



Universitat Autònoma de Barcelona

**ADVERTIMENT.** L'accés als continguts d'aquesta tesi queda condicionat a l'acceptació de les condicions d'ús establertes per la següent llicència Creative Commons:  [http://cat.creativecommons.org/?page\\_id=184](http://cat.creativecommons.org/?page_id=184)

**ADVERTENCIA.** El acceso a los contenidos de esta tesis queda condicionado a la aceptación de las condiciones de uso establecidas por la siguiente licencia Creative Commons:  <http://es.creativecommons.org/blog/licencias/>

**WARNING.** The access to the contents of this doctoral thesis it is limited to the acceptance of the use conditions set by the following Creative Commons license:  <https://creativecommons.org/licenses/?lang=en>

Role of the RecA protein in the  
structuration and function of *Salmonella*  
*enterica* chemotaxis signalling  
complexes

By

Elisabet Frutos Grilo

Directed by

Prof. Jordi Barbé Ph.D, Prof. Susana Campoy Ph.D and Maria Marsal Ph.D

Genetics and Microbiology Department

Universitat Autònoma de Barcelona



Universitat Autònoma  
de Barcelona

June, 2022



A thesis submitted in partial fulfilment of the requirements for the degree of  
DOCTOR OF PHILOSOPHY  
from the Doctoral Programme in Microbiology

By  
Elisabet Frutos Grilo

With the approval of the supervisors,

Prof. Jordi Barbé

Prof. Susana Campoy

Dra. Maria Marsal

Bellaterra, June 2022







Science does not know its debt to imagination.

Ralph Waldo Emerson



## Abstract

*Salmonella enterica* is a primary enteric pathogen infecting both humans and animals and it is the most frequently reported cause of foodborne illness. *S. enterica* can spread to people through contaminated food from farms, causing symptoms such as vomiting and diarrhea, among others related to the gastric system. The number of multiple-antibiotic-resistant isolates is increasing, accelerating the difficulty of their control and treatment. Thereby, these bacteria are considered a high priority by the World Health Organization (WHO), making this species important to study.

Chemotaxis is the ability of bacteria to orient their movement towards more favourable gradients for themselves and it is widely distributed in the *Bacteria* domain. Furthermore, chemotaxis has been described to be important for colonization and subsequent infection in host tissues by many pathogens. For chemotaxis, the chemoreceptor signalling core complexes is needed, which are built of CheA, CheW and methyl-accepting chemotaxis proteins (MCPs), and it modulates the switching of bacterial flagella rotation that drives cell motility.

These complexes, through the formation of heterohexameric rings composed of CheA and CheW, form large clusters at the cell poles. Previous studies demonstrated that RecA, the main bacterial recombinase and the activator of the SOS system, plays a key role in polar cluster formation, interacting with CheW and impairing the assembly when the SOS response is activated.

The results presented herein demonstrate RecA-CheA protein interaction. The interface associated with this interaction has been characterized, revealing some of the essential residues. On one hand, the residues Ala214, Arg222, Asp224, Iso228, Val247 and Lys250 are involved in the interaction of RecA with CheA. On the other

hand, residues Gly537, Lys590, Thr591, Ser628 and Ser646 from the P5-domain of CheA are implied in its interaction with RecA. These findings point out not only surface contacts of RecA with CheA or CheW but also with both proteins. The binding of RecA with both CheA and CheW proteins is needed for wild-type polar cluster formation. In addition, STED microscopy imaging demonstrated that all core unit components (CheA, CheW, and MPCs) have the same subcellular location as RecA: distributed within the cell instead of remaining at the cell pole when SOS response is activated.

Our *in silico* models showed that one RecA molecule, attached to one signalling unit, fits within a CheA-CheW ring without interfering with the complex formation or array assembly. A model for the chemoreceptor arrays disruption according to the acquired results is proposed. The activation of the SOS response is followed by an increase in RecA, which rises up the number of signalling complexes associated with this protein. This suggests the presence of allosteric inhibition in the CheA-CheW interaction and thus of heterohexameric ring formation, impairing the array assembly. CheA- and CheW-RecA interactions are also crucial for chemotaxis, which is maintained when the SOS response is induced and the signalling units are dispersed.

To conclude, the results of the present work provide new molecular level insights into the function of RecA in chemoreceptor clustering and chemotaxis determining that the impaired chemoreceptor clustering not only inhibits swarming but also modulates chemotaxis in SOS-induced cells, thereby modifying bacterial motility in the presence of DNA-damaging compounds, such as antibiotics. These peculiar findings of the chemotactic system of *S. enterica* could give rise to new therapeutic targets for the control of this major pathogen.

## Resumen

*Salmonella enterica* es un patógeno entérico primario que infecta tanto a humanos como animales y es la causa más frecuente de enfermedades transmitidas por alimentos. *S. enterica* puede llegar a las personas a través de alimentos contaminados provenientes de granjas, provocando síntomas como vómitos y diarrea, entre otros relacionados con el sistema gástrico. El número de aislados resistentes a múltiples antibióticos está aumentando, acelerando la dificultad de su control y tratamiento. Por lo tanto, estas bacterias son consideradas de alta prioridad por la Organización Mundial de la Salud (OMS), por lo que es importante estudiar esta especie.

La quimiotaxis es la capacidad de las bacterias para orientar su movimiento hacia gradientes más favorables para ellas y está ampliamente distribuida en el dominio Bacteria. Además, se ha descrito que la quimiotaxis es importante para la colonización y la subsiguiente infección en los tejidos del huésped por parte de muchos patógenos. Para la quimiotaxis se necesitan los complejos centrales de señalización de quimiorreceptores, que están formados por CheA, CheW y proteínas de quimiotaxis que aceptan metilo (MCP), y modulan el cambio de rotación de flagelos bacterianos que impulsa la motilidad celular.

Estos complejos, a través de la formación de anillos heterohexaméricos compuestos por CheA y CheW, forman grandes grupos en los polos celulares. Estudios previos demostraron que RecA, la principal recombinasa bacteriana y el activador del sistema SOS, juega un papel clave en la formación de cúmulos polares, interactuando con CheW y perjudicando el ensamblaje cuando se activa la respuesta SOS.

Los resultados presentados aquí demuestran la interacción de la proteína RecA-CheA. Se ha caracterizado la interfase asociada a esta interacción, revelando así algunos de

los residuos esenciales. Por un lado, los residuos Ala214, Arg222, Asp224, Iso228, Val247 y Lys250 de RecA están involucrados en dicha interacción. Por otro lado, los residuos Gly537, Lys590, Thr591, Ser628 y Ser646 del dominio P5 de CheA están implicados en su interacción con RecA. Estos hallazgos señalan no sólo los contactos de superficie de RecA con CheA o CheW, sino también con ambas proteínas a la vez. La unión de RecA con las proteínas CheA y CheW es necesaria para la formación de grupos polares de tipo salvaje. Además, las imágenes con microscopía STED demuestran que todos los componentes de la unidad central (CheA, CheW y MPC) tienen la misma ubicación subcelular que RecA: distribuidos dentro de la célula en lugar de permanecer en el polo celular cuando se activa la respuesta SOS.

Nuestros modelos *in silico* mostraron que una molécula de RecA, unida a una unidad de señalización, encaja dentro de un anillo CheA-CheW sin interferir con la formación del complejo o el ensamblaje de la matriz. Se propone un modelo para la disrupción de las matrices de quimiorreceptores de acuerdo con los resultados adquiridos. La activación de la respuesta SOS induce un aumento de RecA, lo que eleva el número de complejos de señalización asociados a esta proteína. Esto sugiere la presencia de inhibición alostérica en la interacción CheA-CheW y, por lo tanto, de formación de anillos heterohexaméricos, perjudicando así el ensamblaje de la matriz. Las interacciones CheA- y CheW-RecA también son cruciales para la quimiotaxis, la cual se mantiene cuando se induce la respuesta SOS y se dispersan las unidades de señalización.

Para concluir, los resultados del presente trabajo brindan nuevos conocimientos a nivel molecular sobre la función de RecA en la asociación de quimiorreceptores y la quimiotaxis, lo que determina que el agrupamiento de quimiorreceptores alterado no sólo inhibe el movimiento en enjambre sino que también modula la quimiotaxis en las células inducidas por SOS, modificando así la motilidad bacteriana en presencia de compuestos que dañan el ADN, como los antibióticos. Estos peculiares hallazgos del sistema quimiotáctico de *S. enterica* podrían dar lugar a nuevas dianas terapéuticas para el control de este importante patógeno.

## Resum

*Salmonella enterica* és un patògen entèric primari que infecta tant humans com animals i és la causa més freqüent de malalties transmeses per aliments. *S. enterica* es pot propagar a les persones a través d'aliments contaminats de granges, provocant símptomes com vòmits i diarrea, entre d'altres relacionats amb el sistema gàstric. El nombre d'aïllats resistents a múltiples antibiòtics està augmentant, accelerant així la dificultat del seu control i tractament. D'aquesta manera, aquest bacteri és considerat d'alta prioritat per l'Organització Mundial de la Salut (OMS), cosa que fa que sigui important estudiar aquesta espècie.

La quimiotaxi és la capacitat dels bacteris per orientar el seu moviment cap a gradients més favorables per a ells mateixos i està àmpliament distribuïda al domini Bacteria. A més, s'ha descrit que la quimiotaxi és important per a la colonització i la posterior infecció del teixit hoste per molts patògens. Per a la quimiotaxi es necessiten els complexos bàsics de senyalització de quimiorceptors, que estan formats per CheA, CheW i proteïnes de quimiotaxi acceptadores de metil (MCP, de l'anglès *Methyl-accepting Chemotaxis Protein*) i modulen la commutació de la rotació dels flagels bacterians que impulsa la motilitat cel·lular.

Aquests complexos, mitjançant la formació d'anells heterohexamèrics compostos per CheA i CheW, formen grans agregacions als pols cel·lulars. Estudis anteriors van demostrar que RecA, la principal recombinasa bacteriana i l'activador del sistema SOS, té un paper clau en la formació de clúster polar, interactuant amb CheW i perjudicant el conjunt quan s'activa la resposta SOS.

Els resultats que es presenten aquí demostren la interacció de la proteïna RecA-CheA. S'ha caracteritzat la interfície associada a aquesta interacció, revelant alguns dels



residus essencials. D'una banda, els residus Ala214, Arg222, Asp224, Iso228, Val247 i Lys250 de RecA es troben implicats en la interacció de RecA amb CheA. D'altra banda, els residus Gly537, Lys590, Thr591, Ser628 i Ser646 del domini P5 de CheA estan implicats en la seva interacció amb RecA. Aquestes troballes assenyalen no només els contactes de superfície de RecA amb CheA o CheW, sinó també amb ambdues proteïnes a la vegada. La unió de RecA amb proteïnes CheA i CheW és necessària per a la formació d'agregats polar de tipus salvatge. A més, les imatges amb microscòpia STED van demostrar que tots els components de la unitat central (CheA, CheW i MPC) tenen la mateixa ubicació subcel·lular que RecA: es distribueixen dins de la cèl·lula en lloc de romandre al pol cel·lular quan s'activa la resposta SOS.

Els nostres models *in silico* van demostrar que una molècula RecA, connectada a una unitat de senyalització, encaixa dins d'un anell CheA-CheW sense interferir amb la formació complexa o el conjunt de matrius. Es proposa un model per a la interrupció de les matrius de quimiorceptors segons els resultats adquirits. L'activació de la resposta SOS va seguida d'un augment de RecA, que augmenta el nombre de complexos de senyalització associats a aquesta proteïna. Això suggereix la presència d'inhibició al·lostèrica en la interacció CheA-CheW i, per tant, de formació d'anells heterohexamèrics, perjudicant així el conjunt de la matriu. Les interaccions CheA- i CheW-RecA també són crucials per a la quimiotaxi, que es manté quan s'indueix la resposta SOS i es dispersen les unitats de senyalització.

Per concloure, els resultats del present treball proporcionen nous coneixements a nivell molecular sobre la funció de RecA en l'associació de quimiorceptors i la quimiotaxi, determinant que l'agrupament de quimiorceptors deteriorats no només inhibeix el moviment en eixam, sinó que també modula la quimiotaxi a les cèl·lules induïdes per SOS, modificant així la motilitat bacteriana en la presència de compostos perjudicials per a l'ADN, com els antibiòtics. Aquestes peculiars troballes del sistema quimiotàctic de *S. enterica* podrien donar lloc a noves dianes terapèutiques per al control d'aquest important patògen.

# Contents

|            |                                                       |    |
|------------|-------------------------------------------------------|----|
| 1.         | Introduction                                          | 1  |
| 1.1.       | Two-component systems in bacteria                     | 3  |
| 1.1.1.     | Signal detection and transmission                     | 4  |
| 1.1.2.     | Kinase activation and phosphotransfer                 | 5  |
| 1.1.3.     | Response generation                                   | 6  |
| 1.2.       | Chemotaxis and motility                               | 6  |
| 1.2.1.     | Non-flagella-mediated chemotaxis                      | 9  |
| 1.2.2.     | Pili-mediated chemotaxis                              | 9  |
| 1.2.2.1.   | Twitching                                             | 9  |
| 1.2.2.1.1. | Pilus motor structure                                 | 9  |
| 1.2.2.1.2. | Chemotaxis components of pili-mediated chemotaxis     | 10 |
| 1.2.3.     | Non-appendage-mediated chemotaxis: Gliding            | 13 |
| 1.2.4.     | Flagella-mediated chemotaxis                          | 13 |
| 1.2.4.1.   | Swimming                                              | 13 |
| 1.2.4.1.   | Swarming                                              | 17 |
| 1.2.4.2.   | Flagellar motor structure                             | 21 |
| 1.2.4.3.   | Chemotaxis components of flagella-mediated chemotaxis | 23 |
| 1.2.4.3.1. | Methyl-accepting chemotaxis protein                   | 25 |
| 1.2.4.3.2. | Histidine kinase protein: CheA                        | 27 |
| 1.2.4.3.3. | Coupling proteins: CheW and CheV                      | 28 |
| 1.2.4.3.4. | Phosphotransfer protein: CheY                         | 30 |
| 1.2.4.3.5. | Regulation: CheZ                                      | 30 |
| 1.2.4.3.6. | Adaptation: CheB, CheR and others                     | 31 |

|          |                                                                     |     |
|----------|---------------------------------------------------------------------|-----|
| 1.2.4.4. | Core signalling complexes and clusters                              | 32  |
| 1.2.4.5. | Chemoreceptor cluster location                                      | 35  |
| 1.3.     | Flagella-mediated chemotaxis in virulence and pathogenesis          | 38  |
| 1.3.1.   | Chemoreceptors to sense animal and plant molecules                  | 39  |
| 1.3.2.   | Biofilm production linked to chemotaxis                             | 39  |
| 1.4.     | <i>Salmonella enterica</i> serovar Typhimurium                      | 42  |
| 1.4.1.   | Classification                                                      | 43  |
| 1.4.2.   | Pathogenesis                                                        | 43  |
| 1.4.3.   | Antimicrobial treatment and resistance                              | 45  |
| 1.4.4.   | Flagella-mediated chemotaxis and motility in <i>Salmonella</i>      | 46  |
| 1.4.4.1. | The SOS System                                                      | 47  |
| 1.4.4.2. | The RecA protein                                                    | 49  |
| 1.4.4.3. | Relationship between the SOS system and chemoreceptor clustering    | 51  |
| 2.       | Objectives                                                          | 55  |
| 3.       | Results                                                             | 59  |
| 3.1.     | RecA and CheA interaction                                           | 61  |
| 3.2.     | RecA as a part of the chemoreceptor signalling core unit            | 69  |
| 3.3.     | RecA interacts with both CheW and CheA <i>in vivo</i>               | 71  |
| 3.4.     | Location of CheA and Tar proteins within SOS response-induced cells | 73  |
| 3.5.     | SOS response-induced cells present normal chemotaxis response       | 78  |
| 4.       | Discussion                                                          | 81  |
| 5.       | Conclusions                                                         | 91  |
| 6.       | Material and methods                                                | 95  |
| 7.       | Abbreviations                                                       | 131 |
| 8.       | Annex I                                                             | 135 |
| 8.1.     | Media, solutions and buffers                                        | 137 |
| 8.2.     | Buffers and solutions                                               | 140 |
| 9.       | Annex II                                                            | 147 |
| 9.       | References                                                          | 175 |
| 10.      | Acknowledgements                                                    | 201 |

# 1 INTRODUCTION



# 1. Introduction

## 1.1. Two-component systems in bacteria

Bacteria are present in our daily life, in the most suspect and unsuspected places. They represent 70Gt of carbon of biomass, whereas the human biomass equals to 0.06Gt of carbon<sup>1</sup>. Do we still think that we are the ones who dominate the Earth?

The presence of bacteria is possible by the ability of cells to communicate with environment, which is constantly changing. Bacterial cells possess numerous transmembrane signalling systems that receive stimuli from the environment and they transduce this information into an intracellular signal that triggers cellular responses. Thanks to that, they can colonize a wide variety of environmental niches and survive the challenges associated with them by a tight regulation of expression<sup>2</sup>.

Two-component systems (TCSs) play a major role in these regulatory transmembrane signalling networks<sup>2</sup>. These TCSs have been implicated in mediating the response of bacteria to a wide range of signals and stimuli, including nutrients, cellular redox state, changes in osmolarity, quorum signals, antibiotics, etc<sup>3</sup>. These pathways, constituted by sensor histidine kinases (HKs) and their cognate response regulator (RR), are found in nearly every sequenced bacterial genome, with some of them encoding as many as 200 genes (see a few examples in Table 1.1). Their prevalence underscores their tremendous versatility and their utility to bacteria<sup>4</sup>.

Each HKs and RRs comprise paralogous gene families and the members of each family share significant homology at both primary sequence and structural levels. The

similarity of these signalling proteins raises the possibility of cross-talking between different two-component pathways<sup>5</sup>.

The elegance of the TCS is embodied in its modularity. The most commonly occurring phosphotransfer system is composed of a single HK and a single RR. However, there are other systems in which the combination of HK and RR domains has been exploited creating a more complex signalling circuit, known as phosphorelay system<sup>6</sup>.

**Table 1.1.** Some of the known bacterial two-component systems.

| Histidine kinase | Regulatory protein                | Control function                                      | Reference                                 |
|------------------|-----------------------------------|-------------------------------------------------------|-------------------------------------------|
| ArcB             | ArcA                              | Anaerobiosis                                          | Bekker <i>et al.</i> , 2010 <sup>7</sup>  |
| CheA             | CheY                              | Chemotaxis, flagellar motility                        | Prüß, 2017 <sup>8</sup>                   |
| EnvZ             | OmpR                              | Osmosensing                                           | Caby <i>et al.</i> , 2018 <sup>9</sup>    |
| FrzE             | FrzE (internal receiver) and FrzZ | Fruiting body formation                               | Inclán <i>et al.</i> , 2007 <sup>10</sup> |
| LuxQ and LuxN    | LuxO                              | Bioluminescence                                       | Freeman and Bassler, 1999 <sup>11</sup>   |
| PhoP             | PhoQ                              | Adaptation to Mg <sup>2+</sup> -limiting environments | Groisman, 2001 <sup>12</sup>              |
| NarQ             | NarP                              | Regulation of anaerobic respiration                   | Stewart, 2003 <sup>13</sup>               |
| VanS             | VanR                              | Cell-wall biosynthesis                                | Arthur <i>et al.</i> , 1992 <sup>14</sup> |
| VirA             | VirG                              | Host recognition, transformation                      | Gao and Lynn, 2005 <sup>15</sup>          |
| WalK             | WalR                              | Cell-wall metabolism and structure in cell division   | Takada and Yoshikawab, 2018 <sup>16</sup> |

### 1.1.1. Signal detection and transmission

Extracellular stimuli are sensed by the HK, and this signalling also serves to modulate its own activity. Most HKs are homodimeric membrane receptors. Their ~350 amino acids in length catalytic core comprises two domains:

- i. at N-terminal, a variable extracellular sensor domain
- ii. at C-terminal, the cytoplasmic portion, which contains the catalytic machinery.

Both domains are connected via transmembrane helices<sup>17</sup>. In typical transmembrane HKs, sensing domains directly bind ligands or detect other physical stimuli. More complex schemes involve indirect detection of signals through interaction with other

protein components, as occurs with the soluble HK CheA from the chemotaxis pathway, which forms a complex with transmembrane receptors and an adapter protein CheW<sup>6,18</sup>.

With the diversity of signal detection domains, several models for signal transmission have been described. For instance, studies focusing on the *Escherichia coli* chemoreceptor Tar suggest an asymmetric piston shift model<sup>19</sup>. Furthermore, structures of various sensing domains in apo- and ligand-bound states have also point out two other possible signal transmission modes, named scissoring or helical rotation as described, for example, for PhoQ and LuxQ, respectively<sup>20</sup>. However, these modes of shifts are not mutually exclusive and they can act in combination as occurs in the NarQ protein<sup>21</sup>.

### 1.1.2. Kinase activation and phosphotransfer

All HKs are identified by unique signature sequences called H, N, G, D and F boxes. The H box contains a conserved histidine that serves as the initial phosphoacceptor from ATP, whereas the N, G, D and F are involved in ATP binding. On the basis of HK domain organization, the HKs have been grouped into two major classes. In HK class I, the H box-containing region is directly linked to the region that displays the other four conserved boxes. However, in HK class II, the H box-containing region is distant from the catalytic and ATP-binding domain (CA) by having distinct domain insertions between them<sup>17,22</sup>.

Hence, once detection occurs, signal is transmitted throughout the transmembrane protein helices and it arrives to the C-terminal. Here, the CA domain binds ATP, which then donates its  $\gamma$ -phosphate group to the conserved histidine residue on the H box<sup>17,23</sup>. Then, transphosphorylation from the H box to receiving domains of the cognate RRs is developed through a common four-helix bundle motif<sup>17</sup>.



### 1.1.3. Response generation

The RR protein is the key element to execute the specific cellular output in response to the input detected by the HK. The modular architecture of the RR is observed for the vast number of known RRs, combining any imaginable signal to a cellular response. Hence, the RR is one of the most intriguing and intensively studied bacterial proteins<sup>2</sup>.

Early studies revealed a modular architecture of the typical RR, which usually comprises two domains: a conserved N-terminal receiver domain (REC) and a variable effector domain. Therefore, REC domain is connected to a hypervariable C-terminal effector domain by a non-conserved flexible linker. Besides, it catalyses the transfer of the phosphoryl group from the associated HK onto itself. This develops in a self-activation in a phosphorylation-dependent manner. Finally, the activated effector domain of the RR in turn triggers the specific cellular output response<sup>24</sup>. Just the modular architecture of the RR can guarantee to combine a specific stimulus to a specific cellular response<sup>2,25</sup>.

## 1.2. Chemotaxis and motility

Chemotaxis, and concretely the flagella-mediated chemotaxis, is a signal transduction system present in bacteria formed by TCS<sup>6</sup>, and it is the main axis in which the present thesis turns around.

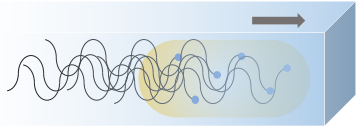
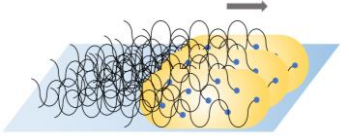
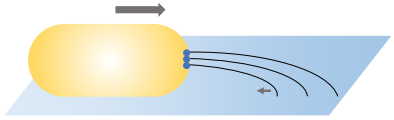
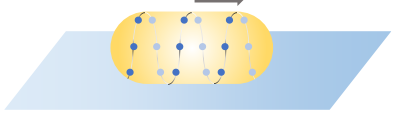
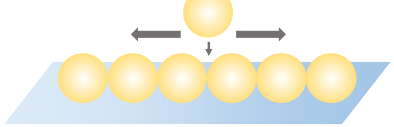
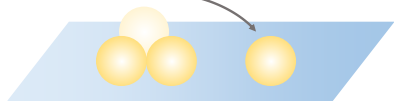
Chemotaxis is the ability of bacteria to direct rapidly their movement towards more favourable conditions by detecting changes and gradients of concentrations of different environmental physical or chemical repellents and attractants<sup>26</sup>. Described evidence which led to the understanding of this process began in 1881, when Engelmann observed a rapid cellular aggregation of microorganisms in the vicinity of the *Spirogyra* algae<sup>27</sup>. His studies developed a sensitive method following the production of photosynthetic oxygen by determining the attraction of these bacteria to this element (currently known as aerotaxis)<sup>28</sup>. A few years later, in 1884, Pfeffer discovered the same phenomenon in male gametes towards an oocyte<sup>29-31</sup>.

For decades, chemotaxis has been widely investigated in all domains. Many studies have been focused on bacteria and this research has been exploited to obtain applied strategies such as in cancer treatment<sup>32-34</sup> or in biosensors usage<sup>35-37</sup>.

Despite its importance, not all bacteria possess a chemotaxis behaviour. An analysis of 450 prokaryotic genomes showed that only 54% of them presented chemosensory signalling genes<sup>38</sup>. This fact suggests that prokaryotes take two different strategies: either they invest in chemotactic capabilities, or they adopt a lifestyle that does not require chemotactic motility<sup>39</sup>. The main evolutionary advantage offered by chemotaxis is the search for food and a quick escape from the immediacy of harmful substances. In addition, it is very important for bacteria such as *E. coli* and *Salmonella enterica*, as ubiquitous colonizers of animal intestines, to orient their motility for host colonization<sup>32,40</sup>.

The output of the TCS networks is a multitude of phenotypic changes in response to variations in the environment. Among these phenotypic changes, some chemotactic TCSs control motility<sup>8</sup>. Up to 6 types of bacterial motilities have been described: swimming (Table 1.2.A), swarming (Table 1.2.B), twitching (Table 1.2.C), gliding (Table 1.2.D), sliding (Table 1.2.E) and darting (Table 1.2.F) (note some authors do not consider the last behaviour as a motility). Chemotaxis signal transduction pathways are conserved, and the genes encoding them are found in the genomes of bacteria movable by pili (twitching), flagella (swimming or swarming) or by other mechanisms that occur in the absence of identified appendages (gliding)<sup>41-43</sup>. The last two enumerated motilities, sliding and darting, are not well studied and non-directly implied two-component system has been identified yet<sup>44-46</sup>.

**Table 1.2.** Main features of the leading types of surface motility<sup>46,47</sup>. The direction of cell movement is indicated by a grey arrow and the motors that power the movement are indicated by blue-coloured circles. Figures adapted from Kearns, 2010<sup>48</sup>. NC, non-characterized feature.

| Types of motility | Motive organelle | Cell differentiation | Movement | Colony expansion rate ( $\mu\text{m/s}$ ) | Schematic models                                                                      | Bacteria genus examples with the described motility                                                                            |
|-------------------|------------------|----------------------|----------|-------------------------------------------|---------------------------------------------------------------------------------------|--------------------------------------------------------------------------------------------------------------------------------|
| Swimming          | Flagella         | No                   | Active   | 25-160                                    |    | <i>Bacillus, Clostridium, Vibrio, Escherichia, Proteus, Salmonella, Pseudomonas, Yersinia, Enterobacter</i>                    |
| Swarming          | Flagella         | In some cases        | Active   | 2-10                                      |    | <i>Bacillus, Clostridium, Vibrio, Escherichia, Proteus, Salmonella, Pseudomonas, Yersinia</i>                                  |
| Twitching         | Type IV pili     | No                   | Active   | 0.06-0.3                                  |    | <i>Aeromonas, Acinetobacter, Legionella, Myxococcus, Neisseria, Pasteurella, Vibrio, Pseudomonas, Streptococcus</i>            |
| Gliding           | Unknown          | No                   | Active   | 0.025-10                                  |   | <i>Anabaena, Cytophaga, Flavobacterium, Flexibacter, Mycoplasma, Myxococcus, Staphylococcus</i>                                |
| Sliding           | None             | No                   | Passive  | 0.03-3                                    |  | <i>Acinetobacter, Alcaligenes, Bacillus, Escherichia, Flavobacterium, Vibrio, Mycobacterium, Streptococcus, Staphylococcus</i> |
| Darting           | None             | NC                   | Passive  | NC                                        |  | <i>Staphylococcus</i>                                                                                                          |

## 1.2.1. Non-flagella-mediated chemotaxis

### 1.2.2. Pili-mediated chemotaxis

#### 1.2.2.1. Twitching

Twitching, also accepted as social gliding or S-motility, is a slow surface movement of bacteria where cells are able to move at 0.06-0.3  $\mu\text{m/s}$  (Table 1.2.C). This form of bacterial movement was hypothesized by D. Bradley because of the repeated extension, tethering and retraction of the type IV pili (T4P)<sup>49</sup>. Examples of twitching bacteria include species such as *Pseudomonas aeruginosa*, *Neisseria gonorrhoeae* or *Acinetobacter*<sup>50,51</sup>.

This movement based on extension and retraction of the pilus is observed on solid surfaces, interfaces or media with moderate viscosities (1% agar) and it has an implication in virulence, host colonization and other forms of complex colonial behaviour, including biofilm development and fruiting bodies<sup>52,53</sup>. Although twitching motility is mainly a social activity that involves the formation of organized and compact rafts, it has also been demonstrated that individual cells can move by twitching<sup>47,52</sup>. The environmental signals that control twitching motility are not well understood. However, there is evidence that this motility is influenced by nutritional status, cell density and may also involve self-generated soluble and cell contact-dependent intercellular signals<sup>50</sup>.

##### 1.2.2.1.1. Pilus motor structure

The pili of bacteria (Fig. 1.1) are long extracellular polymers that mediate diverse functions apart from the movement, such as bacterial attachment and substrate transport. There are five classes of pili in bacteria, but T4P are the effector module involved in the pili associated to chemotaxis and twitching motilities in *P. aeruginosa*, both controlled by the *pil-chp* pathway<sup>54</sup>.

These dynamic extracellular appendages range between 6-9 nm in diameter and can reach several micrometres in length. They are found in Gram-negative and Gram-positive bacteria, and also in Archaea. In Archaea, such systems are responsible for the assembly of the archaeal flagellum or archaellum<sup>55</sup>.

The pili are composed by subunits of pilin PilA, which are further organized in a helical conformation with 5 subunits per turn. Prior to the assembly, PilA is processed by the prepilin peptidase PilD. The *pilA* gene is regulated by a two-component system constituted by PilS and PilR. Here, PilS is the HK sensor which its autophosphorylation induces the phosphorylation of the RR PilR. The kinase activation finally increases the *pilA* transcription<sup>52</sup>.

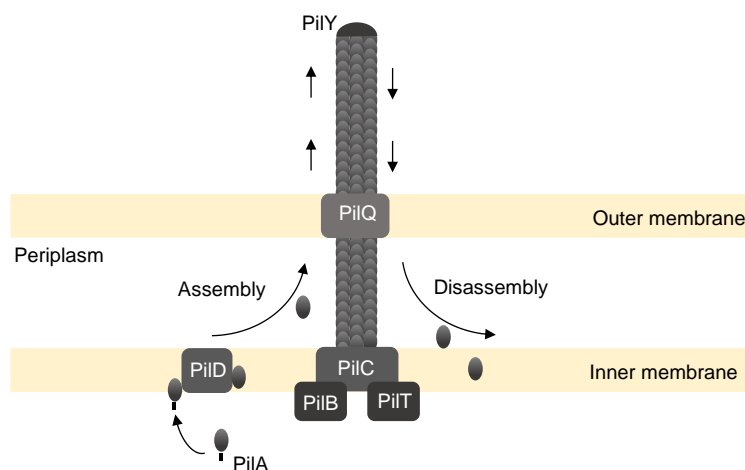


Figure 1.1. Type IV pili structure. Adapted from Burdman S. *et al.*, 2011<sup>56</sup>.

#### 1.2.2.1.2. Chemotaxis components of pili-mediated chemotaxis

T4P can bind to a variety of surfaces, including inert materials, and other bacterial and eukaryotic cells, where they can mediate both colonization and intimate contact through pili retraction<sup>57</sup>. The extension and retraction of these pili are controlled by the Chp chemosensory pathway (Fig. 1.2), and by the FimS/AlgR network, which controls the levels of the cyclic AMP (cAMP) and c-di-GMP as secondary messengers<sup>42</sup>.

Encoded within the *chp* gene cluster, are two RR proteins (PilG and PilH), two coupling proteins (Pill and ChpC), a methyltransferase protein (PilK), a methylesterase protein (ChpB), a complex HK protein with a REC domain (ChpA), and one surface contact and chemical sensing protein (PilJ)<sup>58</sup>.

PilJ detects changes in the concentration of attractant or repellent, such as phosphatidylethanolamine<sup>59</sup>, and it senses surface contact by mechanosensing in response to tension generated within the pilus. In both cases, this detection by PilJ relays the signalling into the two HKs: ChpA and FimS. On one hand, FimS phosphorylates its RR, AlgR, leading to the activation of its regulon (T4P, virulence, the diguanylate cyclase *mucR* and *pilY* genes)<sup>42,54</sup>. On the other hand, signal is also relayed via Pill and ChpC adaptor proteins to ChpA, which autophosphorylates itself and there is a phosphotransfer to ChpB, PilG and PilH. PilG-P mediates pilus extension by interacting with the complex which includes the ATPases PilB, PilZ, and the c-di-GMP -producer FimX. By contrast, PilH-P mediates pilus retraction by interacting with the ATPases PilT. Whether the two RRs PilG and PilH compete for phosphorylation is unclear and it remains to be determined<sup>54</sup>. However, it is known that the adaptation in this pathway is achieved by modulating the ratios of the opposing involved receptor-specific methylesterase ChpB and methyltransferase PilK<sup>60</sup>.

In this manner, as shown in Figure 1.2, the rise of chemoattractant concentration deactivates the autophosphorylation of ChpA and thus, promoting the T4P filament extension. In contrast, ChpA activates its autophosphorylation in absence of chemoattractants and therefore, it stimulates the frequency of pilus retraction.

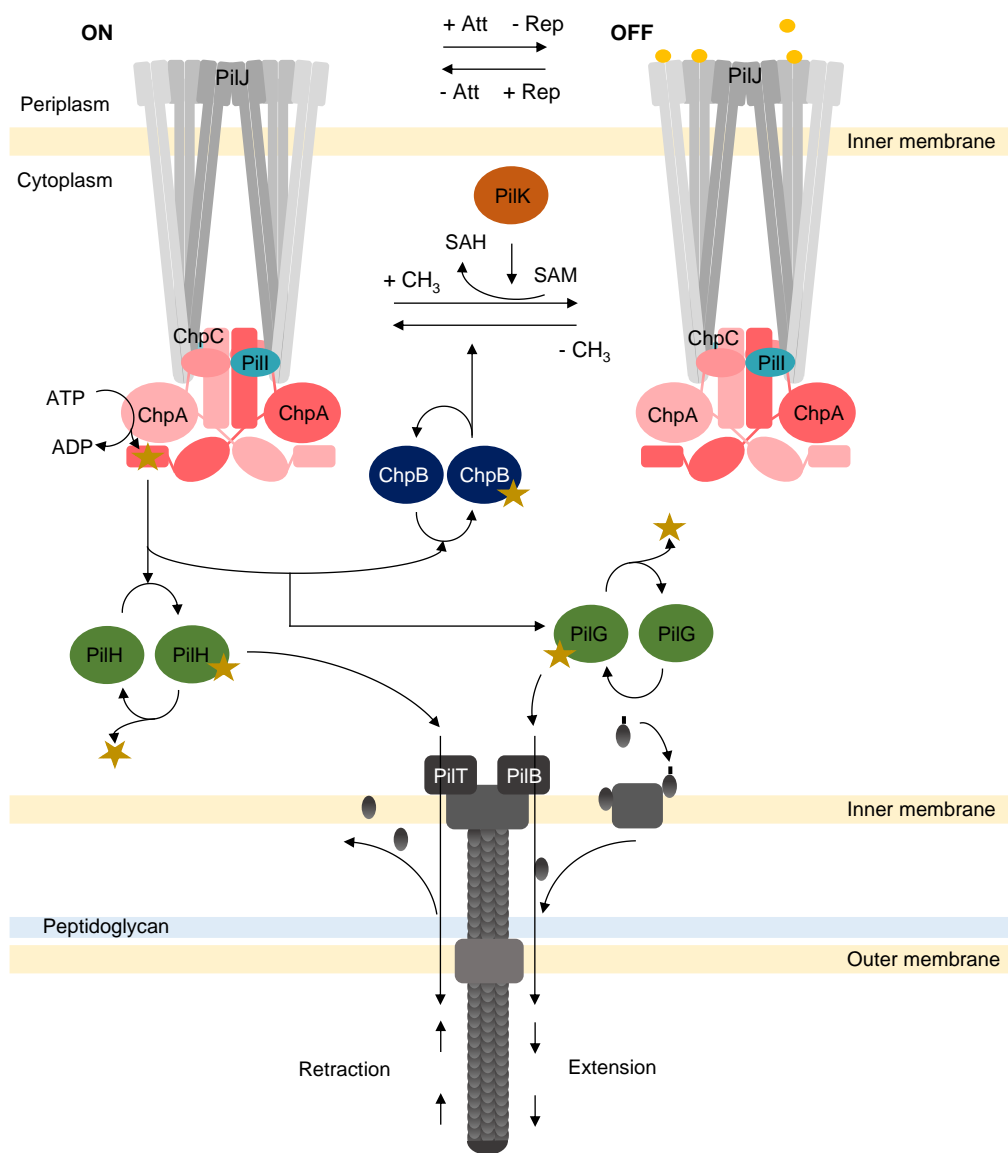


**Figure 1.2.** The Chp pathway, chemotactic system involved in the surface attachment and twitching motility from *P. aeruginosa*. (De) methylations (-CH<sub>3</sub>/+CH<sub>3</sub>) PilJ occur according to their activity state. Attractants (Att) favour OFF states and thus pilus extension occurs more frequently; surface contact and repellents (Rep) favour ON states and pilus retraction. The T4P motor and the associate Chp proteins (ChpA, PilI, ChpC, ChpB, PilH, PilG, PilK) are also represented. Phosphoryl groups are characterized by a yellow star. Adapted from Sampedro *et al.*, 2015 and Francis *et al.*, 2017<sup>42,54</sup>.

### 1.2.3. Non-appendage-mediated chemotaxis: Gliding

In the case of gliding, also known as adventurous gliding or A-motility, there are present a great variability in velocity depending on the species, that can be up to 0.1  $\mu\text{m/s}$  for *Myxococcus xanthus*, 2  $\mu\text{m/s}$  for *Flavobacterium johnsonae* or 2-4.5  $\mu\text{m/s}$  for *Mycoplasma mobile*<sup>61</sup> (Table 1.2.D). This fact suggests the presence of a different efficient motility apparatus<sup>62</sup>. Despite the similarities between twitching and gliding where both types of surface translocation are independent of flagella and the micromorphology of the spreading zone is similar (scattered cells over the agar surface), the pattern is different. In this context, gliding cells are highly organized, whereas that of twitching organisms is only slightly so the spreading from a twitching motility, however, stops before that<sup>44</sup>. Furthermore, spreading of a gliding strain usually continues until bacteria cover the entire agar surface<sup>44</sup>.

In addition, *Myxococcus*, *Flavobacterium* and *Mycoplasma* spp. have different involved chemotaxis signal transduction pathways in its gliding movement. For example, in *M. xanthus*, the Frz chemosensory pathway controls the reversal frequency between its own gliding and twitching motilities<sup>62</sup>. However, although detailed mechanisms and regulation are still under investigation, type IX secretory system (T9SS) provides the development of this movement in *F. johnsonae*<sup>63</sup>. Thus, no common chemotaxis signal transduction is clear in gliding bacteria despite the evidence of many involved TCSs.

### 1.2.4. Flagella-mediated chemotaxis

#### 1.2.4.1. Swimming

Swimming motility is a mode of bacterial movement powered by rotating flagella that take place as individual cells moving in aqueous environments<sup>48</sup> (Fig. 1.3). This movement is widely spread within *Bacteria* domain, but the speed can vary between species: *E. coli* swims at a rate of 25-35  $\mu\text{m/s}$ , whereas *Bdellovibrio bacteriovorus* can reach 160  $\mu\text{m/s}$ <sup>64,65</sup>.



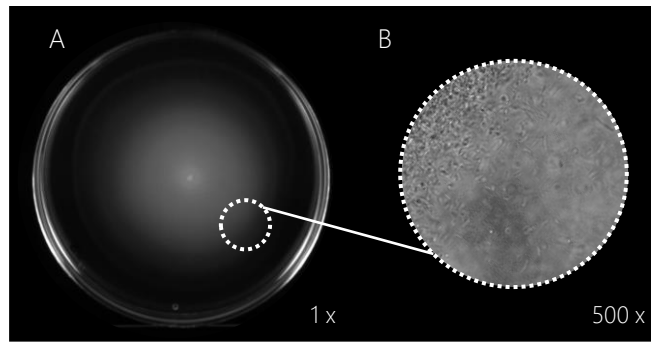


**Figure 1.3.** Colony pattern during swimming translocation of *Enterobacter cloacae*. **(A)** Macroscopic and **(B)** microscopic views under bright-field optical microscopy. Own source.

The bacterium monitors changes according to the concentration of attractants or repellents to orient its trajectory and modulate it according to a constant evaluation. This evaluation is provided by the TCS which controls the flagellar motion in order to directly move along gradients. The sense of flagellar rotation is controlled by the type of molecules detected by the receptors on the surface of the cell: in the presence of an attractant gradient, the rate of smooth swimming increases, whilst the presence of a repellent gradient increases the rate of tumbling<sup>66,67</sup> (Fig. 1.4).

Moreover, the ability to swim involves over 60 structural and regulatory proteins that are required for processing sensory cues and the function and assembly of operating flagella<sup>18</sup>. Different types of cell flagellation are found depending on the number and arrangement of the flagella on the cell surface. In polar flagellation, the flagella are present at one or both ends of the cell. At once, a single flagellum can be attached at one pole (monotrichous) and a tuft of flagella can be located at one pole (lophotrichous) or at both ends (amphitrichous). In contrast, in peritrichous flagellation, the flagella are distributed in different locations around the cell surface. Nevertheless, variations within this classification can be found, like lateral and subpolar flagellation<sup>68</sup>. In all cases, when flagella are present, swimming has been described<sup>69-73</sup>. However, an isolated case of non-flagellated swimming bacterium has been identified and studied in *Synechococcus* spp.. In this case, the cell is completely covered of fine hairs a few nm in diameter and about 0.15  $\mu\text{m}$  long, named spicules, which are used as oars<sup>74,75</sup>.

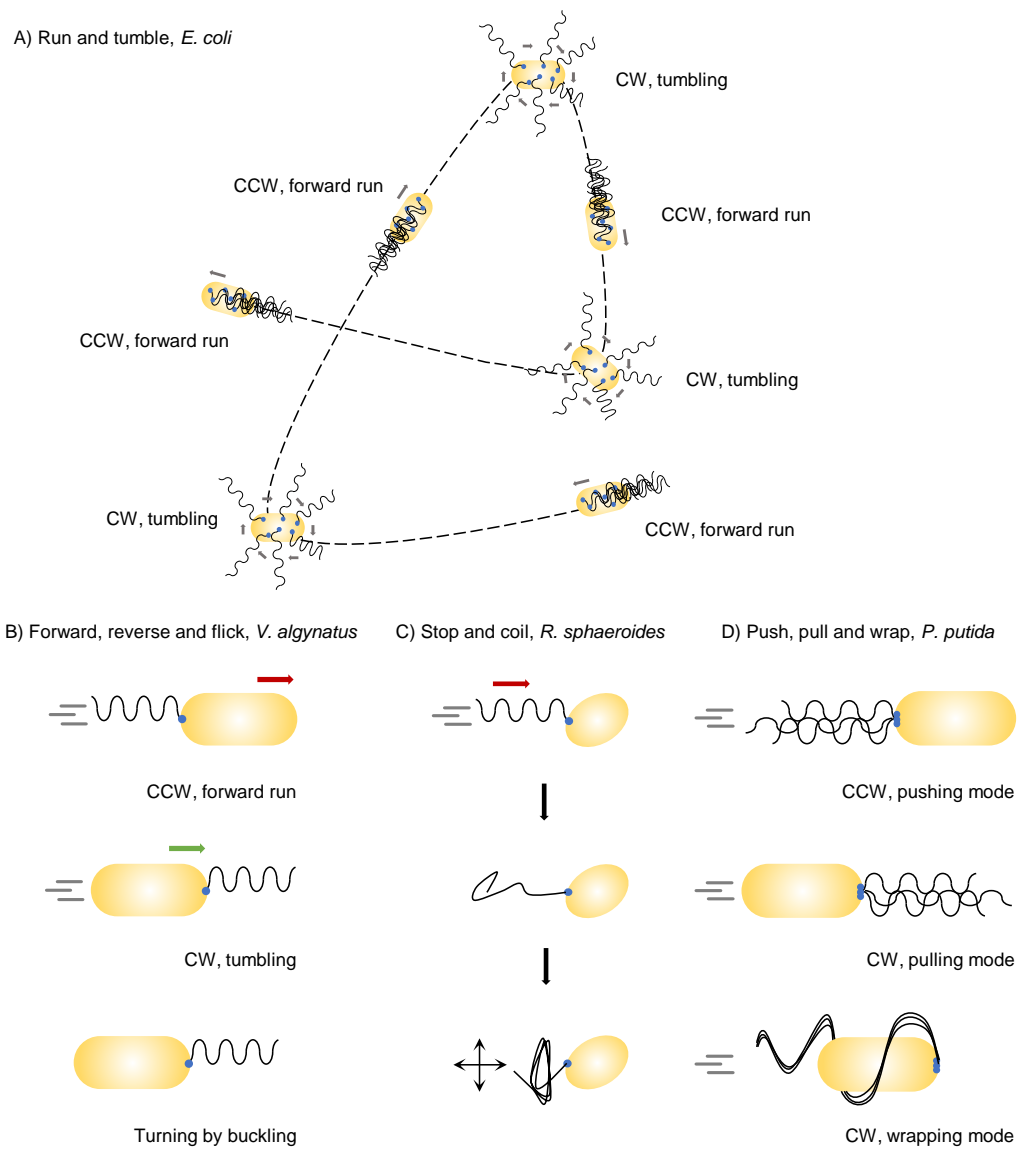


**Figure 1.4.** Swimming strategies of **A)** *E. coli*, **B)** *V. alginatus*, **C)** *R. sphaeroides* and **D)** *P. putida*. CCW and CW mean counter-clockwise and clockwise, respectively. Adapted from Bastos-Arrieta et al., 2018<sup>68</sup>.

The archetype of bacterial swimming is represented by the well-studied model organism *E. coli*, which performs a run-and-tumble swimming pattern (Fig. 1.4.A) with its peritrichous flagellation. In this way, during the swim movement of bacteria, they are usually running following in a direction parallel to their axis for a 1 second-period approximately (running). At this period, all their flagella turn counter-clockwise (CCW). These flagella are intertwined with each other towards the distal end of the body

forming a larger helix for their propulsion. Between these races, some episodes of switching to clockwise (CW) rotation results in a reorientation (tumbling) of the bacterium for a tenth of a second, until a new race begins. After the tumbling event, straight swimming is recovered in a new direction. Thus, translocation depends on the frequency of changes in the direction of flagellar rotation<sup>66,76,77</sup>. In this way, the bacterium monitors changes according to the concentration of attractants or repellents in order to orient its trajectory and modulate it for a constant evaluation: when swimming in chemoeffector gradients, the cell responds in longer runs in favourable directions; in contrast, tumbling events are more frequent in unfavourable zones until chemoattractants are detected.

However, the type of swimming movement varies significantly with the species and number/distribution of flagella on the cell body. For example, *V. alginolyticus*, has a single polar flagellum and it swims in a cyclic three-step (forward, reverse and flick) pattern (Fig. 1.4.B). In other words, the flagellum pushes the cell head to a forward swimming, but it is able to turn 180° to pulling the head upon motor reversal for backward swimming. In addition, the cells can flick by an angle around 90°<sup>78</sup>. Alternatively, *Rhodobacter sphaeroides* has subpolar monotrichous flagellation and it represents another motility strategy. Its cell body reorients stopping and coiling its flagellum (Fig. 1.4.C), which only rotates in one direction against itself from time to time<sup>79</sup>. In the lophotrichous bacterium *Pseudomonas putida*, alternates between three swimming modes: pushing, pulling and wrapping (Fig. 1.4.D). In the pushing mode, the CCW-rotating flagella drive the motion from the rear end of the cell body in straight manner. In contrast, the CW-rotating flagellar bundle is pointing ahead in the pulling mode and the cell swims straight or left bend trajectories. Finally, *P. putida* can also swim by wrapping the filament bundle around its cell body, with the posterior pole pointing in the direction of motion. In that case, the flagellar bundle takes the form of a left-handed helix that turns in CW direction and the trajectories are predominantly straight<sup>68,70</sup>. The wrapping mode has not been found in other species from the same genus, apart from *P. aeruginosa* or *P. fluorescens*.

### 1.2.4.1. Swarming

Swimming motility has been described before as being the best studied model in chemotaxis works<sup>41,48</sup>. However, chemotaxis system has also a crucial role in swarming migration<sup>80</sup>.

Swarming motility is a rapid (2-10  $\mu\text{m/s}$ ) (Table 1.2.B) and coordinated translocation of a bacterial population across solid or semi-solid surfaces; it is the most rapid surface motility known so far<sup>47,52</sup>. As swimming, it is indeed dependent on flagella<sup>81</sup> and, in this case, it also depends on massive flagellation, cell-to-cell communication by quorum sensing<sup>82,83</sup> and the presence of a surfactant<sup>48,84</sup>. These facts are not always accomplished, for example, *P. aeruginosa* differentiates into elongated hyperflagellated cells depending on media and conditions in which swarming is performed<sup>85</sup>.

G. Hauser first described swarming in *Proteus* species in 1885<sup>86</sup> and from then until now has been studied in many other members of Gram-negative and Gram-positive, as *Escherichia*<sup>87</sup>, *Serratia*<sup>88</sup>, *Salmonella*<sup>89</sup>, *Aeromonas*<sup>90</sup>, *Yersinia*<sup>91</sup>, *Pseudomonas*<sup>54</sup>, *Vibrio*<sup>92</sup>, *Bulkholderia*<sup>93</sup>, *Azospirillum*<sup>94</sup>, *Sinorhizobium*<sup>95</sup> and *Bacillus*<sup>96,97</sup>.

Swarming involves movement of cells in groups aligned along their long axis in multicellular rafts (Fig. 1.5). Isolated swarmer cells almost never move, and it could be related to the amount of slime encasing a group of cells versus individual cells. This is because wetting agents in the slime provide a hydrated environment for flagellar function<sup>98</sup>. This notion is consistent with inactivity of cells at the edge of the advancing swarm front, while vigorous motility is evident just behind the front<sup>47</sup>.

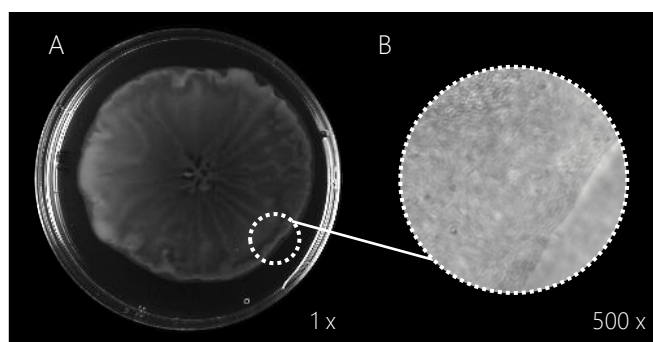


**Figure 1.5.** Colony pattern during swarming translocation of *S. enterica*. **(A)** Macroscopic and **(B)** microscopic views under bright-field optical microscopy. Own source.

Bacterial mechanisms have to surpass surface challenges derived from the intrinsic properties present on the agar surface and not encountered during swimming. For that, bacteria display mechanisms which will allow themselves to swarm within a surface where there is no free water by (i) attracting water to the surface, (ii) overcoming frictional forces and (iii) reducing surface tension<sup>41</sup>. Therefore, some bacteria appear to use osmolytes, polysaccharides, lipopolysaccharides, and other family-specific surface proteins to draw water toward the cells<sup>41</sup>. Furthermore, swimmers regulate the synthesis of the osmoprotectants glutamate and proline in *P. aeruginosa*<sup>99</sup>, potassium uptake in *B. cereus*<sup>100</sup> and a sodium/solute symporter in *Vibrio parahaemolyticus*<sup>101</sup>. Additionally, many swarming bacteria synthesize and secrete surfactants (short for “surface active agent”). Surfactants are amphipathic molecules that reduce tension and frictional forces between the substrate and the bacterial cell to permit spreading over surfaces<sup>102</sup>. Some surfactants to spread over solid surfaces are surfactin<sup>103</sup>, rhamnolipid, HAA<sup>104</sup> and serrawettin W2<sup>105</sup>.

Other related environmental factors that affect swarming are the availability of nutrients and the temperature. Several well-studied bacteria are known to exhibit swarming motility on surfaces of varying nutrient availability, like in members of the genera *Salmonella*, *Bacillus*, *Chromobacterium*, *Clostridium*, *Escherichia*, *Proteus* and *Vibrio*<sup>47,106</sup>. Even though it is possible to observe swarming motility in minimal media, a

carbon source supplementation is usually required, typically glucose or casamino acids in some species<sup>47</sup>.

The swarming motility is widely distributed throughout flagellated bacteria and it is associated with their colonization of host surfaces<sup>107</sup>, the increased expression of virulence factors and antibiotic resistance<sup>108,109</sup>. Regarding their ability to displace over the moist surfaces, swarming bacteria can be divided into two categories: robust swimmers, that can swarm across hard surfaces (1.5% agar and above), and temperate swimmers, that can only swarm over soft surfaces (0.4% to 0.8% agar)<sup>41,47,110</sup>.

The robust swimmers include polarly flagellated bacteria, which display a peritrichous hyperflagellation and cell hyperelongation in contact with the surface. For instance, *Azospirillum*, *Rhodospirillum*, *Proteus*, *Vibrio* and *Aeromonas* species are typically robust swimmers. This gain in number of flagella allows them more facility to swarm on harder agar than their broth-grown (swimming) counterparts. Instead, temperate swimmers include, among others, *Escherichia*, *Bacillus*, *Pseudomonas*, *Rhizobium*, *Salmonella*, *Serratia* and *Yersinia* species<sup>41,111–113</sup>.

Some signalling pathways influence swarming, but with different outcomes in different bacteria:

- i. Chemotaxis has been determined that is required for outward migration of the swarm swarming colony in *V. parahaemolyticus* and *V. alginolyticus*<sup>114,115</sup>, but not for any of the other bacteria examined to date. In other studied species a functional chemotaxis system is crucial, but not chemotaxis *per se*<sup>80,116</sup>. It has been demonstrated that null mutants in the chemotaxis pathway (Che), which rotate motors CCW-only or CW-only fail to swarm whereas those that are able to switch their motors are also able to swarm although do not respond to fluctuations in the environment. That switching has been determined that aids in the lubrication of the surface by obtaining water from the underlying agar, thereby facilitating cell movement<sup>80,117</sup>. However, recent studies observed a

remodelation of the chemotaxis pathway to stimulate a low level of tumble bias, which is apparently optimal for swarm expansion<sup>118</sup>.

- ii. Quorum sensing. Surfactant synthesis is under quorum sensing control in *Serratia liquefaciens*<sup>119</sup>, *Bacillus subtilis*<sup>120</sup>, *Yersinia enterocolitica*<sup>91</sup> and *Bhirkolderia cepacia*<sup>93</sup> and facilitates swarming as described above<sup>41</sup>. Quorum sensing is activated by the production and release of autoinducers, whose external concentration rises with increasing cell density<sup>41</sup>.
- iii. c-di-GMP. bis-(3'-5')-cyclic dimeric guanosine monophosphate (c-di-GMP) is an important signalling molecule in the transition between motile and sessile forms of bacterial life<sup>121,122</sup>. In *E. coli*, *Salmonella* and *B. subtilis*, c-di-GMP complexed with a receptor protein inhibits flagellar motility at the level of either gene expression, flagellar assembly and function<sup>41,123,124</sup>. A variety of signals, such as a mechanical pressure, promote a response through varied TCSs and activate the production of c-di-GMP<sup>42,125</sup>.

It has been studied that TCSs, which receptors are commonly located in the cell envelope, or regulators that increase flagella synthesis, allow bacteria to overcome the above requirements. Thus, the cell envelope and the flagellum are considered to be the sensors implicated in sensing surface contact in more than one bacterial species<sup>41,47,126</sup>. The best evidence for the flagellum as a sensor comes from the marine bacterium *V. parahaemolyticus*<sup>127,128</sup>. Numerous lateral flagella are induced in this bacterium upon contact with a surface<sup>129</sup>. Furthermore, perturbations of the C-terminal periplasmic segment of the flagellar stator-associated protein affect induction of swarming-related proteins in *P. mirabilis*<sup>130,131</sup>. Besides, surface sensors sense perturbation of the membrane, cell wall or periplasmic space. Some of these sensors are TCSs, which generate the canonical stress systems and thereby alert the bacteria about cell-to-surface contact<sup>110,132,133</sup>.

### 1.2.4.2. Flagellar motor structure

In the case of the model bacteria *E. coli* and also in *S. enterica*, they are propelled by flagellar motion. The flagellum is a rigid organelle that rotates in the form of a helix that drives the cell motility, allowing it to infect hosts or to adhere non-pathogenically on abiotic surfaces, colonize soil particles, among other<sup>39,134–136</sup>.

The flagellum structure is complex and involved different proteins. It is well characterized in model bacteria such as *E. coli*. In this context, the flagellum structure is formed by FliM, FliN and FliG form the C ring found on the cytoplasmic face of the MS ring, which is composed of FliE and FliF (Fig. 1.6). The C and MS rings together act as a rotor of the flagellar motor and they are coupled in the outer membrane, whilst P and L rings are embedded in the inner membrane and formed by FlgI and FlgH, respectively<sup>137</sup>. The basal body of the flagellum includes all these rings and also the protein export apparatus, composed of the transmembrane export complexes FlhA, FlhB, FliP, FliQ and FliR, and the cytoplasmic ATPase complex, consisting of FliH, FliI and FliJ. In addition, there are a dozen stators composed of four copies of MotA and two copies of MotB, which surround the C and MS rings and couple the proton flow through a proton channel between cytoplasm and periplasm. MotB anchors MotA on the periplasmic face of the cell wall structure to allow the transmission of the torsion to the flagellar filament by interaction with FliG. The flagellar motor itself regulates the number of active stator units around the rotor in response to changes in the external load and the motive force of the ions through the cytoplasmic membrane<sup>77,138</sup>.

FliE, FlgB, FlgC, FlgF, FlgG form the rod, a rigid tubular structure composed of 11 protofilaments and acts as a driving axis connecting the basal body with the hook and exposing it outside the outer membrane<sup>22,77</sup>. The hook is flexible and consists of FlgE and its associated proteins, FlgK and FlgL.



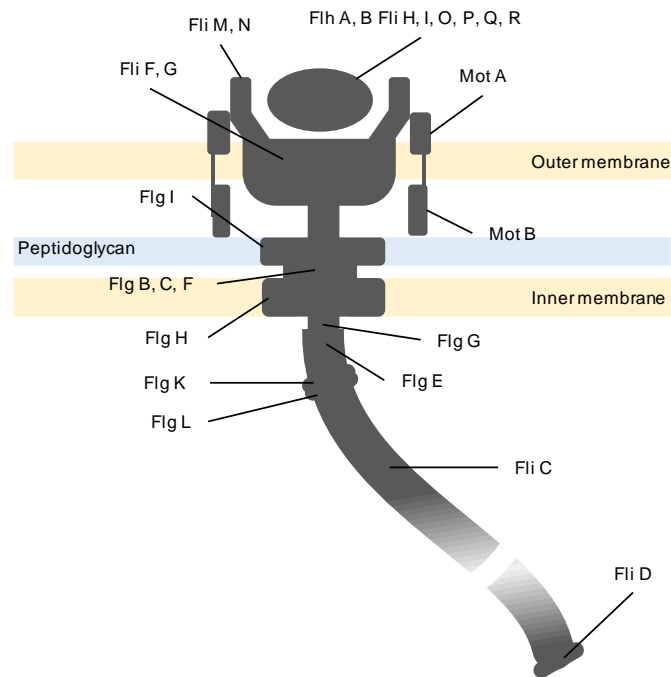


**Figure 1.6.** Schematic diagram of the flagellar motor. The different proteins are named for their coding genes. Adapted from Berg *et al.*, 2003<sup>77</sup>.

Finally, the filament continues, which measures approximately 10-15 nm in length and it is constructed by up to 20.000 sub-units of the flagellin protein (FliC), and finishes with FliD covering the end. This plug is generated at the beginning of the filament formation by FlgL, so the flagellin monomers are subsequently joined, thus lengthening the filament. For the assembly of all the components that form the flagellum, specific chaperones such as FlgN, FliJ, FliS and FliT are necessary<sup>77</sup>.

The flagellar motor structure and its organization are highly conserved among bacterial species<sup>138</sup>. Archaeella and cilia has a common ancestry with flagella, but they have evolved independently from different precursors, specifically flagella from a primordial translocase with further evolution into injectosome/type III secretory systems<sup>139</sup>.

### 1.2.4.3. Chemotaxis components of flagella-mediated chemotaxis

When swarming or swimming occur in either semisolid or liquid media, a band of cells is formed and propagated as a result of the self-organization of these bacteria that dynamically respond to gradients in chemoattractants or changes in cellular energy levels<sup>140</sup>. The chemotaxis system in these both flagellar motilities consist of transmembrane chemoreceptors composed mainly of methyl-accepting chemotactic proteins (MCPs) and the six core components: the HK CheA, the receptor coupling protein CheW, the phosphotransfer RR CheY, the phosphatase CheZ, the methyl esterase CheB and the methyltransferase CheR (Fig. 1.7) in *E. coli*. In both ancient and modern literature, many times has been used the term chemotaxis referring to this flagellar-dependent pathway.

Although general features of chemotactic signalling appear to be conserved across bacteria and even archaea, studies of chemotaxis in species other than *E. coli* revealed diversity at several levels. This variety includes the exact composition of the signalling pathway, the number and specificities of chemoreceptors, and the details of the signal transduction<sup>141</sup>. For instance, in *E. coli* and in the most bacteria, attractants decrease HK activity of the chemotaxis system (Fig. 1.7)<sup>142</sup>, whereas in *B. subtilis* occurs the opposite.

Furthermore, *E. coli* possesses a single chemotaxis pathway with only one copy of each described cytoplasmic signalling protein. Nevertheless, most of the sequenced bacterial species have multiple chemotaxis gene copies in their genome<sup>143,144</sup>. Most of those additional pathways appear to control chemotaxis of swimming bacteria, although some of them regulate alternative cellular functions such as biofilm formation in *P. putida*<sup>145</sup> or productive infection in *Borrellia burgdorferi*<sup>146</sup>.

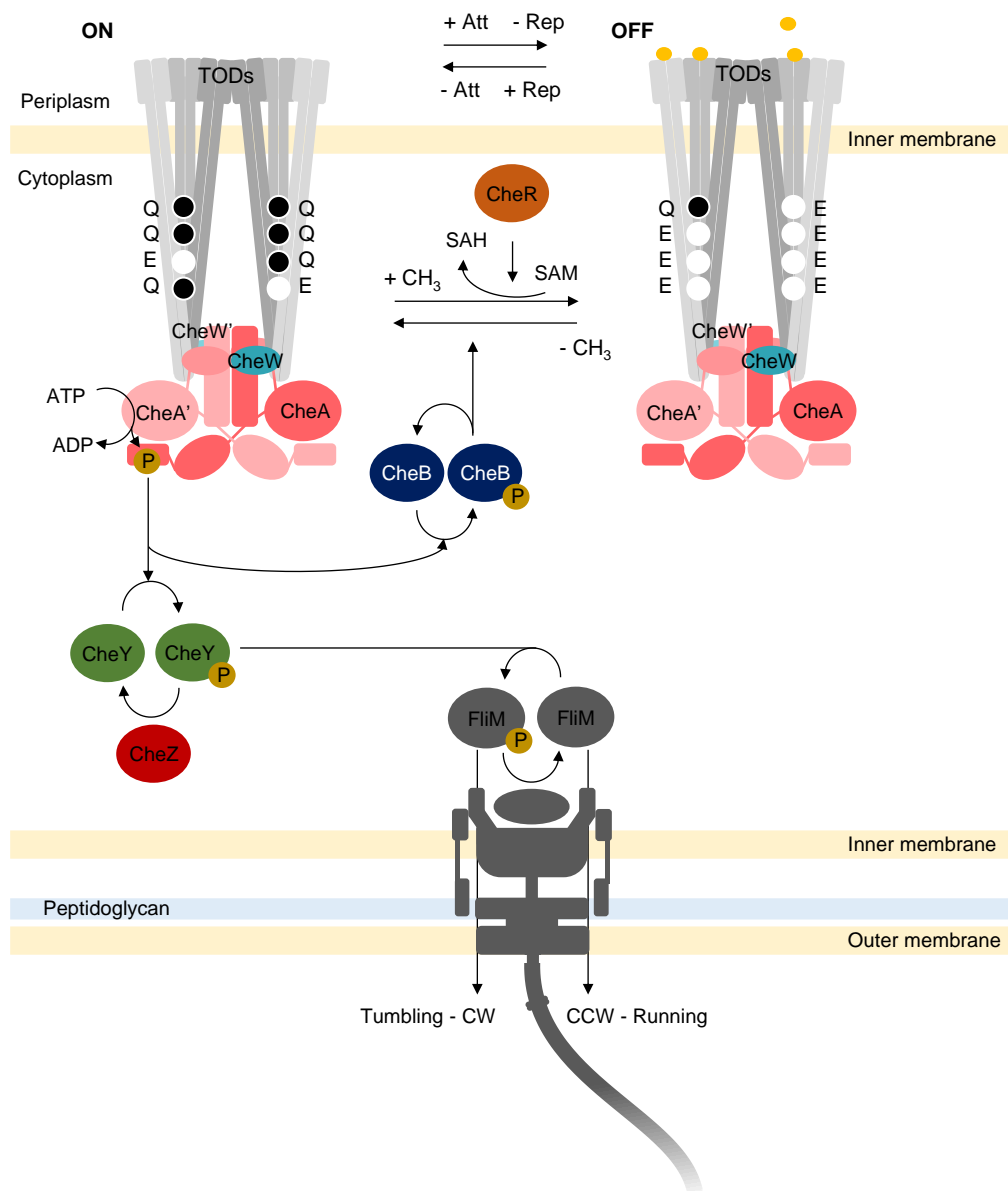


**Figure 1.7.** Chemotaxis pathway in *E. coli*, with its signal transduction and adaptation modules. (De) methylations (-CH<sub>3</sub>/+CH<sub>3</sub>) of trimers-of-dimers chemoreceptors (TODs) occur according to their activity state. Attractants (Att) favour OFF states and thus CCW motor rotation and cell runs; repellents (Rep) favour ON states, CW rotations and cell tumbles. Methylation in the glutamic acid residue (E) turns it in glutamine residue (Q) in the receptor helices. Inorganic phosphate is represented with a single P letter. The flagellar motor and the associate Che proteins (CheA, CheW, CheB, CheR, CheY and CheZ) are also represented. Phosphoryl groups are characterized by a yellow star. Adapted from Colin and Sourjik, 2017<sup>147</sup>.

#### 1.2.4.3.1. Methyl-accepting chemotaxis protein

The MCPs are the most common receptors in bacteria and archaea, and they are responsible for perceiving chemoeffectors, which include chemical (e.g., pH, osmolarity, concentration) and physical (e.g., contact, light, temperature, magnetic field) attractants and repellents<sup>148</sup>. For example, some MCPs function as photoreceptors and direct bacterial movement in response to light (exemplified by the phototaxis of halophilic marine archaea *Halobacterium salinarum*)<sup>149–151</sup>. MCPs are involved in the regulation of various aspects of cellular activities, including biofilm formation, flagellum biosynthesis<sup>152</sup>, the degradation of xenobiotic compounds<sup>153</sup>, the encysting, the formation of fruiting bodies<sup>152</sup> and the production of exopolysaccharides<sup>154</sup> and toxins<sup>155</sup>. Thus, play an important role in cell survival, biodegradation and pathogenesis in many bacteria including *P. aeruginosa*<sup>54</sup>, *Campylobacter jejuni*<sup>156</sup>, *Cronobacter sakazakii*<sup>157</sup> and *Vibrio cholerae*<sup>158</sup>.

Some typical chemoreceptors are embedded in the inner membrane of the cell, locating its N-terminal sensory domain on the periplasm face. This is where it receives the signal (with its ligand-binding domain, LBD), passes through HAMP (histidine kinase, adenyl cyclase, methyl-accepting chemotaxis protein and phosphatase) region, and then it is finally transmitted by its C-terminal signalling domain (SD) located in the cytoplasm. The SD domain interacts with the regulatory protein HK CheA, the receptor coupling protein CheW, the methyltransferase CheR and the methyl esterase CheB<sup>26,148</sup>. This domain also contains the different regions of methylation helices, flexible bundles and the signalling subdomain (SSD)<sup>148</sup>.

MCPs form homodimers and these also interact with each other to establish the final trimers-of-dimers structure<sup>148,159,160</sup>. In the form of homodimer, it can perform the functions of ligand binding, transmembrane signalling and adaptive modification, but unlike in the trimer-of-dimer form, it cannot control the kinase activation<sup>161</sup>.

Several studies show that the conformational signal induced by the binding of the attractant to the LBS brings a small slip (~2Å) similar to a piston in one of the

transmembrane helices of the MCP dimer, in the normal direction to the plane of the membrane<sup>148,162</sup>. This fact causes a twist towards the inside of the propeller so that it improves the stability of HAMP, causing this domain to tighten more and, consequently, that the packaging of the methylation subdomain becomes looser.

Signalling can occur in the opposite direction when the methylation subdomain contracts, so that HAMP is freer. Methylation happens in a glutamic acid residue (Glu, E), which it became in glutamine residue (Gln, Q), producing a neutral moiety and, therefore, the MCP itself have a greater mobility than the unmethylated forms. In this manner, the state of the signalling subdomain is controlled by the modulation of the packaging geometry of the methylation domain<sup>148,163</sup>.

In summary, ligand binding and adaptive modification move the signalling helix between its two piston positions, changing the balance between deactivated kinase (OFF) and activated kinase (ON)<sup>159</sup>.

MCPs are classified according to their LBD and membrane topology into four classes:

- **Class I.** Most MCPs in both bacteria and archaea, including the Tar, Tsr, Trg, and Tap receptors of *E. coli* (which sense aspartate, serine, ribose/galactose and peptides, respectively), have this sensory topology<sup>164</sup>. This class is the most common and, such as described above, it is characterized by the presence of those LBD region located in the periplasm, and the HAMP and SD in the cytoplasmic face.
- **Class II.** Unlike the previous one, it has the LBD region in the cytoplasm, like the rest of the components, all of them spatially close. Transmembrane helices anchor the complex in the membrane and separate the LBD from the rest at the amino acid sequence level. It is very rare in bacteria (3%) compared to the other classes of receptors. It is usually related to aerotaxis or signalling of the cellular redox state.
- **Class III.** It can have a variable number of transmembrane helices, with the LBD domain located within the membrane part (subclass III<sub>m</sub>), or in the

cytoplasm, after the last transmembrane helix (subclass IIIc), and followed by the HAMP and SD region cytoplasmic. This class is more common in archaea than in bacteria.

- **Class IV.** In this case, the LBD domain may or may not be identified, but it is characterized as being an entire cytoplasmic complex, therefore, it does not have transmembrane helices. Like the previous class, it is more represented in archaea than in bacteria<sup>148,165</sup>.

#### 1.2.4.3.2. Histidine kinase protein: CheA

CheA (Fig. 1.8) is the HK of this TCS and it is linked to a sensory unit that responds to changes in physical conditions by modulating its kinase activity. Most HKs are homodimers that use ATP to transphosphorylate a specific substrate histidine residue on the adjacent subunit within the dimer<sup>67</sup>. The dimeric CheA kinase has five domains per subunit: P1 contains the phosphorylatable His residue, P2 docks CheY and CheB for phosphotransfer from P1, P3 dimerizes the kinase, P4 binds ATP and transfers the  $\gamma$ -phosphate to P1 and finally, P5 binds to CheW and the receptor tip<sup>166</sup>.

Receptors in membranes are considered single dimers, dimers-of-dimers, trimers-of-dimers, and CheA- bound trimers of dimers, but only active CheA-bound trimers of dimers can phosphorylate CheY<sup>167</sup>. The kinase, which is up-regulated by either the repellent-occupied or empty receptor but is down-regulated by the attractant-occupied receptor, phosphorylates itself on a specific histidine sidechain<sup>168</sup>. The phosphoryl group is then transferred from histidine to a specific aspartyl residue on a RR domain that may be a separate protein or attached to the HK. Most common separate proteins are CheB and CheY, which are the second components of the system. These RRs, when phosphorylated, act directly to modify an effector, leading to a change in the cellular behaviour<sup>67,169</sup>.

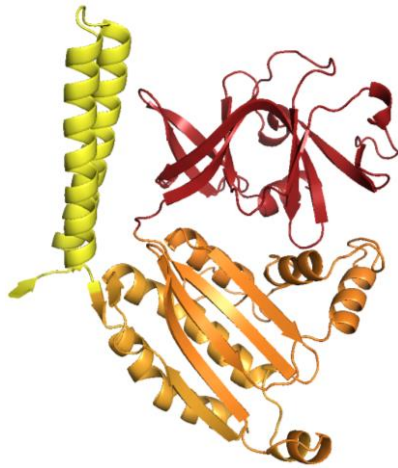


**Figure 1.8.** Structural model of P3- (yellow), P4- (orange) and P5- (red) CheA domains in *E. coli*. P1 and P2 domains are not represented because of its not well-defined structural model due the indeterminate regions between P1-P2 and P2-P3. From PDB: 6S1K.

#### 1.2.4.3.3. Coupling proteins: CheW and CheV

The coupling proteins in bacterial chemotaxis systems have a basic architecture in *E. coli*. CheW is a canonical chemotaxis coupling protein with two subdomains<sup>170,171</sup> (Fig. 1.9). Subdomain 1 is formed by the  $\beta 1$ ,  $\beta 2$  and  $\beta 8$ - $\beta 10$ , while subdomain 2 is formed by the  $\beta 3$ - $\beta 7$  strands<sup>169</sup>. The CheA-P5 subdomain and CheW subdomain 2 interact, allowing CheW bridges the chemoreceptors and CheA to form a stable core signalling complex<sup>147,169,171</sup>. The CheW functionality are so conserved that it has been shown that CheW from evolutionarily distant species can rescue a system with a *cheW* knockout, despite the low level of amino acid identity between the homologs<sup>172</sup>.

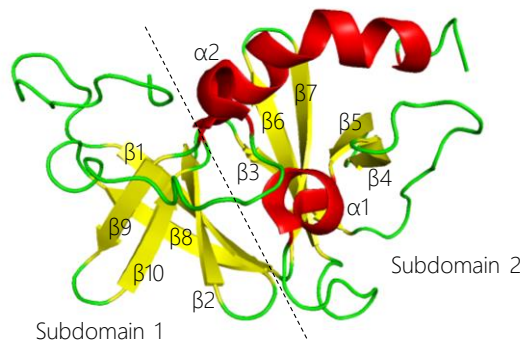


**Figure 1.9.** Protein structure of *E. coli* CheW. Dashed line defines the boundary between the two subdomains. The figure was generated using the program PyMOL. From PDB: 2H09.

In contrast, CheV is a hybrid protein with an N-terminal CheW-like domain fused to a C-terminal receiver domain that can be phosphorylated<sup>173</sup>. *E. coli* lacks CheV protein, however it is present in several other chemotactic enterobacteria (*Salmonella*, *Yersinia*, *Enterobacter*, *Erwinia*, and *Pectobacterium* species)<sup>144</sup>. The role of this protein in bacterial chemotaxis was examined in distantly related species *B. subtilis* and *Helicobacter pylori*, but it is still not well understood<sup>172</sup>. It is known that CheV is an additional adaptor for accommodating specific chemoreceptors within the chemotaxis signalling complex. Some results do not support the idea that CheV participates in the complex array as a part of the CheA-P5/CheW hexagonal ring. Indeed, when CheW lacks, chemoreceptors cannot assemble, thus CheV are unable to balance this deficiency. To explain that, two models have been proposed: CheV may occupies empty rings which does not interact with CheA-P5 or CheW (Fig. 1.10.A) or where CheV might be incorporated with CheW and CheA-P5 into the hexagonal ring (Fig. 1.10.B). In both models, CheV is considered as an accessory protein<sup>172</sup>.

The distribution of *cheW* in the genomes of completely sequenced bacteria and archaea is wider than that of *cheV*. However, in some Firmicutes species appear to only have a CheV coupling protein, such as *Bacillus* spp. and *Listeria* spp., which implies that CheV can completely substitute CheW in these bacteria<sup>174</sup>.

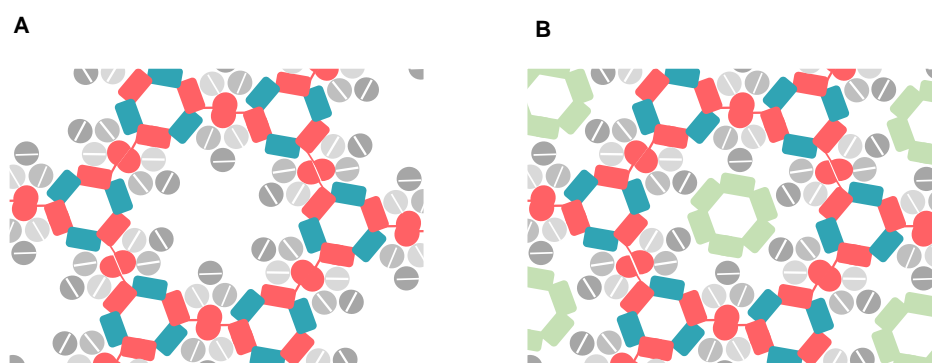


**Figure 1.10.** Schematic models of possible integration of CheV into the chemoreceptor array of *S. enterica*. Top-view of the two models (**A** and **B**) of chemotaxis component arrangement showing the interaction sites between chemoreceptor trimers (grey), CheA (pink) and CheW (cyan), as well as potential locations of CheV (green). Modified from Ortega and Zhulin, 2016<sup>172</sup>.



#### 1.2.4.3.4. Phosphotransfer protein: CheY

CheY is a monomeric globular protein and the chemotactic RR involved in the transmission of sensory signals from the chemoreceptors to the flagellar motors. As therefore mentioned, CheY is phosphorylated by CheA. Phosphorylated CheY (CheY-P) dissociates from the signalling complex and diffuses to the rotary motor where it docks and increases the probability of the CW motor rotation, thereby favouring the formation of the tumbling state. The steady state level of CheY-P thus serves as a diffusible tumble signal that controls the overall frequency of tumbling. This tumble signal is modulated by two opposing reactions: creation of CheY-P by the receptor-kinase complex, and destruction of CheY-P by hydrolysis of its acyl phosphate. CheZ speeds the latter hydrolysis reaction, acting as a phosphatase.

The change of rotation between CW and CCW is given spontaneously, which is increased by the concentration of CheY-P. CheY-P binds more closely than CheY to FliM and FliN, thus inducing the conformational cooperative change of the C ring responsible for switching the direction of flagellar motor switching<sup>175-178</sup>.

In short, repellents stimulate the HK activity and speed the production of CheY-P, whereas attractants inhibit the HK and slow CheY-P formation, thereby raising or lowering the steady state tumble signal, respectively<sup>147,148,168</sup>.

#### 1.2.4.3.5. Regulation: CheZ

CheZ is a monomeric protein, with a fibrous and a globular subdomains, which plays an important role in bacterial chemotaxis signal transduction pathway by accelerating the dephosphorylation of CheY-P.

Dephosphorylation of CheY-P mediated by the phosphatase CheZ enables rapid (sub-second) response to the environmental changes, and it further ensures that on the second timescale the level of CheY-P reflects the fraction of active CheA<sup>147</sup>. The process by which the cell recovers after being stimulated, while the stimulus is still

present, is essential because it allows responding to new stimuli in the presence of constant levels of chemoattractants or chemorepellents<sup>82</sup>.

It is important to highlight that relative levels of activity of CheA and CheZ in the chemotaxis pathway determine the basal behaviour of motile cells<sup>179</sup>. Whereas a basal levels of CheA and CheZ is defined in swimming cell, swimmers cells alter their physiology by increasing the levels of the CheZ phosphatase relative to those of other proteins in the chemotaxis pathway and thus, decreasing the level of tumble bias<sup>118</sup>.

#### 1.2.4.3.6. Adaptation: CheB, CheR and others

An important aspect of chemotaxis is adaptation, where cells respond only transiently to changes in attractants or repellent concentrations and return to their prestimulus random behavior<sup>180</sup>.

Adaptation in chemotaxis can follow one or various of the following described systems. The first system concerns receptor methylation, which can we observe in *E. coli*. Here, CheR is a constitutively expressed and activated methyltransferase which couples with phosphorylated CheB to reset the activity of CheA<sup>169</sup>. CheR methylates the conserved glutamate or deamidated glutamine residues from the helix methylation bundle subdomain (MH) of the chemoreceptors using S-adenosylmethionine as a cofactor. Elevated methylation results in inhibition of MCP signalling, which is the core adaptation mechanism. The activity of methyl esterase CheB is controlled by the levels of activated CheA: that phosphorylates and activates CheB. The activated CheB removes methyl groups from MCPs and thereby restores their signalling capacity. CheB and CheR act in coordination to allow the cell to modulate its stimulation level<sup>148</sup>. Hence, these antagonizing proteins ensure that the fraction of active and inactive receptors always returns to pre-stimulus levels<sup>179</sup>.

In other bacteria, different to *E. coli*, can also find up to two more adaptation systems. For instance, the second system, involves phosphorylation of CheV performed by CheA. Thus, CheV-P inhibit kinase activity by disrupting the coupling between the

receptors and CheA<sup>181</sup>. Finally, the third system includes CheC, CheD, FliY and CheY-P, where the cornerstone of this system is CheD. CheD is a receptor deamidase and activates the CheA kinase by binding to the receptors, and this binding is controlled by CheC, a CheY-P phosphatase, through a competitive binding mechanism. Moreover, CheY-P increases the affinity of CheD for CheC. The essence of this adaptation mechanism is that CheY-P controls CheD binding to the receptors through its interactions with CheC. When CheY-P levels are high, CheC is a better binding target for CheD than the receptors. The result is that CheA activity is decreased as less CheD is bound to the receptors. FliY is a multi-domain phosphatase protein, C-terminal domain of which is homologous to the FliN flagellar component of *E. coli* and the N-terminal domain to CheC. Its location is in the C ring, where it contributes in the dephosphorylation of CheY-P, as CheC<sup>142,182</sup>. These two last systems can be found in species such as *B. subtilis* and *Thermotoga maritima*<sup>181</sup>.

Other bacteria, such as *B. halodurans*, incorporate in its adaptation system another extra CheY-P phosphatase: CheX. It is more powerful phosphatase than CheC and FliY, and it is also the analogous protein of CheZ in *E. coli*. Its role in chemotaxis lies in forming homodimer and thereby, dephosphorylating CheY-P<sup>183</sup>. For *B. burgdorferi*, CheX is the unique CheY-P phosphatase, thus making it essential for its motility and chemotaxis<sup>184</sup>.

Certainly, any of these described adaptation systems enable the cell to navigate in gradients of signals (attractive or repellents) over a broad range of concentrations, ranging from nanomolar to millimolar<sup>185</sup>.

#### 1.2.4.4. Core signalling complexes and clusters

In *E. coli*, the core signalling complex is the minimal signalling functional unit which consists of two receptor trimer-of-dimers, a CheA kinase dimer, and two CheW molecules<sup>171,186</sup> (Fig. 1.11). Trimers can contain receptor dimers with different detection specificities that associate through interactions of conserved residues at the receptor

tip. In fact, reported results support the idea that a mixture of receptors enhances receptor-dependent stimulation of CheA<sup>187,188</sup>. CheW and P5 domain from CheA have homologous structures composed of two similar subdomains (subdomain 1 and subdomain 2). Both of them interact separately with the receptor tip and with each other through the subdomain 1 from P5-CheA to CheW subdomain 2 (interface 1)<sup>171</sup> (Fig. 1.12.A).

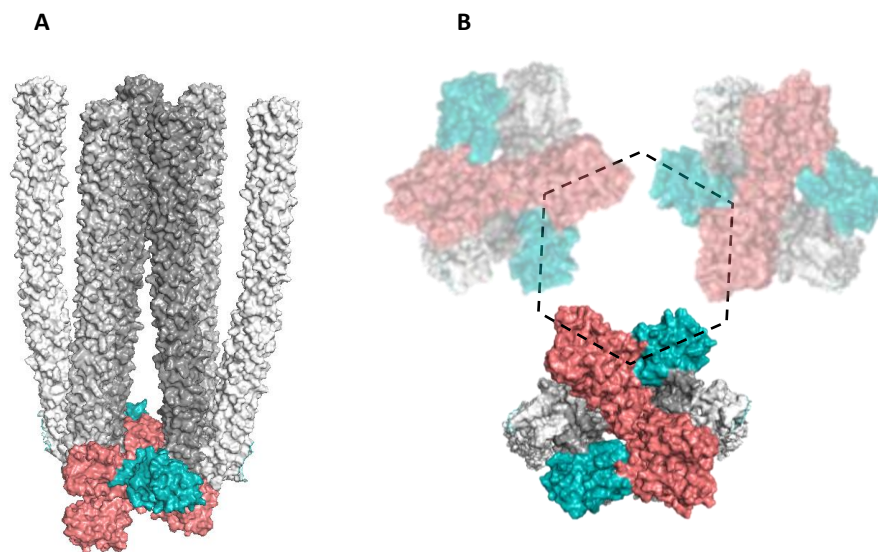


**Figure 1.11.** Structure of the chemotactic core signalling complex of *E. coli*. TODs are represented in grey scale, CheA in pink and CheW in blue. Proteins are shown with the sphere representation, both **(A)** side and **(B)** bottom views. The bottom position is amplified in respect to the side view, and a black dashed hexagon is added in order to better appreciate the hexagonal structure when three chemoreceptors are in array disposition. PyMOL program has been used to visualize and edit the protein structures. From PDB:6S1K.

In addition, the core signalling complex are able to further organize into a dense interconnected hexagonal signalling lattice (array) (Fig. 1.12.B) that localizes to the cell poles, forming the named clusters<sup>186,189</sup>. Cryo-EM and crystallography studies refined the structure of the *E. coli* chemosensory array and revealed that the interaction between CheW subdomain 1 and the P5 subdomain 1 of CheA (interface 2) is the structural key link between core signalling units in the array<sup>186,190-194</sup>. This array shows

interconnected core complexes organized around P5/CheW rings, producing this hexagonal arrangement of receptor trimers (Fig. 1.12B, C).

In addition to P5/CheW rings, six-member CheW rings link the receptor dimers that do not directly contact CheA or CheW in the core complexes<sup>194</sup>. Moreover, thanks to the presence of flexible hinges located in the HAMP domain, chemoreceptors can bind with themselves avoiding steric clashes between neighbouring receptors that would block the formation of core signalling complexes and chemoreceptor arrays<sup>195</sup>.

Arrayed chemoreceptors control multiple CheA molecules in highly cooperative responses to chemoeffector ligands, and the molecular interactions responsible for this behaviour have been studied<sup>171,196</sup>. Piñas *et al.* found that amino acid replacements affecting the interface 2 interaction cause severe array clustering defects and abolished response cooperativity. It means that interface 2 is the route for transmitting signalling related to conformational changes throughout the array<sup>171</sup>.

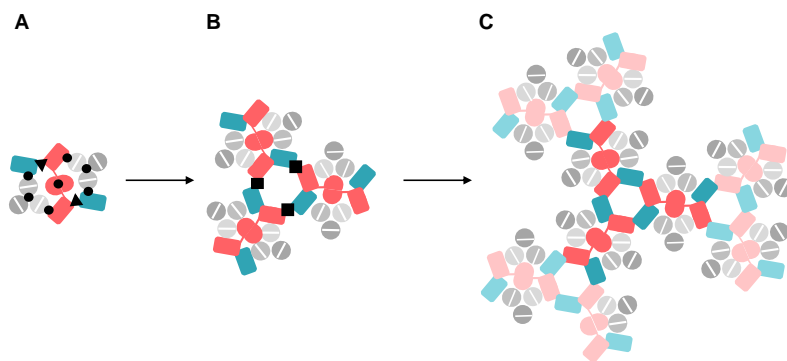


**Figure 1.12.** Structural organization of chemoreceptor arrays. **(A)** Cross-section through the receptor tip and CheA/CheW baseplate, viewed from the cytoplasmic membrane. Critical CheA-CheW interfaces responsible for core complex assembly and function are indicated with black symbols: CheA-P5-receptor, CheW-receptor, trimer contacts and P3-P3' with circles; P5 subdomain 2-CheW subdomain 1 (interface 1) with triangles. **(B)** A lattice unit of the receptor array where interface 2 interactions are symbolised with black squares. **(C)** An extended array showing interconnected core complexes organized around P5/CheW rings. Based on Piñas *et al.*, 2016<sup>171</sup>.

Frank *et al.* studied the behaviour of a prototypical interface 2 defect in adaptation-proficient cells to directly assess the contribution of receptor networking to stimulus signalling and gradient-tracking performance. They found that in a high-activity state, dispersed receptor complexes were more sensitive and less cooperative than their networked counterparts. However, in a low-activity state, such as is typical of adaptation-proficient cells, dispersed receptor complexes were less sensitive but faster than their networked counterparts<sup>196</sup>.

#### 1.2.4.5. Chemoreceptor cluster location

Chemoreceptor arrays have also been described in many different bacterial species such as *T. maritima*, *Listeria monocytogenes*, *Acetonebma longum*, *Borrelia burgdorferi*, *Treponema primitia*, *Caulobacter crescentus*, *Magnetospirillum magneticum*, *R. sphaeroides*, *V. cholerae*, *Halothiobacillus neapolitanus*, *Campylobacter jejuni*<sup>197</sup>, *S. enterica*, *B. subtilis*<sup>186</sup> and *H. hepaticus*<sup>186,197</sup>. *A. longum* and *B. burgdorferi* have typically subpolar arrays but inconsistently positioned, whereas all rest of species have a polar location<sup>197</sup>.

To move usefully through the environment, many specie cells need to be chemotactic<sup>198</sup>. Data suggests that being motile and chemotactic is a survival advantage for many bacteria. That is why daughter cells need to not only be flagellated, but also inherit a chemosensory array on division to respond to the local environment<sup>199</sup>. Thus, in new-divided *E. coli* cells are one or more chemosensory arrays, the largest of which localizes in the old pole. As the cell grows, arrays are formed in the new pole, as well as in the lateral membranes, whilst the pre-constructed polar clusters are positioned at the old poles of the daughter cells (Fig. 1.13).

Therefore, existing mechanisms to ensure that large arrays are inherited on division is critical. If the arrays are localised to only one cell pole before division, then the daughter cell will not inherit a chemosensory network and, thus, will be non-

chemotactic and unable to compete until a new array is expressed and assembled. If clusters are arbitrarily distributed, then causality dictates that a proportion of daughter cells will also not inherit a chemosensory network; therefore, both the numbers and positioning of chemosensory clusters must be controlled<sup>200,201</sup>.

Certainly, in some species with more than one chemosensory pathway show variation in positioning of the clusters reflecting the function of the different pathways. Hence, that above priority for the poles is not an innate attribute of the MCPs or the position of the flagella, as previously thought<sup>199</sup>.

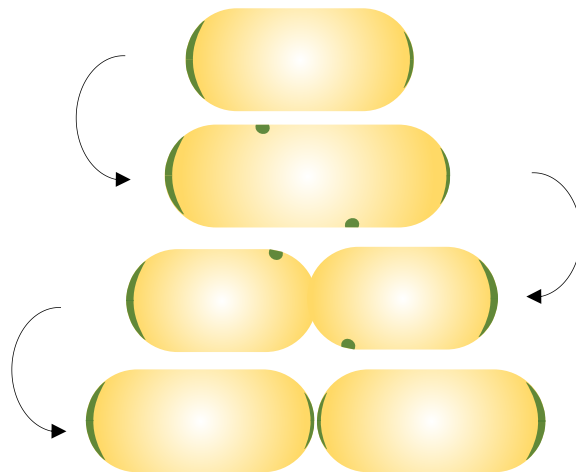


**Figure 1.13.** Cluster positioning during division. Adapted from Jones and Armitage, 2015<sup>199</sup>.

The lateral clusters distribution along the cell body are also poorly understood. They are distributed in a periodic manner, with the peak positions roughly corresponding to  $1/8$ ,  $1/4$ ,  $3/8$ ,  $1/2$ ,  $5/8$ ,  $3/4$ , and  $7/8$  of the distance between polar regions (Fig. 1.14). Many protein complexes in bacteria appear to localize along helical filaments, and it has been recently shown that receptors become inserted into the cytoplasmic membrane along the helically distributed Sec complexes<sup>202</sup>.

Nevertheless, Thiem *et al.* found that replication machinery and lateral clusters are anchored by the same structure<sup>200</sup>. Subsequently, two models have been proposed to explain these evidences. The first expound that the periodically distributed anchoring

sites can be created by the crossing of two helical structures with an opposite direction but the same pitch (Fig. 1.14.A). However, it is inconsistent with the observation that the replication machinery does not co-localise with the lateral clusters at a quarter of the cell length. The second model, in contrast, defends periodically positioned ring-like or short helical structures with the mode of a replisome movement (Fig. 1.14.B)<sup>202,203</sup>.

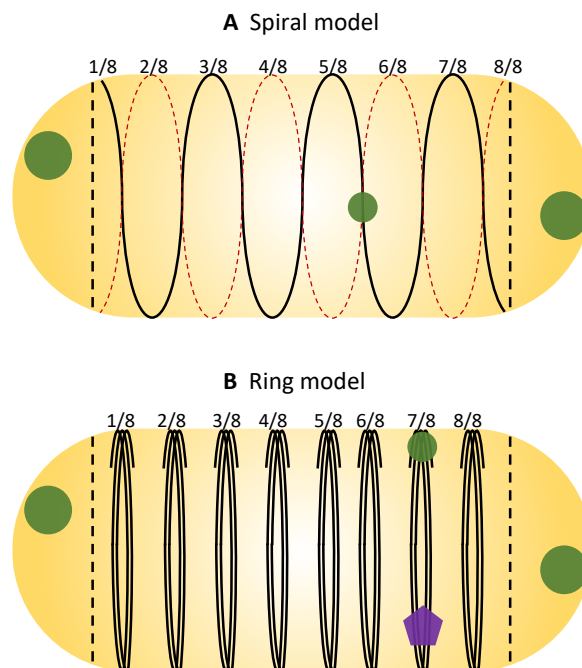


**Figure 1.14.** Models of chemoreceptor cluster positioning in *E. coli* cells. Two possible ways to generate periodic marks for cluster positioning along the cell axis: **A)** spiral and **B)** ring models. Receptor clusters are shown in green and the replisome in purple. Adapted from Thiem *et al.*, 2007<sup>200</sup>.

Some species, such as in *R. sphaeroides*, contain multiple homologues of MCPs and often include both transmembrane and cytoplasmic receptors<sup>144</sup>. In 2009, it was shown that its cytoplasmic chemoreceptors form trimers of dimers packed hexagonally into large cytoplasmic arrays with the same spacing as transmembrane clusters<sup>197,204</sup>. Transmembrane receptors are positioned in a pattern similar to *E. coli*, with predominantly polar clusters and some smaller lateral clusters. Besides, in



transmembrane arrays, the LBDs are positioned in the periplasm arranged in just one layer.

However, the cytoplasmic chemoreceptors arrange themselves in a two-layer sandwich-like structure, where LBDs are located in the middle of the sandwich<sup>197,199</sup>. This configuration does not inhibit access to signalling molecules because the receptor arrangement is much more porous than the outer membrane for which extracellular ligands need to cross in order to be detected by the transmembrane arrays<sup>197,204</sup>. The signalling implications of this arrangement remain unclear, but it is intriguing to think that ligand binding in the middle of the sandwich could result in CheA activation in both baseplates, facilitating signal amplification<sup>205</sup>.

Clusters of soluble receptors are located approximately in the middle of the cell body. So how do the two daughter cells inherit this cytoplasmic cluster? An additional cluster is formed as the cell cycle progresses and the two clusters are placed at  $\frac{1}{4}$  and  $\frac{3}{4}$  positions, such that each daughter cell inherits one cluster at the middle on division<sup>199</sup>.

### 1.3. Flagella-mediated chemotaxis in virulence and pathogenesis

As mentioned before, another important implication of chemotaxis is that it also plays a decisive role in infection and disease. Chemotaxis signalling pathways are broadly distributed across a variety of pathogenic bacteria<sup>39</sup>. Furthermore, several studies indicate that chemotaxis is essential for the initial stages of infection by different human, animal and plant bacterial pathogens. Some studies reveals that in many bacteria such as *P. aeruginosa*, *P. syringae* and *S. enterica*, gene deficiencies in components of the cytosolic *che* pathway, significantly reduces the colonization of host animal and plant tissues<sup>39</sup>. As if that were not enough, unforeseen links between chemotaxis regulators, a pore forming toxin phobalysin and the association of the marine bacterium *Photobacterium damsela* with target cells were revealed in 2018<sup>206</sup>.

### 1.3.1. Chemoreceptors to sense animal and plant molecules

Other studies have succeeded in identifying physiologically relevant signals and corresponding chemoreceptors which senses chemoeffectors that are associated with pathogenicity-relevant chemotaxis. Many of the identified chemoeffectors serve as nitrogen and/or carbon sources for growth or as electron acceptors for metabolism as we have seen before (sugars, amino- and organic acids, dipeptides, aromatic and aliphatic hydrocarbons, nucleotide bases, polyamines and oxygen)<sup>54</sup>, but also plant hormones<sup>207</sup>, inorganic phosphate<sup>208</sup>, metal ions<sup>209</sup>, neurotransmitters<sup>210</sup> and quorum-sensing signals<sup>211</sup>.

For instance, the major causative agent in peptic ulcer disease, *H. pylori*, survives poorly in the lumen of the stomach and must rapidly colonise the gastric epithelial surface in flagella- and chemotaxis-dependent manner. It possesses chemoreceptors to taxis arginine, bicarbonate and pH<sup>212,213</sup> and even metabolites emanating from the human gastric epithelium such as urea<sup>213</sup>. Another example is the case of the most aggressive soil-borne plant pathogen, *Ralstonia solanacearum*. It shows chemotactic response to L-malate and tomato root exudate. Additionally, *R. solanacearum* has two aerotaxis chemoreceptors which its absence impairs the capacity of the bacterium to rapidly localise and colonise tomato roots<sup>214</sup>.

Despite the importance of chemoreceptors in virulence of both animal and plant tissues, the observed abundance of chemosensory signalling and chemoreceptor genes in plant pathogens is superior to that of animal/human bacterial pathogens<sup>39</sup>. In Matilla and Krell, 2018<sup>39</sup> review data relevant to the chemotaxis in other animal, human and plant pathogens, providing information of the bacterial chemoreceptors that appear to be involved in the detection of pathogenicity-associated signal molecules.

### 1.3.2. Biofilm production linked to chemotaxis

Both chemotaxis and biofilm formation are survival strategies that allow microorganisms to successfully find and live in surface environments. Biofilm

production, a virulence-related process of cell attachment and growing in aggregates on surfaces, is a regulated process that has been extensively investigated in model organisms, such as in *Pseudomonas* species<sup>215</sup>. *P. aeruginosa* responds to growth on surfaces by activating the Wsp chemosensory system (Fig. 1.15). This pathway controls the production of the c-di-GMP, which decreases expression of flagellar genes and promotes biofilm formation. As the Chp chemosensory system, the Wsp complex forms a signal transduction arrangement homologous to the Che system. Here, mechanical pressure associated with surface growth activates WspA protein (the MCP homologue), which promotes the autophosphorylation of WspE (the CheA homologue). WspE phosphorylates two RRs, the methyltransferase, WspF, and the diguanylate cyclase, WspR (CheB and CheY homologues, respectively)<sup>42</sup>.

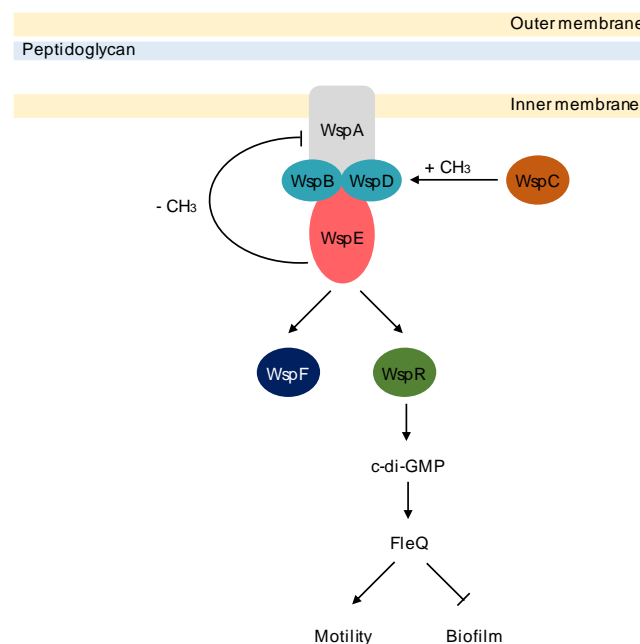


**Figure 1.15.** The Wsp chemosensory pathway of *P. aeruginosa*. Adapted from Francis *et al.*, 2017<sup>42</sup>.

When WspR-P aggregates to form cytoplasmic clusters, where its diguanylate cyclase activity is increased and, thereby, also the production of c-di-GMP. Meanwhile, WspF-P acts to reset the system by removing methyl groups from WspA, thus reducing its

ability to activate WspE. The increasing levels of c-di-GMP inhibits the transcriptional factor FleQ. FleQ promotes flagellar genes and downregulates biofilm-associated genes, but constrained by the binding of c-di-GMP, biofilm formation is upgraded. At one, the system is adapted by the constitutive methyltransferase activity of WspC, the opposed to the methylesterase activity of WspF<sup>42,216</sup>.

Similarly, in the genome of the promising organism for bioremediation *Comamonas testosteroni*, contains one chemotaxis-like (*flm*) gene cluster and nineteen chemoreceptor genes<sup>217</sup>. Studies in this Wsp homolog pathway revealed that not only chemoreceptors from chemotaxis and biofilm formation pathways can be exchanged between the two pathways, but also the CheA protein can phosphorylate FlmD (the WspR in *C. testosteroni*), in addition to CheY. This demonstrates a cross-talk which involves in the coordination of these two types of cell behaviour, chemotaxis and biofilm formation<sup>218</sup>. It has also been observed in the phytopathogen *Xanthomonas citri*<sup>219</sup>. Moreira *et al.*, theorizes that flagellar movements of *X. citri* could trigger swimming, favouring a possible shift to the interior of the plant, or swarming type, which would initiate the process of formation of mature biofilm from planktonic cells, giving way to hyperplasia and necrosis on the plant tissue<sup>219</sup> (Fig. 1.16). This theory could also be extended to bacterial colonization of other hosts and their tissues.

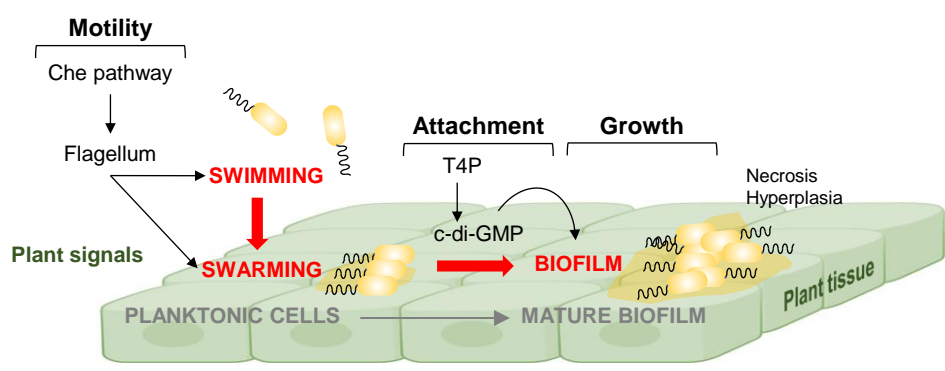


**Figure 1.16.** Steps involved in colonization and biofilm formation in *X. citri* process. Distinct signs of the plant could enable flagellar movements until the formation of mature biofilm. Adapted from Moreira *et al.*, 2015<sup>219</sup>.

#### 1.4. *Salmonella enterica* serovar Typhimurium

In the present work, *S. Typhimurium* was selected as Gram-negative temperate swarmer and chemotactic model organism for the study of swarming and chemotaxis behaviours.

This non-spore-forming and rod-shaped microorganism ranges in diameter from around 0.7 to 1.5  $\mu\text{m}$ , with a length of 2 to 5  $\mu\text{m}$ . The cells are facultative anaerobes and show predominantly peritrichous motility. This genus refers to primary intracellular pathogens leading to different clinical manifestations in the development of infection in humans<sup>220</sup>. It proliferates by cell division each 40 minutes at 37°C. This temperature is its optimal temperature for grow, but it also can do it at a wide range of temperatures, from 6 to 46°C<sup>221</sup>.

*S. enterica* is the most frequently reported cause of foodborne illness throughout the world. In fact, the economic costs due foodborne diseases caused by *Salmonella* spp. from 2013 to 2018 were \$475,579,129 in EEUU<sup>222</sup>. The bacteria are generally transmitted to humans through consumption of contaminated food of animal origin, mainly meat, poultry, eggs and milk. Its impact is so important as to research and find new therapeutic targets for this microorganism, and chemotaxis may be one of them.

Its identification in the clinical laboratory is performed by the growth of stool samples on different solid media. Plates are examined after 24 h of growth at 37°C based on the macroscopic characteristics, generally using MacConkey agar plates in which *Salmonella* colonies are colourless due to the lack of lactose fermentation. However, other solid selective media, such as *Salmonella-Shigella* agar (SS), xylose-lysine-deoxycholate agar (XLD), and hektoen enteric agar plates (HE), are used for more specific isolation and identification. Hydrogen sulfide production, a metabolic trait characteristic of this genus, is shown by colonies with black point in the middle in these three types of selective media<sup>220</sup>.

### 1.4.1. Classification

The genus *Salmonella* is classified inside the  $\gamma$ -proteobacteria class and belongs to the *Enterobacteriaceae* family. This genus name was erected by J. Lignières in 1901, in honour of the veterinary pathologist D. Salmon, who discovered what would be later known as the first *Salmonella* specie (*Salmonella enterica* var. *choleraesuis*) in 1885<sup>223</sup>. According to the Centers for Disease Control and Prevention (CDC), the genus *Salmonella* is further subdivided into two species, *bongori* and *enterica*. The last specie is also divided into five main recognized subspecies that are: *enterica* (serotype I), *salamae* (II), *arizonae* (IIIa), *diarizonae* (IIIb), *houtenae* (IV) and *indica* (V)<sup>224</sup>.

### 1.4.2. Pathogenesis

The two major clinical syndromes caused by *Salmonella* infection in humans are enteric or typhoid fever and colitis/diarrheal disease. Enteric fever is a systemic invasive illness caused by the exclusively human pathogens *S. enterica* serovar Typhi and *S. enterica* serovar Paratyphi A and B<sup>225,226</sup>. The symptoms of *Salmonella* infection usually appear 12-72 hours after infection, and include fever, abdominal pain, diarrhoea, nausea and sometimes vomiting. The illness usually lasts 4-7 days, and most people recover without treatment. However, in the very young and the elderly people, and in cases when bacteremia is present, antibiotherapy may be needed<sup>227</sup>. Without treatment, the mortality is 10 to 15%<sup>228</sup>, decreasing to <1% among patients treated with the appropriate antibiotics<sup>225</sup>.

In contrast to typhoid fever, which is common in the developing world, the non-typhoidal *Salmonella* (NTS) occurs worldwide in humans and can, in addition, infect a wide range of animal hosts<sup>229</sup>. Interestingly, various non-typhoidal serovars have more potential to cause extraintestinal infections than others, such as Typhimurium, Dublin and Choleraesuis<sup>226</sup>.

*S. Typhimurium* infection usually occurs by ingestion of contaminated food or water by the faecal-oral route. The acidic pH of the stomach represents a significant initial

barrier to infect the host. To protect itself against severe acid shock, *S. Typhimurium* activates the acid tolerance response, which provides an inducible pH-homeostatic function to promote survival in these host environments<sup>226,228</sup>. To overcome this infective step in humans, it implies a minimum cell number to trigger the disease, being the lowest dose causing illness about  $2 \times 10^9$  microorganisms<sup>230</sup>.

After entering the small bowel, *Salmonella* must reach and cross the intestinal mucus layer before encountering and adhering to intestinal epithelial cells. *Salmonella* uses flagella to move to the proximity of the intestinal epithelial cells, or to aid cells escape from macrophages<sup>231,232</sup>. Besides, the expression of several fimbriae contributes to their ability to bind the extracellular matrix glycoprotein laminin and mediate adhesion to the host cell<sup>226,228</sup>. Then, the invasion process appears because of translocation mediated by type III secretion system 1 (T3SS-1), a virulence factor encoded by *Salmonella* pathogenicity island 1 (SPI1)<sup>233</sup>. It causes a cytoskeletal rearrangement and leads the formation of membrane ruffles that engulf adherent bacteria in large vesicles called *Salmonella*-containing vacuoles (SCV), the only intracellular compartment in which *Salmonella* cells survive and replicate in the cytoplasm<sup>234</sup> of the M-cells covering Peyer's patches<sup>235</sup>. Moreover, these SCVs inhibit intracellular trafficking by blocking their fusion with lysosomes<sup>236</sup>. Once inside, the second type III secretion system 2 (T3SS-2) is expressed in order to secrete proteins that prevent the production of reactive oxygen species and enables *Salmonella* to survive inside non-phagocytic epithelial cells and, once across the intestinal epithelium, in macrophages<sup>220,233</sup>. This transfer to basolateral side through an exocytosis process leads the bacteria remain in the interstitial space of the *lamina propria* and be randomly phagocyted by the neutrophils, macrophages, or dendritic cells<sup>237</sup>.

Infected phagocytes, predominantly macrophages, migrates and facilitates systemic dissemination of the bacteria to lymph nodes and to extraintestinal tissues via the bloodstream<sup>220</sup>, such as the spleen and liver<sup>238</sup>. Alternatively, direct blood access of *Salmonella*-infected phagocytes from the basolateral side of the intestine has also

been suggested to contribute to systemic dissemination. Either way, the pathogen dissemination renders a systemic infection into the host<sup>239</sup>.

### 1.4.3. Antimicrobial treatment and resistance

For gastroenteritis from NTS infections and other bacteria or viruses, treatment of fluid and electrolyte imbalances by oral or intravenous rehydration is necessary when fluid loss is substantial<sup>240</sup>. In NTS type of disease, the symptoms usually last between 5 and 7 days and resolve spontaneously. Antimicrobial therapy is indicated only for patients who are severely ill, when positive signs of invasive disease have been detected, and for patients with risk factors (such as immunocompromised, children under 5 years old and elder people). However, there is controversy about the efficacy of antibiotics in decreasing either the duration of illness or the severity of symptoms and usually, 3 to 7 days of treatment is reasonable<sup>220,241</sup>. In healthy people with *Salmonella* infection, antibiotics generally do not shorten the duration of illness, diarrhoea, or fever. Unnecessary antibiotic use also contributes to antibiotic resistance, *Salmonella* carriage and disturbance of the microbiome<sup>242</sup>. Efficient therapies include treatment with fluoroquinolones, trimethoprim-sulfamethoxazole, ampicillin, or expanded-spectrum cephalosporins (e.g., ceftriaxone or cefixime) and can usually be successfully completed within 10 to 14 days of therapy<sup>220</sup>.

However, multi-drug resistance (MDR) can be particularly high among *S. Typhimurium* isolates (see examples in USA in Table 1.3). Spread of this MDR phenotype is supported by dissemination of dominant resistant clones, such as definitive phage type DT104, which carries several chromosomally located genes conferring the ACSSuT resistance type (resistance to ampicillin, chloramphenicol, streptomycin, sulfonamides, and tetracycline). On the other hand, dissemination of strains carrying hybrid plasmids is a potential problem. ACSSuT resistance *Salmonella* have already been detected in Spain and the United Kingdom<sup>243</sup>. These facts compromise the use of these drugs and it is a serious public health issue. As a result, use of a third-



generation cephalosporin or fluoroquinolone is reasonable if susceptibilities are unknown. Unfortunately, in line with these therapeutic strategies, an increasing rate of resistance has been observed, not only to nalidixic acid but also to expanded-spectrum cephalosporins, which are also widely used in the clinical setting<sup>220,243,244</sup>.

**Table 1.3.** Percentage resistant registered in 2018 in USA towards most common antibiotics in all nontyphoidal and Typhimurium salmonellae<sup>245</sup>.

| Antibiotic                   | Percentage resistant (%) |                       |
|------------------------------|--------------------------|-----------------------|
|                              | NTS                      | <i>S. Typhimurium</i> |
| Amoxicilin-clavulanic acid   | 2.5                      | 6.9                   |
| Ampicillin                   | 8.6                      | 17.3                  |
| Azithromycin                 | 0.8                      | 0.3                   |
| Cefoxitin                    | 2.4                      | 6.5                   |
| Ceftriaxone                  | 3.5                      | 7.2                   |
| Chloramphenicol              | 4.7                      | 13.4                  |
| Ciprofloxacin                | 0.6                      | 0.0                   |
| Gentamicin                   | 1.1                      | 1.0                   |
| Meropenem                    | 0.0                      | 0.0                   |
| Nalidixic acid               | 6.8                      | 2.3                   |
| Streptomycin                 | 11.2                     | 19.3                  |
| Sulfameth/sulfiz             | 9.5                      | 19.0                  |
| Tetracycline                 | 12.1                     | 18.0                  |
| Trimetoprim-suldamethoxazole | 2.7                      | 1.1                   |

#### 1.4.4. Flagella-mediated chemotaxis and motility in *Salmonella*

The chemotaxis pathway of *Salmonella* is identical to *E. coli* except for the presence of CheV. As mentioned, it is known that the chemotaxis system, but not chemotaxis, is essential for swarming, and it also occurs in *S. Typhimurium*<sup>116</sup>. Furthermore, studies in *S. Typhimurium* reveal that RecA protein plays a role in the chemotactic response and chemoreceptor clustering of this bacteria. Concretely, the increase in the concentration of the RecA protein, generated by the SOS system activation, impairs chemoreceptor polar cluster formation and also reversibly inhibits swarming motility<sup>246,247</sup>. But, what are RecA and the SOS system?

#### 1.4.4.1. The SOS System

In order to survive in various environmental conditions, bacterial cells have a collection of genetically controlled networks such as the SOS response, an inducible DNA repair system that allows bacteria to persist after massive DNA damage. The importance of the SOS response is underscored by the observation that this system is widely present in the Bacteria domain, reflecting the need for all living cells to maintain the integrity of their genome<sup>248,249</sup>.

This system is activated when, after UV irradiation or the presence of any other DNA damage inductor, DNA breaks and the concentration of single-stranded DNA (ssDNA) increases inside the cell. When the amount of detected damage is low, DNA repair is basically done by homologous recombination. For this, RecA, a ubiquitous protein which specifically binds to this ssDNA, forms a nucleoprotein complex. This RecA filament catalyses ATP-driven homologous pairing and strand exchange of DNA molecules necessary for DNA recombinational repair and DNA Pol I fills the derived gaps<sup>250</sup>.

Instead, at higher amounts of ssDNA, SOS system is activated. Initially, when DNA lesions occur, the ssDNA originated from double-strand breaks (Fig. 1.17.A) is encased by RecA which binds to this ssDNA (Fig. 1.17.B), prompting the nucleofilamentation (Fig. 1.17.C). Filament formation requires ATP binding, but not ATP hydrolysis. When ATP is hydrolysed, it causes filament disassembly, also in the 5' to 3' direction, generating activated RecA (RecA\*)<sup>251</sup> (Fig. 1.17.D). The principal role of this RecA\* lies in LexA protein autocatalytic cleavage reaction (Fig. 1.17.E). The autocleavage is performed near the middle of the protein, at a specific Ala84-Gly85 bond in *E. coli*<sup>252</sup>. Furthermore, LexA autocleavage is induced proportionally to intracellular RecA\* presence and, as a result, the pool of non-cleaved LexA protein begins to decrease, leading to de-repression of SOS genes which includes at least 43 known genes in *E. coli*, such as *recA*<sup>251,253</sup> (Fig. 1.17.F).

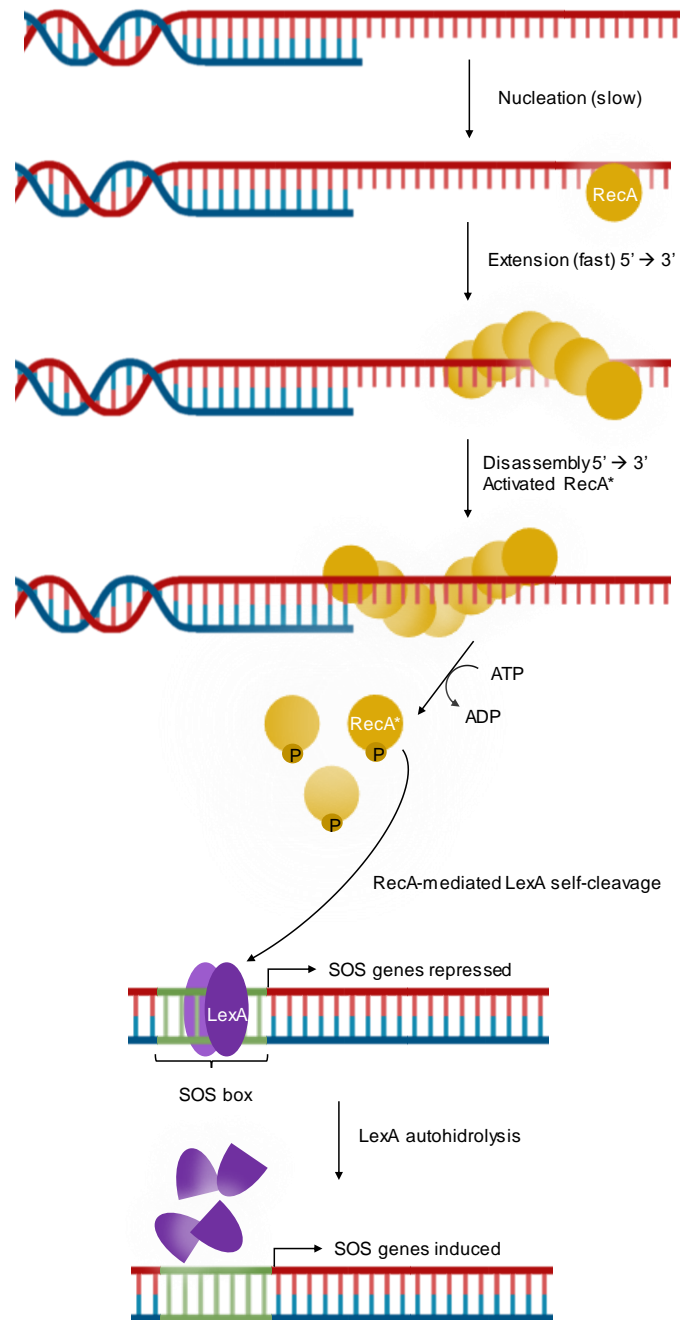


**Figure 1.17.** Schematized SOS induction process. Inorganic phosphate is represented with a single P letter. Adapted from Patel *et al.*, 2010 and Maslowska *et al.*, 2019<sup>251,253</sup>.

Some other activated SOS genes are *umuDC* (DNA Pol V), *polB* (DNA Pol II) and *dinP* (DNA Pol IV), polymerases with a rapid but low fidelity of copy ability. In the early phase of SOS, the first genes induced are the *uvr* genes for excision of damaged

nucleotides, followed by *recA* and other homologous recombination protein coding genes (*ruvAB*, *recN*). Next are *polB* and *dinB* encoding DNA polymerase II and DNA polymerase IV, respectively. The division inhibitor Sula is also induced to give the bacterium time to complete the repairs before the cell division. Finally, if the damage was extensive and not fully repaired, the error-prone DNA polymerase V (encoded by *umuC* and *umuD* genes) is induced, causing elevated mutation levels but allowing DNA replication and thus, cell survival. Importantly, *lexA* itself is also a SOS gene. The constant production of LexA during the SOS process ensures that as soon as DNA repair occurs and ssDNA decreases inside the cell, the disappearance of the inducing signal will allow LexA to reaccumulate and repress again the SOS genes<sup>253-256</sup>.

In summary, the call of the SOS response helps the cell to create a checkpoint, stops replication and allows time to repair DNA lesions and continue living at the expense of the generation of extra mutations. Beyond being a solid model of a DNA repair system, the SOS response has played an important role in shaping the bacterial world as we know it today.

Several research studies correlate this system and the induction of resistance to antibiotics. Diverse works agree that sublethal concentrations of certain SOS-inducing antibiotics induced resistance to other unrelated antibiotics<sup>257-260</sup>. These and other related works have caught their attention in whether SOS inhibitors could block emergence of antibiotic resistance<sup>261</sup>. Interestingly, it has been reported in laboratories of Buffalo University that zinc blockade of SOS response inhibits horizontal transfer of antibiotic resistance genes in enteric bacteria<sup>262</sup>.

#### 1.4.4.2. The RecA protein

RecA family is a plenty conserved group of recombinase proteins which are found in essentially all bacteria. Therefore, *recA* acts as a phylogenetic marker for molecular systematic studies of bacteria<sup>263-265</sup>. Not only is important in bacteria, but also this protein has homologs in mammals, such as Rad51 and Dmc1<sup>266,267</sup>. The gene encoding

*recA* was first shown in 1965 to be essential for genetic recombination and resistance to ultraviolet irradiation<sup>268</sup>. Due to its importance, the full understanding of RecA protein has been crucial since its discovering and many super resolution structures have been resolved by electron microscopy, NMR and X-ray in its monomer and filament form<sup>269–271</sup>.

RecA is an oligomeric protein with a molecular mass of 38 KDa in *E. coli*. Structurally, the RecA monomer consists of mainly three domains (Fig. 1.18):

- The 30-residue N-terminal  $\alpha$ -helix and short  $\beta$ -strand motif<sup>250</sup>. The N-terminal domain is involved in monomer-monomer interactions<sup>272</sup>. Mutations within this domain exhibited defects in the formation of free protein oligomers, but not DNA-RecA complexes<sup>273</sup>.
- The 240-residue  $\alpha/\beta$  ATPase core<sup>250</sup>. This part makes this protein an allosteric enzyme, whereas the conformation stabilized by the binding of ATP has a higher affinity for DNA than the apo-protein form<sup>274</sup>.
- The 89-residue globular domain at the C-terminal. It binds to ssDNA using its ATPase core<sup>250</sup>. The last 25 residues are not visible in the electron density map and they are presumably disordered<sup>275</sup> but, interestingly, exhibits a preponderance of negatively charged amino acids neutralized by bound magnesium ions in solution, important for the conformation change, and/or to the hydrolysis of ATP in the new conformation<sup>276</sup>.

RecA is a multi-functional protein that combines several roles. Aside from being a protease protein<sup>252</sup> and the prototypical recombinase, having its responsibility for search and strand exchange of homologous DNA during double-strand break repair<sup>277</sup>, RecA is associated with the cell membrane forming filaments bundles because of its binding to the anionic phospholipids<sup>278</sup>.

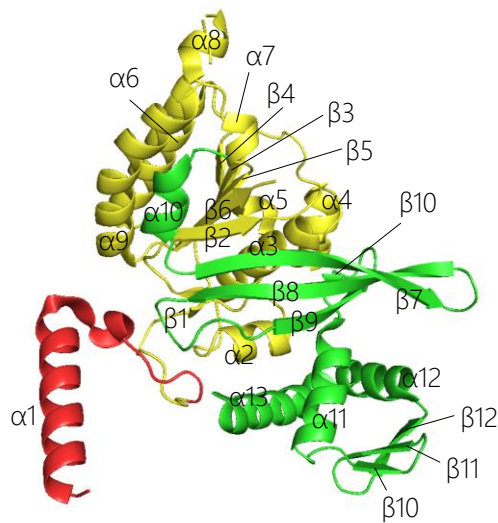


**Figure 1.18.** RecA ternary structure of *E. coli*. Monomer-monomer interaction domain is represented in red,  $\alpha/\beta$  ATPase core in yellow and the globular domain in green. From PDB: 2REB.

Recently, an additional conferred function into RecA is its relationship with motility. As aforementioned, the ability of *E. coli* cells to develop swarming migration on semisolid surfaces was suppressed in the absence of RecA. However, swimming motility was not affected<sup>279</sup>. Likewise, protein interaction network experiments in *E. coli* revealed a direct physical interaction between the RecA and the CheW protein<sup>279,280</sup>. Similarly, it has also been observed direct interaction between RecA and the CheW-like required for surface-associated motility of *A. baumannii*<sup>281</sup>. In the case of *S. Typhimurium* it has been described that SOS response plays a critical role in the prevention of DNA damage by abolishing bacterial cell swarming in the presence of a genotoxic compound<sup>282</sup>.

#### 1.4.4.3. Relationship between the SOS system and chemoreceptor clustering

Despite the non-canonical role played by the RecA protein, swarming modulation activity is exclusively dependent on this protein and not the SOS machinery itself. Even more, none of the yet known RecA activities, i.e., SOS response activation,

recombinational DNA repair, or genetic recombination, seem to be necessary for the control of swarming motility<sup>246</sup>. Moreover, RecA is needed for standard flagellar rotation switching, implying its essential role not only in swarming motility but also in the normal chemotactic response of *S. Typhimurium*<sup>247</sup>.

Previous work demonstrates the direct interaction between RecA and the CheW coupling protein<sup>247,283</sup> (Fig. 1.19).

Moreover, it was found that the molecular balance between RecA and CheW proteins is crucial to allow polar cluster formation in *S. enterica* cells. These results suggested that bacterial populations moving over surfaces make use of specific mechanisms to avoid contact with DNA-damaging compounds<sup>246</sup> (Fig. 1.20).

All presented data appoint out that the RecA molecule might form part of the chemosensory array and a physiological reason was planted. However, further work is needed to elucidate how RecA form parts of this complexes and its role in the modulation of swarming.

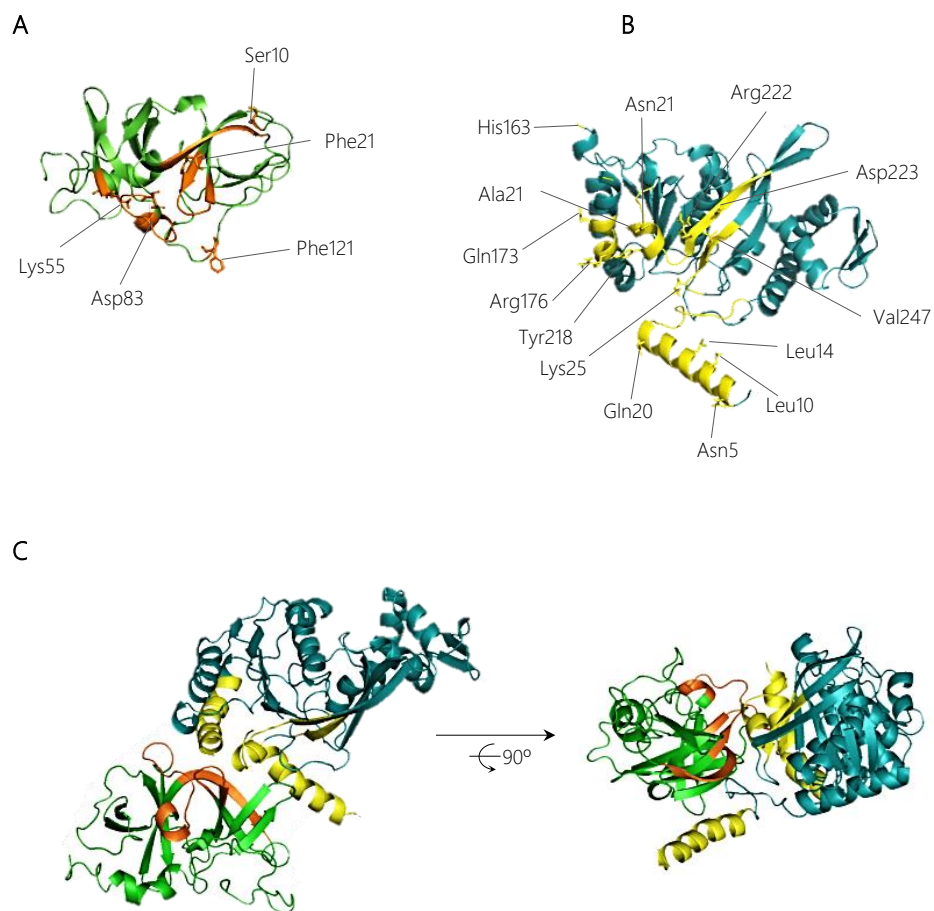


**Figure 1.19.** *In silico* model for the interaction of *S. enterica* RecA and CheW proteins. The predicted tertiary structures of CheW (**A**) and RecA (**B**) proteins are shown. The putative interface of RecA and CheW involved in the reciprocal interaction of the two proteins is highlighted in yellow and orange, respectively. The residues selected for site-directed mutagenesis and their locations are also indicated. (**C**) Ribbon diagrams of one of the highest-scoring models generated for RecA-CheW pair formation analyzed in this study. The two views of the interaction are rotated 90° about the x-axis. From Irazoki *et al.*, 2016<sup>283</sup>.





# 2 OBJECTIVES



## 2. Objectives

The objective of the present work is to elucidate how RecA is involved in the structuration and function of the chemoreceptor signalling complexes at molecular level in *S. enterica*.

The evidence of RecA and CheW interaction which were previously described<sup>247,283</sup> open the door to think the following questions: "If P5-CheA domain is CheW-like<sup>171</sup>, is there also an interaction of RecA with CheA?". If there is interaction between these proteins, which is the purpose? The absence or the overexpression of RecA abolishes the formation of chemoreceptor arrays and the swarming motility<sup>246,247</sup>. Why does it occur?

To answer these questions, the main objectives that are proposed are to:

- I. Determine the molecular interaction between the recombinase RecA and the chemotaxis component CheA.
- II. Determine the *in vivo* location of RecA and its ability to interact with CheW and CheA.
- III. Determine the distribution of the signalling complexes *in vivo* during SOS induction.
- IV. Determine the role of RecA in chemotaxis and motility.



# 3 RESULTS



## 3. Results

To better understand the association of the SOS response and RecA with chemoreceptor cluster formation and chemotaxis, the interaction between RecA and the P5-CheA domain and the region involved in that interaction were explored. In addition, the location within SOS-response activated cells of the major chemoreceptor core unit-components and the impact of this intracellular distribution on chemotaxis were determined.

### 3.1. RecA and CheA interaction

To further determine the role which RecA plays in the signalling complex structuration, the RecA and CheA interaction were proposed because of P5 domain structural similarity with CheW.

For that, co-immunoprecipitation (CoIP) assays (see Section 6.6.7) were conducted to determine whether, as with CheW, RecA was able to interact with CheA<sup>247,280</sup>. Thus, RecA-FLAG and CheA-6xHis tagged proteins were overexpressed in *S. enterica*  $\Delta recA\Delta cheA$  strains carrying the corresponding plasmids. Whole cell-lysates were incubated together to allow interaction of the proteins. Then, magnetic beads pre-coated with anti-FLAG (Beads FLAG) or anti-6xHis antibodies (Beads His) were able to bind specifically corresponding tagged proteins and also pulldown those attached. Proteins attached to the beads were recovered and separated by SDS-PAGE and assessed by Western blotting using both anti-FLAG and anti-6xHis primary antibodies. Thus, as appear in Figure 3.1., when both recombinant proteins were present in the protein mixture, anti-FLAG antibody-coated beads recovered both RecA-FLAG and CheA-6xHis from the supernatants (Fig. 3.1). Consequently, when anti-6xHis antibody-



coated beads were added to the mixture, RecA-FLAG proteins were also recovered along with CheA-6xHis. These results provide strong evidence supporting the *in vitro* pairing of RecA and CheA proteins, in which manner CheA are able to hijack RecA and *vice versa*.

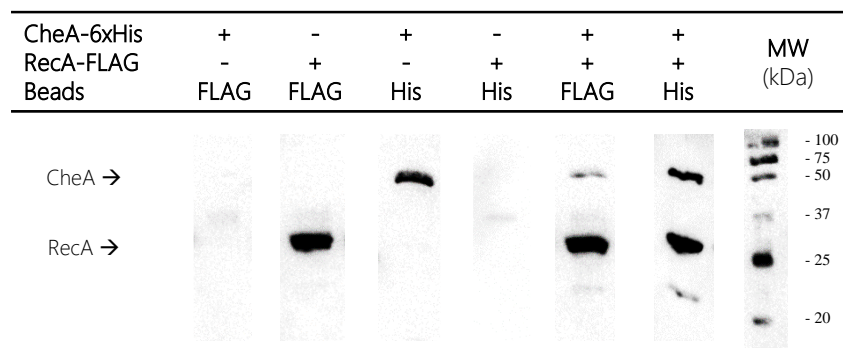


**Figure 3.1.** Co-immunoprecipitation assays of *S. enterica* RecA and CheA. The presence or absence of RecA-FLAG, CheA-6xHis or magnetic beads coated with antibodies in the corresponding lysate mixture is indicated (+, added protein; -, non-added protein). The CoIP positive controls consisted in mixtures containing only RecA-FLAG or CheA-6xHis overexpressing lysates with Beads FLAG or Beads His respectively. In contrast, negative controls were conducted mixing RecA-FLAG or CheA-6xHis overexpressing lysates with Beads His or Beads FLAG, respectively. The experiments were done at least in triplicate. Black arrows show the position of CheA-6xHis and RecA-FLAG; MW, molecular mass marker, in kDa.

Thus, once the interaction between these two proteins were confirmed, an *in silico* modelling experiment was then conducted, with the purpose to identify the putative RecA and CheA residues participating in this interaction. Protein-protein interaction docking (see Section 6.8.4) was performed by RaptorX<sup>284</sup> using, as reference structures, the *E. coli* RecA (PDB: 2REB)<sup>275</sup> and the *Thermotoga maritima* CheA (PDB: 3JA6.C)<sup>194</sup>, which includes the crystallized structures of P3-, P4- and P5-CheA domains. Balanced-coefficient docking models were considered for the analysis of the RecA-CheA interaction<sup>285</sup>.

Thirty of the highest-scoring models were analysed for each combination of RecA receptor protein and CheA ligand and also for the reverse combination. Although the

spatial arrangement was not the same in each combination, the putative interacting regions were considered to be those repeated in all of the studied models (Figure 3.2).

In CheA, both P5 subdomains (1 and 2) interacted with RecA. In some of the *in silico* models, residues of the P3 domain were also exposed to the RecA-CheA interface (Fig. 3.2, Table 3.1). In the case of RecA, the putative interface with CheA was located in the N-terminal and central domains (at  $\alpha 1$ ,  $\alpha 12$ ,  $\alpha 13$ ,  $\beta 11$  and  $\beta 15$ ) (Fig. 3.2, Table 3.2).

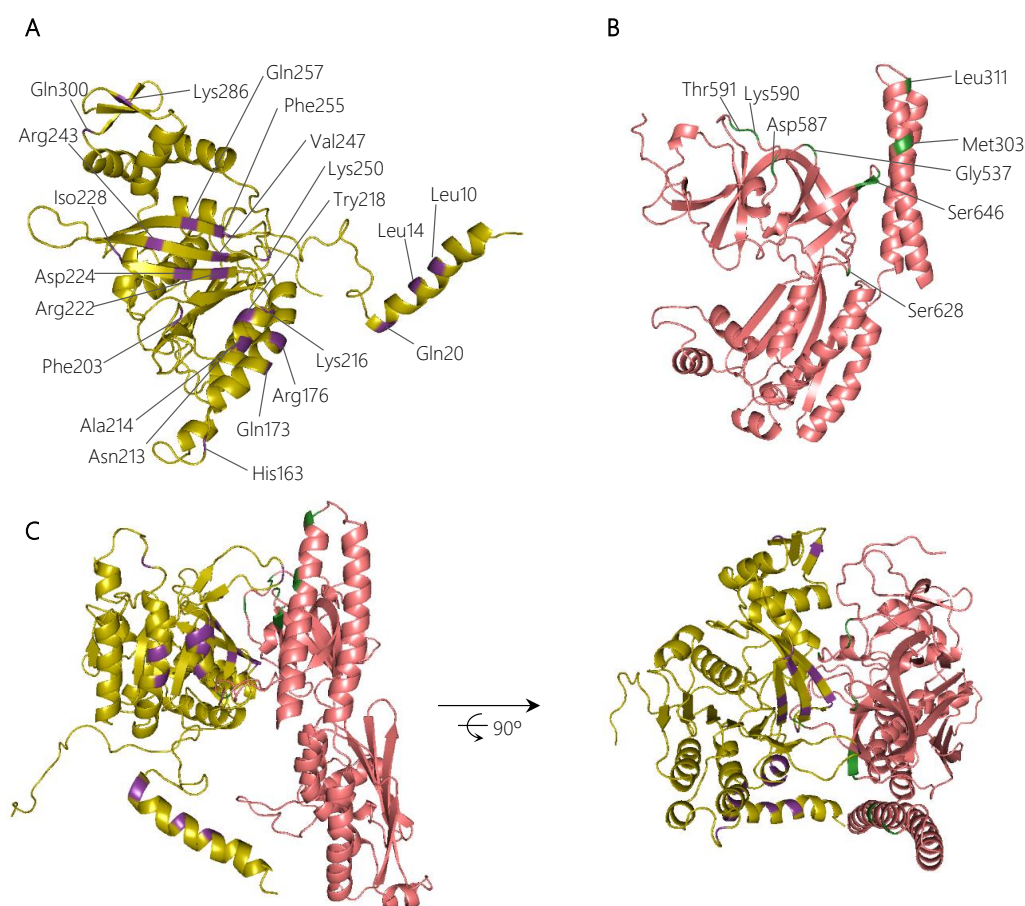


**Figure 3.2.** *In silico* model of the RecA and CheA protein interaction. The predicted ternary structures of (A) *S. enterica* RecA (yellow) and (B) CheA (P3-, P4- and P5-domains, pink) proteins are shown. Residues of RecA and CheA selected for site-directed mutagenesis and their locations are highlighted in purple and green, respectively. (C) Ribbon diagrams of one of the highest-scoring models of the RecA-CheA interaction. The two views of the interaction, obtained using PyMOL software, were achieved rotating 90° about the x-axis.

To confirm these interaction interfaces, site-directed mutagenesis (see Section 6.5.2) was used to construct the corresponding mutant derivatives for each protein. 21 and 8 residues from RecA and CheA, respectively, were selected based on their exposure and their potential ability to mediate RecA-CheA pair formation according to the *in silico* analysis (Tables 3.1 and 3.2). Except for the RecA A214V mutant, in which the Ala residue was changed to a Val, all selected residues were converted to an Ala (Tables 3.1 and 3.2), which is considered to be a non-reactive amino acid<sup>286</sup>. The corresponding *recA* and *cheA* gene mutants constructed *in vitro* were 6xHis-tagged and the effects of the substitutions on the RecA-CheA interaction were determined by ColP assays using the corresponding FLAG-tagged wild type RecA or CheA protein (Fig. 3.3). The results are summarized in the Tables 3.1 and 3.2.

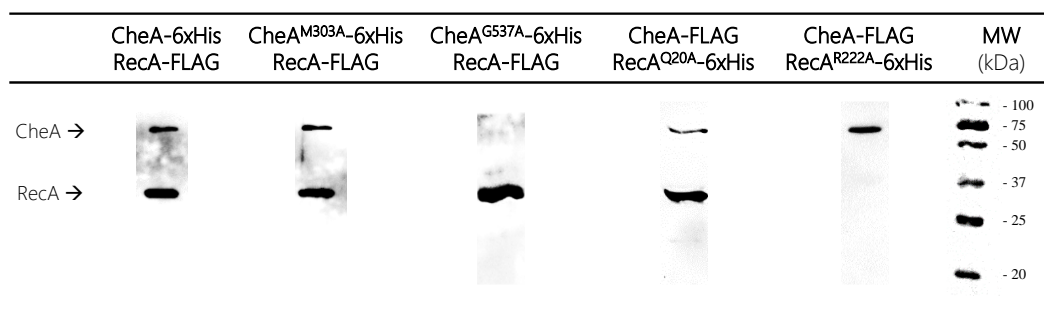


**Figure 3.3.** Co-immunoprecipitation assays of *S. enterica* RecA and CheA mutant derivatives. Representative images of the ColP of mutant derivatives that allow (CheA M303A or RecA R20A) or impair (CheA G537A or RecA R222A) RecA-CheA interaction. Each lane contains a mixture of *S. enterica*  $\Delta recA \Delta cheA$  cell lysates containing the corresponding 6xHis-tagged overexpressed mutant derivative and the wild type FLAG-tagged protein. The immunoprecipitates were obtained using anti-FLAG coated magnetic beads. All experiments were done at least in triplicate. Black arrows indicate RecA and CheA protein bands. MW, molecular mass marker, in kDa.

**Table 3.1.** *In vitro* interaction of CheA mutant derivatives with wild type RecA.

| CheA protein mutated residue <sup>a</sup> | CheA domain containing the mutation <sup>b</sup> | Interaction with wild type RecA <sup>c</sup> |
|-------------------------------------------|--------------------------------------------------|----------------------------------------------|
| Wild type                                 | NA <sup>c</sup>                                  | +                                            |
| M303A                                     | P3                                               | +                                            |
| L311A                                     | P3                                               | +                                            |
| G537A                                     | P5, subdomain 1                                  | -                                            |
| D587A                                     | P5, Subdomain 2                                  | +                                            |
| K590A                                     | P5, Subdomain 2                                  | -                                            |
| T591A                                     | P5, Subdomain 2                                  | -                                            |
| S628A                                     | P5, Subdomain 1                                  | -                                            |
| S646A                                     | P5, Subdomain 1, Strand $\beta$ 9                | -                                            |

According to these results, for CheA, only P5 domain was associated with the RecA interaction because the mutations in the P3-CheA domain did not disturb wild type RecA binding (Table 3.1). Five residues located in P5-CheA domain (G537, K590, T591, S628 and S646) were found to be directly involved in the interaction with RecA as a result of their substitution by Ala which prevented the RecA-CheA pair formation (Fig. 3.3, Table 3.1).

On the other hand, analyses of the 21 RecA mutants showed that only five were unable to bind wild type CheA (A214V, R222A, D224A, I228A and K250A). Thus, for RecA, the CheA binding interface is located at its N-terminal, between residues 214 and 250 (Fig. 3.3, Table 3.2). However, RecA Q20A and R176A mutants, while unable to bind CheW<sup>283</sup>, interacted with wild type CheA (Table 3.2, Fig. 3.3). Similarly, the involvement of residues A214, D224 and I228 was limited to the RecA-CheA interaction, as they had no effect on RecA-CheW binding (Table 3.2). Only two mutant derivatives, R222A and K250A, abolished the interactions of CheA and CheW with RecA (Table 3.2).

**Table 3.2.** *In vitro* interaction of *S. enterica* RecA mutant derivatives with wild type CheA and CheW. Residues involved in the interaction with CheA, CheW or both, are highlighted in blue, yellow or green, respectively.

| RecA protein <sup>a</sup> | Secondary structure region containing the mutated residue | Interaction with wild type CheA <sup>b</sup> | Interaction with wild type CheW <sup>c</sup> |
|---------------------------|-----------------------------------------------------------|----------------------------------------------|----------------------------------------------|
| Wild type                 | NA                                                        | +                                            | +                                            |
| L10A                      |                                                           | +                                            | + <sup>d</sup>                               |
| L14A                      | Helix $\alpha$ 1                                          | +                                            | + <sup>d</sup>                               |
| Q20A                      |                                                           | +                                            | - <sup>d</sup>                               |
| H163A                     | NR                                                        | +                                            | + <sup>d</sup>                               |
| Q173A                     |                                                           | +                                            | + <sup>d</sup>                               |
| R176A                     | Helix $\alpha$ 12                                         | +                                            | - <sup>d</sup>                               |
| F203                      | NR                                                        | +                                            | +                                            |
| N213A                     |                                                           | +                                            | + <sup>d</sup>                               |
| A214V                     | Helix $\alpha$ 13                                         | -                                            | + <sup>d</sup>                               |
| K216A                     |                                                           | +                                            | + <sup>d</sup>                               |
| Y218A                     |                                                           | +                                            | + <sup>d</sup>                               |
| R222A                     |                                                           | -                                            | - <sup>d</sup>                               |
| D224A                     |                                                           | -                                            | + <sup>d</sup>                               |
| I228A                     |                                                           | -                                            | +                                            |
| R243A                     | Strand $\beta$ 11                                         | +                                            | +                                            |
| V247A                     |                                                           | -                                            | + <sup>d</sup>                               |
| K250A                     |                                                           | -                                            | - <sup>d</sup>                               |
| F255A                     | NR                                                        | +                                            | +                                            |
| Q257A                     | Strand $\beta$ 12                                         | +                                            | +                                            |
| K286A                     | NR                                                        | +                                            | +                                            |
| Q300                      | Strand $\beta$ 15                                         | +                                            | +                                            |

NA, not applicable; NR, non-resolved secondary structure.

<sup>a</sup> The mutated residue and the substitution of each tagged mutant derivative are indicated.

<sup>b, c</sup> Results of co-immunoprecipitation (CoIP) assays using each RecA derivative and either CheA or CheW wild type proteins. The maintenance (+) or abolishment (-) of CheA-RecA or CheW-RecA complex formation is shown.

<sup>d</sup> Based on the results of previously described CoIP assays<sup>283</sup>.

These results not only revealed the residues associated with RecA-CheA pairing but also demonstrated the ability of RecA to interact with both CheA and CheW through different interfaces. Furthermore, while both P5-CheA subdomains 1 and 2 participate in the RecA-CheA interaction (Table 3.1), the involved CheA-residues do not overlap with those of the CheA-CheW interaction<sup>194</sup>.

With the exception of A214, all involved residues were located on the  $\beta$ 11 strand, shown in previous studies to be associated with monomer-monomer interactions as well as RecA filament formation and stabilization<sup>250,287,288</sup>. Recombinase assays with the RecA mutants (see Section 6.3.3) showed, in almost all cases, a clear decrease in the recombination activity of the residues associated with RecA-CheA pair formation (Figure 3.4).

Overall, these results validate the *in silico* models and permits understand how RecA interacts with CheA.

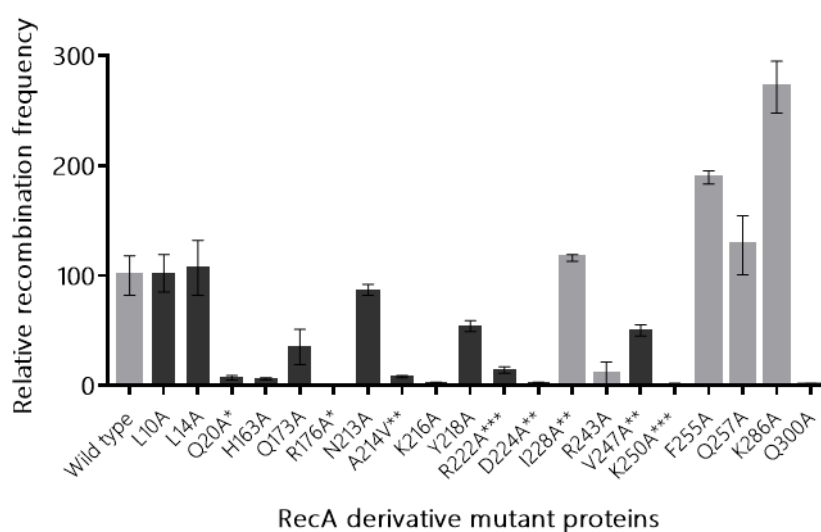


**Figure 3.4.** *In vivo* recombination activity of the RecA mutant derivatives. The relative recombination frequency was calculated as the recombination efficiency of each mutant derivative with respect to that of the strain overexpressing wild type *recA*. The recombination efficiency of each strain is the number of transductants compared with the initial recipient cell concentration. RecA mutant derivatives unable to interact with CheW, with CheA or both proteins are indicated by asterisks (\*, \*\* or \*\*\* respectively). Recombination activity of RecA mutants previously done by Irazoki *et al.*,<sup>283</sup> have also been plotted. The relative recombination frequencies were calculated as the mean of three independent experiments. Error bars indicate the standard deviations.

In addition, the residue conservation percentages among *Salmonella* genus and *Enterobacteriaceae* family were determined for each involved amino acid (Fig. 3.5, see 6.8.2). The RecA residues involved in CheA and CheW interactions were highly conserved (100% identity; Fig. 3.5.A), except for residue I228 (96.4%). Among the CheA residues associated with the RecA interaction, all were conserved in *Salmonella* (100% identity), except G537, which differed in *S. bongori*, resulting in a slightly lower identity (99.2%). The CheA residues were also highly conserved in *Enterobacteriaceae* (>75% identity), again except G537 (7.7%). Finally, for the involved residues of CheW, the results were similar, with 100% identity in *Salmonella* and >80% in *Enterobacteriaceae*. According to these findings, the ability of RecA to interact with CheW and CheA may occur not only in *Salmonella* species besides *S. enterica* but also in *Enterobacteriaceae*.

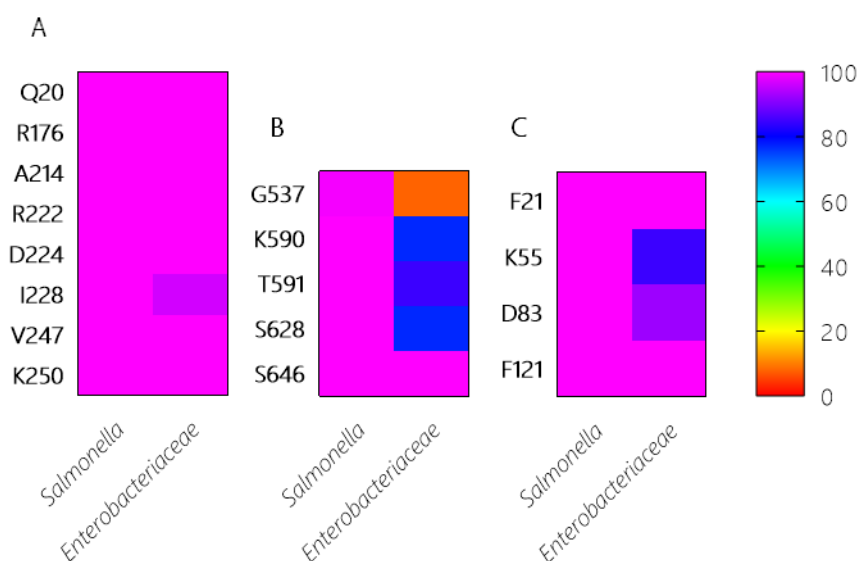


**Figure 3.5.** Conservation of RecA-associated residues among *Salmonella* and other representative *Enterobacteriaceae*. The percentage of conserved residues in the interaction between (A) RecA, (B) CheA and (C) CheW from *S. enterica* was calculated based on the number of residues in the studied sequences that differed from the query sequence. The studied residues were compared with their homologues in *Salmonella* and in one representative of each available genus within the family *Enterobacteriaceae*. Identities closer to 0% are shown in red, and those closer to 100% in pink. Intermediate percentages are represented by other colors in the legend. All sequences were downloaded on November 14, 2019.

### 3.2. RecA as a part of the chemoreceptor signalling core unit

The cellular location of CheW in absence or presence of RecA were determined in previous work<sup>283</sup>. Both proteins localize at cell poles, except when SOS-inductor were added, where these proteins redistribute along the cell-axis.

Using  $\Delta recA$ ,  $\Delta recA \Delta cheA$  and  $\Delta recA \Delta cheW \Delta cheA$  strains complemented with a pUA1108 plasmid containing a  $recA::CLIP$ , the location of RecA were determined under fluorescence microscopy (see Section 6.7.3). When CheA protein was not present, RecA protein was majorly not locate at the cell poles, and as expected, also occurs in absence of both CheA and CheW proteins (Fig. 3.6). This fact confirms the importance of the presence of these chemotactic proteins for the pole-cell location of RecA.

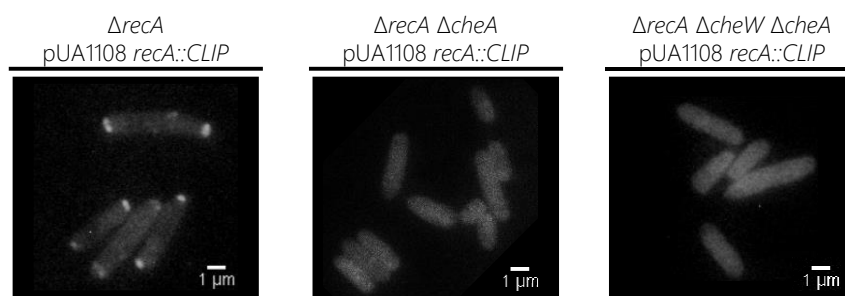


**Figure 3.6.** RecA localization in absence of CheA or both CheA and CheW. Representative fluorescence images of  $\Delta recA$ ,  $\Delta recA \Delta cheA$  and  $\Delta recA \Delta cheW \Delta cheA$  strains complemented with a pUA1108 plasmid containing a  $recA::CLIP$ . RecA protein was labelled with the permeable dyes CLIP-Cell™ TMR-Star. The samples were examined under an Axio Imager M2 microscope (Carl Zeiss Microscopy) equipped with the Rhod (Zeiss filter set 20) filter set.

According to the results, they indicated the differential interaction of RecA with CheW and CheA (Table 3.2) and the importance of both proteins for RecA cell-pole location (Fig. 3.6). Furthermore, RecA interfaces with CheA and CheW (Tables 3.1 and 3.2) did not overlap with the regions of CheA-CheW binding, nor with those involved in MCP interaction<sup>169,171,194</sup>. These observations suggested that RecA may be part of a signalling complex, a possibility explored by generating *in silico* interaction models that included the entire signalling core unit (Fig. 3.7).



The RaptorX-generated structures for all *S. enterica* proteins were compared with the structure of the *T. maritima* chemotaxis signalling complex (PDB:3JA6)<sup>194</sup> and modelled using PyMOL software<sup>289</sup>. The RecA interaction was placed according to the residues determined to be directly involved in the CheA-RecA and CheW-RecA interfaces (Tables 3.1 and 3.2). The *in silico* docking analysis in PyMOL established that RecA interaction could be fitted to the chemoreceptor signalling complex without any allosteric interference (Fig. 3.7), as the P5-CheA subdomain 1 was still able to interact with CheW subdomain 2 (interface 1)<sup>290</sup>.

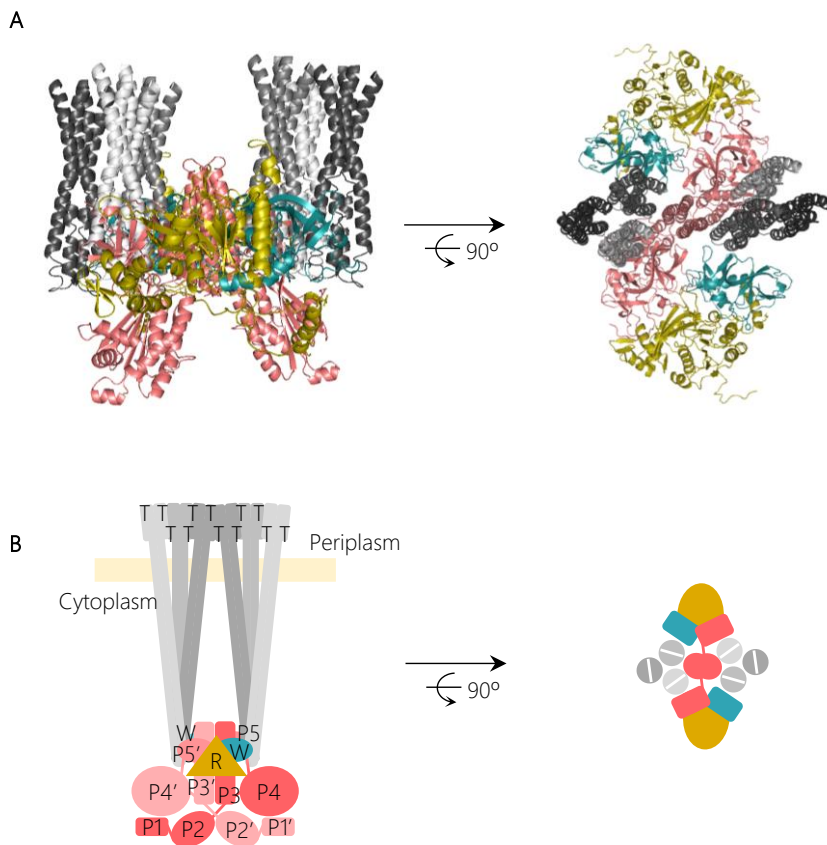


**Figure 3.7.** *In silico* model of the interaction of RecA-CheA-CheW proteins forming the core signalling complex. **(A)** The predicted ternary structures of *S. enterica* RecA (R, yellow), CheW (W, blue), CheA (P3-P5, pink) and Tar (T, gray) are represented in cartoon form. Model images are cross-sections through the receptor tip and CheA/CheW baseplate, viewed perpendicular (left) and parallel (right) to the cytoplasmic membrane. The proteins were modelled using PyMOL software according to the studied protein-protein interfaces responsible for RecA-CheW<sup>283</sup>, RecA-CheA (in this study) and CheA-CheW-Tar interactions<sup>171</sup>. **(B)** Schematic representation of the above *in silico* model including the P1 and P2 domains.

### 3.3. RecA interacts with both CheW and CheA *in vivo*

To corroborate the results of the *in silico* models and study the importance of the RecA-CheA interaction for chemoreceptor polar cluster formation *in vivo*, the location of CheA and Tar proteins was analysed using the stimulated emission depletion (STED) microscopy, a super-resolution fluorescence imaging technique that increases the spatial resolution of biological samples up to 20–40 nm<sup>291</sup>. To guarantee minimal space between the protein and the label and maintain intact the cell envelope, SNAP and CLIP technologies were applied.

The SNAP and CLIP tags are self-labelling enzymes derived from the human DNA repair protein O<sup>6</sup>-alkylguanine-DNA alkyltransferase. Appropriate permeable dyes directly attach to the target protein with high reactivity and labelling specificity, thus preventing bacterial cell membrane alteration. The SNAP-tag binds O<sup>6</sup>-benzylguanine derivatives<sup>292</sup>, and the CLIP-tag O<sup>2</sup>-benzylcytosine derivatives<sup>293</sup>. Due to these differences, the two tags, with their permeable dyes suitable for STED imaging (SNAP-Cell® 505-Star and CLIP-Cell™ TMR-Star, respectively), can be employed simultaneously to specifically label target proteins in living cells. Furthermore, thanks to the permeability of these enzyme-dyes, possible artifacts which can alter the location of the proteins of the study are avoided<sup>293</sup>.

Hence, *S. enterica cheA::SNAP tar::CLIP* and  $\Delta recA cheA::SNAP tar::CLIP$  tagged strains were constructed and tested in chemoreceptor clustering and swarming assays under non-DNA damage conditions to verify that tag addition did not alter their chemoreceptor array phenotypes. No changes in either chemoreceptor polar clusters or swarming motility<sup>294,295</sup> were observed for *S. enterica cheA::SNAP tar::CLIP* strain (Figure 3.8.A). Its phenotype was the same as that of *S. enterica* wild type. Also, *S. enterica  $\Delta recA cheA::SNAP tar::CLIP$*  was unable to swarm and the number of chemoreceptor polar clusters was drastically reduced (Fig. 3.8.B) due RecA is essential for both swarming and polar array cluster formation<sup>247</sup>.

The RecA complementation and overexpression assays were performed using the pUA1108 vector containing wild type *recA* and its derivatives unable to interact with CheA (RecA A214V) or CheW (RecA R222A) or both proteins (RecA R176A) under the control of the Ptac IPTG-inducible promoter. The plasmids were transformed into *S. enterica* *cheA::SNAP tar::CLIP* and  $\Delta recA$  *cheA::SNAP tar::CLIP* strains (Table 6.1), and the intracellular location of CheA and Tar was then determined.

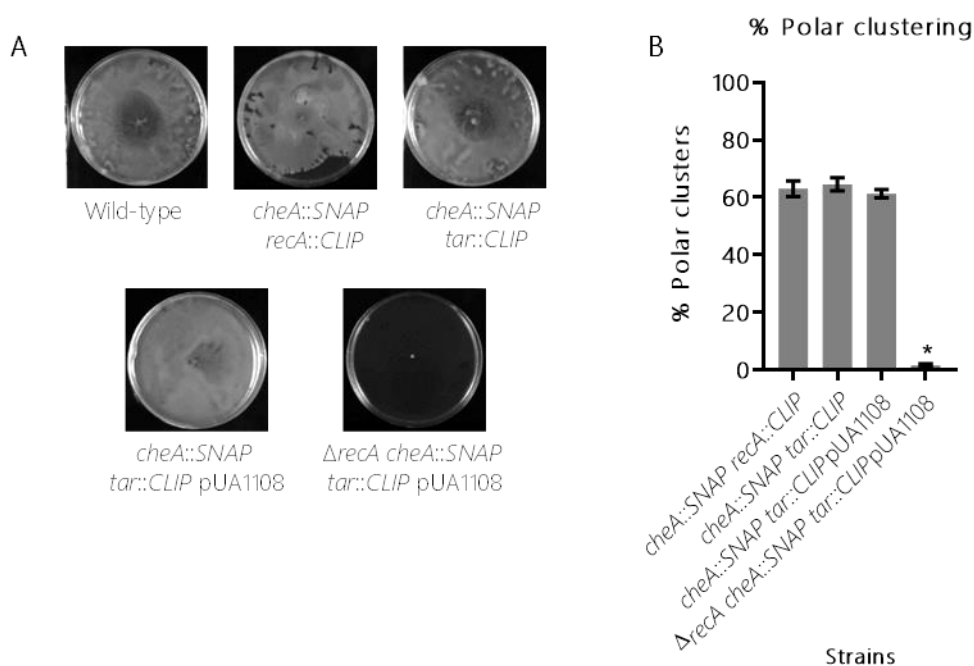


**Figure 3.8.** Swarming assays and chemoreceptor polar clustering of *S. enterica* tagged strains. **(A)** Swarming motility and **(B)** chemoreceptor polar clustering were assayed to confirm that addition of the corresponding tag had no effect on the phenotype of the tested *S. enterica* strains. Swarming assays were performed as previously described<sup>247</sup>. The experiment was done at least in triplicate. The results are the mean of at least three independent imaging studies. One-way ANOVA multiple comparison test with Bonferroni correction were used for statistical analysis. The results are the mean of three independent experiments and error bars represent the standard deviation. P < 0.01 was determined as statistically highly significant (\*).

As known, the absence of RecA impairs chemoreceptor array formation<sup>247</sup>. Certainly, in complementation assays, the basal expression of the wild type *recA* gene cloned in the pUA118 vector was enough to restore chemoreceptor array formation, causing CheA and Tar location were again in cell poles (Fig. 3.9.A)<sup>247</sup>. Nevertheless, in the presence of a non-CheA-interacting RecA, no chemoreceptor polar clusters were formed (Fig. 3.9.A) and CheA and Tar were distributed along the cell. The same phenotype was observed using a RecA mutant unable to interact with CheW (Fig. 3.9.A) or with both CheA and CheW (Fig. 3.9.A).

On the other hand, the RecA overexpression inhibited polar cluster assembly in a wild type genetic background<sup>246</sup>. Then, as expected, the IPTG-induced expression of a wild type *recA* gene within *S. enterica cheA::SNAP tar::CLIP* promoted the redistribution of CheA and Tar along the cell (Fig. 3.9.B). However, the increased expression mediated by IPTG of *recA* mutants unable to bind CheA, CheW or both proteins did not alter the CheA and Tar location, which remained at the cell poles (Fig. 3.9.B). Together, the results indicate that the interaction of RecA with both CheA and CheW is needed for chemoreceptor polar array formation and that both interactions occur *in vivo*.

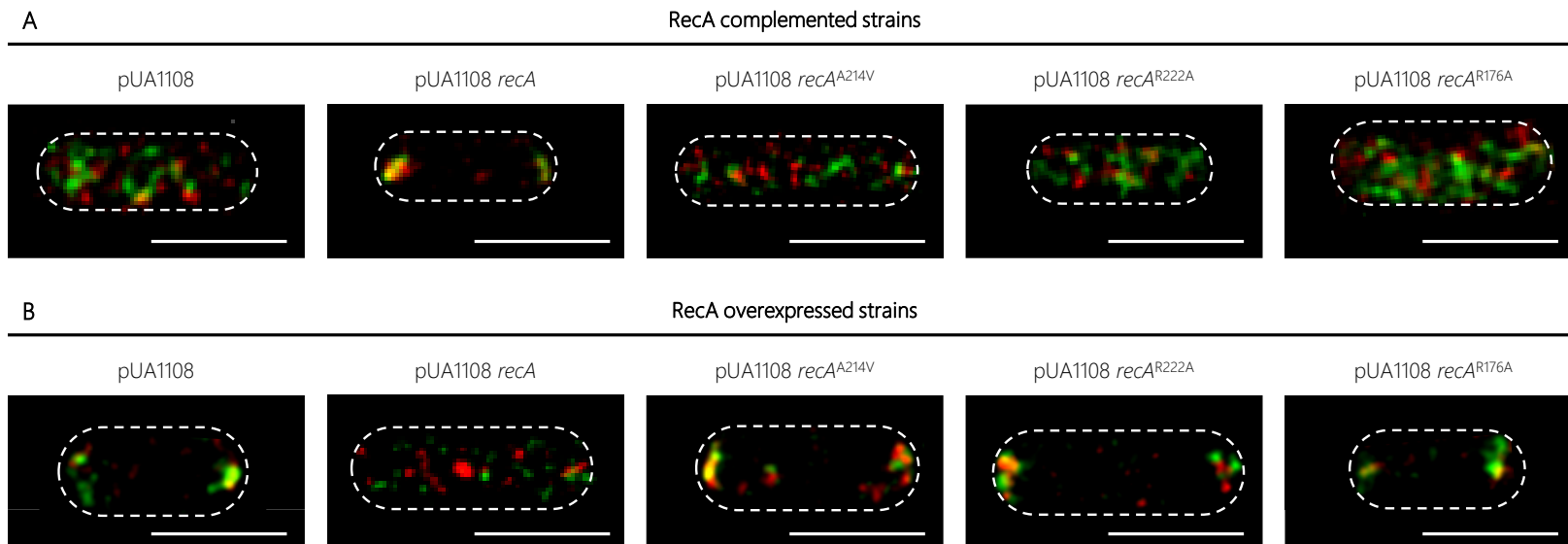


**Figure 3.9.** Representative STED images of the locations of CheA and Tar within *S. enterica*. Cells containing the pUA1108 expression vector, either empty or carrying wild type *recA*, a non-CheA interacting *recA* mutant derivative (A214V), a non-CheW interacting (R222A) or a *recA* mutant derivative that interacts with neither CheA nor CheW (R176A) are shown. The corresponding plasmids were included in the genetic backgrounds of **(A)** *S. enterica*  $\Delta recA$  *cheA::SNAP tar::CLIP* and **(B)** *S. enterica* *cheA::SNAP tar::CLIP*. CheA and Tar proteins were labelled with the permeable dyes CLIP-Cell™ TMR-Star and SNAP-Cell® 505-Star, respectively. For all images, overlapped channel results of CheA (in red) and Tar (in green) location are presented. White bar represents 1  $\mu\text{m}$  of length. The maximum intensity projection images of the obtained z-stacks are shown. All experiments were done at least in triplicate.

### 3.4. Location of CheA and Tar proteins within SOS response-induced cells

The polar cluster array proteins CheW, CheA and Tar are located mainly at the cell poles in bacteria grown in liquid medium under non-DNA damaging conditions<sup>201,296,297</sup>. Also, several studies have shown that RecA also localizes at the poles<sup>246,298,299</sup>. However, previous work demonstrated that during SOS response activation, RecA and CheW are no longer located at the cell poles but in small foci distributed along the cell<sup>283</sup>. It was suggested that the increasing number of RecA molecules when SOS response is activated could kidnap the CheW molecules from the poles clusters, and thus, disrupting the polar clustering<sup>283</sup>. After knowing the direct interaction between RecA and CheA, RecA might kidnap not only CheW but also the entire signalling chemoreceptor complex, and thereby, also CheA and Tar.

To further understand the association of RecA with CheA and the signalling core units, the location of CheA and Tar proteins in SOS-response-induced cells was studied in *S. enterica* *cheA::SNAP tar::CLIP* and *cheA::SNAP recA::CLIP* tagged strains by STED imaging.

The herein results demonstrated that under non-DNA-damaging condition, RecA, CheA and Tar were, as expected, located at the poles of *S. enterica* cells (Figures 3.10 and 3.11). However, the addition of a sublethal concentration of SOS-inducer resulted in cell filamentation and the redistribution of CheA and Tar (Fig. 3.10) to follow that of RecA (Fig. 3.11) and CheW<sup>283</sup>. Thus, under non-DNA-damaging conditions and during activation of the SOS response, the intracellular distributions of CheA, CheW, Tar and RecA were the same, moving from the cell poles to along the cell axis<sup>283</sup> (Figures 3.9 and 3.11).

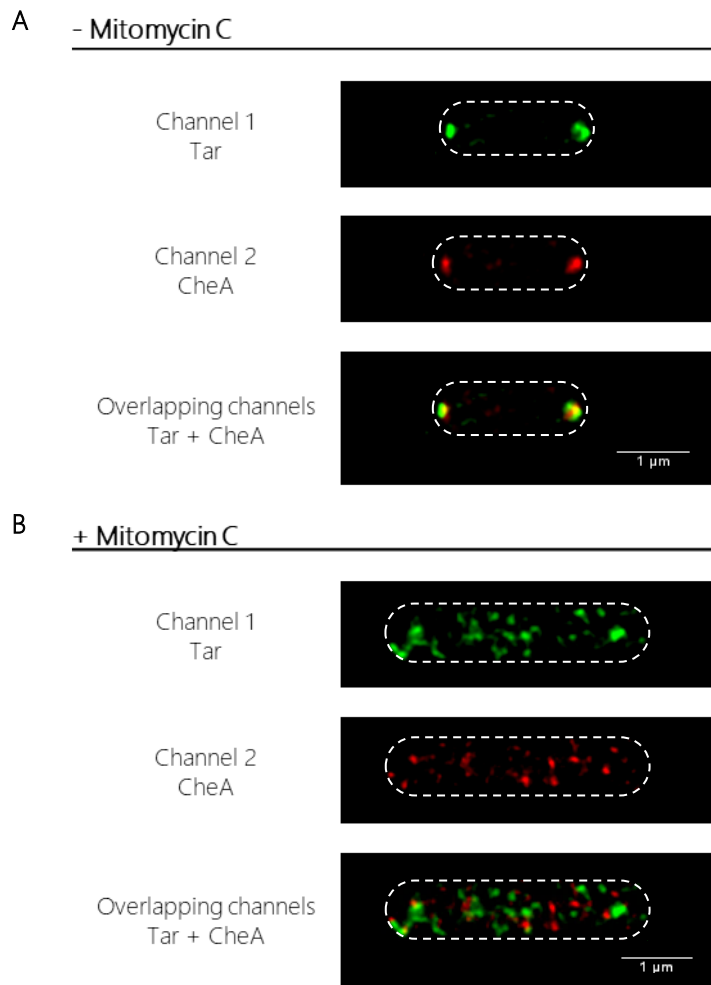


**Figure 3.10.** Representative STED images of the subcellular locations of Tar and CheA in *S. enterica cheA::SNAP tar::CLIP* cells in the **(A)** absence or **(B)** presence of SOS inducer. The Tar and CheA proteins were labelled with the permeable dyes CLIP-Cell™ TMR-Star (channel 1, in green) and SNAP-Cell® 505-Star (channel 2, in red), respectively. When appropriate, mitomycin C was added at a final concentration of 0.08  $\mu\text{g}/\text{mL}$ . For all images, each channel is shown both individually and overlapped. The maximum intensity projection images of the z-stacks are shown. All experiments were done at least in triplicate.

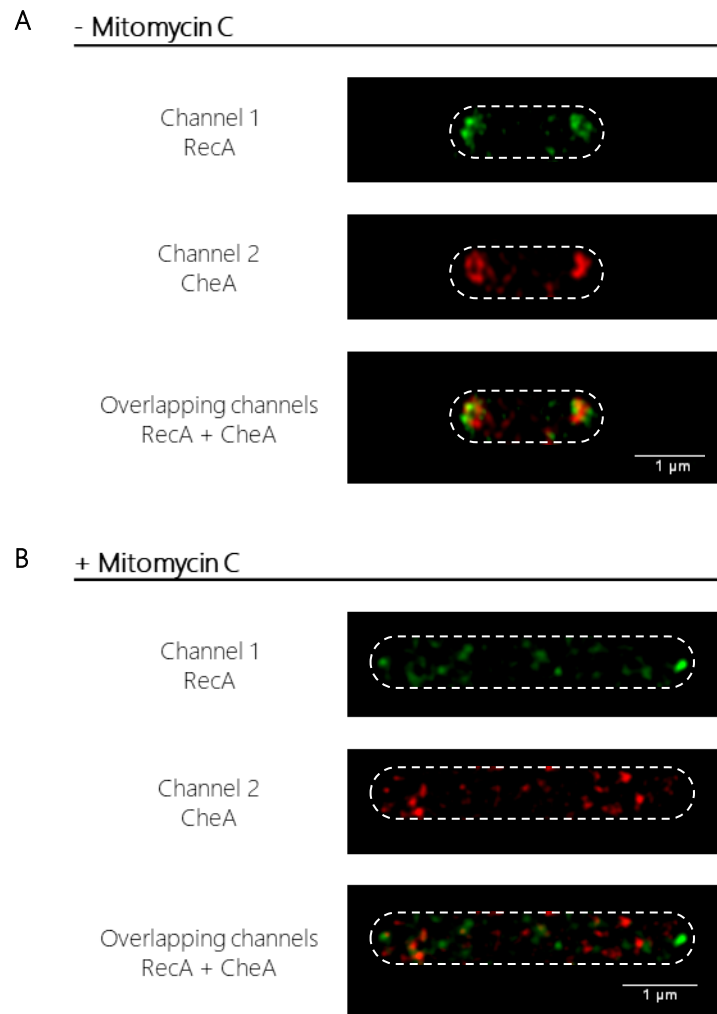


**Figure 3.11.** Representative STED images of the subcellular locations of CheA and RecA in *S. enterica cheA::SNAP recA::CLIP* cells in the **(A)** absence or **(B)** presence of SOS inducer (0.08 µg mitomycin C/mL). RecA and CheA proteins were labelled with the permeable dyes CLIP-Cell™ TMR-Star (channel 1, represented in green) and SNAP-Cell® 505-Star (channel 2, in red), respectively. For all images, each channel is shown both individually and overlapped. The maximum intensity projection images of the obtained z-stacks are also shown. All experiments were done at least in triplicate.



### 3.5. SOS response-induced cells present normal chemotaxis response

STED images of Figures 3.9 and 3.11 demonstrated that RecA and the chemotactic proteins CheA and Tar follow the same intracellular distribution as well as CheW<sup>283</sup> when RecA concentration is increased by either SOS response activation or *recA* overexpression. Hence, RecA could kidnap the entire signalling complex preserving the structure and thus, the chemotactic signalling.

To further demonstrate that RecA is a component of the signalling core unit and that the structure of this unit is preserved during SOS response activation, chemoreceptor polar clustering and chemotaxis assays were performed by exposing cells of different genetic backgrounds to a sublethal concentration of mitomycin C and then monitoring the chemotaxis response.

As shown in Figure 3.12, the presence of mitomycin C did not affect *S. enterica* wild type strain chemotaxis. The same results were obtained when the wild type *recA* was overexpressed in bacterial cells by the addition of IPTG. Under these conditions, i.e., in the presence of mitomycin C or *recA* overexpression, the absence of chemoreceptor polar clusters did not lead to an inhibition of the chemotaxis response. Interestingly, in the presence of mitomycin C, chemoreceptor polar array formation in the  $\Delta recA$  strain was lower than that observed in either SOS-induced or RecA-overexpressing wild type cells (Fig. 3.12).

Furthermore, as previously published<sup>247</sup>,  $\Delta recA$  cells were unable to respond to a chemoeffector or swarm, abilities that were restored only by the addition of wild type *recA*. Neither polar cluster array formation, chemotaxis (Figures 3.9 and 3.12) were restored in a  $\Delta recA$  strain complemented with *recA* mutant derivatives unable to interact with CheA, CheW or both. According to these results, the formation of active signalling core units and, therefore, chemoreceptor polar arrays, require the binding of RecA to both CheA and CheW.

Similarly, in Figure 3.13, cells are able to complement the lack of RecA and restore swarming ability only with the plasmid containing the wild type gene, but not if RecA

cannot interact with CheA and/or CheW within the  $\Delta recA$  strain. By contrast, in cells with basal expression of RecA (wild-type), an increase in cytosolic wild-type RecA abolishes swarming, whereas swarming is maintained in the presence of the other RecA mutant derivatives.

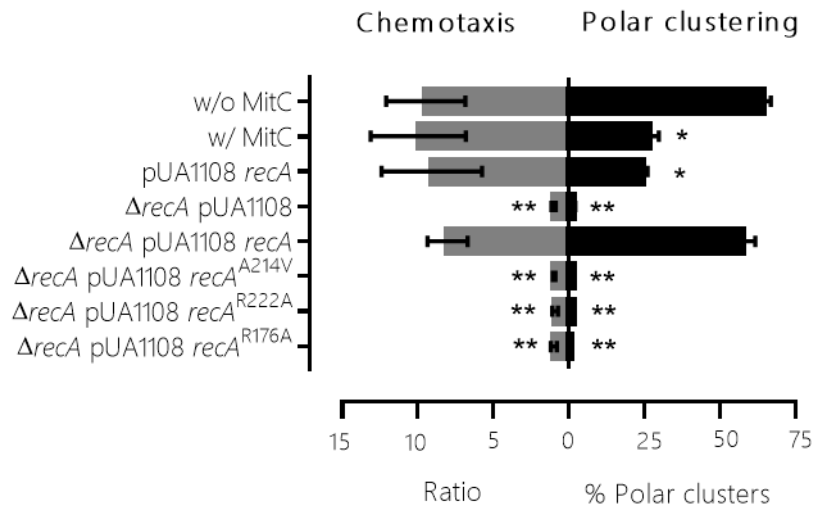


**Figure 3.12.** Chemotaxis ability and chemoreceptor polar clustering of *S. enterica* strains. Chemotaxis assay percentages of chemoreceptor polar clusters in *S. enterica cheA::SNAP tar::CLIP* and  $\Delta recA cheA::SNAP tar::CLIP$  ( $\Delta recA$ ) strains are represented. As needed, the cells were grown in the absence (w/o MitC) or presence (w/ MitC) of mitomycin C (0.08  $\mu\text{g}/\text{mL}$ ). When indicated, they were transformed with either empty pUA1108 or the plasmid carrying wild type *recA* or a *recA* mutant derivative [non-CheA-interacting (A214V), non-CheW-interacting (R222A) or interacting with neither CheA nor CheW (R176A)]. The chemotaxis ratios were calculated as the ratio of viable bacteria inside capillary tubes with vs. without aspartate. One-way ANOVA multiple comparison test were used for statistical analysis. The results are the mean of three independent experiments and error bars represent the standard deviation.  $P < 0.05$  was determined as statistically significant (\*) and  $p < 0.01$  as highly significant (\*\*).

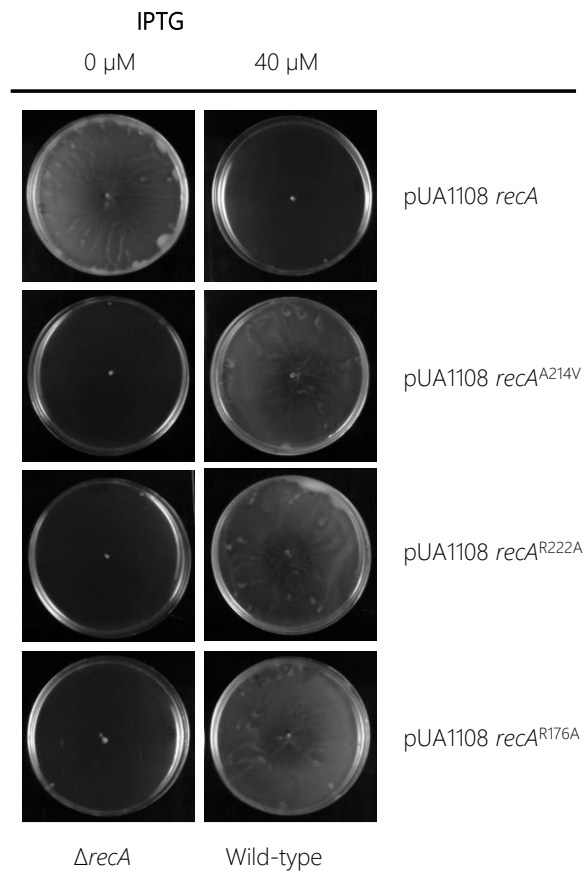


**Figure 3.13.** Swarming assays from *S. enterica*  $\Delta$ *recA* and wild-type strains containing pUA1108 carrying the *recA* gene or the corresponding mutant derivatives. As needed, the cells were tested in the absence or presence of 40  $\mu$ M IPTG swarming agar plates. When indicated,  $\Delta$ *recA* or Wild-type strains were transformed with plasmid carrying wild type *recA* or a *recA* mutant derivative [non-CheA-interacting (A214V), non-CheW-interacting (R222A) or interacting with neither CheA nor CheW (R176A)]. Assays were performed per triplicate.

# 4 DISCUSSION



## 4. Discussion

The results described above provide strong evidence supporting the interaction of RecA with P5-CheA domain (Fig. 3.1), which is structurally similar to CheW<sup>300</sup> (Table 3.1). While both P5-CheA subdomains 1 and 2 participate in the RecA-CheA interaction (Table 3.1), the involved CheA-residues do not overlap with those of the CheA-CheW interaction<sup>194</sup>. For RecA, the CheA binding interface is located at its NH2-terminus, between residues 214 and 250 (Fig. 3.2 and Table 3.2). This region is mainly associated with monomer-monomer interaction as well as RecA filament formation and stabilization<sup>250,287,288</sup>. Moreover, almost all residues involved in RecA-CheA pair formation had a very low recombinase activity (Fig. 3.4). *In silico* docking established that the RecA interaction could be fitted to the chemoreceptor signalling complex without any allosteric interference (Fig. 3.7), as the P5-CheA subdomain 1 was still able to interact with CheW subdomain 2 (also known as interface 1)<sup>290</sup>.

Despite the similarity of CheW and P5-CheA, only RecA Arg222 and Lys250 residues, located at the  $\beta$ 11 strand, were associated with both RecA-CheA and RecA-CheW pair formation<sup>283</sup> (Table 3.2). Interestingly, these two amino acids are approximately located in the union between CheA-CheW. The rest of the identified RecA residues (Ala214, located in the  $\alpha$ 13 helix, and Asp224, Ile228, and Val247, all of them in the  $\beta$ 11 strand) are only associated with CheA binding, and their mutation did not affect the RecA-CheW interaction (Table 3.2). RecA binding to CheW is mediated not only by the  $\beta$ 11 strand but also by the  $\alpha$ 1 and  $\alpha$ 12 helices of RecA<sup>283</sup>. As in the RecA-CheA interaction, RecA-CheW pairing does not interfere with the binding of any of the other CheW binding partners identified so far (CheA, CheW and MCPs)<sup>283</sup>. Moreover, all residues involved in RecA-CheA and RecA-CheW interfaces were highly conserved not

only in *S. enterica* but also in other members of *Enterobacteriaceae* (Fig. 3.5), pointing out the importance of the conservation of these residues. The association of the SOS response with chemoreceptor signalling complexes may be extended to *Enterobacteriaceae* and perhaps also to other families of bacteria.

*In vivo* assays showed that chemoreceptor polar clustering requires the interaction of RecA with both CheA and CheW. Indeed, RecA was distributed along the cell when polar clusters are not built (Fig. 3.6). Further, RecA mutants unable to bind CheA, CheW, or both proteins neither restored wild type chemoreceptor polar cluster assembly in cells with a  $\Delta recA$  genetic background (Fig. 3.9.A) nor abolished polar cluster formation in wild type cells overexpressing RecA<sup>246</sup> (Fig. 3.9.B).

According to these results, the interaction of RecA not only with CheW but also with CheA is essential for chemoreceptor array formation and this evidence could be linked with the stoichiometry of the chemoreceptor components. Previous studies showed that the stoichiometry of chemoreceptor core unit components within the cell is crucial for polar array assembly. For instance, the absence or overexpression of CheW abolishes chemoreceptor cluster formation<sup>295</sup>. The same phenotype occurs in a knock out *recA* mutant<sup>247</sup> or when the RecA concentration is increased, whether by SOS response activation or by its overexpression<sup>246,279</sup>. Earlier work proposed that RecA prompts the titration of CheW, thus preventing chemoreceptor assembly and, in turn, polar cluster array formation during activation of the SOS response<sup>283</sup>. The same sequence of events may describe the CheA-RecA interaction.

Nevertheless, the results described herein clearly determine that RecA protein present different binding interfaces with CheA and CheW, that do not overlap with those associated with CheA-CheW interaction or with their binding to MCPs. Together with the fact that, in the absence of RecA there is no chemotaxis response<sup>247</sup>, suggested the direct interaction of RecA with the chemoreceptor core unit.

STED imaging of the tagged strains indicated that RecA, CheA, Tar (Figures 3.9 and 3.11) and CheW<sup>283</sup>, the main components of the signalling core unit, follow the same

intracellular distribution when RecA concentration is increased following the activation of the SOS response or *recA* overexpression, moving from the cell poles to along the cell axis<sup>283</sup> (Figures 3.9 and 3.11). Furthermore, the polar cluster arrays of *S. enterica*  $\Delta recA$  cells were not restored by the presence of a *recA* mutant unable to bind CheA, CheW, or both, such that chemotaxis was inhibited (Fig. 3.12). Only the addition of wildtype RecA reestablished chemotaxis (Fig. 3.12), and the RecA molecule is, and not the SOS general response or activated RecA (RecA\*), responsible of these results.

Taken together, these findings demonstrate that RecA and its ability to bind CheA and CheW are not only crucial for the functionality of the signalling core complex, but also for chemotaxis. The direct association of RecA with the chemoreceptor core unit also explains the impaired formation of chemoreceptor polar clusters in the presence of increased RecA (Fig. 4.1). Chemoreceptor arrays consist of hexagonal lattices of MCPs stabilized by interconnected heterohexameric rings of CheA and CheW<sup>194</sup>. The rings are formed by the alternated interactions between P5-CheA and CheW of three unit core complexes that give rise to interface 2, composed of the P5-CheA subdomain 2 and CheW subdomain 1. This key link with the fact that signalling core complexes in the array is needed for cluster assembly<sup>194,290</sup>.



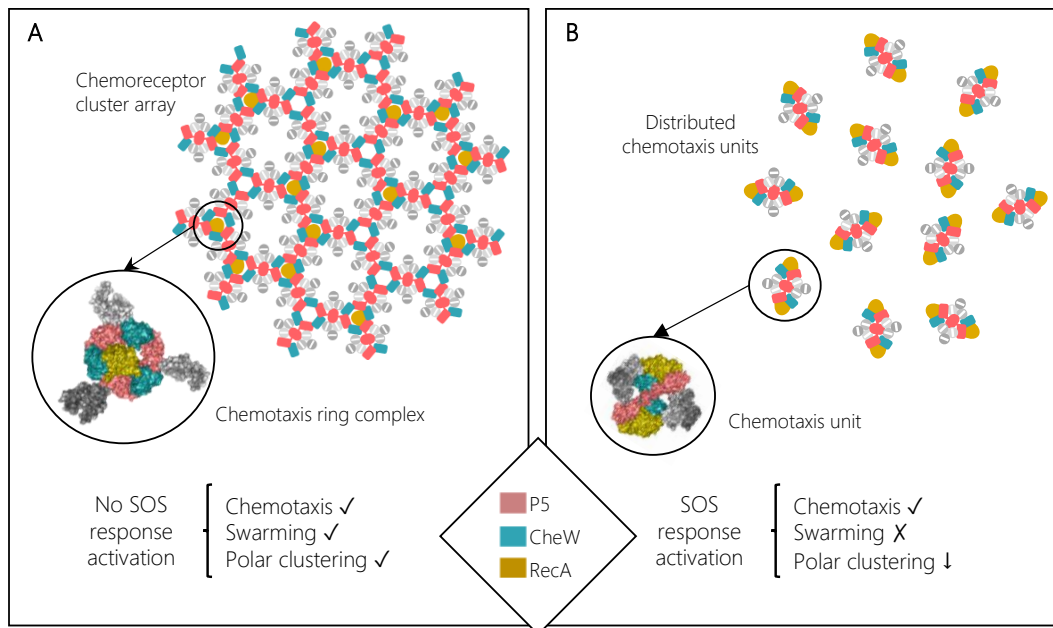


**Figure 4.1.** Proposed model of chemoreceptor assembly inhibition during activation of the SOS response. **(A)** Under non-DNA damaging conditions, only one RecA molecule fits within the inner aspect of the heterohexameric ring. **(B)** Activation of the SOS response is followed by a high increase in the RecA concentration. This induces an increase in the number of RecA-associated signalling complexes. In that context, the heterohexameric ring formation is allosterically disturbed by the presence of more than one RecA molecule. As a result, chemoreceptor polar clusters are unable to form and chemoreceptor signalling units remain distributed along the cell. These cells are unable to swarm but retain a chemotaxis response

As shown in Figure 4.1, there is enough space within a ring to fit one RecA molecule interacting with one of the three internal faces of the CheW-CheA<sub>2</sub>-CheW heterohexameric ring, without altering its hexagonal structure. When SOS response activation increases the intracellular RecA concentration, the protein becomes associated with a greater number of signalling core units. Thus, the build-up of heterohexameric rings is prevented by the high levels of RecA, which impair the formation of CheW-P5-CheA interface 2 and consequently, the array assembly is inhibited. RecA seems to be not able to destroy previously formed clusters, which would explain why micrographies of the bacterial population where the amount of RecA is higher, either for SOS induction or RecA overexpression, show percentages roundly 35% of clusters (Fig. 3.12). These clusters could be formed before the rise of RecA. This is consistent with previously published data, where confirm that chemotaxis

clusters are array structures difficult to be destroyed<sup>201</sup>. Nonetheless, further studies kinetic and *in vivo* imaging are needed to confirm this suggestion.

It is important to note that the chemotaxis response is not associated with the presence of polar chemoreceptor clusters, unlike swarming. Thus, in the *S. enterica* wild type strain, while either SOS response activation by mitomycin C or the overexpression of wild type *recA* impaired chemoreceptor array formation and therefore swarming motility<sup>246</sup> (Fig. 3.13), there was no effect on chemotaxis (Fig. 3.12). The signalling core units were completely functional, even in the absence of chemoreceptors arrays, only in the presence of wild type RecA, not a RecA mutant unable to bind CheA, CheW, or both (Fig. 3.12). These results indicate, in agreement with previously reported data, that although the absence of polar clustering clearly impairs swarming ability<sup>196,246,295</sup>, the chemotaxis pathway remains functional<sup>171,186,196,301</sup>.

Furthermore, the complementations (Fig. 3.9) and the locations (Figures 3.10 and 3.11) reject the idea that RecA sequesters CheW or CheA (or even both proteins) from the chemoreceptor unit. It was thought due the P5-CheA homology with CheW, hence, increase in number of RecA molecules could interact with CheW unabling CheW-CheA interaction. Another explanation was that RecA sequester CheA or both CheA-CheW, without the TODs. Any of proposed cases would impair the cluster formation and chemotaxis, but chemotaxis remains functional despite non-polar cluster prevalent phenotype (Fig. 3.12). Hence, a determination of dissociation constants between RecA and CheA or CheW would be unnecessary knowing that related critical interaction with these two proteins.

In previous results, CheW overexpression re-established polar cluster assembly in a RecA-overexpressing strain<sup>246</sup>, exemplifying the increased availability of CheW restores chemosensory array assembly. Our results are also consistent with this CheW and RecA titration, but the explanation is different. It is worth noting that CheW decompensation with CheA protein levels disable polar clustering. Thus, when RecA is induced or overexpressed, the excess of available CheW molecules is balanced with RecA and this complex remains unlocated in the cell, whilst a portion of CheW and

RecA are clustering with CheA and Tar at the poles, allowing both swarming and chemotaxis.

Further, it is also known that chemotaxis is not affected when *E. coli* cells are treated with cephalixin<sup>301</sup>, a  $\beta$ -lactam antibiotic that induces the SOS response<sup>302</sup>. As seen, the over production of RecA due SOS response activation by the presence of DNA-damaging compounds or antibiotics, increases the number of signalling core units associated to RecA. Consequently, this increase modulates the architecture of chemoreceptor arrays, by impairing the heterohexameric CheA-CheW ring formation (Fig. 4.1). It is known that the chemotaxis of bacterial cells is enhanced by the networking of chemoreceptors<sup>196</sup>. Nevertheless, Frank *et al.*, 2016, showed that the CheA kinase levels and flagellar motor switching are similar in cells with and without polar clusters. The same authors found that, under conditions of high CheA kinase activity, cells with dispersed receptor complexes are more sensitive to chemoeffectors than cells with polar clusters<sup>196</sup>. However, cells can remodel their chemotaxis signalling pathway to enhance swarming motility<sup>294</sup>. Thus, the distribution of chemoreceptor signalling units in *Salmonella* modulates not only swarming motility in cells growing on a surface, to prevent exposure to higher concentrations of SOS-inducer compounds<sup>246</sup>, but also the chemotaxis performance of the SOS-induced cells. This behaviour is different that in the presence of chemorepellents, so in a manner, the cell prefers stopping its surface movement and stay near the SOS inducer, sub-lethal conditions, than run away. It would be to take advantage of this SOS induction and conserve provoked mutations which could be benefit in other surroundings. Another explanation is the impossibility for cell to have chemoreceptors for every existing, and to exist, chemorepellents. Hence, when cell is near to conditions which produces DNA lesions, prefers disrupting than continuing towards its death (or suicide). In this case, RecA act as "sensor" in front of many different chemical compounds which act in the same target, the DNA destruction. Certainly, the diffusion of a SOS-inducer compound is different in liquid than semi-solid environment. Thus, in this fatidic condition, stop is not an option for the swimmer cells due the speed and scope in

liquid media. Here, these cells conserve chemotaxis and they are able to be more sensitive to chemoeffectors, promoting changes in their movement and thus, move away from the toxic compound.

The high degree of conservation of residues associated with the CheA-RecA-CheW interaction in *Enterobacteriaceae* (Fig. 3.5) suggested that the relationship between the SOS response, chemotaxis and swarming to modulate bacterial motility in the presence of antibiotics and other injurious or potentially lethal compounds may be extended to other species of this bacterial group.



# 5 CONCLUSIONS



## 5. Conclusions

- I. The obtained results unequivocally determine the interaction between *S. enterica* RecA and CheA proteins. The interface involved in the interaction of RecA with CheA concerns the residues Ala214, Arg222, Asp224, Iso228, Val247 and Lys250 of the RecA protein, which also participate in the recombinase activity of this protein. On the other hand, in P5-domain of CheA, the residues Gly537 and Ser646 of subdomain 1, and Lys590, Thr591 and Ser646 of subdomain 2 are essential for the interaction with RecA.
- II. The characterized RecA-binding CheA interface does not overlap with any of CheA-, CheW- or MCP-binding regions identified so far. Certainly, RecA is able to interact with both CheA and CheW. Furthermore, all residues involved in RecA-CheA and RecA-CheW interfaces are highly conserved in *S. enterica* and among other members of *Enterobacteriaceae* family.
- III. Based on *in silico* protein modelling described herein, the chemoreceptor signalling complex fits one RecA molecule without any allosteric interference, thus permitting CheA interaction with both CheW and MCP and, in addition, the formation of chemotaxis ring complexes.
- IV. RecA interacts with both CheA and CheW *in vivo*. Indeed, only the presence of RecA able to interact with both proteins restore the CheA and Tar pole-clustering, and thus, the signalling complex formation in *S. enterica*  $\Delta recA$  mutants. Likewise, the chemotactic polar arrangements are disrupted with the overexpression of wild type RecA. This interaction with both proteins is also essential for the chemotaxis and the swarming motility of *S. enterica*.



- V. The activation of the SOS response or *recA* overexpression changes the intracellular distribution of RecA, CheA, CheW and Tar proteins, moving from the cell poles to along the cell axis.
- VI. Our proposed model suggests that when SOS response is activated (or when *recA* is overexpressed), the number of RecA molecules interacting with CheA and CheW is higher. Hence, the formation of new polar-clustering arrays is disrupted because of the unfeasibility to join chemotaxis units between them. The RecA-associated signalling complexes remain distributed along, abolishing also swarming displacement.
- VII. The results reject the idea that RecA sequesters either CheA, CheW or both proteins from the chemoreceptor unit. Instead, all the chemotaxis signal complex is associated with RecA once SOS response (or *recA* overexpression) is activated. Consequently, the SOS response activation does not abolish the chemotaxis ability of *S. enterica*.
- VIII. The obtained results determine the role of RecA protein in chemoreceptor signalling complexes and allow to understand the association of SOS response with chemotaxis and swarming motility of *S. enterica* at a molecular-level.

# 6 MATERIAL AND METHODS



## 6. Material and methods

### 6.1. Strains, plasmids and bacteriophages

Strains, plasmids and bacteriophages used in this study are listed in Table 6.1.

**Table 6.1.** List of strains, plasmids and bacteriophages used in this work.

| Strain or plasmid | Relevant characteristic(s)                                                                                                                                                                       | Source or reference                               |
|-------------------|--------------------------------------------------------------------------------------------------------------------------------------------------------------------------------------------------|---------------------------------------------------|
| <b>Strain</b>     |                                                                                                                                                                                                  |                                                   |
| DH5 $\alpha$      | <i>E. coli supE4 <math>\Delta</math>lacU169 (p80 <math>\Delta</math>lacZ <math>\Delta</math>M15) hsdR17, recA1, endA1, gyrA96, thi-1, relA1</i>                                                  | Clontech                                          |
| ATCC 14028        | <i>S. enterica</i> Typhimurium wild type strain                                                                                                                                                  | ATCC                                              |
| UA1927            | <i>S. Typhimurium <math>\Delta</math>recA</i>                                                                                                                                                    | 247                                               |
| UA1941            | <i>S. Typhimurium <math>\Delta</math>recA <math>\Delta</math>cheA</i>                                                                                                                            | This work                                         |
| UA1915            | <i>S. Typhimurium <math>\Delta</math>recA <math>\Delta</math>cheW</i>                                                                                                                            | 247                                               |
| UA1942            | <i>S. Typhimurium cheA::SNAP tar::CLIP</i>                                                                                                                                                       | This work                                         |
| UA1943            | <i>S. Typhimurium cheA::SNAP recA::CLIP</i>                                                                                                                                                      | This work                                         |
| UA1945            | <i>S. Typhimurium <math>\Delta</math>recA cheA::SNAP tar::CLIP</i>                                                                                                                               | This work                                         |
| UA1952            | <i>S. Typhimurium <math>\Delta</math>recA <math>\Delta</math>cheA <math>\Delta</math>cheW</i>                                                                                                    | This work                                         |
| <b>Plasmid</b>    |                                                                                                                                                                                                  |                                                   |
| pKOBEGA           | Vector containing the $\lambda$ Red recombinase system, Amp <sup>R</sup> , temperature sensitive                                                                                                 | Generous gift of Prof. G. M. Ghigo <sup>303</sup> |
| pCP20             | Vector carrying FLP system, OriV <sup>ts</sup> , Amp <sup>R</sup> , Cm <sup>R</sup>                                                                                                              | 304                                               |
| pKD4              | Vector carrying FRT-Kan construction, Amp <sup>R</sup> , Kan <sup>R</sup>                                                                                                                        | 304                                               |
| pUA1108           | pGEX 4T-1 derivative plasmid carrying without the GST fusion tag, carrying only the <i>Ptac</i> IPTG-inducible promoter and the <i>lacI<sup>q</sup></i> gene; Amp <sup>R</sup>                   | 247                                               |
| pGEMT             | Cloning vector, Amp <sup>R</sup>                                                                                                                                                                 | Promega                                           |
| pUA1135           | pGEMT derivative plasmid containing the <i>SNAP</i> -tag gene and kanamycin cassette flanked with FRT sequences under the control of the <i>Ptac</i> promoter, Amp <sup>R</sup> Kan <sup>R</sup> | This work                                         |
| pUA1136           | pGEMT derivative plasmid containing the <i>CLIP</i> -tag gene and kanamycin cassette flanked with FRT sequences under the control of the <i>Ptac</i> promoter, Amp <sup>R</sup> Kan <sup>R</sup> | This work                                         |
| pUA1130           | pUA1108 derivative plasmid containing the native <i>S. Typhimurium recA</i> gene under the control of the <i>Ptac</i> promoter, Amp <sup>R</sup>                                                 | 247                                               |

|                       |                                                                                                                                                                                                             |           |
|-----------------------|-------------------------------------------------------------------------------------------------------------------------------------------------------------------------------------------------------------|-----------|
| pUA1137               | pUA1108 derivative plasmid containing the <i>S. Typhimurium</i> <i>recA</i> <sup>A214V</sup> mutant under the control of the <i>Ptac</i> promoter, Amp <sup>R</sup> [pUA1108 <i>recA</i> <sup>A214V</sup> ] | This work |
| pUA1138               | pUA1108 derivative plasmid containing the <i>S. Typhimurium</i> <i>recA</i> <sup>R222A</sup> mutant under the control of the <i>Ptac</i> promoter, Amp <sup>R</sup> [pUA1108 <i>recA</i> <sup>R222A</sup> ] | This work |
| pUA1139               | pUA1108 derivative plasmid containing the <i>S. Typhimurium</i> <i>recA</i> <sup>R176A</sup> mutant under the control of the <i>Ptac</i> promoter, Amp <sup>R</sup> [pUA1108 <i>recA</i> <sup>R176A</sup> ] | 305       |
| pUA1141               | pUA1108 derivative plasmid containing the <i>S. Typhimurium</i> <i>recA</i> <sup>L10A</sup> mutant under the control of the <i>Ptac</i> promoter, Amp <sup>R</sup>                                          | This work |
| pUA1142               | pUA1108 derivative plasmid containing the <i>S. Typhimurium</i> <i>recA</i> <sup>L14A</sup> mutant under the control of the <i>Ptac</i> promoter, Amp <sup>R</sup>                                          | This work |
| pUA1143               | pUA1108 derivative plasmid containing the <i>S. Typhimurium</i> <i>recA</i> <sup>Q20A</sup> mutant under the control of the <i>Ptac</i> promoter, Amp <sup>R</sup>                                          | This work |
| pUA1144               | pUA1108 derivative plasmid containing the <i>S. Typhimurium</i> <i>recA</i> <sup>H163A</sup> mutant under the control of the <i>Ptac</i> promoter, Amp <sup>R</sup>                                         | This work |
| pUA1145               | pUA1108 derivative plasmid containing the <i>S. Typhimurium</i> <i>recA</i> <sup>F203A</sup> mutant under the control of the <i>Ptac</i> promoter, Amp <sup>R</sup>                                         | This work |
| pUA1146               | pUA1108 derivative plasmid containing the <i>S. Typhimurium</i> <i>recA</i> <sup>N213A</sup> mutant under the control of the <i>Ptac</i> promoter, Amp <sup>R</sup>                                         | This work |
| pUA1147               | pUA1108 derivative plasmid containing the <i>S. Typhimurium</i> <i>recA</i> <sup>K216A</sup> mutant under the control of the <i>Ptac</i> promoter, Amp <sup>R</sup>                                         | This work |
| pUA1148               | pUA1108 derivative plasmid containing the <i>S. Typhimurium</i> <i>recA</i> <sup>Y218A</sup> mutant under the control of the <i>Ptac</i> promoter, Amp <sup>R</sup>                                         | This work |
| pUA1149               | pUA1108 derivative plasmid containing the <i>S. Typhimurium</i> <i>recA</i> <sup>D224A</sup> mutant under the control of the <i>Ptac</i> promoter, Amp <sup>R</sup>                                         | This work |
| pUA1150               | pUA1108 derivative plasmid containing the <i>S. Typhimurium</i> <i>recA</i> <sup>I228A</sup> mutant under the control of the <i>Ptac</i> promoter, Amp <sup>R</sup>                                         | This work |
| pUA1151               | pUA1108 derivative plasmid containing the <i>S. Typhimurium</i> <i>recA</i> <sup>R243A</sup> mutant under the control of the <i>Ptac</i> promoter, Amp <sup>R</sup>                                         | This work |
| pUA1152               | pUA1108 derivative plasmid containing the <i>S. Typhimurium</i> <i>recA</i> <sup>LV247A</sup> mutant under the control of the <i>Ptac</i> promoter, Amp <sup>R</sup>                                        | This work |
| pUA1153               | pUA1108 derivative plasmid containing the <i>S. Typhimurium</i> <i>recA</i> <sup>LK250A</sup> mutant under the control of the <i>Ptac</i> promoter, Amp <sup>R</sup>                                        | This work |
| pUA1154               | pUA1108 derivative plasmid containing the <i>S. Typhimurium</i> <i>recA</i> <sup>F255A</sup> mutant under the control of the <i>Ptac</i> promoter, Amp <sup>R</sup>                                         | This work |
| pUA1155               | pUA1108 derivative plasmid containing the <i>S. Typhimurium</i> <i>recA</i> <sup>Q257A</sup> mutant under the control of the <i>Ptac</i> promoter, Amp <sup>R</sup>                                         | This work |
| pUA1156               | pUA1108 derivative plasmid containing the <i>S. Typhimurium</i> <i>recA</i> <sup>K286A</sup> mutant under the control of the <i>Ptac</i> promoter, Amp <sup>R</sup>                                         | This work |
| pUA1157               | pUA1108 derivative plasmid containing the <i>S. Typhimurium</i> <i>recA</i> <sup>Q300A</sup> mutant under the control of the <i>Ptac</i> promoter, Amp <sup>R</sup>                                         | This work |
| pUA1140               | pUA1108 derivative plasmid containing the <i>S. Typhimurium</i> <i>recA::CLIP</i> under the control of the <i>Ptac</i> promoter, Amp <sup>R</sup>                                                           | This work |
| pUA1158               | <i>recA</i> <sup>A214V::CLIP</sup> mutant under the control of the <i>Ptac</i> promoter, Amp <sup>R</sup>                                                                                                   | This work |
| pUA1159               | <i>recA</i> <sup>R222A::CLIP</sup> mutant under the control of the <i>Ptac</i> promoter, Amp <sup>R</sup>                                                                                                   | This work |
| pUA1160               | <i>recA</i> <sup>R176A::CLIP</sup> mutant under the control of the <i>Ptac</i> promoter, Amp <sup>R</sup> [pUA1108 <i>recA</i> <sup>R176A</sup> ]                                                           | This work |
| <b>Bacteriophages</b> |                                                                                                                                                                                                             |           |
| P22int7 (HT)          | High transductant <i>Salmonella</i> bacteriophage                                                                                                                                                           | 306       |

## 6.2. Oligonucleotides

Oligonucleotides used in this study are listed in Table 6.2. Invitrogen (Thermo Scientific) is the nucleotide supplier and all oligonucleotide vials were received in lyophilized form. All vials were reconstituted in sterile conditions with MQ water to a final concentration of 100  $\mu$ M.

**Table 6.2.** List of pair-primers used in *Salmonella* related work. Primer sequence are indicated, where priming sites are marked in capital letters.

| Primer name | Sequence                                                                                               | Application                                                                              |
|-------------|--------------------------------------------------------------------------------------------------------|------------------------------------------------------------------------------------------|
| Tar_clip_F  | agtgaacgctcagtcggcaataacgccgagtcattagccgccagggatgatgcgaa<br>ctgggaaaccttcGCCTCCGCCGCCCTCCATGGACAAAGAC  | Oligonucleotides to introduce CLIP-tag after <i>tar</i> gene                             |
| Tar_clip_R2 | ttttgctttatctatgcaaccagacgaaaggtatcgcggggtcgcaaattaatcgat<br>aaccgacagcgcacgtcgaATGGGAATTAGCCATGGTCC   |                                                                                          |
| R_clip_F    | taatcagaatgccacgcccgatttcgccgttgacgatagcgaagcggtgcagaaacc<br>aacgaagattttGCCTCCGCCGCCCTCCATGGACAAAGAC  | Oligonucleotides to introduce CLIP-tag after <i>recA</i> gene                            |
| R_clip_P2   | cataaatgcagcccttgatggtaattaacgttttgctgaatggcggtctgtttgcccgc<br>cccaccatcacctgatgaATGGGAATTAGCCATGGTCC  |                                                                                          |
| W_snap_F    | ggtgaatatcgaaaaactgctaacagcgaagagatggcgctgctggatatcgcagc<br>atcacacgtcggcctccgccgcccctccatggacaagaagac | Oligonucleotides to introduce SNAP-tag after <i>cheW</i> gene                            |
| W_snap_P2   | cgatgaagaggcactctcaccgctggcgaagcataacggatgaattgcccgatgg<br>cgcgacgccatccggcaacgtaATGGGAATTAGCCATGGTCC  |                                                                                          |
| A_snap_F    | cgcgctgattgtgatgtttccgattgcagggttaaacccggaacaacgtatggcgat<br>cacagccgcccctccgccgcccctccatggacaagaagac  | Oligonucleotides to introduce SNAP-tag after <i>cheA</i> gene                            |
| A_snap_P22  | caggaattcctgacctgacggctcggcggcagtttgcttacattactataccggtcata<br>ttattcccttctactcaaATGGGAATTAGCCATGGTCC  |                                                                                          |
| cApKO3BF    | agggatccTTCGATAATTCACCAGAATCAG                                                                         | Oligonucleotides for checking 500 bp downstream and upstream of its STOP codon           |
| cApKO3BR    | agggatccGATGTGGTGAAACGTAACAT                                                                           |                                                                                          |
| cheA_fw     | acacaggaacagttacatATGAGCATGGATATTAGCG                                                                  | Oligonucleotide to amplify since start of <i>cheA</i>                                    |
| cWpKO3BF    | agggatccCATTCTGGAGTAAATCCGT                                                                            | Oligonucleotides for checking 500 bp downstream and upstream of its STOP codon           |
| cWpKO3BR    | agggatccACCGGTATGAGTAATGTAAGC                                                                          |                                                                                          |
| pNAS_RecAf  | ttcacacaggaacagttacaATGGCTATCGACGAAAAC                                                                 | Oligonucleotides for checking <i>recA</i> gene from its start and final <i>recX</i> gene |
| recX_HF_f   | gggatcgcgccgaccggatccTCAATCTGCAAAATTCGCC                                                               |                                                                                          |
| tarpKO3BF   | AGggatccATGGCGATACTGTAAGTTCT                                                                           | Oligonucleotides for checking 500 bp downstream and upstream of its STOP codon           |
| tarpKO3BR   | agggatccACTAACATTCTGGCGCTGA                                                                            |                                                                                          |
| M304A F     | TACCCAGTCAgcgTTGGCCCAGC                                                                                | Oligonucleotides for CheA M303A mutant derivative construction                           |
| M304A R     | ATCACTAACTCGCCGACC                                                                                     |                                                                                          |
| L312A F     | TTCTAACGAGcgGACCCGGTAAACC                                                                              | Oligonucleotides for CheA L311A mutant derivative construction                           |
| L312A R     | CGCTGGGCCAACATTGAC                                                                                     |                                                                                          |

|         |                                      |                                                                |
|---------|--------------------------------------|----------------------------------------------------------------|
| G538A_F | TCGCGTGGCGgcgGAAGTTTTTA              | Oligonucleotides for CheA G537A mutant derivative construction |
| G538A_R | ACCGACATCCCATCGAGG                   |                                                                |
| D588A_F | GTTTGACGTGgcgGGGGCGAAAAC             | Oligonucleotides for CheA D587A mutant derivative construction |
| D588A_R | ACTTCCACAATTTCGACC                   |                                                                |
| K591A_F | GGACGGGGCGgcaACCGAAGCCA              | Oligonucleotides for CheA K590A mutant derivative construction |
| K591A_R | ACGTCAAACACTTTCACAATTTCGACC          |                                                                |
| T592A_F | CGGGGCGAAAgccGAAGCCACGC              | Oligonucleotides for CheA T591A mutant derivative construction |
| T592A_R | TCCACGTCAAACACTTTCACAATTTCGACC       |                                                                |
| S629A_F | AAATCTGGAAGccAATTATCGCAAGGTACCGG     | Oligonucleotides for CheA S628A mutant derivative construction |
| S629A_R | TTGACCACCACCTGGTGC                   |                                                                |
| S647A_F | GGGCGACGGCgccGTCGCGCTGA              | Oligonucleotides for CheA S646A mutant derivative construction |
| S647A_R | AGGATCGTCGCGGGCGGAAATC               |                                                                |
| F204A_F | TGGCGTGATGgcgGGTAACCCGG              | Oligonucleotides for RecA F203A mutant derivative construction |
| F204A_R | ATCTTCATACGGATCTGG                   |                                                                |
| I229A_F | TATCCGTCGTgcgGGCGCGGTGA              | Oligonucleotides for RecA I228A mutant derivative construction |
| I229A_R | TCAAGACGAACAGAGGCG                   |                                                                |
| R244A_F | TAGCGAAACGgcgGTGAAAGTGGTGAAAACAAAATC | Oligonucleotides for RecA R243A mutant derivative construction |
| R244A_R | CCCACGACATTATCGCCC                   |                                                                |
| F256A_F | CGCCGCGCCGgcgAAGCAGGCCG              | Oligonucleotides for RecA F255A mutant derivative construction |
| F256A_R | ATTTTGTTTTCACCACTTTCACACGCGTTTC      |                                                                |
| Q258A_F | GCCGTTTAAGgcgGCCGAGTTCC              | Oligonucleotides for RecA Q257A mutant derivative construction |
| Q258A_R | GCGGCGATTTTGTTTTC                    |                                                                |
| K287A_F | GCTGATCGAGgcgGCGGGCGCAT              | Oligonucleotides for RecA K286A mutant derivative construction |
| K287A_R | TTCTCTTTCACGCCAGG                    |                                                                |
| Q301A_F | GAAGATTGGCgcgGGTAAAGCGAACG           | Oligonucleotides for RecA Q300A mutant derivative construction |
| Q301A_R | TCGCCGTTGTAGCTGTAC                   |                                                                |

### 6.3. Microbiological methods

#### 6.3.1. Media and culture conditions

During this study, either solid, liquid or semisolid media were used. The composition of every medium and solution used in this study is described in detail in Annex 8.1. All solutions are diluted in MQ water, except when specifically indicated.

Unless otherwise noted, strains were cultured in Luria-Bertani (LB) broth (Table 8.1.1). Other media used in this work are: brain heart infusion (BHI) medium (Table 8.1.2), LB swarming (Table 8.1.3), LB swimming (Table 8.1.4), super optimal broth (SOB) medium (Table 8.1.5), super optimal broth with catabolite (SOC) medium (Table 8.1.6), tryptone broth (TBr) medium (Table 8.1.7), green agar plates (Table 8.1.8) and top agar (Table 8.1.9).

When necessary, antibiotics were added to growth medium with a microorganism-dependent final concentration, which are indicated in the Table 6.3. Other supplements used in different applications are mentioned in each specific case.

**Table 6.3.** Final antibiotic concentration ( $\mu\text{g/ml}$ ) in order to select the figured bacterial strains.

| Antibiotic           | Source    | Dose for microorganism ( $\mu\text{g/ml}$ ) |                    |
|----------------------|-----------|---------------------------------------------|--------------------|
|                      |           | <i>E. coli</i>                              | <i>S. enterica</i> |
| Ampicillin (Amp)     | Roche     | 100                                         | 100                |
| Chloramphenicol (Cm) | Roche     | 34                                          | 34                 |
| Kanamycin (Kan)      | Applichem | 50                                          | 75                 |

In all cases, culture media were sterilized by wet heat at 121°C during 15 minutes in an autoclave. Antibiotics and other non-autoclavable supplements were sterilised by filtration with 0.45  $\mu\text{m}$  pore diameter filters (Whatman).

After sterilisation, liquid media were allowed to cool progressively at room temperature (RT) and stored at 4°C until they were needed, where liquid were tempered at room temperature. Solid media were allowed to cool to 50°C and, when required, filtered antibiotics or other supplements were added while shaking. After that, solid media were plated into 9 Sterilin™ Petri dishes (ThermoFisher), allowed to solidify at room temperature and stored at 4°C.

The vast majority of experiments made in this work required the use of liquid cultures growing in early or mid-exponential phase. Overnight cultures (approx. 16 h) were diluted, usually 1/100, and incubated at 37°C with a constant shaking at 24.000 g



(Excella® shaker E5, New Brunswick Scientific) until the growth phase required was achieved. For those strains harbouring thermosensitive plasmids, incubations were made at 30°C to maintain the plasmid or at 42°C to curate it.

### 6.3.2. Swarming and swimming motility assays

Swarming and swimming motility assays were conducted to test *S. Typhimurium* behaviours regarding on different genetic mutant backgrounds. Fresh solid LB plates (Table 8.1.1) were streaked with the corresponding strains and incubated overnight at 37°C for *S. Typhimurium*. At the following day, new solid LB plates (Table 8.1.1) were streaked again from the overnight plate culture and incubated during 6 hours at the same mentioned temperatures.

Fresh LB swarming plates (Table 8.1.3) or swimming plates (Table 8.1.4) were also prepared the day of the assay. Small volume bottles were prepared and sterilized as described before (Section 6.3.1). After sterilization, 20 mL of medium was plated on 9 cm Petri dishes with constantly shaking to ensure homogenization of the agar. Supplements, such as sterile isopropyl  $\beta$ -D-1-thiogalactopyranoside (IPTG) (NZYTech), should be added at that point. After solidification, plates were placed with the lid ajar in an airflow cabin and allowed to dry during 15 minutes.

The inoculum was applied with a sterile toothpick. A single colony was picked and inoculated at the centre of the plate avoiding medium penetration in any case. After inoculation, plates were upwards incubated at 37°C during a controlled period of time, usually 9 to 12 hours for *S. Typhimurium*. This time is required to let wild type strain to reach the plate border. Plates were photographed when necessary (ChemiDoc™ XRS+ system, Bio-Rad).

### 6.3.3. Transduction assay

#### 6.3.3.1. Lysate preparation

Generalized transduction using the P22int7 (HT) phage was used to move several resistance markers between *S. Typhimurium* strains. The overall procedure is based on the guidelines published by Davis *et al.*, 1980<sup>307</sup>.

To prepare phage lysate, as previously described<sup>306</sup>, an overnight culture of the desired strains carrying the antibiotic marker of interest (donor) were processed. 1/100 dilution in fresh 10 mL of LB (Table 8.1.1) medium and incubated at 37°C until reach 0.5 OD<sub>550</sub> using Thermo Scientific Genesys 10S UV-Vis spectrophotometer. Then, culture was infected with 0.1-1 MOI of P22int7(HT) phage and incubated during 15 minutes at room temperature without shaking to allow phage absorption, and later incubated for 3 hours at 37°C with shaking. Finally, phages were recovered centrifuging the culture for 10 min at 15.000 g, keeping supernatant phase and filtering with 0.22 µm pore diameter filters (Whatman). Phage lysates were tittered and kept at 4°C.

#### 6.3.3.2. Phage titter

Lysates were quantified using the simple spot titering method. For that, a mixture of 100 µL of an overnight culture of a wild type *S. Typhimurium* and 2.5 mL of melted top agar (Table 8.1.9) was spreaded over a solid LB plate (Table 8.1.1). Once solidified, 100 µL of dilutions 10<sup>-6</sup>, 10<sup>-7</sup>, 10<sup>-8</sup> and 10<sup>-9</sup> of the phage lysate were spreaded on previous plates and allowed to dry with the lid ajar. Note that phages were always diluted with 10mM MgSO<sub>4</sub> (Table 8.2.3). The plates were then incubated overnight at 37°C. The number of plaques in each dilution-plate was counted and the average number of plaque-forming unit per each millilitre (PFU/mL) was calculated according to Formula 1.

**Formula 1.** Formula to calculate PFU/mL.

$$\frac{\text{PFU}}{\text{mL}} = \frac{\text{N}^{\circ} \text{ of plaques}}{\text{Volume of diluted lysate} \times \text{Dilution factor}}$$

### 6.3.3.3. Marker transduction

To perform phage transduction, an overnight culture of the desired strains of interest (receptor) were processed. 1/100 dilution in fresh 10 mL of LB (Table 8.1.1) medium and incubated at 37°C until reaching 0.5 OD<sub>550</sub>. Then, 1.5 mL tubes were prepared with the following mixes:

- 200 µL cells (as cellular control)
- 200 µL cells + phage at MOI 1
- 200 µL cells + phage at MOI 10
- 200 µL LB + phage at MOI 10 (as phage control)

Tubes were incubated during 15 minutes at room temperature without shaking to ensure the phage-cell contact, and later 1 hour at 37°C. After the incubation, the cells were recovered by centrifugation (10.000 g, 5 min), and re-suspend them in 100 µL of fresh LB (Table 8.1.1). The whole volume was plated in LB plates (Table 8.1.1) supplemented with the appropriate antibiotic (Table 6.3) and the plates were incubated ON at 37°C.

The absence of the prophage in the transductants was determined by streaking them onto green plates (Table 8.1.8) as described later (Section 6.3.3.4).

Transduction assay were used for two purposes:

- *recA* gene removal for the construction of *S. enterica*  $\Delta recA\Delta cheA$  and  $\Delta recA\Delta cheA\Delta cheW$  strains. In this case, strains obtainment was conducted as described in this section, taking advantage of the presence of kanamycin resistance disrupting the gene of interest.
- Recombinase assay of *recA* gene derivative mutants. In this other case, assay was attended with few modifications. Here, lysate preparation of *S. enterica*  $\Delta STM0363\Omega Km$  were prepared as donor strain and *S. enterica*  $\Delta recA$  carrying the derivative *recA* gene mutants were used as receptor. In marker transduction procedure, 1.5 mL tubes were prepared uniquely mixing 500 µL cells with 500 µL phage lysate at MOI 1. Finally, transductants were counted

and compared with *S. enterica*  $\Delta recA$  carrying the *recA* wild type plasmid (Formula 2).

**Formula 2.** Formula to calculate recombination activity of the RecA mutant derivatives.

$$\text{Recombinase activity} = 100 \times \frac{\text{N}^\circ \text{ of colonies } recA \text{ mutant derivative plate}}{\text{N}^\circ \text{ of colonies wild type } recA \text{ plate}}$$

#### 6.3.3.4. Phage removal

In order to remove phage of the transductant cells, a colony from the desired strain was spread and incubated at 37°C overnight in a green plate (Table 8.1.8) for acquire isolate single cells. After incubation, isolated light green colonies were selected and plated them in a new green plate (Table 8.1.8) again. The process was repeated at least 3 times until the whole bacterial mass was light green.

To test the presence of lysogenic phages, a virulence assay was performed. Hence, 5  $\mu\text{L}$  of P22int7(HT) phage is added in the middle of a green plate (Table 8.1.8). After let air-dry the drop, each isolated light green colony was inoculated with a microstreaker, from one side of the plate to the opposite side, crossing over the phage drop, and then plate was incubated overnight at 37°C.

The day after, plate could be analysed. Therefore, if the light green colony line becomes dark after cross the phage inoculation, it means that isolated strain could be infected. Those strains able to perform that were selected, always from as far away from the phage drop as possible.

#### 6.3.4. Chemotaxis capillary assay

Chemotaxis assays were conducted essentially as described by Adler in 1973<sup>136</sup> but some modifications were necessary to adapt it for *S. Typhimurium*<sup>308,309</sup>.

The chemotaxis chambers and capillary tubes were set using sterile forceps during all process in sterile conditions. In one hand, chemotaxis chambers were formed by laying three sterile V-shaped needles (40mm 18G needle, Nipro) under a 24 x 65 mm microscope cover slip n° 1.5 (thickness of 0.17mm required for super resolution microscopy, Menzel-Gläsner). Chemotaxis chambers were built inside of an aseptic Petri Dish (Deltalab). In the other hand, one end of the capillary tubes (1  $\mu$ L - 3 cm long Microcaps, Drummond Scientific Co.) were heat-sealed in a Bunsen flame and then autoclaved to ensure sterility. After that, the sealed capillaries were heated quickly passing four times through a flame and immediately dropped, with the open-end down, into a small vial containing 1 mL of tethering buffer (Table 8.2.1) and tethering buffer with 30 mM L-aspartate (Panreac) for *S. Typhimurium* (Fig. 6.1.A). Vials containing capillaries were cool-down for at least 30 minutes at 30°C (Fig. 6.1.B).

For the preparation of cell suspensions, each strain was cultured in 5mL TBr broth (Table 8.1.7) overnight at 30°C with shaking. The cultures were diluted 1:100 in 10mL of fresh TBr broth (Table 8.1.7) and incubated at 30°C until OD<sub>600</sub> reached 0.5. Cultures were pelleted by low-speed centrifugation (4500 g) for 15 minutes at room temperature. Then, pellets were washed twice with tethering buffer (Table 8.2.1) and adjusted with the same buffer at an OD<sub>600</sub> of 0.1. Finally, this suspension was diluted 1:10, which corresponds to approximately 5·10<sup>6</sup> CFU/mL.

Each chemotaxis chambers (Fig. 6.1.D) were filled with 2 mL of the strain dilution (Fig. 6.1.E). Then, filled capillaries were distributed with the open-end in contact with the suspension inner the chemotaxis chambers and incubated for 1 hour at 30°C (Fig. 6.1.F). Total of six capillaries were used for each strain, three filled with buffer (Table 8.2.1) and other three filled with buffer and chemoattractant.

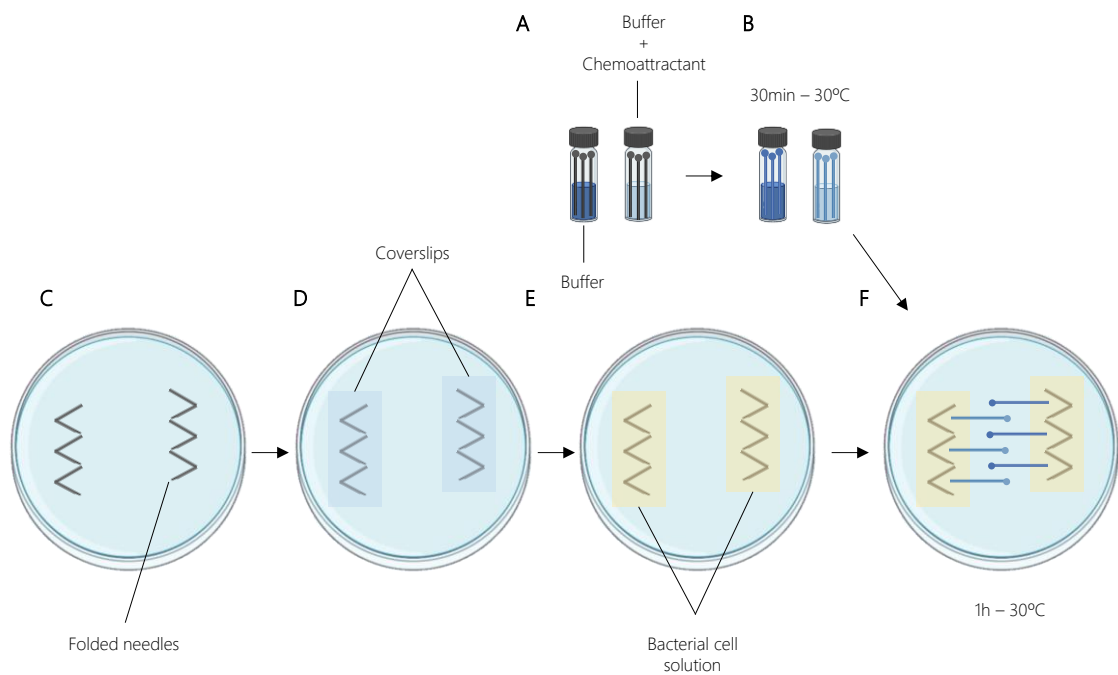


**Figure 6.1.** Step-by-step chemotaxis capillary procedure. **(A)** and **(B)** represent the capillary filled with buffer and buffer with chemoattractant. **(C-F)** describe chemotaxis chamber building and application.

After the incubation, the open-end of filled capillaries were rinsed with 200  $\mu$ L of saline solution (Table 8.2.4). Then, the sealed end of each capillary was broken with the forceps and these capillaries were emptied using the rubber bulb into a 1.5 mL microcentrifuge tube filled of 1 mL saline solution (Table 8.2.4). Re-filled tubes were diluted and plated into LB plates (Table 8.1.1). After overnight incubation at 37°C, CFU/mL were calculated.

### 6.3.5. Electrocompetent cell preparation

The preparation method was described by Dower *et al.* (1988) and it was used with some slight modifications.

For that, LB (Table 8.1.1) overnight cultures of bacterial strains were incubated at 37°C, or 30°C for bacterial strains carrying thermosensitive plasmids. The day after, the

required volume of LB medium (Table 8.1.1) was inoculated (1/100 dilution from the overnight) and allowed to grow at a convenient temperature with constant shaking until OD<sub>550</sub> 0.5-0.6 was reached. The culture was then transferred to previously chilled 50 mL Falcon tubes (Thermo Scientific) and centrifuged for 10 minutes at 24,000 g and 4°C. After that, the pellet was washed twice with 1 volume of cold MQ water. Preparation of electrocompetent cells for transformation at high voltages require the final cell suspension to have a very low conductivity. Thus, cells were twice washed with 0.5 volumes of sterilized ice cold 10 % glycerol (Panreac). Finally, cells were harvested and resuspended in 0.001 volumes of ice cold 10 % glycerol (Panreac). The resulting suspension was 50 µL distributed in 1.5 mL aliquots and frozen at -80°C until needed.

Note the case of electrocompetent cell preparation for gene-replacement method is detailed in Section 6.5.1.2.

### 6.3.6. Electrotransformation

Electrotransformation was conducted following the methods described by Dower *et al.* (1988)<sup>310</sup> and O'Callaghan and Charbit (1990)<sup>311</sup>, with some modifications.

The desired amount of DNA (plasmid DNA, 100-200 ng) was mixed with competent cells previously thawed on ice. The cells-DNA mix was then subjected to an electrical pulse (Bio-Rad Gene Pulser, Bio-Rad) with the electrical requirements noted in Table 6.4. Just after electroporation, cells were immediately recovered with 1 mL of LB medium (Table 8.1.1). Transformed cells were transferred to a glass tube, incubated at 37°C for 1 hour and finally spreaded into appropriate selective LB plates (Table 8.1.1).

**Table 6.4.** Relevant features microorganism-dependent for electroporation.

| Strain             | Cuvette length (mm) | Voltage (kV) | Time (ms) |
|--------------------|---------------------|--------------|-----------|
| <i>E. coli</i>     | 20                  | 2.5          | ≈5        |
| <i>S. enterica</i> | 20                  | 2.5          | ≈5        |

Note the case of electrocompetent cell transformation for gene-replacement method is detailed in Section 6.5.1.2.

#### **6.4. Nucleic acids manipulation methods**

##### **6.4.1. Nucleic acid quantification**

Quantification, purity and cleanness from all suspended DNA and RNA, being it either plasmid, genome, PCR-product or RNA extraction, was evaluated with absorbance measuring (Nanodrop 2000; Thermo Scientific):  $1.8 \leq A_{260}/A_{280} \leq 2.0$  and  $2.0 \leq A_{260}/A_{230} \leq 2.2$ , respectively. MQ water was always used to measure as blank.

##### **6.4.2. Agarose gel electrophoresis**

In order to check DNA or RNA integrity, plasmid digestions or PCR amplifications, agarose gel electrophoresis were performed regularly.

In short, the required amount of conventional agarose E (Condalab) was mixed with TAE 1X buffer (Table 8.2.5) in an Erlenmeyer to a final desired concentration. The mixture was heated in a microwave until agarose was dissolved and RedSafe™ Nucleic Acid Staining Solution (INtRON) at final concentration of 0.005 % (v/v) was added and agitated to homogenize solution. Then, solution was placed in a gel tray with the desired gel combs to form wells. Depending on the molecular weight of the samples to be loaded, agarose concentration ranged between 0.5 % and 2 % (w/v) were used.

Samples to be load were prepared by adding a tenth part of DNA loading buffer (Table 8.2.6) and mixed. Once gel was solidified and put in the buffer tank, wells were filled with the previously prepared sample, always using a suitable molecular weight marker. Electrophoresis was conducted at 120 V during 30 minutes, sufficient time to allow correct DNA bands separation, and using TAE 1X (Table 8.2.5) as running buffer.

Visualization of DNA gels was conducted by placing them on a UV-transillumination and image capture device (E-box-1000/20 M; Vilber Loumat).



### 6.4.3. DNA extraction

#### 6.4.3.1. Genomic DNA extraction

Genomic DNA extractions of needed strains (*S. Typhimurium* and derivative mutants) were performed using the commercial kit Easy-DNA™ (Invitrogen). Fresh overnight spreaded plate of bacterial strain were resuspended in PBS 1X (Table 8.2.16) and proceeded following manufacturer's instructions. Concentration and purity of extracted DNA were determined as described (Section 6.4.1). Resulted genomic DNA was finally stored at 20°C for long-term storage and diluted aliquots were stored at 4°C for short-term storage.

Genomic DNA extractions of needed strains were loaded on a 0.5 % agarose gel (Section 6.4.2) to check its DNA integrity.

#### 6.4.3.2. Plasmid DNA extraction

Small volume plasmid DNA extractions were performed using NZYMiniprep (NZYTech) as manufacturer's instructions. Concentration and purity of extracted DNA were determined as described (Section 6.4.1). Resulted genomic DNA was finally stored at 20°C for long-term storage and diluted aliquots were stored at 4°C for short-term usage.

Genomic DNA extractions of needed strains were loaded on a 0.75 % agarose gel (Section 6.4.2) to check its DNA integrity.

### 6.4.4. Polymerase chain reaction (PCR)

#### 6.4.4.1. DNA amplification for cloning

For cloning amplifications, where high fidelity was required, Phusion® High Fidelity DNA polymerase (Thermo Scientific) was used following manufacturer's instructions. Final concentrations of reaction mixture constituents for this polymerase are described in Table 6.5. The maximum final reaction volume used was 100 µL divided in two 0.2

ml PCR tubes, maintaining concentration ratios between master mix constituents. Same reactions were placed and recovered (Section 6.4.5) together.

**Table 6.5.** Composition for Phusion®-PCR mix.

| Component                 | Supplier          | Amount $\mu\text{L}$ |
|---------------------------|-------------------|----------------------|
| High Fidelity Buffer      | Thermo Scientific | 5                    |
| dNTPs 2 mM                | NZY               | 4                    |
| DMSO                      | Thermo Scientific | 2                    |
| Primer forward            | Thermo Scientific | 5                    |
| Primer reverse            | Thermo Scientific | 5                    |
| Polymerase                | Thermo Scientific | 0.4                  |
| DNA 100 ng/ $\mu\text{L}$ |                   | 1                    |
| MQ water                  |                   | To 100               |

#### 6.4.4.2. DNA amplification for plasmid construction screenings

Colony PCR was routinely used for screening purposes when performing cloning steps. Briefly, a single colony was picked using a sterile toothpick and resuspended in 50  $\mu\text{L}$  of MQ water in a 0.2 mL PCR tube and repeated in batches of 8 colonies for each ligation transformed. Tubes were placed in a thermocycler during 10 minutes at 90°C in order to boil samples and let DNA emerge from cells. Then, tubes were centrifuged until cell debris were pelleted. The supernatant from these boiled tubes were used as DNA template for the PCR.

PCR reaction was performed using the kit DNA polymerase (Biotools®), with the final concentration of the reaction constituents defined in the Table 6.6, adjusting to approximately 15  $\mu\text{L}$  as final volume.

**Table 6.6.** Composition for Biotools®-PCR mix.

| Component      | Supplier          | Amount $\mu\text{L}$ |
|----------------|-------------------|----------------------|
| Buffer         | Biotools          | 1.25                 |
| dNTPs 2 mM     | NZY               | 0.5                  |
| Primer forward | Thermo Scientific | 0.625                |
| Primer reverse | Thermo Scientific | 0.625                |
| Polymerase     | Biotools          | 0.025                |
| Boiled colony  |                   | 1                    |
| MQ water       |                   | 10                   |

#### 6.4.4.3. DNA amplification for chromosomal construction screening

To screening edited bacterial chromosomes (Section 6.5.1), Invitrogen™ Standard *Taq* DNA Polymerase (Thermo Scientific) was used as described in Table 6.7. Here, purified genomic DNA as detailed previously (Section 6.4.3.1) was used as DNA template. Final used volume was 25  $\mu\text{L}$  for screening, whereas 100  $\mu\text{L}$  as final volume from positive clone was used to be recovered (Section 6.4.5) and finally sequenced (Section 6.5.3).

**Table 6.7.** Composition for Invitrogen™ Standard *Taq*-PCR mix.

| Component                 | Supplier          | Amount $\mu\text{L}$ |
|---------------------------|-------------------|----------------------|
| Buffer                    | Thermo Scientific | 2.5                  |
| DNTPs 2 mM                | NZY               | 1                    |
| $\text{MgCl}_2$           | Thermo Scientific | 0,75                 |
| Primer forward            | Thermo Scientific | 1.25                 |
| Primer reverse            | Thermo Scientific | 1.25                 |
| Polymerase                | Thermo Scientific | 0.1                  |
| DNA 100 ng/ $\mu\text{L}$ |                   | 0.5                  |
| MQ water                  |                   | To 25                |

#### 6.4.4.4. DNA amplification for $\lambda$ Red recombination method

Invitrogen™ Standard *Taq* DNA Polymerase (Thermo Scientific) was also used to acquire DNA product needed for the  $\lambda$  Red one-step inactivation (Section 6.5.1). The maximum final reaction volume used was 200  $\mu\text{L}$  divided in four 0.2 ml PCR tubes,

maintaining concentration ratios between master mix constituents from Table 6.7. Same reactions were placed and recovered (Section 6.4.5) together.

#### 6.4.5. PCR products recovery and DNA purification

DNA derived from PCR amplifications or digestions were recovered using NZYGelpure (NZYTech) following the manufacturer's recommendations. Quantification, cleanness and purity of the recovered DNA were performed as previously described (Section 6.4.1).

#### 6.4.6. DNA cloning

##### 6.4.6.1. Restriction DNA polymerases

All restriction endonucleases were mainly supplied by Roche and New England Biolabs. Every reaction was performed following the manufacturer's recommendations for each enzyme. The reaction volume was usually 20  $\mu$ L. When a large amount of DNA needs to be processed, the reaction volume became 100  $\mu$ L. All reactions were finally purified as described (Section 6.4.5).

In the case of double digestions, the best compatible buffer enzyme was chose attending NEBcloner (<https://nebcloner.neb.com/#!/redigest>) online server.

##### 6.4.6.2. Dephosphorylation

Digested vectors were dephosphorylated to prevent re-ligation during cloning procedures. Briefly, 1.5 U of recombinant shrimp alkaline phosphatase (NEB) was mixed with DNA and 10X dephosphorylation buffer (supplied) in a final volume of 40  $\mu$ L adjusted with MQ water. The mix was then incubated for 30 minutes at 37°C. After that, another 1.5 U of phosphatase were added to the mix, gently shacked, and incubated another 30 minutes at the same temperature. Finally, the phosphatase was

inactivated by placing the mixture at 65°C for 10 minutes and the DNA was recovered as previously explained (Section 6.4.5).

#### 6.4.6.3. HiFi DNA assembly

HiFi DNA Assembly technology relies on homologous recombination to assemble adjacent DNA fragments sharing end-terminal homology. NEBuilder HiFi DNA Assembly Master Mix (NEB), provided in the HiFi DNA assembly cloning kit (NEB), includes: exonucleases to create single-stranded 3' overhangs, DNA polymerase to fill gaps within each annealed fragment, and DNA ligase to seal nicks in the assembled DNA.

To proceed the protocol, the reaction was kept on ice and the components were mixed as described in Table 6.8. Insert DNA amount was calculated as the Formula 3 describes.

After assembly, product always was dialyzed. To perform dialysis, ligation was delivered upon a 0.05 µm pore size membrane filter (Millipore) floating over an empty plate filled with 10 mL MQ water. Disk-membrane can exchange salt ions from ligation solution to MQ water. After 10 minutes, ligation was recovered and kept at 4°C until its use.

**Formula 3.** Formula to calculate the required mass of insert to put in the HiFi DNA assembly mix.

$$\text{required mass insert (ng)} = \frac{\text{insert DNA length} \times \text{ratio [insert / vector length]}}{\text{vector DNA mass of vector (ng)}}$$

**Table 6.8.** HiFi DNA assembly mix composition.

| Components                                              | Value         |
|---------------------------------------------------------|---------------|
| 2x NEBuilder HiFi DNA Assembly Master Mix (NEB)         | 5 $\mu$ l     |
| Vector DNA                                              | 60 ng         |
| Insert DNA fragment (ratio [insert/vector lengths] 5:1) | To calculate  |
| MQ water                                                | To 10 $\mu$ l |

## 6.5. Mutant construction

### 6.5.1. $\lambda$ Red recombination procedure

#### 6.5.1.1. DNA preparation

$\lambda$  Red one-step inactivation procedure was primarily described by Datsenko and Wanner (2000)<sup>304</sup> to generate gene deletion in a fast and reliable *E. coli* K-12. In this work, one-step inactivation has been used with some slight modifications to generate some of the *S. Typhimurium* mutant strains, as proceeded previously<sup>246,247</sup>.

The *kan* resistance was amplified from the pKD4 plasmid as described in Section 6.4.4.4. This vector contains a kanamycin resistance gene as selectable marker flanked by FRT in each side, the target sequences for the FLP recombinase.

Suitable primers were designed as follows:

Forward: 5'- H1 + P1 -3'

Reverse: 5'- H2 + P2 -3'

The indicated P1 (5'-GTGTAGGCTGGAGCTGCTTC-3') and P2 (5'-TGGAATTAGCCATGGTCC-3') are priming sites located near the FRT-flanked resistance cassette included in the pKD4 plasmid (Fig. 6.2.A.2). Instead, H1 and H2 refer to the 80bp-homology extensions, which overlap with the region of interest (Fig. 6.2.A.1 and 6.2.B.1).

This method was used not only for gene replacement (Fig. 6.2.A) but also for tag addition (Fig. 6.2.B) with some modifications.

For tag addition, pGEM-T vectors (Promega) containing -SNAP or -CLIP tags from pSNAP-tag® (T7)-2 and pCLIPf vectors (NEB) followed by the kanamycin cassette

from pKD4 vector<sup>304</sup> were constructed using HiFi DNA assembly cloning method (Section 6.4.6.3) giving rise to pUA1135 and pUA1136, respectively. These plasmids were used as the template to amplify the tag followed by the kanamycin cassette as described (Section 6.4.4.4) using the suitable oligonucleotides (Table 6.2). These plasmids contain -SNAP or -CLIP tag, followed by the FRT-flanked kanamycin resistance cassette (Fig. 6.2.B). Hence, appropriate primers were designed as follows:

Forward: 5'\_ H1 + Fw \_3'                      Reverse: 5'\_ H2 + P2 \_3'

Here, Fw indicates the priming site where it hybrids at the ATG-start of the tag gene sequence. The *kan* gene was amplified from these plasmids as described for this gene addition case.

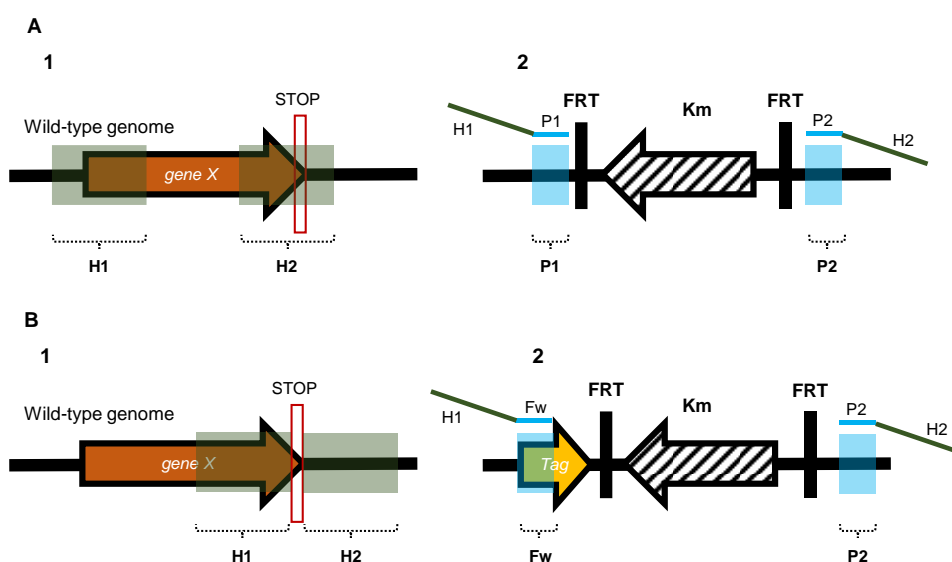


**Figure 6.2.** Scheme representation of primer design for gene replacement or tag addition. Primer design for gene replacement are represented in (A) and for tag addition in (B).

The PCR product was then loaded into an agarose gel (Section 6.4.2) and recovered in 90  $\mu$ L volume (Section 6.4.5). After that, the recovered product was digested with *DpnI* endonuclease for 16 hours at 37°C. This restriction endonuclease cleaves only when its recognition site is methylated, thus only the remaining pKD4 plasmid, but not the amplified DNA, was cut.

After digestion, DNA was directly recovered from solution (Section 6.4.5) in 15  $\mu$ L final volume and quantified (Section 6.4.1).

#### 6.5.1.2. Electrocompetent cell preparation and electrotransformation

Competent cells were prepared as described in Section 6.3.5, with some modifications. The temperature of incubation in this time was 30°C to maintain the sensitive plasmid (pKOBEGA or pKOBEG). Furthermore, the medium growth was SOB with 20 mM DL-arabinose (Sigma) and the pertinent antibiotics (Table 6.3).

Then, the remaining product was finally transformed into a *S. Typhimurium* strain and mutant derivatives harbouring the pKOBEGA plasmid, as explained below (Section 6.3.5). Cells were recovered with 1 mL of SOC medium (Table 8.1.6) and transferred to a 1.5 mL tube. Tubes were incubated at 37°C for 1.5 hours and finally spreaded into selective LB plates (Table 8.1.1).

In all cases, gene replacement in all constructs was verified by PCR using suitable primers followed of sequencing (Section 6.5.3).

#### 6.5.1.3. pKOBEGA removal

Plasmid carrying  $\lambda$  Red recombinase were cured from the mutant strains using incubations at restrictive temperature, hence 42°C.

For incubations, strain was inoculated in 5 mL of fresh LB (Table 8.1.1) and incubated overnight at 42°C. The next day, a 1/100 dilution of the culture was placed over day and allowed to grow at 42°C to stationary phase (approx. 8 hours). Then, the dilutions  $10^{-5}$ ,  $10^{-6}$  and  $10^{-7}$  were plated on LB (Table 8.1.1) and the plates were incubated overnight at 30°C. This procedure allowed the elimination of the pKOBEGA plasmid<sup>304</sup> due to its temperature conditional origin of replication. Finally, individual colonies were picked and replica plated onto LB plates supplemented with kanamycin (to select for the previous gain of the *kan* gene) and LB containing ampicillin or



chloramphenicol (to select cells with pKOBEGA). Colonies growing on LB-kanamycin but not on LB-ampicillin or chloramphenicol were selected and PCR-checked.

#### 6.5.1.4. Antibiotic marker removal

When necessary, pCP20 plasmid harbouring FLP recombinase activity was transformed into the desired recipient strain using the electrotransformation procedure as described on section A. However, incubations (phenotypic expression and overnight on selective plates) were conducted at 30°C due to pCP20 has a thermosensitive replication origin, in ampicillin-chloramphenicol selective plates. The day after, some colonies were inoculated into 5 mL of fresh LB (Table 8.1.1) and then incubated overnight at 42°C.

Again, the next day, an 1/100 dilution of the culture was placed over day and allowed to grow at 42°C to stationary phase. Then, dilutions  $10^{-5}$ ,  $10^{-6}$  and  $10^{-7}$  were plated on LB (Table 8.1.1) and the plates were incubated overnight at 42°C. Finally, individual colonies were picked and replica plated onto LB plates and LB containing chloramphenicol (to select for the loss of the plasmid) and kanamycin (to select for the loss of the *kan* gene). Colonies growing on LB but not on LB-ampicillin and LB-chloramphenicol were selected and PCR-checked (Section 6.4.4.3).

#### 6.5.2. Construction of tagged genes and overexpressing vectors

Co-immunoprecipitation (CoIP) assays were performed using proteins carrying -6xHis and -FLAG tags. Likewise, -CLIP and -SNAP tagged proteins were used for fluorescence and STED microscopy. Plasmids harbouring the corresponding tagged genes were constructed using the appropriate oligonucleotides (Tables 6.2 and 6.3) and the HiFi DNA assembly cloning kit (NEB, Section 6.4.6.3). The tag sequences (-6xHis, -FLAG, -CLIP and -SNAP) were included at the 3' end of the genes preceded by a 3×Gly linker. All PCR products were digested (Section 6.4.8.1), cloned (Section

6.4.8.3) into the pUA1108 overexpression vector<sup>247</sup> and transformed into *E. coli* DH5 $\alpha$ . When needed, site directed mutagenesis kit (Agilent) were also used for introducing specific nucleotide variations to induce the desired amino acid change in the resulting protein.

All constructions were confirmed by PCR (Section 6.4.4.2) and sequencing (Section 6.5.3). In all cases, the expression of corresponding plasmids (Section 6.6.1) was confirmed in SDS-PAGE gel (Section 6.6.4) and the tagged plasmids were confirmed by Western blot (Section 6.6.6).

### 6.5.3. Sequencing of strains and plasmids

In order to check point mutations, insertions or deletions when required, DNA was sequenced using Illumina® technology. Sequencing procedure was conducted by Macrogen Sequencing server in Madrid, Spain.

Needed plasmids were extracted as explained into Section 6.4.3.2. Checks on genomic DNA or plasmid were conducted by previous PCR (Section 6.4.4.2 or 6.4.4.3) using appropriate oligonucleotides (Table 6.2). Service provider required in 10  $\mu$ L at least 250 ng of purified DNA or 500 ng of plasmid, with 50 pmoles of the corresponding primer (Table 6.2).

## 6.6. Protein manipulation methods

### 6.6.1. Protein overexpression

Overnight cultures prepared with LB medium (Table 8.1.1), supplemented with corresponding antibiotics (Table 6.3), were incubated during 16 hours at 37°C. The day after, overnights were 1/100 diluted in 10 - 100 mL fresh LB medium (Table 8.1.1) and they were incubated until reach 0.4-0.6 OD<sub>600</sub>. Hence 1 mM IPTG (NZYTech) were added in cultures, and they were incubated during 3 more hours at the same temperature.

The final culture was pelleted, supernatant discarded and pellets kept at -20°C. In this work, new constructed vectors were checked by this method and little volumes were used. Instead, large volumes were applied in ColP lysates, where high amounts of protein were needed.

In order to check overexpression, 1 mL of the pre-IPTG induction- and final-cultures were recovered. The recovered volume was also pelleted and supernatant discarded, but also diluted with 45 µL MQ water and 15 µL Laemmli 4X buffer (Table 8.2.7). Then, pellets were subjected to 3 freeze-boil cycles to allow cell disruption. Samples were boiled at 100°C for 5 minutes and once samples were adequately fluid, were loaded in SDS-PAGE gel (Section 6.6.4). Resulted overexpression could be compared to its own control (pre-IPTG induction).

#### 6.6.2. Whole-cell lysates preparation

ColP pellets were suspended in lysis buffer (Table 8.2.9). The volume of lysis buffer (Table 8.2.9) added was equivalent to one hundredth of the original culture volume of the pellet. These pellets were then lysed by sonication whereas the cold chain was maintained. Five pulses of 30 second length and 20 % amplitude were applied (Digital Sonifier® 450, Branson). After lysis, lysates were centrifuged 10.000 g during 5 minutes at 4°C to remove cell debris. Supernatants were recovered in a clean, autoclaved microcentrifuge tubes.

#### 6.6.3. Protein quantification

Protein quantification of lysates was performed using a modified Bradford method (Bradford, 1976). BSA (Panreac) in a range of 1,5 to 200 µg/mL was used as standard and BioRad Protein Reagent Dye® (BioRad) was used as Bradford reagent.

In short, four half-serial dilutions of unknown samples were placed in a 96-well flat bottom microtiter plate (Deltalab). The standards and at least four blank replicates were also included.

Briefly, samples and standards were diluted in 140  $\mu$ L final volume of MQ-water. Next, 20  $\mu$ L of 1 M NaOH (Panreac) were added to each well. NaOH (Panreac) is used to ensure that the sample does not precipitate upon addition of Bradford reagent as it facilitates protein solubility, especially for membrane proteins (Stoscheck, 1990). Finally, 40  $\mu$ L of concentrated Bradford reagent were added to each well and pipette-mixed. After a 5 minutes incubation, the  $A_{595}$  was measured using a microtiter plate reader (Sunrise, Tecan). Samples were quantified twice to ensure absorbance.

As obtaining whole-cell lysates for CoIP quantifications was a laborious procedure due to the large number of different lysates to be tested, the BSA calibration method was excluded and only absorbance was considered. Hence, CoIP lysates were diluted with lysis buffer (Table 8.2.9) until all of them reached  $1.00 \pm 0.01 A_{595}$  using the described Bradford method.

#### 6.6.4. SDS-PAGE

SDS-PAGE was routinely used to visualize protein presence and integrity. 15 % polyacrylamide gels were prepared with three quarters of the total gel with separating gel (Table 8.2.8.1) and the superior quarter with stacking gel (Table 8.2.8.2). In these gels, the principal proteins, CheA ( $\approx 72$  KDa), RecA ( $\approx 38$  KDa), CheV ( $\approx 37$  KDa) and CheW ( $\approx 18$  KDa) could be visualized. The electrophoresis was conducted in tris-glycine-SDS buffer (TGS 10X, Laboratorios Conda) at 250 V for 60 minutes.

After that, coomassie staining (Section 6.6.5) was performed to visualize the protein bands, whereas western blotting (Section 6.6.6) was implemented to visualize tagged protein bands.

#### 6.6.5. Coomassie staining

After that, acrylamide gels were stained using Coomassie staining solution (Table 8.2.10) for 10 minutes at room temperature while shaking. To visualize the protein bands, gels were faded in 10 % acetic acid solution (Panreac) until the gel become transparent. If needed, gels were photographed (ChemiDoc™ XRS+ system, Bio-Rad).

Amersham™ ECL™ Rainbow™ (Sigma) was the molecular weight marker used with the purpose of whole cell protein visualization.

#### 6.6.6. Western blot

Supernatants were separated by SDS-PAGE on a 15 % polyacrylamide gel (Section 6.6.4, Table 8.2.8). Then, gel was soaked in western transfer buffer (Table 8.2.12) for 10 minutes.

For membrane activation, 10x10 cm PVDF Immobilon membrane (Merck) was activated by soaking it in methanol 100 % for 10 minutes, then methanol 25 % for 10 minutes and finally, western transfer buffer (Table 8.2.11) for 10 minutes.

Then, proteins from the gel were transfer to the activated membrane in 7 minutes using Thermo Scientific™ Pierce™ Power Blotter (Thermo Scientific). For that, the western blot sandwich is introduced into de power blotter cassette. This sandwich consisted of two 3MM filter papers soaked in western transfer buffer (Table 8.2.11), then the activated membrane, the gel and, finally, two more soaked 3MM filter papers. After protein transfer, transferred membranes were recovered and incubated with 10 mL of western blocking buffer (Table 8.2.12) during 30 minutes at room temperature with orbital shaking. Then, mouse anti-6xHis IgG1 (Merck) and rabbit anti-FLAG® (Merck) were incubated with the membranes during 3 hours. After primary antibody incubation, membranes were washed with western wash buffer (Table 8.2.13) and then, incubated again with horseradish-peroxidase (HRP)-coupled

anti-mouse IgG or anti-rabbit IgG antibodies (Acris) during an hour. After washes with western wash buffer (Table 8.2.13), the membranes were revealed using a HRP chemiluminescent substrate (SuperSignal™ West Pico PLUS Chemiluminescent Substrate, Thermo Scientific) following the manufacturer's instructions. Finally, the membranes were imaged using a ChemiDoc™ XRS+ system (Bio-Rad).

Note that all used antibodies were diluted in 10 mL of western blocking buffer (Table 8.2.12), volume necessary to cover one membrane in a 20 x 15 cm pyrex plate.

Precision Plus Protein™ Western C™ Blotting Standard (Bio-Rad) was the molecular weight marker used with the purpose of tagged cell protein visualization.

#### 6.6.7. Co-immunoprecipitation assay

##### 6.6.7.1. Cell lysis

Cultures of *S. enterica*  $\Delta recA\Delta cheA$  carrying the corresponding overexpression plasmid encoding a *recA* or *cheA* tagged gene and their corresponding mutant derivatives were used (Table 6.1). *S. enterica*  $\Delta recA\Delta cheW$  background was used when *cheW* tagged gene was induced. In all cases, the tagged-gene overexpression was induced by the addition of 1 mM of IPTG (NZYTech) and cell lysates were obtained by sonication (Branson Digital Sonifier). As control, cells lysates harbouring the pUA1108 overexpression vector were obtained following the same procedure.

##### 6.6.7.2. Tagged Protein A magnetic beads

The CoIP assays were performed using Pure Proteome Protein A magnetic beads (Millipore) coated, following the manufacturer's instructions, with either mouse anti-FLAG IgG or anti-6xHis IgG monoclonal primary antibodies (Sigma). In short, magnetic beads were washed with CoIP wash buffer (Table 8.2.14) and incubated with the corresponding antibody with CoIP blocking buffer (Table 8.2.15) during 2 hours at room temperature with soft shacking. Then, coated beads were twice washed to avoid

unspecific antibodies and these beads were incubated with CoIP blocking buffer (Table 8.2.15) 2 hours with gently shaking at room temperature. Finally, the coated magnetic beads were incubated overnight with the control lysates with gently shaking at 4°C to minimize non-specific interactions.

### 6.6.7.3. Co-immunoprecipitation

The CoIP assays were conducted as described previously<sup>247,283</sup> with a few modifications.

Two cell lysates containing the corresponding proteins were mixed and incubated at 30°C for 1 h without shaking to allow protein-protein interaction and kept at 4°C without shaking to maintain specific interactions for 16h. Afterwards, treated coated magnetic beads were added to the lysate mixture for 1h at RT with gently shaking.

Magnetic beads were then recovered, washed 3 times with PBS 1X (Table 8.2.16) and heated for 10 minutes at 90°C. Supernatants were mixed with Laemmli buffer 4X (Table 8.2.7) and results were obtained loading samples in SDS-PAGE gel (Table 8.2.8) to perform a Western blot (Section 6.6.6).

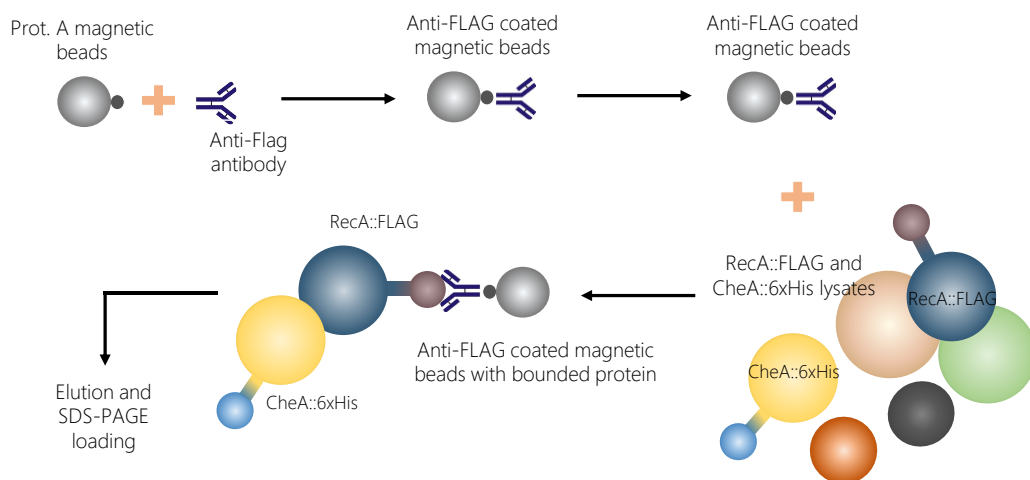


**Figure 6.2.** Schematic representation of coimmunoprecipitation assay of interacting RecA::FLAG and CheA::6xHis proteins.

## 6.7. Microscopy methods

### 6.7.1. SNAP- and CLIP- labelling

*S. enterica* cells were labelled using SNAP-Cell® 505-Star and CLIP-Cell™ TMR-Star permeable dyes, which specifically recognize SNAP- and CLIP- tags, respectively, following the manufacturer's instructions. The SNAP and CLIP technology is briefly described in Figure 6.3.

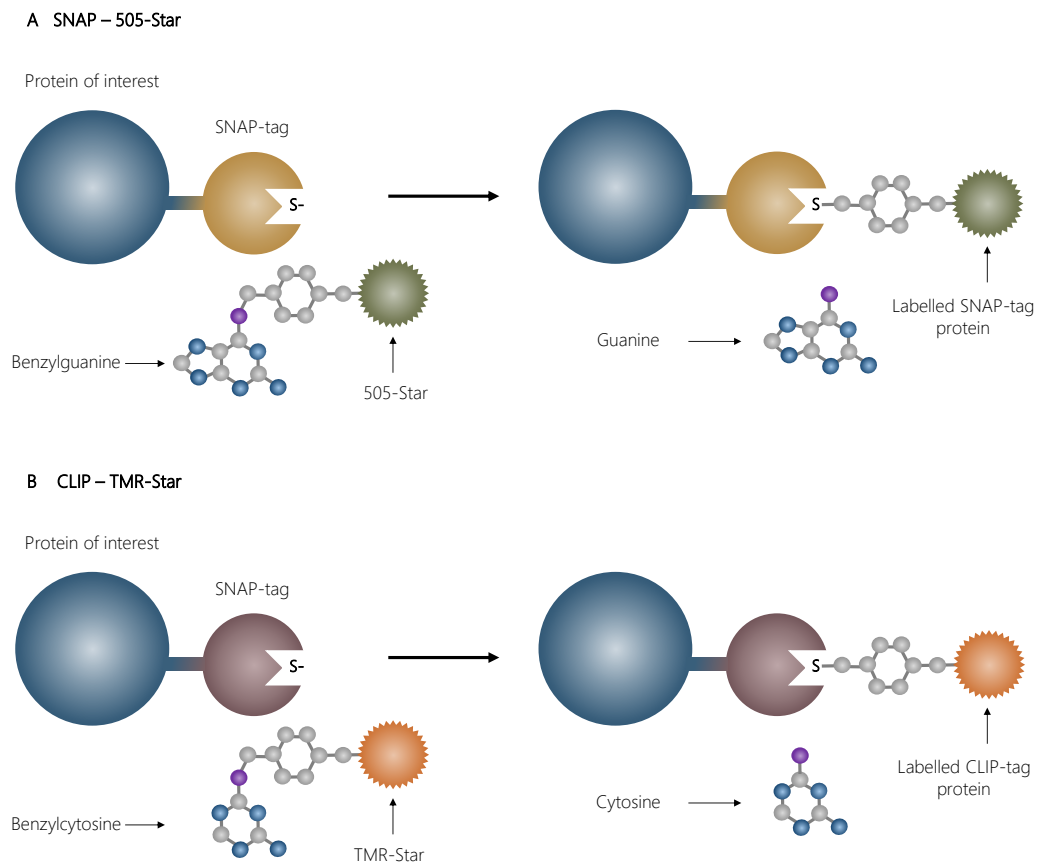


**Figure 6.3.** Representation of **A)** SNAP-Cell® 505-Star and **B)** CLIP-Cell™ TMR-Star technologies. Each O<sup>6</sup>-alkylguanine-DNA-alkyltransferase based protein (SNAP and CLIP) and their corresponding substrate (benzylguanine and benzylcytosine, respectively) are pictured. "S-" means the sulfide bound where follows the enzyme reaction.



Briefly, overnight cultures of the corresponded tagged strains were grown at 30°C in TBr (Table 8.1.7), supplemented, when needed, with corresponding antibiotic (Table 6.3). After 16 hours, overnight cultures were diluted 1:100 in fresh TBr medium (Table 8.1.8) and incubated at 30°C until an OD<sub>600</sub> of 0.08–0.1 was reached. Here, supplements were added (0.08 µg mitomycin C/mL or 40 µM IPTG) if required. All cultures were incubated 2 more hours. Then, cells were collected by centrifugation, washed once using ice-cold tethering buffer (Table 8.2.1) and resuspended in 20–100 µL of the same buffer. Then cells were stained with the permeable dyes SNAP-Cell® 505-Star and CLIP-Cell™ TMR-Star, following the manufacturer's instruction and avoiding light. Finally, cells were fixed with paraformaldehyde, resuspended in PBS 1X (Table 8.2.16), mounted on 35-mm poly-L-lysine-pre-coated coverslips using Mowiol-DABCO mounting medium (Table 8.2.17) and air-dried.

#### 6.7.2. Coverslip mounting

Coverslip mounted was proceeded as described<sup>283</sup>. For that, 35-mm coverslips were incubated with 0.1 % (w/v) in H<sub>2</sub>O poly-L-lysine solution (Sigma) during 1 hour at 37°C. Then, coverslips were twice washed with MQ water and air-dried at room temperature. POSSAR

Labelled cells (Section 6.7.1) were incubated 15 minutes on the poly-L-lysine-pre-coated coverslips, washed with MQ water and mounted on using Mowiol®-DABCO mounting medium (Table 8.2.17) and air-dried. Mowiol® is a hydrolysed polyvinyl alcohol and the mounting medium based on Mowiol polymerizes upon contact with air and sets, usually overnight. The recipe (Table 8.2.17) uses DABCO (1,4-diazabicyclooctane) as antifade reagent and it is almost identical to the mounting medium described below.

### 6.7.3. Chemoreceptor clustering assay

The chemoreceptor polar cluster arrays were visualized as previously described<sup>247</sup>, with a few modifications.

The labelled (Section 6.7.1) and mounted (Section 6.7.2) samples were examined under an Axio Imager M2 microscope (Carl Zeiss Microscopy) equipped with the appropriate filter set [green channel: GFP (Zeiss filter set 38); red channel: Rhod (Zeiss filter set 20)]. Cell fields were photographed and at least 350 cells were visually inspected. All images were acquired under identical conditions. Each experiment was performed at least in triplicate using independent cultures; a minimum of 1050 cells from each studied strain were therefore analysed. The images presented in the figures are representative of the entire image set. ImageJ software (National Institutes of Health) was used to quantify the number of clusters and to prepare images for publication.

### 6.7.4. STED microscopy imaging

The two-colour labelled and mounted samples (Sections 6.7.1 and 6.7.2) were observed using a commercial gated-STED microscope (Leica TCS SP8 STED 3X) equipped with a pulsed white light laser source and three depletion lasers. Prior to STED imaging, samples were examined under an Axio Imager M2 microscope (Carl Zeiss Microscopy) to ensure that at least 90 % of the cells were correctly labelled.

STED illumination of cells tagged with SNAP-Cell® 505-Star was performed using a 505-nm line, and depletion using a 592-nm line. For the CLIP-Cell™ TMR-Star tag, the illumination line was 555 nm and the depletion source 660 nm. Fluorescent light was collected using high-efficiency single-molecule detectors (SMD-HyD), using a HC PL APO CS2 100×/1.40 oil objective. The selected areas were scanned at 600 Hz and the final pixel size was 20 nm.

The selected cells were screened along the z-axis and the brightest plane was chosen. At least three different representative cells were obtained for each sample. The images were deconvoluted using the Lightning GPU-based Deconvolution Leica package. Images for publication were processed and prepared using Fiji ImageJ software (National Institutes of Health).

## 6.8. Informatic methods

### 6.8.1. DNA sequence analysis

Sequencing results were analysed in Seqman software (DNASTar Inc.). Downloaded sequences from Macrogen were aligned with the wild type sequence of interest and compared.

The selection of primers (Table 6.2) was performed using PrimerSelect (DNASTar Inc.) software, NEBuilder Assembly Tool (<https://nebuilder.neb.com/#!/>) and NEBaseChanger (<http://nebasechanger.neb.com/>), online servers. These servers were used for HiFi assemblies (Section 6.4.6.3) and base substitutions (Section 6.5.2), respectively. For all other cases, nucleotides were designed manually and checked by SnapGene Viewer software.

### 6.8.2. Residue conservation percentage

To determine the percent conservation of the involved residues, all complete genomes from *Salmonella* specie and one random genome of each genus of the Enterobacteriaceae family were downloaded from the GenBank database. RecA, CheA and CheW *S. enterica* ATCC 14028 protein sequences (ACY89831.1, ACY88793.1 and ACY88792.1 respectively) were used as queries in the Basic local alignment search tool (BLAST) to identify similar protein sequences, limited using the previously translated nucleotide databases (tBLASTn). RecA matches were obtained for 501 *Salmonella* and 23 *Enterobacteriaceae* genomes, CheA matches for 492 *Salmonella* and 13

*Enterobacteriaceae* genomes and CheW matches for 501 *Salmonella* and 13 *Enterobacteriaceae* genomes. The results were filtered based on cut-offs for the e-value (<10<sup>-20</sup>) and coverage (>75 %). Multiple sequence alignment and data analysis were carried out using the Clustal Omega local server with standard parameters<sup>312</sup>. The data were represented in a heat map obtained using Prism (GraphPad) program.

### 6.8.3. Statistical analysis

The results of the chemotaxis and chemoreceptor-clustering assays were statistically evaluated using a one-way analysis of variance (ANOVA) with Prism (GraphPad), as previously described<sup>247,313,314</sup>. The analyses were followed by the Bonferroni multiple comparison post-hoc test. A p-value <0.05 was considered to indicate statistical significance and <0.01 as highly significance. In all cases, the error bars in the figures indicate the standard deviation.

### 6.8.4. Protein docking

RaptorX<sup>284</sup> custom-generated *S. enterica* RecA, CheW, Tar and CheA protein structures were used in the docking assays. In all cases, the available resolved structures of *E. coli* RecA (PDB: 2REB)<sup>275</sup> and CheW (PDB: 2HO9), and *T. maritima* Tar and CheA (PDB: 3JA6.C)<sup>194</sup> were used to validate the obtained 3D structures.

*In silico* models of the interaction of CheA and RecA was assessed in a simple protein-protein docking study using the ClusPro server<sup>285</sup>. At least 30 of the highest-scoring models, in which RecA was the receptor and CheA the ligand, and vice versa, were analysed in duplicate. The protein structures and the obtained *in silico* models were visualized and analysed using PyMOL software<sup>289</sup>.

Instead, for *in silico* studies of the signalling core unit and ring complex formation, the RaptorX generated structures of *Salmonella* proteins, were compared with the structures documented in *Thermotoga maritima* (PDB:3JA6)<sup>194</sup> and modelled using

PyMOL<sup>289</sup>, with the RecA protein placed according to the identified residues of the CheW-RecA and CheA-RecA interfaces.

#### 6.8.5. Microphotography editing

##### 6.8.5.1. Polar cluster counting

Obtained fluorescence images from Axio Imager M2 microscope (Carl Zeiss Microscopy) were processed adjusting contrast and brightness in order to further highlight the *Salmonella* labelled cells using Adobe Photoshop CS6 (Adobe Inc.) and facilitate the counting of (non)-polar-cluster cells.

##### 6.8.5.2. Fluorescence microscopy image editing

Fluorescence resulting images from Axio Imager M2 microscope (Carl Zeiss Microscopy) were processed adjusting brightness, contrast and colour with ImageJ (NIH) software to improve the quality of the images of the *Salmonella* labelled cells. Furthermore, corresponding scale bars were added.

##### 6.8.5.3. STED microscopy image editing

STED resulting images were deconvolved using LAS X (Leica) program with default features.

Obtained deconvolved STED images were processed in ImageJ (NIH) software. It was used to edit all images and adjust brightness and contrast. Selected images, according to the most representative phenotype, were scaled at 0.02 x 0.02 pixel width x height and corresponding scale bars were added.

# 7 ABBREVIATIONS



## 7. Abbreviations

**ACSSuT:** Ampicillin, chloramphenicol, streptomycin, sulfonamides and tetracycline

**BLAST:** Basic local alignment search tool

**CA:** Catalytic and ATP-binding domain

**cAMP:** Cyclic AMP

**CCW:** Counter-clockwise

**CDC:** Centers for Disease Control and Prevention

**c-di-GMP:** Bis-(3'-5')-cyclic dimeric guanosine monophosphate

**CFU:** Colony forming units

**COG:** Clusters of orthologous groups of proteins

**CoIP:** Co-immunoprecipitation

**Cm:** Chloramphenicol

**CW:** Clockwise

**DNA:** Deoxyribonucleic acid

**HAMP:** Histidine kinase, adenylyl cyclase, methyl-accepting chemotaxis protein and phosphatase

**HK:** Histidine kinase

**IPTG:** isopropyl  $\beta$ -D-1-thiogalactopyranoside

**Kan:** Kanamycin



**LBD:** Ligand-binding domain

**MCP:** Methyl-accepting chemotactic protein

**MDR:** Multi-drug resistance

**MH:** Helix methylation bundle subdomain

**MOI:** Multiplicity of infection

**PFU:** Plaque-forming units

**NTS:** Non-typhoidal *Salmonella*

**REC:** Receiver domain

**RR:** Response regulator

**RT:** Room temperature

**SCV:** *Salmonella*-containing vacuoles

**SD:** Signalling domain

**SPI1:** *Salmonella* pathogenicity island 1

**SSD:** Signalling subdomain

**ssDNA:** Single-stranded deoxyribonucleic acid

**STED:** Stimulated emission depletion

**T3SS-1:** Type III secretion system 1

**T3SS-2:** Type III secretion system 2

**T4P:** Type IV pili

**TCS:** Two-component system

**UTI:** Urinary tract infection

# 8 ANNEX I



## 8. Annex

### 8.1. Media, solutions and buffers

#### 8.1.1. Luria-Bertani (LB) broth and agar

**Table 8.1.1.** Luria-Bertani broth and agar medium composition.

| Component        | Supplier | Concentration (w/v) |
|------------------|----------|---------------------|
| Tryptone         | Condalab | 1.0 %               |
| Yeast extract    | Condalab | 0.5 %               |
| NaCl             | Panreac  | 0.5 %               |
| Agar (if needed) | Condalab | 1.7 %               |
| MQ water         |          | To desired volume   |

#### 8.1.2. Brain heart infusion (BHI) medium

**Table 8.1.2.** Brain heart infusion medium composition.

| Component | Supplier | Concentration (w/v) |
|-----------|----------|---------------------|
| BHI mix   | Oxoid    | 3.7 %               |
| MQ water  |          | To desired volume   |

### 8.1.3. LB swarming

**Table 8.1.3.** LB swarming medium composition.

| Component     | Supplier | Concentration (w/v) |
|---------------|----------|---------------------|
| Tryptone      | Difco    | 1 %                 |
| Yeast extract | Difco    | 0.5 %               |
| NaCl          | Panreac  | 0.5 %               |
| Agar          | Difco    | 0.5 %               |
| D-(+)-glucose | Merck    | 0.5 %               |
| MQ water      |          | To desired volume   |

### 8.1.4. LB swimming

**Table 8.1.4.** LB swimming medium composition for *Salmonella*.

| Component     | Supplier | Concentration (w/v) |
|---------------|----------|---------------------|
| Tryptone      | Difco    | 1 %                 |
| Yeast extract | Difco    | 0.5 %               |
| NaCl          | Panreac  | 0.5 %               |
| Agar          | Difco    | 0.3 %               |
| MQ water      |          | To desired volume   |

### 8.1.5. Super optimal broth (SOB)

**Table 8.1.5.** Super optimal broth medium composition.

| Component     | Supplier | Concentration     |
|---------------|----------|-------------------|
| Tryptone      | Difco    | 2 % (w/v)         |
| Yeast extract | Difco    | 0.5 % (w/v)       |
| NaCl          | Panreac  | 0.05 % (w/v)      |
| KCl           | Panreac  | 1.25 mM           |
| MQ water      |          | To desired volume |

Filtered 20 mM DL-arabinose (Sigma) was added to the broth in the moment of use.

### 8.1.6. Super optimal broth with catabolite (SOC)

**Table 8.1.6.** Super optimal broth medium with catabolite composition.

| Component     | Supplier | Concentration     |
|---------------|----------|-------------------|
| Tryptone      | Difco    | 2 % (w/v)         |
| Yeast extract | Difco    | 0.5 % (w/v)       |
| NaCl          | Panreac  | 0.05 % (w/v)      |
| KCl           | Panreac  | 1.25 mM           |
| MQ water      |          | To desired volume |

Filtered 20 mM DL-arabinose (Sigma) and 20 mM D-(+)-glucose (Merck) were added to the broth in the moment of use.

### 8.1.7. Tryptone broth (TBr)

**Table 8.1.7.** Tryptone broth medium composition.

| Component | Supplier | Concentration (w/v) |
|-----------|----------|---------------------|
| Tryptone  | Difco    | 2 %                 |
| NaCl      | Panreac  | 0.05 %              |
| MQ water  |          | To desired volume   |

### 8.1.8. Green plates

**Table 8.1.8.** Green plates medium composition.

| Component       | Supplier | Concentration (w/v) |
|-----------------|----------|---------------------|
| Tryptone        | Difco    | 0.8 %               |
| Yeast extract   | Difco    | 0.1 %               |
| NaCl            | Panreac  | 0.5 %               |
| Agar            | Difco    | 1.5 %               |
| Alizarin Yellow | Panreac  | 0.083 %             |
| Aniline Blue    | Panreac  | 0.013 %             |
| D-(+)-glucose   | Merck    | 1.3 %               |
| MQ water        |          | To desired volume   |

D-(+)-glucose should be prepared 40 % concentrated and autoclaved apart. Once the previous medium was sterilized and cooled down to around 50°C, 3.4 % (v/v) of this glucose should be added using sterile conditions.

### 8.1.9. Top agar

**Table 8.1.9.** Top agar composition.

| Component     | Supplier | Concentration (w/v) |
|---------------|----------|---------------------|
| Tryptone      | Difco    | 1.0 %               |
| Yeast extract | Difco    | 0.5 %               |
| NaCl          | Panreac  | 1.0 %               |
| Agar          | Difco    | 0.7 %               |
| MQ water      |          | To desired volume   |

## 8.2. Buffers and solutions

### 8.2.1. Tethering buffer

**Table 8.2.1.** Tethering buffer composition.

| Component                 | Supplier | Concentration (mM) |
|---------------------------|----------|--------------------|
| Potassium-Phosphate, pH 7 | Panreac  | 10                 |
| NaCl                      | Panreac  | 67                 |
| Sodium-lactate            | Sigma    | 10                 |
| EDTA                      | Merck    | 0.1                |
| L-methionine              | VWR      | 0.001              |
| MQ water                  |          | To desired volume  |

### 8.2.2. Chemotaxis buffer

**Table 8.2.2.** Chemotaxis buffer composition.

| Component                 | Supplier | Concentration (mM) |
|---------------------------|----------|--------------------|
| Potassium-Phosphate, pH 7 | Panreac  | 10                 |
| EDTA                      | Merck    | 0.1                |
| MgSO <sub>4</sub>         | VWR      | 1                  |
| MQ water                  |          | To desired volume  |

### 8.2.3. MgSO<sub>4</sub> solution

**Table 8.2.3.** MgSO<sub>4</sub> solution composition.

| Component         | Supplier | Concentration (mM) |
|-------------------|----------|--------------------|
| MgSO <sub>4</sub> | Panreac  | 10                 |
| MQ water          |          | To desired volume  |

### 8.2.4. Saline solution

**Table 8.2.4.** Saline solution composition.

| Component | Supplier | Concentration (w/v) |
|-----------|----------|---------------------|
| NaCl      | Panreac  | 0.9 %               |
| MQ water  |          | To desired volume   |

### 8.2.5. TAE 50X

**Table 8.2.5.** TAE 50X composition.

| Component                | Supplier | Concentration     |
|--------------------------|----------|-------------------|
| Trizma Base              | Sigma    | 200 mM            |
| EDTA 0.5 M pH 8 solution | Sigma    | 10 % (v/v)        |
| Acetic acid glacial      | Panreac  | 5.7               |
| MQ water                 |          | To desired volume |



### 8.2.6. DNA loading buffer

**Table 8.2.6.** DNA loading buffer composition.

| Component                | Supplier | Concentration     |
|--------------------------|----------|-------------------|
| Xilene-Cyanol            | Clontech | 0.25 % (w/v)      |
| Bromophenol Blue         | Panreac  | 0.25 % (w/v)      |
| Glycerol                 | Panreac  | 30 % (v/v)        |
| EDTA 0.5 M pH 8 solution | Sigma    | 2 % (v/v)         |
| MQ water                 |          | To desired volume |

### 8.2.7. Laemmli 4X buffer

**Table 8.2.7.** Laemmli 4X buffer composition.

| Component                    | Supplier | Concentration     |
|------------------------------|----------|-------------------|
| SDS                          | Merck    | 8 % (w/v)         |
| Bromophenol Blue             | Panreac  | 0.4 % (w/v)       |
| Glycerol                     | Panreac  | 40 % (v/v)        |
| Stacking buffer 4X (A.2.9.4) |          | 50 % (v/v)        |
| MQ water                     |          | To desired volume |

### 8.2.8. SDS-Polyacrylamide gel electrophoresis (SDS-PAGE) 15 %

#### Separating gel

**Table 8.2.8.1.** Separating gel composition for polyacrylamide gel electrophoresis at 15%.

| Component                      | Supplier | Volume      |
|--------------------------------|----------|-------------|
| Separating buffer 4X (A.2.9.3) |          | 1.9 mL      |
| Acrylamide 4K solution (30 %)  | PanReac  | 3 mL        |
| Ammonium persulfate (APS)      | Amresco  | 100 $\mu$ L |
| TEMED                          | Amresco  | 20 $\mu$ L  |
| MQ water                       |          | 1.9 mL      |

## Stacking gel

**Table 8.2.8.2.** Stacking gel composition for polyacrylamide gel electrophoresis.

| Component                                   | Supplier | Volume     |
|---------------------------------------------|----------|------------|
| Stacking buffer 4X (A.2.9.4)                |          | 0.75 mL    |
| Acrylamide 4K solution (30 %) – Mix 37.5: 1 | PanReac  | 0.3 mL     |
| Ammonium persulfate (APS) 10 %              | Amresco  | 30 $\mu$ L |
| TEMED                                       | Amresco  | 6 $\mu$ L  |
| MQ water                                    |          | 1.75 mL    |

## Separating buffer 4X

**Table 8.2.8.3.** Separating buffer 4X composition.

| Component   | Supplier | Amount |
|-------------|----------|--------|
| Trizma Base | Sigma    | 45.5 g |
| SDS         | Merck    | 1 g    |
| MQ water    |          | 250 mL |

Once prepared adjust to pH 8.8 with HCl previously to SDS addition.

## Stacking buffer 4X

**Table 8.2.8.4.** Stacking buffer 4X composition.

| Component   | Supplier | Amount |
|-------------|----------|--------|
| Trizma Base | Sigma    | 15.1 g |
| SDS         | Merck    | 1 g    |
| MQ water    |          | 250 mL |

Once prepared adjust to pH 6.8 with HCl previously to SDS addition.

### 8.2.9. Lysis buffer

**Table 8.2.9.** Lysis buffer composition.

| Component                       | Supplier | Concentration     |
|---------------------------------|----------|-------------------|
| TBS 10X                         |          | 1X                |
| Glycerol                        | Panreac  | 10 % (v/v)        |
| Triton X-100                    | Roche    | 1 % (v/v)         |
| EDTA 0.5M (pH 8)                |          | 1 mM              |
| Lysozyme                        | Roche    | 1 mg/mL           |
| cOmplete mini EDTA-free tablets | Roche    | 1 tablet/L        |
| MQ water                        |          | To desired volume |

### 8.2.10. Coomassie staining buffer

**Table 8.2.10.** Coomassie staining buffer composition.

| Component                      | Supplier | Concentration (mM) |
|--------------------------------|----------|--------------------|
| Coomassie Brilliant Blue R-250 | Bio-Rad  | 0.1 % (w/v)        |
| Acetic acid 96 %               | Panreac  | 10 % (v/v)         |
| Methanol                       | Panreac  | 40 % (v/v)         |
| MQ water                       |          | To 500 mL          |

### 8.2.11. Western transfer buffer

**Table 8.2.11.** Western transfer buffer composition.

| Component | Supplier | Concentration     |
|-----------|----------|-------------------|
| Tris Base | Bio-Rad  | 25 mM             |
| Glycine   | Roche    | 190 mM            |
| Methanol  | Panreac  | 20 % (v/v)        |
| MQ water  |          | To desired volume |

### 8.2.12. Western blocking buffer

**Table 8.2.12.** Western blocking buffer composition.

| Component      | Supplier | Concentration     |
|----------------|----------|-------------------|
| TBS 10X        |          | 1X                |
| Tween 20       | Panreac  | 0.05 % (v/v)      |
| BSA Fraction V | Panreac  | 3 % (w/v)         |
| MQ water       |          | To desired volume |

### 8.2.13. Western wash buffer

**Table 8.2.13.** Western wash buffer composition.

| Component | Supplier | Concentration     |
|-----------|----------|-------------------|
| TBS 10X   |          | 1X                |
| Tween 20  | Panreac  | 0.05 % (v/v)      |
| MQ water  |          | To desired volume |

### 8.2.14. CoIP wash buffer

**Table 8.2.14.** CoIP wash buffer composition.

| Component    | Supplier | Concentration     |
|--------------|----------|-------------------|
| TBS 10X      |          | 1X                |
| Glycerol     | Panreac  | 10 % (v/v)        |
| Triton X-100 | Roche    | 1 % (v/v)         |
| MQ water     |          | To desired volume |

### 8.2.15. CoIP blocking buffer

**Table 8.2.15.** CoIP blocking buffer composition.

| Component      | Supplier | Concentration     |
|----------------|----------|-------------------|
| TBS 10X        |          | 1X                |
| Glycerol       | Roche    | 10 % (v/v)        |
| Triton X-100   | Roche    | 1 % (v/v)         |
| BSA Fraction V | Panreac  | 3 % (w/v)         |
| MQ water       |          | To desired volume |

### 8.2.16. Phosphate-buffered saline (PBS) 10X

**Table 8.2.16.** Phosphate-buffered saline 10X composition.

| Component                                             | Supplier | Concentration (mM) |
|-------------------------------------------------------|----------|--------------------|
| NaCl                                                  | Panreac  | 13710              |
| KCl                                                   | Panreac  | 27                 |
| Na <sub>2</sub> HPO <sub>4</sub> · 7 H <sub>2</sub> O | Panreac  | 10                 |
| KH <sub>2</sub> PO <sub>4</sub>                       | Panreac  | 18                 |
| MQ water                                              |          | To desired volume  |

Once prepared adjust to pH 7.3 using HCl. For other uses, pH could be slightly modified. PBS could be autoclaved 15 minutes at 121°C if required.

### 8.2.17. Mowiol-DABCO mounting medium

First, 5 g Mowiol® (Sigma) was added in to 20 mL PBS 1X (Table 8.2.17) and stirred overnight. 10 mL glycerol (Panreac) was also added and stirred overnight again. After Mowiol is dissolved, mixture was centrifuged at 250 g for 15 minutes and pellet was discarded. 2.5 % DABCO was added to supernatant and mixed. Solution was adjusted to 8-8.5 pH and afterwards, distributed in 1.5 mL tubes and stored at -20°C until its use.

# 9 ANNEX II





## The Interaction of RecA With Both CheA and CheW Is Required for Chemotaxis

Elisabet Frutos-Grilo<sup>1</sup>, Maria Marsal<sup>2</sup>, Oihane Irazoki<sup>1</sup>, Jordi Barbé<sup>1†</sup> and Susana Campoy<sup>1\*†</sup>

<sup>1</sup> Departament de Genètica i de Microbiologia, Universitat Autònoma de Barcelona, Barcelona, Spain, <sup>2</sup> ICFO-Institut de Ciències Fotòniques, The Barcelona Institute of Science and Technology, Barcelona, Spain

### OPEN ACCESS

#### Edited by:

Hari S. Misra,  
Bhabha Atomic Research Centre  
(BARC), India

#### Reviewed by:

Irfan Ahmad,  
University of Health Sciences,  
Pakistan  
Juan Carlos Alonso,  
Centro Nacional de Biotecnología  
(CNB), Spain

#### \*Correspondence:

Susana Campoy  
susana.campoy@uab.cat

<sup>†</sup> These authors share senior  
authorship

#### Specialty section:

This article was submitted to  
Microbial Physiology and Metabolism,  
a section of the journal  
Frontiers in Microbiology

**Received:** 23 December 2019

**Accepted:** 17 March 2020

**Published:** 07 April 2020

#### Citation:

Frutos-Grilo E, Marsal M,  
Irazoki O, Barbé J and Campoy S  
(2020) The Interaction of RecA With  
Both CheA and CheW Is Required  
for Chemotaxis.  
*Front. Microbiol.* 11:583.  
doi: 10.3389/fmicb.2020.00583

*Salmonella enterica* is the most frequently reported cause of foodborne illness. As in other microorganisms, chemotaxis affords key physiological benefits, including enhanced access to growth substrates, but also plays an important role in infection and disease. Chemoreceptor signaling core complexes, consisting of CheA, CheW and methyl-accepting chemotaxis proteins (MCPs), modulate the switching of bacterial flagella rotation that drives cell motility. These complexes, through the formation of heterohexameric rings composed of CheA and CheW, form large clusters at the cell poles. RecA plays a key role in polar cluster formation, impairing the assembly when the SOS response is activated. In this study, we determined that RecA protein interacts with both CheW and CheA. The binding of these proteins to RecA is needed for wild-type polar cluster formation. *In silico* models showed that one RecA molecule, attached to one signaling unit, fits within a CheA-CheW ring without interfering with the complex formation or array assembly. Activation of the SOS response is followed by an increase in RecA, which rises up the number of signaling complexes associated with this protein. This suggests the presence of allosteric inhibition in the CheA-CheW interaction and thus of heterohexameric ring formation, impairing the array assembly. STED imaging demonstrated that all core unit components (CheA, CheW, and MCPs) have the same subcellular location as RecA. Activation of the SOS response promotes the RecA distribution along the cell instead of being at the cell poles. CheA- and CheW- RecA interactions are also crucial for chemotaxis, which is maintained when the SOS response is induced and the signaling units are dispersed. Our results provide new molecular-level insights into the function of RecA in chemoreceptor clustering and chemotaxis determining that the impaired chemoreceptor clustering not only inhibits swarming but also modulates chemotaxis in SOS-induced cells, thereby modifying bacterial motility in the presence of DNA-damaging compounds, such as antibiotics.

**Keywords:** SOS response system, chemotaxis, RecA, CheA, chemoreceptor polar arrays, STED microscopy, swarming



## INTRODUCTION

Chemotaxis allows bacteria to sense their environment and adjust their flagellar rotation accordingly, resulting in their directed movement toward attractants and away from repellents (Falke et al., 1997; Bi and Lai, 2015). Chemoreceptors are methyl-accepting chemotaxis proteins (MCPs) that detect the presence of chemoeffectors and modulate the activity of the CheA kinase that, via the CheY chemotaxis response regulator, initiates the signaling pathway controlling the flagellar motor (Sourjik and Wingreen, 2012). There are different types of MCPs, being Tar and Tsr the most abundant and studied in *Salmonella enterica* and *Escherichia coli* (Blat and Eisenbach, 1995). In many *Bacteria* and *Archaea*, MCPs group together to form large chemosensory arrays that contain from a few to thousands of chemoreceptor core complexes (Briegel et al., 2009, 2012, 2015; Greenfield et al., 2009). These ordered structures act as “antennae,” amplifying chemoeffector sensing by cooperative networking (Li and Hazelbauer, 2014; Frank et al., 2016; Piñas et al., 2016). Besides chemotaxis, chemoreceptor clusters are essential for swarming motility (Cardozo et al., 2010; Santos et al., 2014; Irazoki et al., 2016b) and are involved in other important processes, including biofilm formation (He and Bauer, 2014; Huang et al., 2019b), cell adhesion (Huang et al., 2017), host colonization (Erhardt, 2016; Johnson and Ottemann, 2018) and antibiotic resistance (Butler et al., 2010; Irazoki et al., 2017).

In *E. coli* and *S. enterica*, the signaling core complexes are formed by two heterotrimers of transmembrane MCP homodimers, each one coupled to a protomer of the CheA kinase by the chemoreceptor adaptor protein CheW (Li and Hazelbauer, 2004, 2011; Koler et al., 2018). CheA is a dimeric histidine kinase that presents five structural and functional domains associated with: histidine-containing phosphotransfer (P1), CheY/CheB binding (P2), dimerization (P3), ATP binding/catalysis (P4), and CheW binding (P5) (Bilwes et al., 1999). The architecture of the chemoreceptor array has been previously elucidated, in which the interaction between CheW and the P5-CheA domain was shown to be the key structural link between core signaling units in the arrays (Liu et al., 2012; Li et al., 2013; Briegel et al., 2014b; Cassidy et al., 2015; Piñas et al., 2016). Specifically, the interaction of CheW with P5-CheA links three core complexes [using (CheW-CheA<sub>2</sub>-CheW) core linkers] and forms a hexagonal ring of receptors, giving rise to a lattice of hexagonally packed receptor trimers of dimers networked by P5-CheA/CheW rings (Briegel et al., 2012, 2014a; Liu et al., 2012; Cassidy et al., 2015). These highly stable structures are located at the cell poles (Maddock and Shapiro, 1993; Sourjik and Berg, 2000; Jones and Armitage, 2015; Koler et al., 2018).

Several conditions can disrupt chemoreceptor array assembly. In *S. enterica* and *E. coli*, the absence of RecA (Gómez-Gómez et al., 2007; Mayola et al., 2014), the stoichiometric excess of CheW (Cardozo et al., 2010; Irazoki et al., 2016b) and an increase in the concentration of the RecA protein prompted by the activation of SOS response (Irazoki et al., 2016b) inhibit polar chemoreceptor array formation and suppress swarming motility. RecA is a multifunctional protein, it is the main bacterial recombinase and is also involved in DNA repair (Cox, 1999;

Lusetti and Cox, 2002; Patel et al., 2010; Keyamura et al., 2013) being the SOS response activator (Little and Mount, 1982; Maslowska et al., 2019). When DNA damage occurs, RecA acquires co-protease activity and thus the ability to promote the auto-cleavage, among others, of LexA, the SOS system repressor. The LexA auto-hydrolysis induces the expression of SOS genes (including *recA*), most of which are involved in DNA repair (Sassanfar and Roberts, 1990). RecA is also essential for chemoreceptor polar array formation and standard flagellar rotation switching (Mayola et al., 2014). In previous work, we showed that RecA interacts with CheW (Irazoki et al., 2016a) impairing chemoreceptor clustering and consequently swarming motility during activation of the SOS response (Irazoki et al., 2016a,b). Specifically, when the SOS response is induced, the intracellular locations of CheW and RecA changes from the poles to along the cell axis (Irazoki et al., 2016a). Only after repair of the DNA damage are the polar arrays restored (Irazoki et al., 2016a,b). However, whether the inhibition of array assembly is due to CheW titration by RecA, thereby altering the stoichiometric balance of these proteins, or to other causes is unclear.

Previous studies showed that the structures of the P5-CheA domain and CheW are paralogous (Vu et al., 2012; Piñas et al., 2018). The mutual substitution of the P5-CheA domain and CheW within the hexagonal rings of chemoreceptors has also been described (Bilwes et al., 1999; Park et al., 2006). Based on these observations, we hypothesized that RecA also interacts with CheA and is part of the chemoreceptor core complexes comprising the chemoreceptor arrays.

Thus, to better understand the association of the SOS response and RecA with chemoreceptor cluster formation and chemotaxis, we explored the interaction between RecA and the P5-CheA domain and identified the region involved in that interaction. In addition, we determined the location within SOS-response-activated cells of the major chemoreceptor core unit-components and the impact of this intracellular distribution on chemotaxis.

## MATERIALS AND METHODS

### Bacterial Strains and Growth Conditions

Except when indicated, all strains were grown at 37°C in Luria-Bertani (LB) broth or on LB plates, supplemented, when necessary, with ampicillin (100 µg/mL), chloramphenicol (34 µg/mL), and/or kanamycin (10 µg/mL). The strains and constructions used in this work are described in **Supplementary Table S1**.

### In silico Docking Analysis

RaptorX (Källberg et al., 2012) custom-generated *S. enterica* RecA, CheW, Tar, and CheA protein structures were used in the docking assays. In all cases, the available resolved structures of *E. coli* RecA (PDB: 2REB) (Story et al., 1992) and CheW (PDB: 2HO9), and *Thermotoga maritima* Tar and CheA (PDB: 3JA6.C) (Cassidy et al., 2015) were used to validate the obtained 3D structures. *In silico* models were generated using the ClusPro server (Comeau et al., 2004).

The interaction of CheA and RecA was assessed in a simple protein-protein docking study. At least 30 of the highest-scoring models, in which RecA was the receptor and CheA the ligand, and *vice versa*, were analyzed in duplicate. The protein structures and the obtained *in silico* models were visualized and analyzed using PyMOL software (Schrödinger, 2010).

For *in silico* studies of the signaling core unit and ring complex formation, the RaptorX generated structures were compared with the structures documented in *T. maritima* (PDB:3JA6) (Cassidy et al., 2015) and modeled using PyMOL (Schrödinger, 2010), with the RecA protein placed according to the identified residues of the CheW-RecA and CheA-RecA interfaces (Tables 1, 2).

### Construction of RecA and CheA Tagged Proteins and Overexpressing Vectors

Co-immunoprecipitation (CoIP) assays were performed using proteins carrying -6xHis and -FLAG tags. Likewise, -CLIP and -SNAP tagged proteins were used for STED microscopy. Plasmids harboring the corresponding tagged genes were constructed using the appropriate oligonucleotides (Supplementary Table S2) and the HiFi DNA assembly cloning kit (NEB). The tag sequences were included at the 3' end of the genes preceded by a 3 × Gly linker (Supplementary Figure S1). All PCR products were digested, cloned into the pUA1108 overexpression vector (Mayola et al., 2014) and transformed into *E. coli* DH5α. The *recA* and *cheA* tagged mutants were obtained using a site directed mutagenesis kit (Agilent). All constructions were confirmed by PCR and sequencing. In all cases, the expression of the corresponding tagged derivative was confirmed by Western blotting (Supplementary Figure S2).

### Co-immunoprecipitation Assays

The CoIP assays were conducted as described previously (Mayola et al., 2014; Irazoki et al., 2016a) with a few modifications. Briefly, cultures of *S. enterica* Δ*recA*Δ*cheA* carrying the corresponding overexpression plasmid encoding a *recA*, or

*cheA* tagged gene and their corresponding mutant derivatives were used (Supplementary Table S1). *S. enterica* Δ*recA*Δ*cheW* background was used when *cheW* tagged gene was induced. In all cases, the tagged-gene overexpression was induced by the addition of 1mM of IPTG and cell lysates were obtained by sonication (Branson Digital Sonifier). As control, cells lysates harboring the pUA1108 overexpression vector were obtained following the same procedure.

The CoIP assays were performed using Pure Proteome Protein A magnetic beads (Millipore) coated, following the manufacturer's instructions, with either mouse anti-FLAG IgG or anti-6xHis IgG monoclonal primary antibodies (Sigma-Aldrich). Before CoIP, the coated magnetic beads were pre-incubated with the control lysates to minimize non-specific interactions. Two cell lysates containing the corresponding proteins were mixed and incubated at 30°C for 1 h without shaking to allow protein-protein interaction and kept at 4°C without shaking to maintain specific interactions for 16 h. Afterward, treated coated magnetic beads were added to the lysate mixture for 1 h at RT with gently shaking. Magnetic beads were then recovered, washed three times and heated for 10 min at 90°C. Supernatants were separated by SDS-PAGE on a 15% polyacrylamide gel

**TABLE 2 |** *In vitro* interaction of RecA mutant derivatives with wild-type CheA and CheW.

| RecA protein <sup>a</sup> | Secondary structure region containing the mutated residue | Interaction with wild-type CheA <sup>b</sup> | Interaction with wild-type CheW <sup>c,d</sup> |
|---------------------------|-----------------------------------------------------------|----------------------------------------------|------------------------------------------------|
| Wild-type                 | NA                                                        | +                                            | +                                              |
| L10A                      | Helix α1                                                  | +                                            | +                                              |
| L14A                      |                                                           | +                                            | +                                              |
| Q20A                      |                                                           | +                                            | -                                              |
| H183A                     | NR                                                        | +                                            | +                                              |
| Q173A                     | Helix α12                                                 | +                                            | +                                              |
| R176A                     |                                                           | +                                            | -                                              |
| F203                      | NR                                                        | +                                            | +                                              |
| N213A                     | Helix α13                                                 | +                                            | +                                              |
| A214V                     |                                                           | -                                            | +                                              |
| K216A                     |                                                           | +                                            | +                                              |
| Y218A                     |                                                           | +                                            | +                                              |
| R222A                     | Strand β11                                                | -                                            | -                                              |
| D224A                     |                                                           | -                                            | +                                              |
| I228A                     |                                                           | -                                            | +                                              |
| R243A                     |                                                           | +                                            | +                                              |
| V247A                     |                                                           | -                                            | +                                              |
| K250A                     |                                                           | -                                            | -                                              |
| F255A                     | NR                                                        | +                                            | +                                              |
| Q257A                     | Strand β12                                                | +                                            | +                                              |
| K286A                     | NR                                                        | +                                            | +                                              |
| Q300                      | Strand β15                                                | +                                            | +                                              |

**TABLE 1 |** *In vitro* interaction of CheA mutant derivatives with wild-type RecA.

| CheA protein mutated residue <sup>a</sup> | CheA domain containing the mutation <sup>b</sup> | Interaction with wild-type RecA <sup>c</sup> |
|-------------------------------------------|--------------------------------------------------|----------------------------------------------|
| Wild-type                                 | NA <sup>c</sup>                                  | +                                            |
| M303A                                     | P3                                               | +                                            |
| L311A                                     | P3                                               | +                                            |
| G537A                                     | P5, subdomain 1                                  | -                                            |
| D587A                                     | P5, Subdomain 2                                  | +                                            |
| K590A                                     | P5, Subdomain 2                                  | -                                            |
| T591A                                     | P5, Subdomain 2                                  | -                                            |
| S628A                                     | P5, Subdomain 1                                  | -                                            |
| S646A                                     | P5, Subdomain 1, Strand β9                       | -                                            |

NA, not applicable. <sup>a</sup>The mutated residue and the substitution of each tagged mutant derivative are indicated. <sup>b</sup>Unless otherwise indicated, the residue is located in a non-resolved secondary structure region of the P5 CheA domain. <sup>c</sup>Results of co-immunoprecipitation assays using each CheA derivative and wild-type RecA. (+) and (-) indicate the maintenance or abolishment of CheA-RecA complex formation, respectively.

NA, not applicable; NR, non-resolved secondary structure. <sup>a</sup>The mutated residue and the substitution of each tagged mutant derivative are indicated. <sup>b,c</sup>Results of co-immunoprecipitation (CoIP) assays using each RecA derivative and either CheA or CheW wild-type proteins. The maintenance (+) or abolishment (-) of CheA-RecA or CheW-RecA complex formation is shown. <sup>d</sup>Based on the results of previously described CoIP assays (Irazoki et al., 2016a).

and analyzed by Western blotting using mouse anti-6xHis IgG1 (Merck) and rabbit anti-FLAG® (Merck) and horseradish-peroxidase (HRP)-coupled anti-mouse IgG or anti-rabbit IgG antibodies (Acris). The membranes were developed using a HRP chemoluminescent substrate (SuperSignal™ West Pico PLUS Chemiluminescent Substrate, Thermo Scientific) following the manufacturer's instructions. The membranes were imaged using a ChemiDoc™ XRS + system (Bio-Rad).

### Construction of *S. enterica* Mutant and Tagged Strains

*S. enterica*  $\Delta cheA$  and *S. enterica*  $\Delta cheA\Delta cheW$  mutants and -SNAP and/or -CLIP tagged strains were constructed according to the  $\lambda$ Red recombinase-based gene replacement method (Datsenko and Wanner, 2000; **Supplementary Figure S1**). pGEM-T vectors (Promega) containing -SNAP or -CLIP tags from pSNAP-tag (T7)-2 and pCLIPf vectors (NEB) followed by the kanamycin cassette from pKD4 vector (Datsenko and Wanner, 2000) were constructed using HiFi DNA assembly cloning kit (NEB) giving rise to pUA1135 and pUA1136, respectively (**Supplementary Table S1**). These plasmids were used as the template to amplify the -SNAP or -CLIP tag followed by the kanamycin cassette using the suitable oligonucleotides (**Supplementary Table S2**). The PCR products were transformed into the corresponding *S. enterica* cells containing the pKOBEGA plasmid (Chaveroche et al., 2000). When necessary, the antibiotic resistance cassettes were eliminated using the pCP20 plasmid (Datsenko and Wanner, 2000).

The *S. enterica*  $\Delta recA\Delta cheA$  and  $\Delta recA\Delta cheA\Delta cheW$  strains were constructed by transduction as previously described (Campoy et al., 2002), using the P22int7(HT) bacteriophage and *S. enterica*  $\Delta recA$  (UA1927), as donor strain (Mayola et al., 2014). The absence of the prophage in the transductants was determined by streaking them onto green plates as described previously (Davis et al., 1980).

In all cases, gene substitution in all constructs was verified by PCR using suitable primers followed by sequencing.

### Residue Conservation Percentage

To determine the percent conservation of the involved residues, all complete genomes from *Salmonella* specie and one random genome of each genus of the *Enterobacteriaceae* family were downloaded from the GenBank database. RecA, CheA, and CheW *S. enterica* ATCC 14028 protein sequences (ACY89831.1, ACY88793.1, and ACY88792.1, respectively) were used as queries in the Basic Local Alignment Search Tool (tBLASTn) to identify similar protein sequences, limited using the previously searched genomes. RecA matches were obtained for 501 *Salmonella* and 23 *Enterobacteriaceae* genomes (**Supplementary Data Sheet S1**), CheA matches for 492 *Salmonella* and 13 *Enterobacteriaceae* genomes (**Supplementary Data Sheet S2**) and CheW matches for 501 *Salmonella* and 13 *Enterobacteriaceae* genomes (**Supplementary Data Sheet S3**). The results were filtered based on cut-offs for the *e*-value ( $<10^{-20}$ ) and coverage ( $>75\%$ ). Multiple sequence alignment and data analysis were carried out using the Clustal Omega local server with standard

parameters (Sievers et al., 2011). The data were represented in a heat map obtained using Prism (GraphPad).

### Stimulated Emission Depletion (STED) Microscopy

*S. enterica* cells were labeled using SNAP-Cell® 505-Star and CLIP-Cell™ TMR-Star permeable dyes, which specifically recognize SNAP- and CLIP- tags, respectively, following the manufacturer's instructions. All strains were cultured and coverslip mounted as described (Irazoki et al., 2016a), supplemented when required with 0.08  $\mu$ g mitomycin C/mL. Previous STED imaging, samples were examined under an AxioImager M2 microscope (Carl Zeiss Microscopy) to ensure that at least 90% of the cells were correctly labeled.

Fluorescence immunolabeling was carried out as described (Buddelmeijer et al., 2013), with a few modifications. The two-color labeled samples were observed using a commercial gated-STED microscope (Leica TCS SP8 STED 3X) equipped with a pulsed white light laser source and three depletion lasers. STED illumination of cells tagged with SNAP-Cell® 505-Star was performed using a 505 nm line, and depletion using a 592 nm line. For the CLIP-Cell™ TMR-Star tag, the illumination line was 555 nm and the depletion source 660 nm. Fluorescent light was collected using high-efficiency single-molecule detectors (SMD-HyD), using a HC PL APO CS2 100 $\times$ /1.40 oil objective. The selected areas were scanned at 600 Hz and the final pixel size was 20 nm.

The selected cells were screened along the *z* axis and the brightest plane was chosen. At least three different representative cells were obtained for each sample. The images were deconvoluted using the Lightning GPU-based Deconvolution Leica package. Images for publication were processed and prepared using Fiji ImageJ software (National Institutes of Health).

### Chemotaxis Capillary Assays

Chemotaxis assays were conducted as previously described (Mayola et al., 2014). Briefly, 1  $\mu$ L capillary tubes (Microcaps, Drummond Scientific Co.) filled with either tethering buffer or 10 mM L-aspartate dissolved in tethering buffer (Block et al., 1983) were placed in contact with 2 mL of the corresponding cell suspension in the chemotaxis chambers formed by placing three V-shaped bent needles (40 mm 18G needle, Nipro). After incubation at 30°C for 1 h, the exterior of capillaries was rinsed under a stream of sterile distilled water. Then capillary tubes were emptied and the cell concentration was determined by plating. Chemotaxis ratios were calculated as the ratio of viable bacteria inside capillary tubes with vs. without aspartate.

### Chemoreceptor Polar Clustering Assay

The chemoreceptor polar cluster arrays were visualized as previously described (Mayola et al., 2014), with a few modifications. Briefly, overnight cultures of the corresponded tagged strains were grown at 30°C in tryptone broth, supplemented, when needed, with ampicillin and/or 40  $\mu$ M IPTG. Overnight cultures were diluted 1:100 in tryptone broth



supplemented with IPTG and incubated at 30°C until an OD<sub>600</sub> of 0.08–0.1 was reached. Then cells were collected by centrifugation, washed once using ice-cold tethering buffer (10 mM potassium-phosphate pH 7, 67 mM NaCl, 10 mM Na-lactate, 0.1 mM EDTA, and 0.001 mM l-methionine) and resuspended in 20–100 µL of the same buffer. Then cells were stained with the permeable dyes SNAP-Cell® 505-Star and CLIP-Cell™ TMR-Star, following the manufacturer's instruction. Finally, cells were fixed with paraformaldehyde, resuspended in 1 × PBS, mounted on 35 mm poly-L-lysine-pre-coated coverslips using Mowiol-DABCO mounting medium and air-dried.

The samples were examined under an Axio Imager M2 microscope (Carl Zeiss Microscopy) equipped with the appropriate filter set [green channel: GFP (Zeiss filter set 38); red channel: Rhod (Zeiss filter set 20)]. Cell fields were photographed and at least 350 cells were visually inspected. All images were acquired under identical conditions. Each experiment was performed at least in triplicate using independent cultures; a minimum of 1,050 cells from each studied strain were therefore analyzed. The images presented in the figures are representative of the entire image set. ImageJ software (National Institutes of Health) was used to quantify the number of clusters and to prepare images for publication.

### Statistical Analysis

The results of the chemotaxis and chemoreceptor-clustering assays were statistically evaluated using a one-way analysis of variance (ANOVA) with Prism (GraphPad), as previously described (Brennan et al., 2013; Raterman and Welch, 2013; Mayola et al., 2014). The analyses were followed by the Bonferroni multiple comparison *post hoc* test. A *p*-value < 0.01 was considered to indicate statistical significance. In all cases, the error bars in the figures indicate the standard deviation.

## RESULTS

### RecA and CheA Interaction

Given the structural similarities of the P5-CheA domain and CheW (Vu et al., 2012; Piñas et al., 2018), we conducted co-immunoprecipitation (CoIP) assays to determine whether, as with CheW, RecA is able to interact with CheA (Arifuzzaman et al., 2006; Mayola et al., 2014). Thus, RecA-FLAG and CheA-6xHis tagged proteins were overexpressed in *S. enterica*  $\Delta$ recA $\Delta$ cheA strains carrying the corresponding plasmids (Supplementary Table S1). When both recombinant proteins were present in the protein mixture, anti-FLAG antibody-coated beads recovered both RecA-FLAG and CheA-6xHis from the supernatants (Figure 1). When anti-6xHis antibody-coated beads were added to the mixture, RecA-FLAG proteins were also recovered along with CheA. These results demonstrated the *in vitro* pairing of RecA and CheA.

An *in silico* modeling experiment was then conducted, aimed at identifying the putative RecA and CheA residues participating in the interaction of these proteins. Protein-protein interaction docking was performed with RaptorX (Källberg et al., 2012) using, as reference structures, the *E. coli* RecA (PDB:

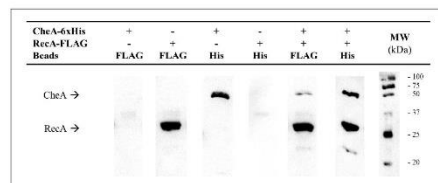
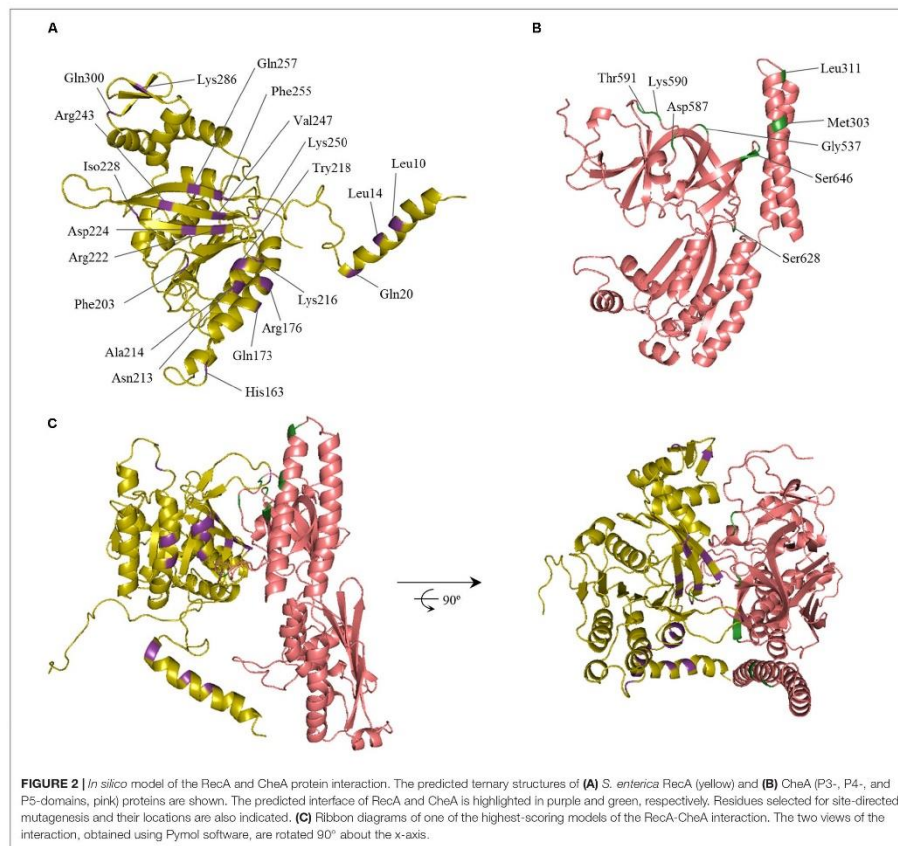


**FIGURE 1 |** Co-immunoprecipitation assays of *S. enterica* RecA and CheA. Cell-lysates prepared from *S. enterica*  $\Delta$ recA $\Delta$ cheA cultures overexpressing either RecA-FLAG- or CheA-6xHis-tagged proteins were incubated together to allow interaction of the proteins. Co-immunoprecipitation (CoIP) was performed by adding magnetic beads coated with anti-FLAG (Beads FLAG) or anti-6xHis antibodies (Beads His), attached proteins were recovered and separated by SDS-PAGE. The CoIP controls consisted of mixtures containing only RecA-FLAG or CheA-6xHis overexpressing lysates. The presence in the recovered supernatants of each tagged-protein was assessed by Western blotting using both anti-FLAG and anti-6xHis primary antibodies. The presence or absence of RecA-FLAG, CheA-6xHis, or both tagged proteins in the corresponding lysate is indicated. The experiments were done at least in triplicate. Black arrows show the position of CheA-6xHis and RecA-FLAG. +, added protein; -, non-added protein; MW, molecular mass marker, in kDa.

2REB) (Story et al., 1992) and the *T. maritima* CheA (PDB: 3JA6.C) (Cassidy et al., 2015), which includes the P3-, P4-, and P5-CheA domains. Balanced-coefficient docking models were considered to be the most accurate for the analysis of the RecA-CheA interaction (Comeau et al., 2004). Thirty of the highest-scoring models were analyzed for each combination of RecA receptor protein and CheA ligase and for the reverse combination. Although the spatial arrangement was not exactly the same in each combination, the putative interacting regions were considered to be those repeated in all of the studied models (Figure 2).

As expected, the results were similar to those obtained for the CheW-RecA interaction. In CheA, both P5 subdomains (1 and 2) interacted with RecA. In some of the *in silico* models, residues of the P3 domain were also exposed to the RecA-CheA interface (Figure 2 and Table 1). With respect to RecA, the putative interface with CheA was located in the NH<sub>2</sub>-terminal and central domains (at  $\alpha$ 1,  $\alpha$ 12,  $\alpha$ 13,  $\beta$ 11, and  $\beta$ 15) (Figure 2 and Table 2).

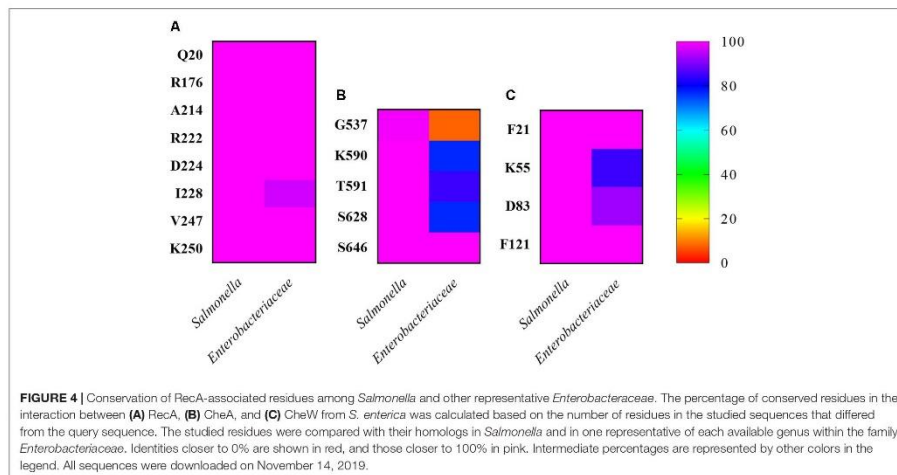
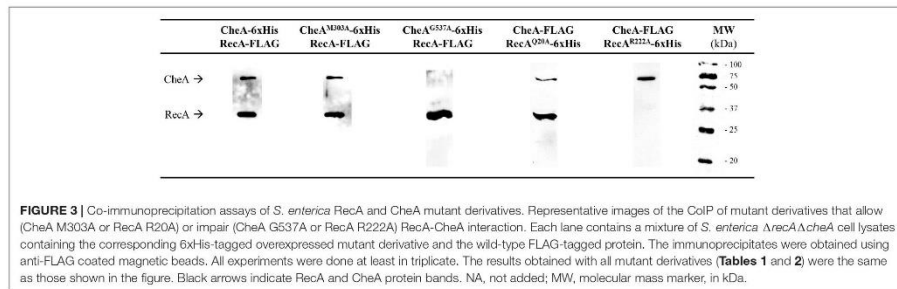
To confirm these interaction interfaces, site-directed mutagenesis was used to construct the corresponding mutant derivatives for each protein. The 21 RecA and 8 CheA residues were selected based on their exposure and their potential ability to mediate RecA-CheA pair formation (Tables 1, 2). With the exception of the RecA A214V mutant, in which the Ala residue was changed to a Val, all selected residues were converted to an Ala (Tables 1, 2), which is considered to be non-reactive amino acid (Cunningham and Wells, 1989). The corresponding *recA* and *cheA* gene mutants constructed *in vitro* were 6xHis-tagged and the effects of the substitutions on the RecA-CheA interaction were determined by CoIP assays using the corresponding FLAG-tagged wild-type RecA or CheA protein (Figure 3). The results are summarized in Tables 1 and 2. For CheA, only



P5 domain was associated with the RecA interaction; CheA mutations in the P3 domain did not disturb wild-type RecA binding (Table 1). Within the P5-CheA domain, five residues (G537, K590, T591, S628, and S646) were found to be directly involved in the interaction with RecA. Their substitution by Ala prevented RecA-CheA pair formation (Table 1 and Figure 3). Analyses of the 21 RecA mutants showed that only five were unable to bind wild-type CheA (A214V, R222A, D224A, K250A, and I228A). With the exception of A214, all of the residues were located on the  $\beta$ 11 strand, shown in previous studies to be associated with monomer-monomer interactions as well as RecA filament formation and stabilization (Skiba et al., 1999; Zaitsev and Kowalczykowski, 1999; Chen et al., 2008). Recombinase assays with the RecA mutants showed, in almost all cases, a clear

decrease in the recombination activity of the residues associated with RecA-CheA pair formation (Supplementary Figure S3).

However, not all of the residues involved in the CheW-RecA interaction were also associated with the CheA-RecA interaction. Thus, RecA Q20A and R176A mutants, while unable to bind CheW (Irazoki et al., 2016a), interacted with wild-type CheA (Table 2 and Figure 3). Similarly, the involvement of residues A214, D224, and I228 was limited to the RecA-CheA interaction, as they had no effect on RecA-CheW binding (Table 2). Only two mutant derivatives, R222A and K250A, abolished the interactions of CheA and CheW with RecA (Table 2). These results not only revealed the residues associated with RecA-CheA pairing but also demonstrated the ability of RecA to interact with both CheA and CheW through different interfaces. In addition, when CheA and



CheW proteins were not present RecA protein was majorly not located at the cell poles (Supplementary Figure S4).

In addition, we determined the residue conservation percentages among *Salmonella* and *Enterobacteriaceae* for each involved amino acid (Figure 4). The RecA residues involved in CheA and CheW interactions were highly conserved (100% identity; Figure 4A), except for residue I228 (96.4%). Among the CheA residues associated with the RecA interaction, all were conserved in *Salmonella* (100% identity), except G537, which differed in *S. bongori*, resulting in a slightly lower identity (99.2%). The CheA residues were also highly conserved in *Enterobacteriaceae* (>75% identity), again except G537 (7.7%). Finally, for the involved residues of CheW, the results were similar, with 100% identity in *Salmonella* and >80% in *Enterobacteriaceae*. According to these findings, the ability of RecA to interact with CheW and CheA may occur not only in *Salmonella* species besides *S. enterica* but also in

*Enterobacteriaceae*. These results pointed out that the association of the SOS response with chemoreceptor signaling complexes may be extended to *Enterobacteriaceae* and perhaps also to other families of bacteria.

### RecA as a Part of the Chemoreceptor Signaling Core Unit

Our results also indicated the differential interaction of RecA with CheW and CheA (Table 2). RecA interfaces with CheA and CheW do not overlap with the regions of CheA-CheW binding, nor with those involved in MCP interaction (Cassidy et al., 2015; Piñas et al., 2016; Huang et al., 2019a). These observation suggested that RecA may be part of a signaling complex, a possibility explored by generating *in silico* interaction models that included the entire signaling core unit (Figure 5). The RaptorX-generated structures for all *S. enterica* proteins

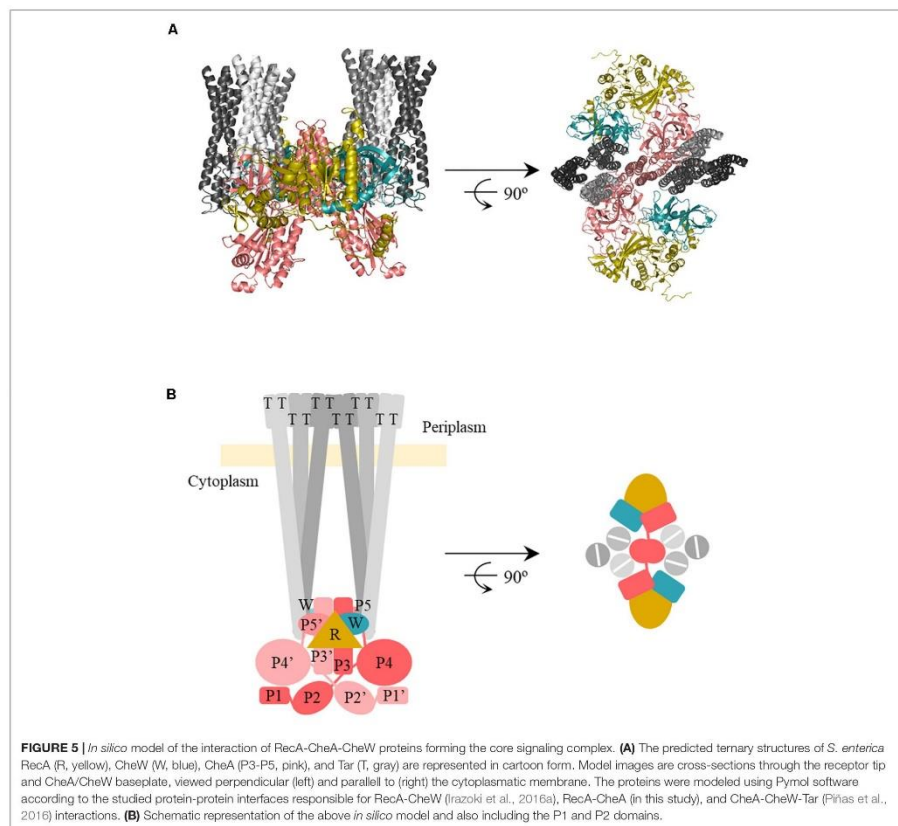
were compared with the structure of the *T. maritima* chemotaxis signaling complex (PDB:3JA6) (Cassidy et al., 2015) and modeled using PyMOL software (Schrödinger, 2010). The RecA interaction was placed according to the residues determined to be directly involved in the CheA-RecA or CheW-RecA interfaces (Tables 1, 2). As seen in Figure 5, the RecA fits into the chemoreceptor signaling complex without allosteric interference.

### RecA Interacts With Both CheW and CheA *in vivo*

To corroborate the results of the *in silico* models and study the importance of the RecA-CheA interaction for chemoreceptor polar cluster formation *in vivo*, the location of CheA and Tar proteins was analyzed using the stimulated emission depletion

microscopy (STED), a super-resolution fluorescence imaging technique that increases the axial resolution of biological samples up to 20–40 nm (Han and Ha, 2015).

*S. enterica cheA:SNAP tar:CLIP* and  $\Delta recA cheA:SNAP tar:CLIP$  tagged strains were constructed and were tested in chemoreceptor clustering and swarming assays under non-DNA damage conditions to verify that tag addition did not alter their chemoreceptor array phenotypes. No changes in either chemoreceptor polar clusters or swarming motility (Cardozo et al., 2010; Partridge et al., 2019) were observed for *S. enterica cheA:SNAP tar:CLIP* strain. Its phenotype was the same as that of *S. enterica* wild-type (Supplementary Figure S5). Also, *S. enterica*  $\Delta recA cheA:SNAP tar:CLIP$  was unable to swarm and the number of chemoreceptor polar clusters was drastically reduced (Supplementary Figure S5) since RecA is





essential for both swarming and polar array cluster formation (Mayola et al., 2014).

The RecA complementation and overexpression assays were performed using the pUA1108 vector containing wild-type *recA* and its derivatives unable to interact with CheA (RecA A214V) or CheW (RecA R222A) or both proteins (RecA R176A) under the control of the Ptac IPTG-inducible promoter. The plasmids were transformed into *S. enterica* *cheA:SNAP tar:CLIP* and  $\Delta$ *recA* *cheA:SNAP tar:CLIP* strains (Supplementary Table S1), and the intracellular location of CheA and Tar was then determined.

The SNAP and CLIP tags are self-labeling enzymes derived from the human DNA repair protein *O*<sup>6</sup>-alkylguanine-DNA alkyltransferase. Appropriate permeable dyes directly attach to the target protein with high reactivity and labeling specificity. The SNAP-tag binds *O*<sup>6</sup>-benzylguanine derivatives (Keppeler et al., 2003), and the CLIP-tag *O*<sup>2</sup>-benzylcytosine derivatives (Gautier et al., 2008). Due to these differences, the two tags, with their permeable dyes suitable for STED imaging (SNAP-Cell<sup>®</sup> 505-Star and CLIP-Cell<sup>™</sup> TMR-Star, respectively), can be employed simultaneously to specifically label target proteins in living cells (Gautier et al., 2008).

The absence of RecA impairs chemoreceptor array formation (Mayola et al., 2014). For complementation assays, the basal expression of the wild-type *recA* gene cloned in the pUA1108 vector was enough to restore chemoreceptor array formation and cell CheA and Tar were located again in cell poles (Figure 6A; Mayola et al., 2014). Nevertheless, in the presence of a non-CheA-interacting RecA, no chemoreceptor polar clusters were formed (Figure 6A) and CheA and Tar were distributed along the cell. The same phenotype was observed using a RecA mutant unable to interact with CheW (Figure 6A) or with both CheA and CheW (Figure 6A).

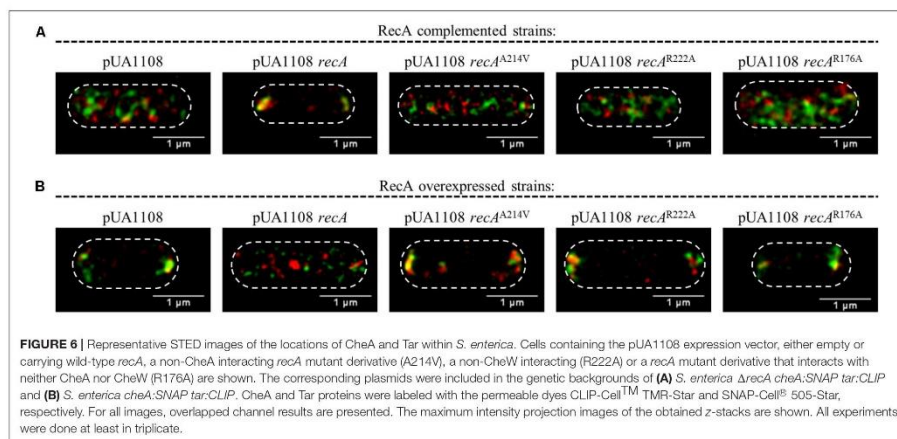
On the other hand, the RecA overexpression inhibited polar cluster assembly in a wild-type genetic background

(Irazoki et al., 2016b). Then, as expected, the IPTG-induced expression of a wild-type *recA* gene within *S. enterica* *cheA:SNAP tar:CLIP* promoted the redistribution of CheA and Tar along the cell (Figure 6B). However, the increased expression mediated by IPTG of *recA* mutants unable to bind CheA, CheW or both proteins did not alter the CheA and Tar location, that remained at the cell poles (Figure 6B). Together, the results indicate that the interaction of RecA with both CheA and CheW is needed for chemoreceptor polar array formation and that both interactions occur *in vivo*.

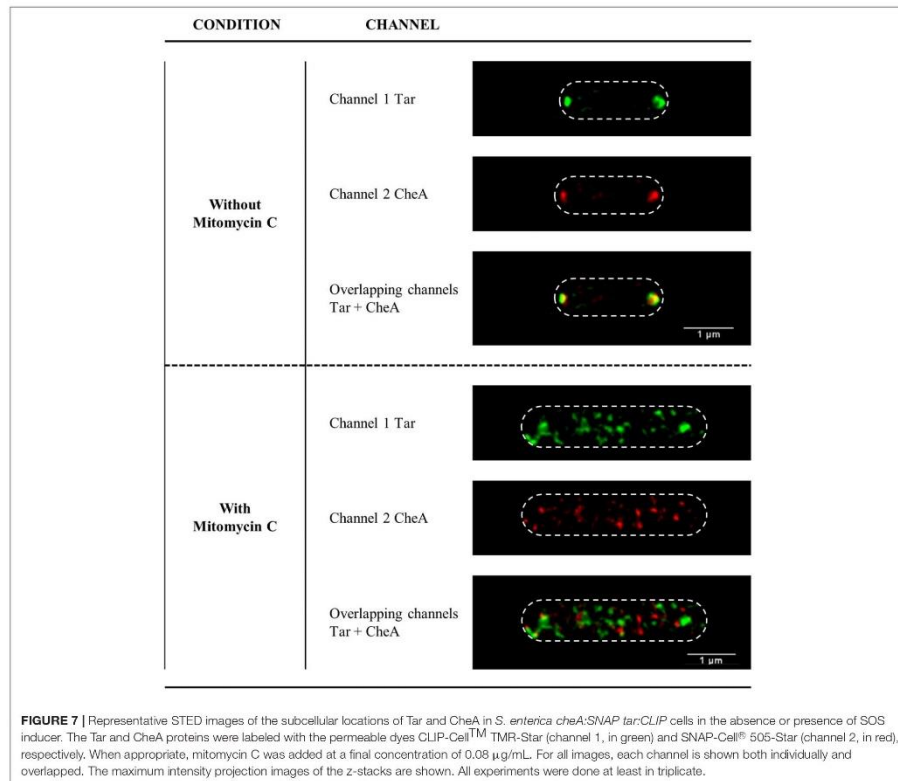
### Location of CheA and Tar Proteins Within SOS Response-Induced Cells

In bacteria grown in liquid medium under non-DNA damaging conditions, the polar cluster array proteins CheW, CheA, and Tar are located mainly at the cell poles (Sourjik and Berg, 2000; Greenfield et al., 2009; Koler et al., 2018). Several studies have shown that RecA also localizes at the poles (Lusetti and Cox, 2002; Lesterlin et al., 2014; Irazoki et al., 2016b). Our previous work demonstrated that during SOS response activation, RecA and CheW are no longer located at the cell poles but in small foci distributed along the cell (Irazoki et al., 2016a). To further understand the association of RecA with CheA and the signaling core units, the location of CheA and Tar proteins in SOS-response-induced cells was studied in *S. enterica* *cheA:SNAP tar:CLIP* and *cheA:SNAP recA:CLIP* tagged strains by STED imaging.

Under non-DNA-damaging condition, RecA, CheA, and Tar were, as expected, located at the poles of *S. enterica* cells (Figure 7 and Supplementary Figure S6). However, the addition of a sublethal concentration of SOS-inducer resulted in cell filamentation and the redistribution of CheA and Tar (Figure 7) to follow that of RecA (Supplementary Figure S6)







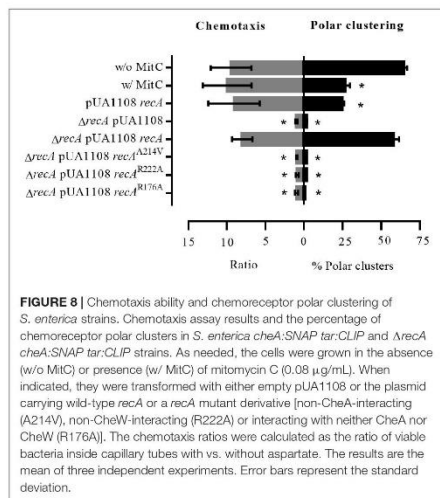
and CheW (Irazoki et al., 2016a). Thus, under non-DNA-damaging conditions and during activation of the SOS response, the intracellular distributions of CheA, CheW, Tar and RecA were the same.

### SOS Response-Induced Cells Present Normal Chemotaxis Response

To further demonstrate that RecA is a component of the signaling core unit and that the structure of this unit is preserved during SOS response activation, chemoreceptor polar clustering and chemotaxis assays were performed by exposing cells of different genetic backgrounds to a sublethal concentration of mitomycin C, and then monitoring the chemotaxis response.

As shown in **Figure 8**, the presence of mitomycin C did not affect *S. enterica* wild-type strain chemotaxis. The same results were obtained when the wild-type *recA* was

overexpressed in bacterial cells by the addition of IPTG. Under these conditions, i.e., in the presence of mitomycin C or *recA* overexpression, the absence of chemoreceptor polar clusters did not lead to an inhibition of the chemotaxis response. Interestingly, in the presence of mitomycin C, chemoreceptor polar array formation in the  $\Delta recA$  strain are lower than that observed in either SOS-induced or RecA-overexpressing wild-type cells (**Figure 8**). Further, as previously published (Mayola et al., 2014),  $\Delta recA$  cells were unable to respond to a chemoeffector, an ability that was restored only by the addition of wild-type *recA*. Neither polar cluster array formation nor chemotaxis (**Figures 6, 8**) were restored in a  $\Delta recA$  strain complemented with *recA* mutant derivatives unable to interact with CheA, CheW or both. According to these results, the formation of active signaling core units and therefore chemoreceptor polar arrays requires the binding of RecA to both CheA and CheW.



## DISCUSSION

Our results provide strong evidence supporting the interaction of RecA with P5-CheA domain (Figure 1), which is structurally similar to CheW (Vu et al., 2012; Table 1). While both P5-CheA subdomains 1 and 2 participate in the RecA-CheA interaction (Table 1), the involved CheA-residues do not overlap with those of the CheA-CheW interaction (Cassidy et al., 2015). For RecA, the CheA binding interface is located at its NH<sub>2</sub>-terminus, between residues 214 and 250 (Figure 2 and Table 2). This region is mainly associated with monomer-monomer interaction as well as RecA filament formation and stabilization (Skiba et al., 1999; Zaitsev and Kowalczykowski, 1999; Chen et al., 2008). Moreover, almost all of the residues involved in RecA-CheA pair formation had a very low recombinase activity (Supplementary Figure S3).

*In silico* docking established that the RecA interaction could be fitted to the chemoreceptor signaling complex without any allosteric interference (Figure 5), as the P5-CheA subdomain 1 was still able to interact with CheW subdomain 2 (also known as interface 1) (Natale et al., 2013). Despite the similarity of CheW and P5-CheA, only RecA Arg222 and Lys250 residues, located at the β11 strand, were associated with both RecA-CheA and RecA-CheW pair formation (Table 2; Irazoki et al., 2016a). The rest of the identified RecA residues (Ala214, located in the α13 helix, and Asp224, Ile228, and Val247, all of them in the β11 strand) are only associated with CheA binding, and their mutation did not affect the RecA-CheW interaction (Bilwes et al., 1999; Cassidy et al., 2015). RecA binding to CheW is mediated not only by the β11 strand but also by the α1 and α12 helices of RecA (Table 2; Irazoki et al., 2016a). As in the RecA-CheA interaction, RecA-CheW pairing does not interfere with the binding of any

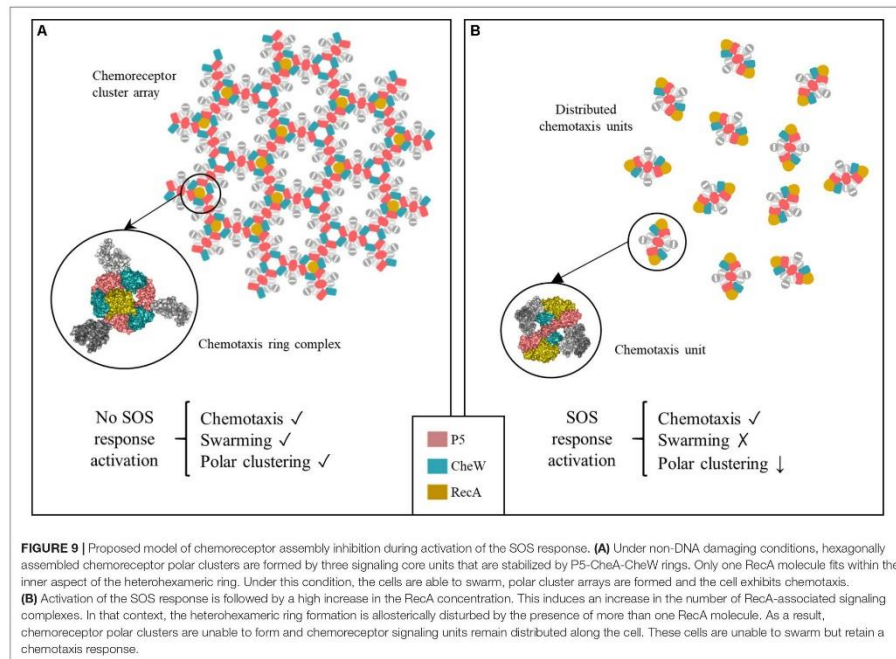
of the other CheW binding partners identified so far (CheA, CheW, and MCPs) (Irazoki et al., 2016a). Moreover, all residues involved in RecA-CheA and RecA-CheW interfaces were highly conserved not only in *S. enterica* but also in other members of *Enterobacteriaceae* (Figure 4).

*In vivo* assays showed that chemoreceptor polar clustering requires the interaction of RecA with both CheA and CheW. Indeed, RecA was distributed along the cell when polar clusters are not built (Supplementary Figure S4). Further, RecA mutants unable to bind CheA, CheW, or both proteins neither restored wild-type chemoreceptor polar cluster assembly in cells with a *ΔrecA* genetic background (Figure 6A) nor abolished polar cluster formation in wild-type cells overexpressing RecA (Irazoki et al., 2016b; Figure 6B). According to these results, the interaction of RecA not only with CheW but also with CheA is essential for chemoreceptor array formation.

Previous studies showed that the stoichiometry of chemoreceptor core unit components within the cell is crucial for polar array assembly. For example, the absence or overexpression of CheW abolishes chemoreceptor cluster formation (Avram Sanders et al., 1989; Cardozo et al., 2010). The same phenotype occurs in a knock out *recA* mutant (Mayola et al., 2014) or when the RecA concentration is increased, whether by SOS response activation or by its overexpression (Gómez-Gómez et al., 2007; Irazoki et al., 2016b). In earlier work, we proposed that RecA prompts the titration of CheW, thus preventing chemoreceptor assembly and, in turn, polar cluster array formation during activation of the SOS response (Irazoki et al., 2016a). The same sequence of events may describe the CheA-RecA interaction. Nevertheless, the results described herein clearly determine that RecA protein present different binding interfaces with CheA and CheW, that do not overlap with those associated with CheA-CheW interaction or with their binding to MCPs. Together with the fact that, in the absence of RecA there is no chemotaxis response (Mayola et al., 2014), suggested the direct interaction of RecA with the chemoreceptor core unit.

STED imaging of the tagged strains indicated that RecA, CheA, Tar (Figure 6 and Supplementary Figure S6) and CheW (Irazoki et al., 2016a), the main components of the signaling core unit, follow the same intracellular distribution when RecA concentration is increased following the activation of the SOS response or *recA* overexpression, moving from the cell poles to along the cell axis (Figure 6 and Supplementary Figure S6; Irazoki et al., 2016a). Furthermore, the polar cluster arrays of *S. enterica* *ΔrecA* cells were not restored by the presence of a *recA* mutant unable to bind CheA, CheW, or both, such that chemotaxis was inhibited (Figure 8). Only the addition of wild-type RecA reestablished chemotaxis (Figure 8). Taken together, these findings demonstrate that RecA and its ability to bind CheA and CheW are crucial for the functionality of the signaling core complex and for chemotaxis.

The direct association of RecA with the chemoreceptor core unit also explains the impaired formation of chemoreceptor polar clusters in the presence of increased RecA (Figure 9). Chemoreceptor arrays consist of hexagonal lattices of MCPs stabilized by interconnected heterohexameric rings of CheA and CheW (Cassidy et al., 2015). The rings are formed by the



alternated interactions between P5-CheA and CheW of three unit core complexes that give rise to interface 2, composed of the P5-CheA subdomain 2 and CheW subdomain 1. This key link between signaling core complexes in the array is needed for cluster assembly (Natale et al., 2013; Cassidy et al., 2015). As shown in **Figure 9**, there is enough space within a ring to fit one RecA molecule interacting with one of the three internal face of (CheW-CheA<sub>2</sub>-CheW) heterohexameric ring, without altering its hexagonally structure. When SOS response activation increases the intracellular RecA concentration, the protein becomes associated with a greater number of signaling core units. However, the build-up of heterohexameric rings is prevented by the high levels of RecA, which impair the formation of CheW-P5-CheA interface 2 and consequently, the array assembly is inhibited.

It is important to note that the chemotaxis response is not associated with the presence of polar chemoreceptor clusters, unlike swarming. Thus, in the *S. enterica* wild-type strain, while either SOS response activation by mitomycin C or the overexpression of wild-type *recA* impaired chemoreceptor array formation and therefore swarming motility (**Supplementary Figure S7**; Irazoki et al., 2016b), there was no effect on chemotaxis (**Figure 8**). The signaling core units were completely functional,

even in the absence of chemoreceptors arrays, only in the presence of wild-type RecA, not a RecA mutant unable to bind CheA, CheW, or both (**Figure 8**). Our results indicates, in agreement with previously reported data, that although the absence of polar clustering clearly impairs swarming ability (Cardozo et al., 2010; Frank et al., 2016; Irazoki et al., 2016b), the chemotaxis pathway remains functional (Maki et al., 2000; Briegel et al., 2014b; Frank et al., 2016; Piñas et al., 2016). These results are in Further, it is also known that chemotaxis is not affected when *E. coli* cells are treated with cephalixin (Maki et al., 2000), a  $\beta$ -lactam antibiotic that induces the SOS response (Bano et al., 2014).

The chemotaxis of bacterial cells is enhanced by the networking of chemoreceptors (Frank et al., 2016). Nevertheless, Frank et al. (2016) showed that the CheA kinase levels and flagellar motor switching are similar in cells with and without polar clusters. The same authors found that, under conditions of high CheA kinase activity, cells with dispersed receptor complexes are more sensitive to chemoeffectors than cells with polar clusters (Frank et al., 2016). However, cells can remodel their chemotaxis signaling pathway to enhance swarming motility (Partridge et al., 2019). The over production of RecA due SOS response activation by the presence of DNA-damaging



compounds or antibiotics, increase the number of signaling core units associated to RecA, and consequently modulate the architecture of chemoreceptor arrays, by impairing the heterohexameric CheA-CheW ring formation (Figure 9). Thus, the distribution of chemoreceptor signaling units modulates not only swarming motility in cells growing on a surface, to prevent exposure to higher concentrations of SOS-inducer compounds (Irazoki et al., 2016b), but also the chemotaxis performance of the SOS-induced cells. The high degree of conservation of residues associated with the CheA-RecA-CheW interaction in *Enterobacteriaceae* (Figure 4) suggested that the relationship between the SOS response, chemotaxis and swarming to modulate bacterial motility in the presence of antibiotics and other injurious or potentially lethal compounds may be extended to other species of this bacterial group.

## DATA AVAILABILITY STATEMENT

All datasets generated for this study are included in the article/Supplementary Material.

## AUTHOR CONTRIBUTIONS

EF-G, OI, and SC performed the *in silico* analyses and site-directed mutagenesis. EF-G and MM performed the fluorescent immunolabeling and STED imaging. EF-G and SC designed, performed, and analyzed the rest of experiments. EF-G, SC, and JB coordinated the research, discussed the findings, and interpreted the results. SC wrote the first draft of the manuscript. EF-G, MM, and OI wrote sections of the manuscript. All authors

contributed conception and design of the study, contributed to manuscript revision, read and approved the submitted version.

## FUNDING

The authors acknowledge financial support from the Spanish Ministry of Economy and Competitiveness through its R&D funding program (BIO2016-77011-R) and the “Severo Ochoa” program for Centres of Excellence in R&D (SEV-2015-0522), from Fundació Privada Cellex, Fundació Mig-Puig and from Generalitat de Catalunya through the CERCA program. The funders had no role in the design of the study, in data collection and analysis, in the decision to publish, or in the preparation of the manuscript.

## ACKNOWLEDGMENTS

We thank Joan Ruiz, Susana Escribano, Marc Gaona, and Miquel Sánchez for their technical support during some of the experimental procedures, and Pablo Loza and Jordi Andilla for their help and guidance on some of the super-resolution microscopy experiments.

## SUPPLEMENTARY MATERIAL

The Supplementary Material for this article can be found online at: <https://www.frontiersin.org/articles/10.3389/fmicb.2020.00583/full#supplementary-material>

## REFERENCES

- Arifuzzaman, M., Maeda, M., Itoh, A., Nishikata, K., Takita, C., Saito, R., et al. (2006). Large-scale identification of protein-protein interaction of *Escherichia coli* K-12. *Genome Res.* 16, 686–691. doi: 10.1101/gr.4527806.8
- Avram Sanders, D., Mendez, B., and Koshland, D. E. (1989). Role of the CheW protein in bacterial chemotaxis: overexpression is equivalent to absence. *J. Bacteriol.* 171, 6271–6278. doi: 10.1128/jb.171.11.6271-6278.1989
- Bano, S., Vankemmelbeke, M., Penfold, C. N., and James, R. (2014). Detection of induced synthesis of colicin E9 using *ColE9p:gfpmut2* based reporter system. *World J. Microbiol. Biotechnol.* 30, 2091–2099. doi: 10.1007/s11274-014-1635-y
- Bi, S., and Lai, L. (2015). Bacterial chemoreceptors and chemoeffectors. *Cell. Mol. Life Sci.* 72, 691–708. doi: 10.1007/s00018-014-1770-5
- Bilwes, A. M., Alex, L. A., Crane, B. R., and Simon, M. I. (1999). Structure of CheA, a signal-transducing histidine kinase. *Cell* 96, 131–141. doi: 10.1016/s0092-8674(00)80966-6
- Blat, Y., and Eisenbach, M. (1995). Tar-dependent and -independent pattern formation by *Salmonella typhimurium*. *J. Bacteriol.* 177, 1683–1691. doi: 10.1128/jb.177.7.1683-1691.1995
- Block, S. M., Segall, J. E., and Berg, H. C. (1983). Adaptation kinetics in bacterial chemotaxis. *J. Bacteriol.* 154, 312–323. doi: 10.1128/jb.154.1.312-323.1983
- Brennan, C. A., DeLoney-Marino, C. R., and Mandel, M. J. (2013). Chemoreceptor VtcA mediates amino acid chemotaxis in *Vibrio fischeri*. *Appl. Environ. Microbiol.* 79, 1889–1896. doi: 10.1128/aem.03794-12
- Briegel, A., Ladinsky, M. S., Oikonomou, C., Jones, C. W., Harris, M. J., Fowler, D. J., et al. (2014a). Structure of bacterial cytoplasmic chemoreceptor arrays and implications for chemotactic signaling. *Elife* 2014, 1–16. doi: 10.7554/eLife.02151
- Briegel, A., Wong, M. L., Hodges, H. L., Oikonomou, C. M., Piasta, K. N., Harris, M. J., et al. (2014b). New insights into bacterial chemoreceptor array structure and assembly from electron cryotomography. *Biochemistry* 53, 1575–1585. doi: 10.1021/bi5000614
- Briegel, A., Li, X., Bilwes, M. A., Hughes, K. T., Jensen, G. J., and Crane, B. R. (2012). Bacterial chemoreceptor arrays are hexagonally packed trimers of receptor dimers networked by rings of kinase and coupling proteins. *Proc. Natl. Acad. Sci. U.S.A.* 109, 3766–3771. doi: 10.1073/pnas.1115719109
- Briegel, A., Ortega, D. R., Huang, A. N., Oikonomou, C. M., Gunsalus, R. P., and Jensen, G. J. (2015). Structural conservation of chemotaxis machinery across *Archaea* and *Bacteria*. *Environ. Microbiol. Rep.* 7, 414–419. doi: 10.1111/1758-2229.12265
- Briegel, A., Ortega, D. R., Tocheva, E. I., Wuichet, K., Li, Z., Chen, S., et al. (2009). Universal architecture of bacterial chemoreceptor arrays. *Proc. Natl. Acad. Sci. U.S.A.* 106, 17181–17186. doi: 10.1073/pnas.0905181106
- Buddelmeijer, N., Aarsman, M., and den Blaauwen, T. (2013). Immunolabeling of proteins *in situ* in *Escherichia coli* K12 strains. *Bio-Protocol* 3:e852.
- Butler, M. T., Wang, Q., and Harshey, R. M. (2010). Cell density and mobility protect swarming bacteria against antibiotics. *Proc. Natl. Acad. Sci. U.S.A.* 107, 3776–3781. doi: 10.1073/pnas.0910934107
- Campos, S., Jara, M., Busquets, N., de Rozas, A. M. P., Padiola, I., Barbé, J., et al. (2002). Intracellular cyclic AMP concentration is decreased in *Salmonella typhimurium* fur mutants. *Microbiology* 148, 1039–1048. doi: 10.1099/00221287-148-4-1039
- Cardozo, M. J., Massazza, D. A., Parkinson, J. S., and Studdert, C. A. (2010). Disruption of chemoreceptor signalling arrays by high levels of CheW, the receptor-kinase coupling protein. *Mol. Microbiol.* 75, 1171–1181. doi: 10.1111/j.1365-2958.2009.07032.x

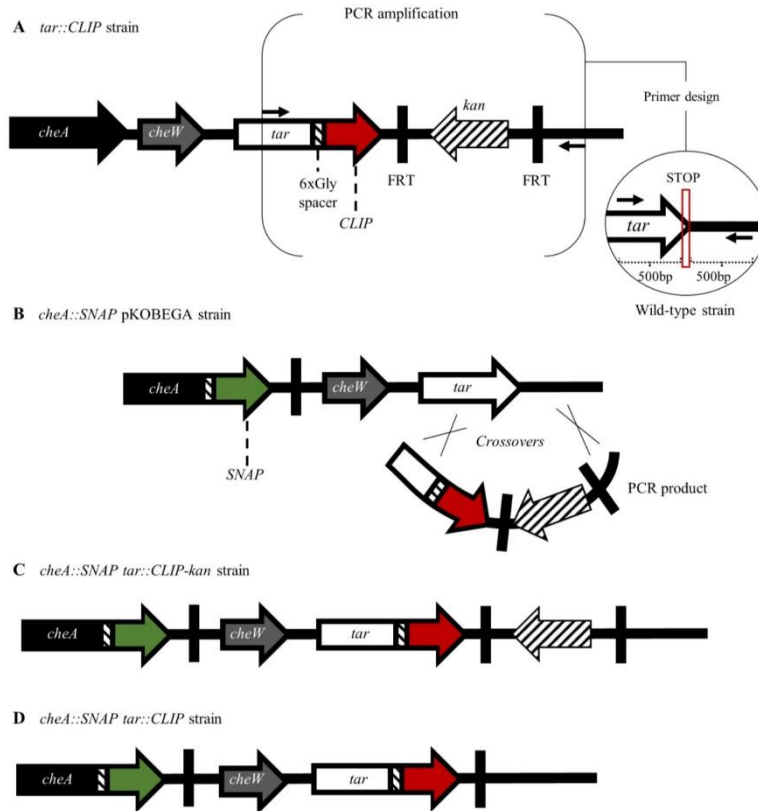
- Cassidy, C. K., Himes, B. A., Alvarez, F. J., Ma, J., Zhao, G., Perilla, J. R., et al. (2015). CryoEM and computer simulations reveal a novel kinase conformational switch in bacterial chemotaxis signaling. *Elife* 4:e08419. doi: 10.7554/eLife.08419
- Chaveroche, M. K., Ghigo, J. M., and d'Enfert, C. (2000). A rapid method for efficient gene replacement in the filamentous fungus *Aspergillus nidulans*. *Nucleic Acids Res.* 28:E97.
- Chen, Z., Yang, H., and Pavletich, N. P. (2008). Mechanism of homologous recombination from the RecA-ssDNA/dsDNA structures. *Nature* 453, 489–484. doi: 10.1038/nature06971
- Comeau, S. R., Gatchell, D. W., Vajda, S., and Camacho, C. J. (2004). ClusPro: a fully automated algorithm for protein-protein docking. *Nucleic Acids Res.* 32, 96–99. doi: 10.1093/nar/gkh354
- Cox, M. M. (1999). Recombinational DNA repair in bacteria and the RecA protein. *Prog. Nucleic Acid Res. Mol. Biol.* 63, 311–366. doi: 10.1016/s0079-6603(08)60726-6
- Cunningham, B., and Wells, J. (1989). High-resolution epitope mapping of hGH-receptor interactions by alanine-scanning mutagenesis. *Science* 244, 1081–1085. doi: 10.1126/science.2471267
- Datsenko, K. A., and Wanner, B. L. (2000). One-step inactivation of chromosomal genes in *Escherichia coli* K-12 using PCR products. *Proc. Natl. Acad. Sci. U.S.A.* 97, 6640–6645. doi: 10.1073/pnas.120163297
- Davis, R., Botstein, D., and Roth, J. (1980). *Advance Bacterial Genetics: Manual for Genetic Engineering*. Cold Spring Harbor, NY: Cold Spring Harbor Laboratory.
- Erhardt, M. (2016). Strategies to block bacterial pathogenesis by interference with motility and chemotaxis. *Science* 398, 185–205. doi: 10.1007/82.2016.493
- Falke, J. J., Bass, R. B., Butler, S. L., Chervitz, S. A., and Danielson, M. A. (1997). The two-component signaling pathway of bacterial chemotaxis: a molecular view of signal transduction by receptors, kinases, and adaptation enzymes. *Annu. Rev. Cell Dev. Biol.* 13, 457–512. doi: 10.1146/annurev.cellbio.13.1.457
- Frank, V., Piñas, G. E., Cohen, H., Parkinson, J. S., and Vaknin, A. (2016). Networked chemoreceptors benefit bacterial chemotaxis performance. *MBio* 7:e1824-16. doi: 10.1128/mBio.01824-16
- Gautier, A., Juillerat, A., Heinis, C., Corrèa, I. R., Kindermann, M., Beauflis, F., et al. (2008). An engineered protein tag for multiprotein labeling in living cells. *Chem. Biol.* 15, 128–136. doi: 10.1016/j.chembiol.2008.01.007
- Gómez-Gómez, J. M., Manfredi, C., Alonso, J. C., and Blázquez, J. (2007). A novel role for RecA under non-stress: promotion of swarming motility in *Escherichia coli* K-12. *BMC Biol.* 5:14. doi: 10.1186/1741-7007-5-14
- Greenfield, D., McEvoy, A. L., Shroff, H., Crooks, G. E., Wingreen, N. S., Betzig, E., et al. (2009). Self-Organization of the *Escherichia coli* chemotaxis network imaged with super-resolution light microscopy. *PLoS Biol.* 7:e1000137. doi: 10.1371/journal.pbio.1000137
- Han, K. Y., and Ha, T. (2015). Dual-color three-dimensional STED microscopy with a single high-repetition-rate laser. *Opt. Lett.* 40, 2653–2656.
- He, K., and Bauer, C. E. (2014). Chemotaxis signaling systems that control bacterial survival. *Trends Microbiol.* 22, 389–398. doi: 10.1016/j.tim.2014.04.004
- Huang, L., Wang, L., Lin, X., Su, Y., Qin, Y., Kong, W., et al. (2017). *mcp*, *aer*, *cheB*, and *cheV* contribute to the regulation of *Vibrio alginolyticus* (ND-01) adhesion under gradients of environmental factors. *Microbiologyopen* 6:e00517. doi: 10.1002/mbo3.517
- Huang, Z., Pan, X., Xu, N., and Guo, M. (2019a). Bacterial chemotaxis coupling protein: Structure, function and diversity. *Microbiol. Res.* 219, 40–48. doi: 10.1016/j.micres.2018.11.001
- Huang, Z., Wang, Y. H., Zhu, H. Z., Andrianova, E. P., Jiang, C. Y., Li, D., et al. (2019b). Cross talk between chemosensory pathways that modulate chemotaxis and biofilm formation. *MBio* 10:e2876-18.
- Irazoki, O., Aranda, J., Zimmermann, T., Campoy, S., Barbe, J., and Barbé, J. (2016a). Molecular interaction and cellular location of RecA and CheW proteins in *Salmonella enterica* during SOS response and their implication in swarming. *Front. Microbiol.* 7:1560. doi: 10.3389/fmicb.2016.01560
- Irazoki, O., Mayola, A., Campoy, S., Barbé, J., and Barbe, J. (2016b). SOS system induction inhibits the assembly of chemoreceptor signaling clusters in *Salmonella enterica*. *PLoS ONE* 11:e0146685. doi: 10.1371/journal.pone.0146685
- Irazoki, O., Campoy, S., and Barbé, J. (2017). The transient multidrug resistance phenotype of *Salmonella enterica* swarming cells is abolished by sub-inhibitory concentrations of antimicrobial compounds. *Front. Microbiol.* 8:1360. doi: 10.3389/fmicb.2017.01360
- Johnson, K. S., and Ottemann, K. M. (2018). Colonization, localization, and inflammation: the roles of *H. pylori* chemotaxis in vivo. *Curr. Opin. Microbiol.* 41, 51–57. doi: 10.1016/j.cmi.2017.11.019
- Jones, C. W., and Armitage, J. P. (2015). Positioning of bacterial chemoreceptors. *Trends Microbiol.* 23, 247–256. doi: 10.1016/j.tim.2015.03.004
- Källberg, M., Wang, H., Wang, S., Peng, J., Wang, Z., Lu, H., et al. (2012). Template-based protein structure modeling using the RaptorX web server. *Nat. Protoc.* 7, 1511–1522. doi: 10.1038/nprot.2012.085
- Kepler, A., Gendreizig, S., Gronemeyer, T., Pick, H., Vogel, H., and Johnsson, K. (2003). A general method for the covalent labeling of fusion proteins with small molecules in vivo. *Nat. Biotechnol.* 21, 86–89. doi: 10.1038/nbt765
- Keyamura, K., Sakaguchi, C., Kubota, Y., Niki, H., and Hishida, T. (2013). RecA protein recruits structural maintenance of chromosomes (SMC)-like RecN protein to DNA double-strand breaks. *J. Biol. Chem.* 288, 29229–29237. doi: 10.1074/jbc.M113.485474
- Koler, M., Peretz, E., Aditya, C., Shimizu, T. S., and Vaknin, A. (2018). Long-term positioning and polar preference of chemoreceptor clusters in *E. coli*. *Nat. Commun.* 9, 1–10. doi: 10.1038/s41467-018-06835-5
- Lesterlin, C., Ball, G., Schermelleh, L., and Sherratt, D. J. (2014). RecA bundles mediate homology pairing between distant sisters during DNA break repair. *Nature* 506, 249–253. doi: 10.1038/nature12868
- Li, M., and Hazelbauer, G. L. (2004). Cellular stoichiometry of the components of the chemotaxis signaling complex. *J. Bacteriol.* 186, 3687–3694. doi: 10.1128/jb.186.12.3687-3694.2004
- Li, M., and Hazelbauer, G. L. (2011). Core unit of chemotaxis signaling complexes. *Proc. Natl. Acad. Sci. U.S.A.* 108, 9390–9395. doi: 10.1073/pnas.1104824108
- Li, M., and Hazelbauer, G. L. (2014). Selective allosteric coupling in core chemotaxis signaling complexes. *Proc. Natl. Acad. Sci. U.S.A.* 111, 15940–15945. doi: 10.1073/pnas.1415184111
- Li, X., Fleetwood, A. D., Bayas, C., Bilwes, A. M., Ortega, D. R., Falke, J. J., et al. (2013). The 3.2 Å resolution structure of a receptor: CheA-CheW signaling complex defines overlapping binding sites and key residue interactions within bacterial chemosensory arrays. *Biochemistry* 52, 3852–3865. doi: 10.1021/bi400383e
- Little, J. W., and Mount, D. W. (1982). The SOS regulatory system of *Escherichia coli*. *Cell* 29, 11–22. doi: 10.1016/0092-8674(82)90085-x
- Liu, J., Hu, B., Morado, D. R., Jani, S., Manson, M. D., and Margolin, W. (2012). Molecular architecture of chemoreceptor arrays revealed by cryoelectron tomography of *Escherichia coli* minicells. *Proc. Natl. Acad. Sci. U.S.A.* 109, E1481–E1488. doi: 10.1073/pnas.1200781109
- Lusetti, S. L., and Cox, M. M. (2002). The bacterial RecA protein and the recombinational DNA repair of stalled replication forks. *Annu. Rev. Biochem.* 71, 71–100. doi: 10.1146/annurev.biochem.71.083101.133940
- Maddock, J. R., and Shapiro, L. (1993). Polar location of the chemoreceptor complex in the *Escherichia coli* cell. *Science* 259, 1717–1723. doi: 10.1126/science.8456299
- Maki, N., Gestwicki, J. E., Lake, E. M., Laura, L., Adler, J., and Kiessling, L. L. (2000). Motility and chemotaxis of filamentous cells of *Escherichia coli*. *J. Bacteriol.* 182, 4337–4342. doi: 10.1128/jb.182.15.4337-4342.2000
- Maslovska, K. H., Makiela-Dzbenka, K., and Fijałkowska, I. J. (2019). The SOS system: a complex and tightly regulated response to DNA damage. *Environ. Mol. Mutagen.* 60, 368–384. doi: 10.1002/em.22267
- Mayola, A., Irazoki, O., Martínez, I. A., Petrov, D., Menolascina, F., Stocker, R., et al. (2014). RecA protein plays a role in the chemotactic response and chemoreceptor clustering of *Salmonella enterica*. *PLoS ONE* 9:e105578. doi: 10.1371/journal.pone.0105578
- Natale, A. M., Duplantier, J. L., Piasta, K. N., and Falke, J. J. (2013). Structure, function and on-off switching of a core unit contact between CheA kinase and CheW adaptor protein in the bacterial chemosensory array: a disulfide mapping and mutagenesis study. *Biochemistry* 52, 7753–7765. doi: 10.1021/bi401159k
- Park, S. Y., Borbat, P. P., Gonzalez-Bonet, G., Bhatnagar, J., Pollard, A. M., Freed, J. H., et al. (2006). Reconstruction of the chemotaxis receptor-kinase assembly. *Nat. Struct. Mol. Biol.* 13, 400–407. doi: 10.1038/msb1085
- Partridge, J. D., Nhu, N. T. Q., Dufour, Y. S., and Harshey, R. M. (2019). *Escherichia coli* remodels the chemotaxis pathway for swarming. *MBio* 10, e316–e319. doi: 10.1128/mBio.00316-19

- Patel, M., Jiang, Q., Woodgate, R., Cox, M. M., and Goodman, M. F. (2010). A new model for SOS-induced mutagenesis: how RecA protein activates DNA polymerase V. *Crit. Rev. Biochem. Mol. Biol.* 45, 171–184. doi: 10.3109/10409238.2010.480968
- Piñas, G. E., DeSantis, M. D., and Parkinson, J. S. (2018). Noncritical signaling role of a kinase-receptor interaction surface in the *Escherichia coli* chemosensory core complex. *J. Mol. Biol.* 430, 1051–1064. doi: 10.1016/j.jmb.2018.02.004
- Piñas, G. E., Frank, V., Vaknin, A., and Parkinson, J. S. (2016). The source of high signal cooperativity in bacterial chemosensory arrays. *Proc. Natl. Acad. Sci. U.S.A.* 113, 3335–3340. doi: 10.1073/pnas.1600216113
- Raterman, E. L., and Welch, R. A. (2013). Chemoreceptors of *Escherichia coli* CFT073 play redundant roles in chemotaxis toward urine. *PLoS ONE* 8:e54133. doi: 10.1371/journal.pone.0054133
- Santos, T. M., Lin, T. Y. Y., Rajendran, M., Anderson, S. M., and Weibel, D. B. (2014). Polar localization of *Escherichia coli* chemoreceptors requires an intact Tol-Pal complex. *Mol. Microbiol.* 92, 985–1004. doi: 10.1111/mmi.12609
- Sassanfar, M., and Roberts, J. W. (1990). Nature of the SOS-inducing signal in *Escherichia coli*. The involvement of DNA replication. *J. Mol. Biol.* 212, 79–96. doi: 10.1016/0022-2836(90)90306-7
- Schrödinger, L. (2010). *The PyMOL Molecular Graphics System, Version 1.3r1*. Available online at: [https://www.scrip.org/\(S\(vtj3fa45qm1ean45vffc255\)\)/reference/ReferencesPapers.aspx?ReferenceID=1571978](https://www.scrip.org/(S(vtj3fa45qm1ean45vffc255))/reference/ReferencesPapers.aspx?ReferenceID=1571978).
- Sievers, F., Wilm, A., Dineen, D., Gibson, T. J., Karplus, K., Li, W., et al. (2011). Fast, scalable generation of high-quality protein multiple sequence alignments using Clustal Omega. *Mol. Syst. Biol.* 7:539. doi: 10.1038/msb.2011.75
- Skiba, M. C., Logan, K. M., and Knight, K. L. (1999). Intersubunit proximity of residues in the RecA protein as shown by engineered disulfide cross-links. *Biochemistry* 38, 11933–11941. doi: 10.1021/BI991118Z
- Sourjik, V., and Berg, H. C. (2000). Localization of components of the chemotaxis machinery of *Escherichia coli* using fluorescent protein fusions. *Mol. Microbiol.* 37, 740–751. doi: 10.1046/j.1365-2958.2000.02044.x
- Sourjik, V., and Wingreen, N. S. (2012). Responding to chemical gradients: bacterial chemotaxis. *Curr. Opin. Cell Biol.* 24, 262–268. doi: 10.1016/j.ceb.2011.11.008
- Story, R. M., Weber, I. T., and Steitz, T. A. (1992). The structure of the *E. coli* RecA protein monomer and polymer. *Nature* 355, 318–325. doi: 10.1038/355318a0
- Vu, A., Wang, X., Zhou, H., and Dahlquist, F. W. (2012). The receptor-CheW binding interface in bacterial chemotaxis. *J. Mol. Biol.* 415, 759–767. doi: 10.1016/j.jmb.2011.11.043
- Zaitsev, E. N., and Kowalczykowski, S. C. (1999). Enhanced monomer-monomer interactions can suppress the recombination deficiency of the recA142 allele. *Mol. Microbiol.* 34, 1–9. doi: 10.1046/j.1365-2958.1999.01552.x

**Conflict of Interest:** The authors declare that the research was conducted in the absence of any commercial or financial relationships that could be construed as a potential conflict of interest.

Copyright © 2020 Frutos-Grilo, Marsal, Irazoki, Barbé and Campoy. This is an open-access article distributed under the terms of the Creative Commons Attribution License (CC BY). The use, distribution or reproduction in other forums is permitted, provided the original author(s) and the copyright owner(s) are credited and that the original publication in this journal is cited, in accordance with accepted academic practice. No use, distribution or reproduction is permitted which does not comply with these terms.

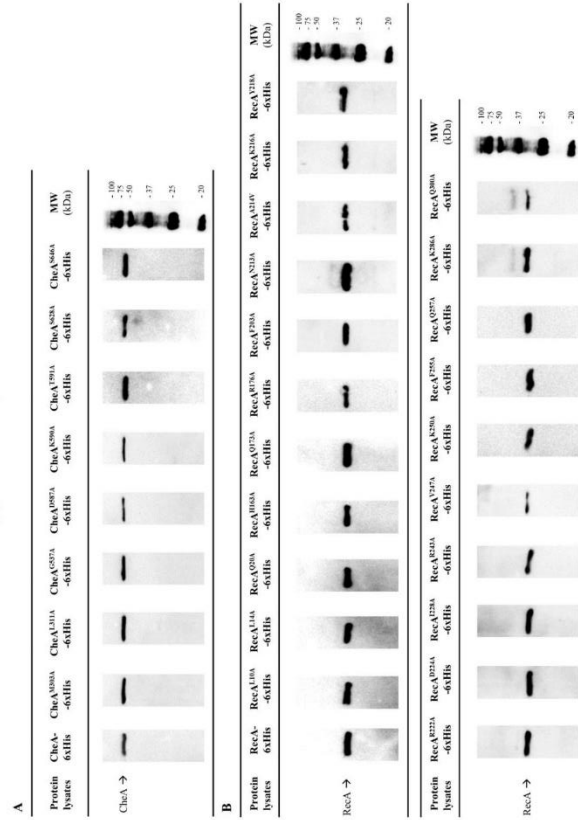
Supplementary Material



**Supplementary Figure 1. Schematic representation of the *S. enterica cheA::SNAP tar::CLIP* strain construct obtained using the  $\lambda$  Red recombination-based gene replacement method. (A) *S. enterica tar::CLIP* was constructed by introducing the tag between the last nucleotide and the STOP triplet of the *tar* gene. To construct the double-tagged strain, a PCR with primers amplifying 500 bp upstream and downstream of the *tar* STOP codon was performed. (B) The PCR product was electroporated into the *S. enterica cheA::SNAP* pKOBEGA strain and double recombination allowed the tagging of *tar* with CLIP, generating the strain (C) *S. enterica cheA::SNAP tar::CLIP-kan*. (D) Kanamycin resistance was removed using pCP20, yielding the *cheA::SNAP tar::CLIP* strain.**



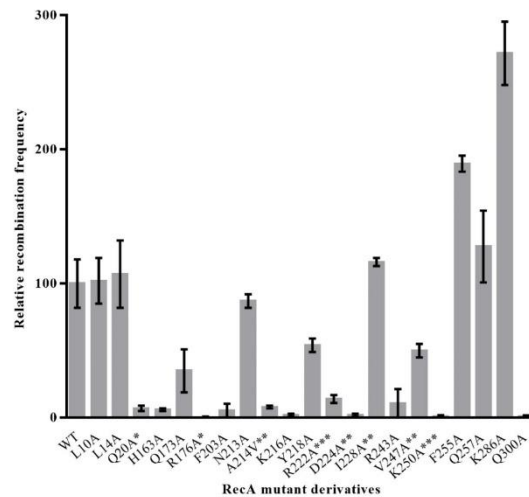
Supplementary Material



**Supplementary Figure 2. Expression of RecA and CheA mutant derivatives.** Western blot assays of the cell lysates expressing the corresponding *S. enterica* (A) CheA or (B) RecA mutant derivative were performed. In both cases, CheA and RecA proteins were detected using anti-6xHis IgG1 (Merck) and horseradish-peroxidase (HRP)-coupled anti-mouse IgG (Acris) was added as secondary antibody.



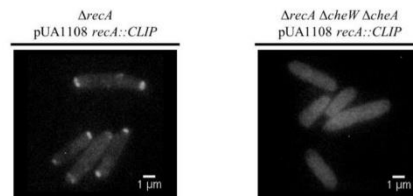
Supplementary Material



**Supplementary Figure 3. *In vivo* recombination activity of the RecA mutant derivatives.** The efficiency of *S. enterica*  $\Delta recA$  strains containing an expression vector carrying the corresponding *recA* mutant derivative and transduced by bacteriophage P22intH7 was tested for use in recombination studies using a selectable genetic marker. The method was performed as described previously (Irazoki et al., 2016). The relative recombination frequency was calculated as the recombination efficiency of each mutant derivative with respect to that of the strain overexpressing wild-type *recA*. The recombination efficiency of each strain is the number of transductants compared with the initial recipient cell concentration. RecA mutant derivatives unable to interact with CheW, with CheA or both proteins are indicated by asterisks (\*, \*\* or \*\*\* respectively). The relative recombination frequencies were calculated as the mean of three independent experiments. Error bars indicate the standard deviations.

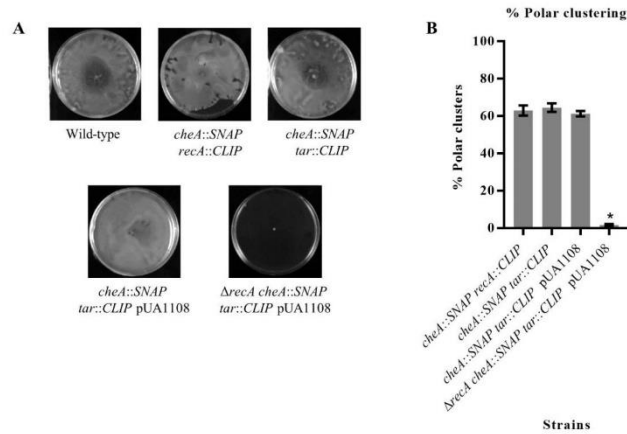
Irazoki, O., Aranda, J., Zimmermann, T., Campoy, S., and Barbé, J. (2016). Molecular interaction and cellular location of RecA and CheW proteins in *Salmonella enterica* during SOS response and their implication in swarming. *Front. Microbiol.* 7, 1560. doi:10.3389/fmicb.2016.01560.

*Supplementary Material*



**Supplementary Figure 4. RecA localization in the absence of CheA and CheW.** Representative fluorescence images of  $\Delta recA$  and  $\Delta recA \Delta cheW \Delta cheA$  strains complemented with a pUA1108 plasmid containing a *recA::CLIP*. RecA protein was labelled with the permeable dyes CLIP-Cell™ TMR-Star. The samples were examined under an Axio Imager M2 microscope (Carl Zeiss Microscopy) equipped with the Rhod (Zeiss filter set 20) filter set.

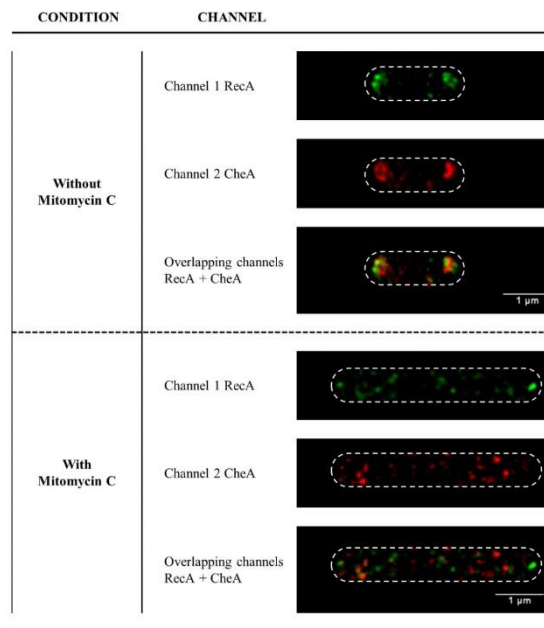
Supplementary Material



**Supplementary Figure 5. Swarming assays and chemoreceptor polar clustering of *S. enterica* tagged strains.** (A) Swarming motility and (B) chemoreceptor polar clustering were assayed to confirm that addition of the corresponding tag had no effect on the phenotype of the tested *S. enterica* strains. Swarming assays were performed as previously described (Mayola et al., 2014). The experiment was done at least in triplicate. Images of the chemoreceptor clustering assays were acquired under identical conditions and at least 350 cells were visually inspected to determine the presence and types of clusters in each sample. The results are the mean of at least three independent imaging studies. Then, a minimum of 1050 cells from each studied strain were analysed. Error bars represent the standard deviation. \* $p < 0.01$  as determined in a one-way ANOVA with a Bonferroni correction.

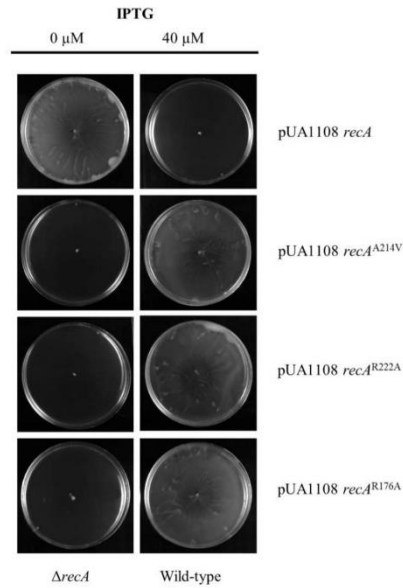
Mayola A, Irazoki O, Martínez IA, Petrov D, Menolascina F, Stocker R, Reycs-Darias JA, Kroll T, Barbé J, Campoy S. 2014. RecA protein plays a role in the chemotactic response and chemoreceptor clustering of *Salmonella enterica*. PLoS One 9:e105578.

*Supplementary Material*



**Supplementary Figure 6. Representative STED images of the subcellular locations of CheA and RecA in *S. enterica cheA::SNAP recA::CLIP* cells in the absence or presence of SOS inducer (0.08 µg mitomycin C/mL). RecA and CheA proteins were labeled with the permeable dyes CLIP-Cell™ TMR-Star (channel 1, represented in green) and SNAP-Cell® 505-Star (channel 2, in red), respectively. For all images, each channel is shown both individually and overlapped. The maximum intensity projection images of the obtained z-stacks are also shown. All experiments were done at least in triplicate.**

*Supplementary Material*



**Supplementary Figure 7. Swarming assays from *S. enterica*  $\Delta$ *recA* and wild-type strains containing pUA1108 carrying the *recA* gene or the corresponding mutant derivative.** Cells are able to complement the lack of RecA and restore swarming ability only with the plasmid containing the wild type gene, but not if RecA cannot interact with CheA and/or CheW within the  $\Delta$ *recA* strain. By contrast, in cells with basal expression of RecA (Wild-type), an increase in cytosolic wild-type RecA abolishes swarming, whereas swarming is maintained in the presence of the other RecA mutant derivatives. Assays were performed per triplicate.

## Supplementary Material

Supplementary Table 1. Bacterial strains and plasmids used in this work.

| Strain or plasmid | Relevant characteristic(s)                                                                                                                                                                                  | Source or reference                                          |
|-------------------|-------------------------------------------------------------------------------------------------------------------------------------------------------------------------------------------------------------|--------------------------------------------------------------|
| <b>Strain</b>     |                                                                                                                                                                                                             |                                                              |
| DH5 $\alpha$      | <i>E. coli</i> supE4 <i>AlacU169</i> ( $\phi$ 80 <i>AlacZ</i> <i>AM15</i> ) <i>hsdR17</i> , <i>recA1</i> , <i>endA1</i> , <i>gyrA96</i> , <i>thi-1</i> , <i>relA1</i>                                       | Clontech                                                     |
| ATCC 14028        | <i>S. enterica</i> Typhimurium wild type strain                                                                                                                                                             | ATCC                                                         |
| UA1927            | <i>S. Typhimurium</i> <i>recA</i> $\Omega$ <i>cat</i> , Cm <sup>R</sup>                                                                                                                                     | (Mayola et al., 2014)                                        |
| UA1941            | <i>S. Typhimurium</i> $\Delta$ <i>recA</i> $\Delta$ <i>cheA</i>                                                                                                                                             | This work                                                    |
| UA1915            | <i>S. Typhimurium</i> $\Delta$ <i>recA</i> $\Delta$ <i>cheW</i>                                                                                                                                             | (Mayola et al., 2014)                                        |
| UA1942            | <i>S. Typhimurium</i> <i>cheA</i> :: <i>SNAP tar</i> :: <i>CLIP</i>                                                                                                                                         | This work                                                    |
| UA1943            | <i>S. Typhimurium</i> <i>cheA</i> :: <i>SNAP recA</i> :: <i>CLIP</i>                                                                                                                                        | This work                                                    |
| UA1944            | <i>S. Typhimurium</i> <i>cheA</i> :: <i>SNAP tar</i> :: <i>CLIP</i> pUA1108                                                                                                                                 | This work                                                    |
| UA1945            | <i>S. Typhimurium</i> $\Delta$ <i>recA</i> <i>cheA</i> :: <i>SNAP tar</i> :: <i>CLIP</i> pUA1108                                                                                                            | This work                                                    |
| UA1946            | <i>S. Typhimurium</i> <i>cheA</i> :: <i>SNAP tar</i> :: <i>CLIP</i> pUA1108 <i>recA</i>                                                                                                                     | This work                                                    |
| UA1947            | <i>S. Typhimurium</i> $\Delta$ <i>recA</i> <i>cheA</i> :: <i>SNAP tar</i> :: <i>CLIP</i> pUA1108 <i>recA</i>                                                                                                | This work                                                    |
| UA1948            | <i>S. Typhimurium</i> <i>cheA</i> :: <i>SNAP tar</i> :: <i>CLIP</i> pUA1108 <i>recA</i> <sup>A214V</sup>                                                                                                    | This work                                                    |
| UA1949            | <i>S. Typhimurium</i> $\Delta$ <i>recA</i> <i>cheA</i> :: <i>SNAP tar</i> :: <i>CLIP</i> pUA1108 <i>recA</i> <sup>A214V</sup>                                                                               | This work                                                    |
| UA1950            | <i>S. Typhimurium</i> <i>cheA</i> :: <i>SNAP tar</i> :: <i>CLIP</i> pUA1108 <i>recA</i> <sup>R222A</sup>                                                                                                    | This work                                                    |
| UA1951            | <i>S. Typhimurium</i> $\Delta$ <i>recA</i> <i>cheA</i> :: <i>SNAP tar</i> :: <i>CLIP</i> pUA1108 <i>recA</i> <sup>R222A</sup>                                                                               | This work                                                    |
| UA1952            | <i>S. Typhimurium</i> $\Delta$ <i>recA</i> $\Delta$ <i>cheA</i> $\Delta$ <i>cheW</i> pUA1108 <i>recA</i> :: <i>CLIP</i>                                                                                     | This work                                                    |
| <b>Plasmid</b>    |                                                                                                                                                                                                             |                                                              |
| pKOBEGA           | Vector containing the $\lambda$ Red recombinase system, Amp <sup>R</sup> , temperature sensitive                                                                                                            | Generous gift of Prof. G. M. Ghigo (Chaveroche et al., 2000) |
| pCP20             | Vector carrying FLP system, OriV <sup>ts</sup> , Amp <sup>R</sup>                                                                                                                                           | (Datsenko and Wanner, 2000)                                  |
| pKD4              | Vector carrying FRT-Kan construction, Amp <sup>R</sup> , Kan <sup>R</sup>                                                                                                                                   | (Datsenko and Wanner, 2000)                                  |
| pUA1108           | pGEX 41-1 derivative plasmid carrying only the <i>Ptac</i> IPGIG-inducible promoter and the <i>lacP</i> gene; used as overexpression vector, Amp <sup>R</sup>                                               | (Mayola et al., 2014)                                        |
| pGEMT             | Cloning vector, Amp <sup>R</sup>                                                                                                                                                                            | Promega                                                      |
| pUA1135           | pGEMT derivative plasmid containing the <i>SNAP</i> -tag gene and kanamycin cassette flanked with FRT sequences under the control of the <i>Ptac</i> promoter, Amp <sup>R</sup> Kan <sup>R</sup>            | This work                                                    |
| pUA1136           | pGEMT derivative plasmid containing the <i>CLIP</i> -tag gene and kanamycin cassette flanked with FRT sequences under the control of the <i>Ptac</i> promoter, Amp <sup>R</sup> Kan <sup>R</sup>            | This work                                                    |
| pUA1130           | pUA1108 derivative plasmid containing the native <i>S. Typhimurium</i> <i>recA</i> gene under the control of the <i>Ptac</i> promoter, Amp <sup>R</sup>                                                     | (Mayola et al., 2014)                                        |
| pUA1137           | pUA1108 derivative plasmid containing the <i>S. Typhimurium</i> <i>recA</i> <sup>A214V</sup> mutant under the control of the <i>Ptac</i> promoter, Amp <sup>R</sup> [pUA1108 <i>recA</i> <sup>A214V</sup> ] | This work                                                    |
| pUA1138           | pUA1108 derivative plasmid containing the <i>S. Typhimurium</i> <i>recA</i> <sup>R222A</sup> mutant under the control of the <i>Ptac</i> promoter, Amp <sup>R</sup> [pUA1108 <i>recA</i> <sup>R222A</sup> ] | This work                                                    |
| pUA1139           | pUA1108 derivative plasmid containing the <i>S. Typhimurium</i> <i>recA</i> <sup>R176A</sup> mutant under the control of the <i>Ptac</i> promoter, Amp <sup>R</sup> [pUA1108 <i>recA</i> <sup>R176A</sup> ] | (Irazoki et al., 2016)                                       |
| pUA1140           | pUA1108 derivative plasmid containing the <i>S. Typhimurium</i> <i>recA</i> :: <i>CLIP</i> under the control of the <i>Ptac</i> promoter, Amp <sup>R</sup>                                                  | This work                                                    |

Chaveroche, M. K., Ghigo, J. M., and d'Enfert, C. (2000). A rapid method for efficient gene replacement in the filamentous fungus *Aspergillus nidulans*. *Nucleic Acids Res.* 28, E97. doi:10.1093/nar/28.22.e97

Datsenko, K., and Wanner, B. L. (2000). One-step inactivation of chromosomal genes in *Escherichia coli* K-12 using PCR products. *Proc. Natl. Acad. Sci. U. S. A.* 97, 6640–6645. doi:10.1073/pnas.120163297.

Irazoki, O., Aranda, J., Zimmermann, T., Campoy, S., and Barbé, J. (2016). Molecular interaction and cellular location of RecA and CheW proteins in *Salmonella enterica* during SOS response and their implication in swarming. *Front. Microbiol.* 7, 1560. doi:10.3389/fmicb.2016.01560.

Mayola, A., Irazoki, O., Martínez, I. A., Petrov, D., Menolascina, F., Stocker, R., et al. (2014). RecA protein plays a role in the chemotactic response and chemoreceptor clustering of *Salmonella enterica*. *PLoS One* 9, e105578. doi:10.1371/journal.pone.0105578.

## Supplementary Material

**Supplementary Table 2.** Primers used in this work.

| Primer name | Sequence                                                                                                 | Application                                                                                    |
|-------------|----------------------------------------------------------------------------------------------------------|------------------------------------------------------------------------------------------------|
| Tar_clip_F  | agtgaacgctcaglcggcaatacggccagtcattagccgagggatgatg<br>cgaactgggaaccttcGCCTCCGCCGCCCTCCATGGAC<br>CAAAGAC   | Oligonucleotides to introduce<br>CLIP-tag after <i>tar</i> gene                                |
| Tar_clip_R2 | ttttgttttatctatcgcaaccagacgaaaggtatcggcgggttcgaaatfaat<br>cgataaccgacagcgacgctgaATGGGAATTAGCCATGGT<br>CC |                                                                                                |
| R_clip_F    | taatcagaatgccaccggcattcggcgttgacgatagcgaagcgttcgaga<br>aaccaacgaagattttGCCTCCGCCGCCCTCCATGGAC<br>AAAGAC  | Oligonucleotides to introduce<br>CLIP-tag after <i>recA</i> gene                               |
| R_clip_P2   | cafaaatgcagcccttgatgfaattfaacgttttgcgnaatggcgttcgtttgc<br>cgccccaccatcactgatgaATGGGAATTAGCCATGGTCC       |                                                                                                |
| W_snap_F    | ggfgaatcgaaaaaactgctaacagcgaagatggcgtgctggatategc<br>agcatcacacgtcggcctccggcgcctccatggacaaaagac          | Oligonucleotides to introduce<br>SNAP-tag after <i>cheW</i> gene                               |
| W_snap_P2   | cgatgaagaggcactctaccctggcgaagcataacggfgaatattgccgg<br>atggcgcgacgcatccggcaacgttaATGGGAATTAGCCATG<br>GTCC |                                                                                                |
| A_snap_F    | cgcgctgattgtagtllccgcatlccagggtltaaccggaacaacgtatgg<br>cgaacacggccgctcgcgcgctccatggacaagac               | Oligonucleotides to introduce<br>SNAP-tag after <i>cheA</i> gene                               |
| A_snap_P22  | caggaattcctgacctgacgctcgcggcagttgcttaactactatacgg<br>gtcatatttcccttctcaactcaaATGGGAATTAGCCATGGTCC        |                                                                                                |
| cApK03BF    | agggatccTTCGATAATCACCAGAATCAG                                                                            | Oligonucleotides for checking<br>500 bp downstream and upstream<br>of its STOP codon           |
| cApK03BR    | agggatccGATGTGGTGAACGTAACAT                                                                              |                                                                                                |
| cheA_fw     | acacaggaacagctacatATGAGCATGGATATTAGCG                                                                    | Oligonucleotide to amplify since<br>start of <i>cheA</i>                                       |
| cWpK03BF    | agggatccCATTCGGAGTAAATCCGT                                                                               | Oligonucleotides for checking<br>500 bp downstream and upstream<br>of its STOP codon           |
| cWpK03BR    | agggatccACCGGATGAGTAATGTAAGC                                                                             |                                                                                                |
| pNAS_RecAf  | ttcacacaggaacagctacaATGGCTATCGACGAAAAC                                                                   | Oligonucleotides for checking<br><i>recA</i> gene from its start and final<br><i>recX</i> gene |
| recX_HF_f   | gggatcgggccggaccggatccTCAATCTGCAAAAATTTTC<br>GCC                                                         |                                                                                                |
| tarpK03BF   | AGggatccATGGCGATACTGTAAGGTCT                                                                             | Oligonucleotides for checking<br>500 bp downstream and upstream<br>of its STOP codon           |
| tarpK03BR   | agggatccACTAACATCTGGCGCTGA                                                                               |                                                                                                |
| M304A F     | TACCCAGTCAgegTTGGCCGAGC                                                                                  | Oligonucleotides for CheA<br>M303A mutant derivative<br>construction                           |
| M304A R     | ATCACTAACTCGCCGACC                                                                                       |                                                                                                |
| L312A F     | TTCTAACGAGgegGACCCGGTAAACC                                                                               | Oligonucleotides for CheA<br>L311A mutant derivative<br>construction                           |
| L312A R     | CGCTGGGCCAACATTGAC                                                                                       |                                                                                                |
| G538A F     | TCGCGTGGCGgegGAAGTTTTTA                                                                                  | Oligonucleotides for CheA<br>G537A mutant derivative<br>construction                           |
| G538A R     | ACCGACAICCCAICGAGG                                                                                       |                                                                                                |
| D588A F     | GTTTGACGTGgegGGGGCGAAAAC                                                                                 | Oligonucleotides for CheA<br>D587A mutant derivative<br>construction                           |
| D588A R     | ACTTTCCACAATTCGACC                                                                                       |                                                                                                |
| K591A F     | GGACGGGGCGgcaACCGAAGCCA                                                                                  | Oligonucleotides for CheA<br>K590A mutant derivative<br>construction                           |
| K591A R     | ACGTCAAACACTTCCACAATTCGAC                                                                                |                                                                                                |

## Supplementary Material

|         |                                           |                                                                      |
|---------|-------------------------------------------|----------------------------------------------------------------------|
| T592A_F | CGGGGCgAAAgccGAAGCCACGC                   | Oligonucleotides for CheA<br>T591A mutant derivative<br>construction |
| T592A_R | TCCACGTCAAACACTTTCACAATTCGACC             |                                                                      |
| S629A_F | AAATCTGGAAgcccAATTATCGCAAGGTACCGG         | Oligonucleotides for CheA<br>S628A mutant derivative<br>construction |
| S629A_R | TTGACCACCACCTGGTGC                        |                                                                      |
| S647A_F | GGGCGACGGCgcccGTCGCGCTGA                  | Oligonucleotides for CheA<br>S646A mutant derivative<br>construction |
| S647A_R | AGGATCGTCGCGCGGAAAATC                     |                                                                      |
| F204A_F | TGGCGTGATGgcccGGTAACCCGG                  | Oligonucleotides for RecA<br>F203A mutant derivative<br>construction |
| F204A_R | ATCTTCATACGGATCTGG                        |                                                                      |
| I229A_F | TATCCGTCGTgcccGGCGCGGTGA                  | Oligonucleotides for RecA I228A<br>mutant derivative construction    |
| I229A_R | TCAAGACGAACAGAGGCG                        |                                                                      |
| R244A_F | TAGCGAAACGgcccGTGAAAGTGGTAAAAACAA<br>AATC | Oligonucleotides for RecA<br>R243A mutant derivative<br>construction |
| R244A_R | CCCACGACATTATCGCCC                        |                                                                      |
| F256A_F | CGCCGCGCCGgcccAAGCAGGCCG                  | Oligonucleotides for RecA<br>F255A mutant derivative<br>construction |
| F256A_R | ATTTTGTTTTTCACCACTTTCACACGCGTTTC          |                                                                      |
| Q258A_F | GCCGTTTAAAggcccGCCGAGTTCC                 | Oligonucleotides for RecA<br>Q257A mutant derivative<br>construction |
| Q258A_R | GCGGCGATTTTGTTTTTC                        |                                                                      |
| K287A_F | GCTGATCGAGgcccGCGGGCGCAT                  | Oligonucleotides for RecA<br>K286A mutant derivative<br>construction |
| K287A_R | TTCTCTTCACGCCCAGG                         |                                                                      |
| Q301A_F | GAAGATTGGCgcccGGTAAAGCGAACG               | Oligonucleotides for RecA<br>Q300A mutant derivative<br>construction |
| Q301A_R | TCGCCGTTGTAGCTGTAC                        |                                                                      |





# 10 REFERENCES



## 10. References

1. Bar-On, Y. M., Phillips, R. & Milo, R. The biomass distribution on Earth. *Proc Natl Acad Sci U S A* **115**, 6506–6511 (2018).
2. Zschiedrich, C. P., Keidel, V. & Szurmant, H. Molecular mechanisms of two-component signal transduction. *Journal of Molecular Biology* vol. 428 3752–3775 (2016).
3. Wolanin, P. M., Thomason, P. A. & Stock, J. B. Histidine protein kinases: Key signal transducers outside the animal kingdom. *Genome Biology* **3**, 1–8 (2002).
4. Laub, M. T. & Goulian, M. Specificity in two-component signal transduction pathways. *Annual Review of Genetics* **41**, 121–145 (2007).
5. Wanner, B. L. Is cross regulation by phosphorylation of two-component response regulator proteins important in bacteria? *Journal of Bacteriology* **174**, 2053–2058 (1992).
6. Bourret, R. B. & Silversmith, R. E. Two-component signal transduction. **13**, 113–115 (2013).
7. Bekker, M. *et al.* The ArcBA two-component system of *Escherichia coli* is regulated by the redox state of both the ubiquinone and the menaquinone pool. *Journal of Bacteriology* **192**, 746–754 (2010).
8. Prüß, B. Involvement of two component signalling on bacterial motility and biofilm development. *Journal of Bacteriology* **199**, 1–12 (2017).
9. Caby, M. *et al.* The EnvZ-OmpR two-component signalling system is inactivated in a mutant devoid of osmoregulated periplasmic glucans in *Dickeya dadantii*. *Frontiers in Microbiology* **9**, 1–13 (2018).
10. Inclán, Y. F., Vlamakis, H. C. & Zusman, D. R. FrzZ, a dual CheY-like response regulator, functions as an output for the Frz chemosensory pathway of *Myxococcus xanthus*. *Molecular Microbiology* **65**, 90–102 (2007).

11. Freeman, J. A. & Bassler, B. L. Sequence and function of LuxU: A two-component phosphorelay protein that regulates quorum sensing in *Vibrio harveyi*. *Journal of Bacteriology* **181**, 899–906 (1999).
12. Groisman, E. A. The pleiotropic two-component regulatory system PhoP-PhoQ. *Journal of Bacteriology* vol. 183 1835–1842 (2001).
13. Stewart, V. & Stewart, V. Nitrate- and nitrite-responsive sensors *NarX* and *NarQ* of proteobacteria. (2003).
14. Arthur, M., Molinas, C. & Courvalin, P. The VanS-VanR two-component regulatory system controls synthesis of depsipeptide peptidoglycan precursors in *Enterococcus faecium* BM4147. *Journal of Bacteriology* **174**, 2582–2591 (1992).
15. Gao, R. & Lynn, D. G. Environmental pH sensing: Resolving the VirA/VirG two-component system inputs for *Agrobacterium* pathogenesis. *Journal of Bacteriology* **187**, 2182–2189 (2005).
16. Takada, H. & Yoshikawa, H. Essentiality and function of Walk/WalR two-component system: The past, present, and future of research. *Bioscience, Biotechnology and Biochemistry* **82**, 741–751 (2018).
17. Dutta, R., Qin, L. & Inouye, M. Histidine kinases: Diversity of domain organization. *Molecular Microbiology* **34**, 633–640 (1999).
18. Blair, D. F. How bacteria sense and swim. *Annual Review of Microbiology* **49**, 489–522 (2002).
19. Chervitz, S. A. & Falke, J. J. Molecular mechanism of transmembrane signalling by the aspartate receptor: A model. *Proc Natl Acad Sci U S A* **93**, 2545–2550 (1996).
20. Mechanisms, M. & Transduction, S. Molecular Mechanisms of Signal Transduction. *Journal of Molecular Biology* **428**, 1–24 (2016).
21. Gushchin, I. *et al.* Sensor histidine kinase *narq* activates via helical rotation, diagonal scissoring, and eventually piston-like shifts. *International Journal of Molecular Sciences* **21**, (2020).
22. Bourret, R. B. & Stock, A. M. Molecular Information Processing: Lessons from Bacterial Chemotaxis. *Journal of Biological Chemistry* **277**, 9625–9628 (2002).
23. Wang, S. Bacterial two-component systems: structures and signalling mechanisms. *Protein Phosphorylation in Human Health* vol. 1, chapter 15 439–466 (2012).
24. Schmidl, S. R. *et al.* Rewiring bacterial two-component systems by modular DNA-binding domain swapping. *Nature Chemical Biology* **15**, 690–698 (2019).

25. Stock, A. M., Robinson, V. L. & Goudreau, P. N. Two-component signal transduction. *Annu. Rev. Biochem* **69**, 183–215 (2000).
26. Miller, L. D., Russell, M. H. & Alexandre, G. Diversity in bacterial chemotactic responses and niche adaptation. *Advances in Applied Microbiology* vol. 66, chapter 3 (Elsevier Inc., 2009).
27. Baracchini, O. & Sherris, J. C. The chemotactic effect of oxygen on bacteria. *The Journal of Pathology and Bacteriology* **77**, 565–574 (1959).
28. Drews, G. Contributions of Theodor Wilhelm Engelmann on phototaxis, chemotaxis and photosynthesis. *Photosynthesis Research* **83**, 25–34 (2005).
29. Sadler, D. R. Chemotaxis. *Elsevier Ltd.* **5**, 1998 (1998).
30. Yoshida, M. Sexual reproduction in animals and plants. 3–11 (2014) doi:10.1007/978-4-431-54589-7.
31. Kaupp, U. B. Milestone in physiology 100 years of sperm chemotaxis. *The Journal of General Physiology* **140**, 583–586 (2012).
32. Kasinskas, R. W. & Forbes, N. S. *Salmonella typhimurium* specifically chemotax and proliferate in heterogeneous tumor tissue *in vitro*. *Biotechnol Bioeng* **94**, 710–721 (2006).
33. Forbes, N. S. Engineering the perfect (bacterial) cancer therapy. *Nat Rev Cancer* **10**, 785–94 (2010).
34. Song, J. *et al.* A microfluidic device for studying chemotaxis mechanism of bacterial cancer targeting. *Scientific Reports* **8**, 1–9 (2018).
35. Ravikumar, S., Baylon, M. G., Park, S. J. & Choi, J. Engineered microbial biosensors based on bacterial two-component systems as synthetic biotechnology platforms in bioremediation and biorefinery. *Microbial Cell Factories* **16**, 1–10 (2017).
36. Roggo, C. *et al.* Heterologous expression of *Pseudomonas putida* methyl-accepting chemotaxis proteins yields *Escherichia coli* cells chemotactic to aromatic compounds. **84**, 1–15 (2018).
37. Jung, K., Fabiani, F., Hoyer, E. & Jung, K. Bacterial transmembrane signalling systems and their engineering for biosensing. (2018).
38. Wuichet, K. & Zhulin, I. B. Origins and diversification of a complex signal transduction system in prokaryotes. *Sci signal* **3**, 1–13 (2010).
39. Matilla, M. A. & Krell, T. The effect of bacterial chemotaxis on host infection and pathogenicity. *FEMS Microbiology Reviews* **42**, 40–67 (2018).

40. Johnson, D. E. *et al.* Role of motility in the colonization of uropathogenic *Escherichia coli* in the urinary tract. *Infection and Immunity* **73**, 7644–7656 (2005).
41. Partridge, J. D. & Harshey, R. M. Swarming: Flexible roaming plans. *Journal of Bacteriology* **195**, 909–918 (2013).
42. Francis, V. I., Stevenson, E. C. & Porter, S. L. Two-component systems required for virulence in *Pseudomonas aeruginosa*. *FEMS Microbiology Letters* **364**, 1–22 (2017).
43. Alexandre, G. Chemotaxis control of transient cell aggregation. *Journal of Bacteriology* **197**, 3230–3237 (2015).
44. Henrichsen, J. Bacterial surface translocation: a survey and a classification. *Bacteriol Rev* **36**, 478–503 (1972).
45. Shrout, J. D. A fantastic voyage for sliding bacteria. *Trends Microbiol* **23**, 244–246 (2015).
46. Pollitt, E. J. G. & Diggle, S. P. Defining motility in the *Staphylococci*. *Cellular and Molecular Life Sciences* **74**, 2943–2958 (2017).
47. Harshey, R. M. Bacterial motility on a surface: Many ways to a common goal. *Annual Review of Microbiology* **57**, 249–273 (2003).
48. Kearns, D. B. A field guide to bacterial swarming motility. *Nat Rev Microbiol* **8**, 634–644 (2010).
49. Bradley, D. E. Evidence for the retraction of *Pseudomonas aeruginosa* RNA phage pili. *Biochemical and Biophysical Research Communications* **47**, 142–149 (1972).
50. Mattick, J. S. Type IV pili and twitching motility. *Annual Review of Microbiology* **56**, 289–314 (2002).
51. Clemmer, K. M., Bonomo, R. A. & Rather, P. N. Genetic analysis of surface motility in *Acinetobacter baumannii*. *Microbiology (N Y)* **157**, 2534–2544 (2011).
52. Burrows, L. L. *Pseudomonas aeruginosa* twitching motility: Type IV pili in action. *Annual Review of Microbiology* **66**, 493–520 (2012).
53. Daniels, R., Vanderleyden, J. & Michiels, J. Quorum sensing and swarming migration in bacteria. *FEMS Microbiology Reviews* **28**, 261–289 (2004).
54. Sampedro, I., Parales, R. E., Krell, T. & Hill, J. E. *Pseudomonas* chemotaxis. *FEMS Microbiology Reviews* **39**, 17–46 (2015).

55. Hospenthal, M. K., Costa, T. R. D. & Waksman, G. A comprehensive guide to pilus biogenesis in Gram-negative bacteria. *Nature Reviews Microbiology* **15**, 365–379 (2017).
56. Burdman, S., Bahar, O., Parker, J. K. & de la Fuente, L. Involvement of type IV pili in pathogenicity of plant pathogenic bacteria. *Genes (Basel)* **2**, 706–735 (2011).
57. Sun, H., Zusman, D. R. & Shi, W. Type IV pilus of *Myxococcus Xanthus* is a motility apparatus controlled by the *frz* chemosensory system. *Current Biology* **10**, 1143–1146 (2000).
58. Whitchurch, C. B., Hobbs, M., Livingston, S. P., Krishnapillai, V. & Mattick, J. S. Characterisation of a *Pseudomonas aeruginosa* twitching motility gene and evidence for a specialised protein export system widespread in eubacteria. *Gene* **101**, 33–44 (1991).
59. Kearns, D. B., Robinson, J. & Shimkets, L. J. *Pseudomonas aeruginosa* exhibits directed twitching motility up phosphatidylethanolamine gradients. *Journal of Bacteriology* **183**, 763–767 (2001).
60. Bertrand, J. J., West, J. T. & Engel, J. N. Genetic analysis of the regulation of type IV pilus function by the Chp chemosensory system of *Pseudomonas aeruginosa*. *Journal of Bacteriology* **192**, 994–1010 (2010).
61. Nan, B. & Zusman, David. R. Novel mechanisms power bacterial gliding motility. *Mol Microbiol* **101**, 186–193 (2017).
62. Mauriello, E. M. F., Mignot, T., Yang, Z. & Zusman, D. R. Gliding motility revisited: how do the *Myxobacteria* move without flagella? *Microbiology and Molecular Biology Reviews* **74**, 229–249 (2010).
63. Lasica, A. M., Ksiazek, M., Madej, M. & Potempa, J. The type IX secretion system (T9SS): highlights and recent insights into its structure and function. *Frontiers in Cellular and Infection Microbiology* **7**, (2017).
64. Howard, C. & Douglas, A. Chemotaxis in *Escherichia coli* analysed by three-dimensional tracking. *Nature* **239**, 500–504 (1972).
65. Lambert, C. *et al.* Characterizing the flagellar filament and the role of motility in bacterial prey-penetration by *Bdellovibrio bacteriovorus*. *Molecular Microbiology* **60**, 274–286 (2006).
66. Berg, H. C. *E. coli in Motion*. (2004).
67. Bilwes, A. M., Alex, L. A., Crane, B. R. & Simon, M. I. Structure of CheA, a signal-transducing histidine kinase. *Cell* **96**, 131–141 (1999).



68. Bastos-Arrieta, J., Revilla-Guarinos, A., Uspal, W. E. & Simmchen, J. Bacterial biohybrid microswimmers. *Frontiers Robotics AI* **5**, (2018).
69. Murat, D. *et al.* Opposite and coordinated rotation of amphitrichous flagella governs oriented swimming and reversals in a magnetotactic spirillum. *Journal of Bacteriology* **197**, 3275–3282 (2015).
70. Hintsche, M. *et al.* A polar bundle of flagella can drive bacterial swimming by pushing, pulling, or coiling around the cell body. *Scientific Reports* **7**, 1–10 (2017).
71. Mears, P. J., Koirala, S., Rao, C. v., Golding, I. & Chemla, Y. R. *Escherichia coli* swimming is robust against variations in flagellar number. *Elife* **2014**, 1–18 (2014).
72. Echazarreta, M. A. & Klose, K. E. *Vibrio* flagellar synthesis. *Frontiers in Cellular and Infection Microbiology* **9**, 1–11 (2019).
73. Padgett, P. J., Friedman, M. W. & Krieg, N. R. Straight mutants of *Spirillum volutans* can swim. *Journal of Bacteriology* **153**, 1543–1544 (1983).
74. Ehlers, K. M., Samuel, A. D. T., Berg, H. C. & Montgomery, R. Do cyanobacteria swim using traveling surface waves? *Proc Natl Acad Sci U S A* **93**, 8340–8343 (1996).
75. Samuel, A. D. T., Petersen, J. D. & Reese, T. S. Envelope structure of *Synechococcus* spp. WH8113, a nonflagellated swimming cyanobacterium. *BMC Microbiology* **1**, 1–8 (2001).
76. Chatterjee, S., da Silveira, R. A. & Kafri, Y. Chemotaxis when bacteria remember: Drift versus diffusion. *PLoS Computational Biology* **7**, (2011).
77. Berg, H. C. The rotary motor of bacterial flagella. *Annual Review of Biochemistry* **72**, 19–54 (2003).
78. Son, K., Guasto, J. S. & Stocker, R. Bacteria can exploit a flagellar buckling instability to change direction. *Nature Physics* **9**, 494–498 (2013).
79. Rosser, G., Baker, R. E., Armitage, J. P. & Fletcher, A. G. Modelling and analysis of bacterial tracks suggest an active reorientation mechanism in *Rhodobacter sphaeroides*. *Journal of the Royal Society Interface* **11**, (2014).
80. Burkart, M., Toguchi, A. & Harshey, R. M. The chemotaxis system, but not chemotaxis, is essential for swarming motility in *Escherichia coli*. *Proc Natl Acad Sci U S A* **95**, 2568–2573 (1998).
81. Harshey, R. M. Bees aren't the only ones: swarming in Gram-negative bacteria. *Molecular Microbiology* **13**, 389–394 (1994).

82. Eisenbach, M. Bacterial Chemotaxis. *Encyclopedia of Life Sciences* (2006) doi:10.1038/npg.els.0001251.
83. Köler, T., Curty, L. K., Barja, F., van Delden, C. & Pechère, J.C. Swarming of *Pseudomonas aeruginosa* is dependent on cell-to-cell signalling and requires flagella and pili. *Journal of Bacteriology* **182**, 5990–5996 (2000).
84. Webre, D. J., Wolanin, P. M. & Stock, J. B. Bacterial chemotaxis. 47–49.
85. Takahashi, C. *et al.* Swarming of *Pseudomonas aeruginosa* PAO1 without differentiation into elongated hyperflagellates on hard agar minimal medium. *FEMS Microbiology Letters* **280**, 169–175 (2007).
86. Hauser, G. Ober fiulniss bacterien und deren beziehungen zur septiciimie. *Leipzig: F. G. W.* vol. 107 (1885).
87. Swiecicki, J. M., Sliusarenko, O. & Weibel, D. B. From swimming to swarming: *Escherichia coli* cell motility in two-dimensions. *Integrative Biology (United Kingdom)* **5**, 1490–1494 (2013).
88. O'Rear, J., Alberti, L. & Harshey, R. M. Mutations that impair swarming motility in *Serratia marcescens* 274 include but are not limited to those affecting chemotaxis or flagellar function. *Journal of Bacteriology* **174**, 6125–6137 (1992).
89. Deditius, J. A. *et al.* Characterization of novel factors involved in swimming and swarming motility in *Salmonella enterica* serovar Typhimurium. *PLoS ONE* **10**, 1–15 (2015).
90. Gavín, R. *et al.* Lateral flagella of *Aeromonas* species are essential for epithelial cell adherence and biofilm formation. *Molecular Microbiology* **43**, 383–397 (2002).
91. Atkinson, S., Chang, C. Y., Sockett, R. E., Cámara, M. & Williams, P. Quorum sensing in *Yersinia enterocolitica* controls swimming and swarming motility. *Journal of Bacteriology* **188**, 1451–1461 (2006).
92. McCarter, L. & Silverman, M. Surface-induced swarmer cell differentiation of *Vibrio parahaemolyticus*. *Molecular Microbiology* **4**, 1057–1062 (1990).
93. Huber, B. *et al.* The *cep* quorum-sensing system of *Burkholderia cepacia* H111 controls biofilm formation and swarming motility. *Microbiology (N Y)* **147**, 2517–2528 (2001).
94. Hall, P. G. & Krieg, N. R. Swarming of *Azospirillum brasilense* on solid media. *Canadian Journal of Microbiology* **29**, 1592–1594 (1983).
95. Soto, M. J., Fernández-Pascual, M., Sanjuan, J. & Olivares, J. A *fadD* mutant of *Sinorhizobium meliloti* shows multicellular swarming migration and is impaired

- in nodulation efficiency on alfalfa roots. *Molecular Microbiology* **43**, 371–382 (2002).
96. Ghelardi, E. *et al.* Requirement of *flhA* for swarming differentiation, flagellin export, and secretion of virulence-associated proteins in *Bacillus thuringiensis*. *Journal of Bacteriology* **184**, 6424–6433 (2002).
  97. Senesi, S. *et al.* Swarming motility in *Bacillus cereus* and characterization of a *fliY* mutant impaired in swarm cell differentiation. *Microbiology (N Y)* **148**, 1785–1794 (2002).
  98. Toguchi, A., Siano, M., Burkart, M. & Harshey, R. M. Genetics of swarming motility in *Salmonella enterica* serovar Typhimurium: Critical role for lipopolysaccharide. *Journal of Bacteriology* **182**, 6308–6321 (2000).
  99. Tremblay, J. & Déziel, E. Gene expression in *Pseudomonas aeruginosa* swarming motility. *BMC Genomics* **11**, 587 (2010).
  100. Salvetti, S., Faegri, K., Ghelardi, E., Kolstø, A. B. & Senesi, S. Global gene expression profile for swarming *Bacillus cereus* bacteria. *Applied and Environmental Microbiology* **77**, 5149–5156 (2011).
  101. Gode-Potratz, C. J. & McCarter, L. L. Quorum sensing and silencing in *Vibrio parahaemolyticus*. *Journal of Bacteriology* **193**, 4224–4237 (2011).
  102. Desai, J. D. & Banat, I. M. Microbial production of surfactants and their commercial potential. *Microbiol Mol Biol Rev* **61**, 47–64 (1997).
  103. Kearns, D. B. & Losick, R. Swarming motility in undomesticated *Bacillus subtilis*. *Molecular Microbiology* **49**, 581–590 (2003).
  104. Déziel, E., Lépine, F., Milot, S. & Villemur, R. *rhlA* is required for the production of a novel biosurfactant promoting swarming motility in *Pseudomonas aeruginosa*: 3-(3-hydroxyalkanoxyloxy)alkanoic acids (HAAs), the precursors of rhamnolipids. *Microbiology (N Y)* **149**, 2005–2013 (2003).
  105. Matsuyama, T. *et al.* A novel extracellular cyclic lipopeptide which promotes flagellum-dependent and -independent spreading growth of *Serratia marcescens*. **174**, 1769–1776 (1992).
  106. Bees, M. A., Andresén, P., Mosekilde, E. & Givskov, M. Quantitative effects of medium hardness and nutrient availability on the swarming motility of *Serratia liquefaciens*. *Bulletin of Mathematical Biology* **64**, 565–587 (2002).
  107. Murray, T. S., Ledizet, M. & Kazmierczak, B. I. Swarming motility, secretion of type 3 effectors and biofilm formation phenotypes exhibited within a large

- cohort of *Pseudomonas aeruginosa* clinical isolates. *Journal of Medical Microbiology* **59**, 511–520 (2010).
108. Lai, S., Tremblay, J. & Déziel, E. Swarming motility: A multicellular behaviour conferring antimicrobial resistance. *Environmental Microbiology* **11**, 126–136 (2009).
  109. Kim, W. & Surette, M. G. Swarming populations of *Salmonella* represent a unique physiological state coupled to multiple mechanisms of antibiotic resistance. *Biological Procedures Online* **5**, 189–196 (2003).
  110. Verstraeten, N. *et al.* Living on a surface: swarming and biofilm formation. *Trends in Microbiology* **16**, 496–506 (2008).
  111. Pearson, M. M., Rasko, D. A., Smith, S. N. & Mobley, H. L. T. Transcriptome of swarming *Proteus mirabilis*. *Infection and Immunity* **78**, 2834–2845 (2010).
  112. Gode-potratz, C. J., Kustusch, R. J., Breheny, P. J., Weiss, D. S. & McCarter, L. L. Surface sensing in *Vibrio parahaemolyticus* triggers a program of gene expression that promotes colonization and virulence. *Mol Microbiol.* Gode-Potratz.2011.pdf. **79**, 240–263 (2012).
  113. Trimble, M. J. & McCarter, L. L. Bis-(3'-5')-cyclic dimeric GMP-linked quorum sensing controls swarming in *Vibrio parahaemolyticus*. *Proc Natl Acad Sci U S A* **108**, 18079–18084 (2011).
  114. Kojima, M., Kubo, R., Yakushi, T., Homma, M. & Kawagishi, I. The bidirectional polar and unidirectional lateral flagellar motors of *Vibrio alginolyticus* are controlled by a single CheY species. *Molecular Microbiology* **64**, 57–67 (2007).
  115. Sar, N., McCarter, L., Simon, M. & Silverman, M. Chemotactic control of the two flagellar systems of *Vibrio parahaemolyticus*. *Journal of Bacteriology* **172**, 334–341 (1990).
  116. Mariconda, S., Wang, Q. & Harshey, R. M. A mechanical role for the chemotaxis system in swarming motility. *Molecular Microbiology* **60**, 1590–1602 (2006).
  117. Ford, K. M., Antani, J. D., Nagarajan, A., Johnson, M. M. & Lele, P. P. Switching and torque generation in swarming *E. coli*. *Frontiers in Microbiology* **9**, 1–10 (2018).
  118. Partridge, J., Nhu, N., Dufour, Y. & Harshey, R. *Escherichia coli* remodels the chemotaxis pathway for swarming. *mBio* **10**, 1–16 (2019).
  119. Miller, M. B. & Bassler, B. L. Quorum sensing in bacteria. **55**, 165–199 (2001).

120. Ghelardi, E. *et al.* Contribution of surfactin and SwrA to flagellin expression, swimming, and surface motility in *Bacillus subtilis*. *Applied and Environmental Microbiology* **78**, 6540–6544 (2012).
121. Krasteva, P. V., Giglio, K. M. & Sondermann, H. Sensing the messenger: The diverse ways that bacteria signal through c-di-GMP. *Protein Science* **21**, 929–948 (2012).
122. Hengge, R. Principles of c-di-GMP signalling in bacteria. *Nature Reviews Microbiology* **7**, 263–273 (2009).
123. Wolfe, A. J. & Visick, K. L. Get the message out: Cyclic-Di-GMP regulates multiple levels of flagellum-based motility. *Journal of Bacteriology* **190**, 463–475 (2008).
124. Hickman, Jason; Harwood, C. Identification of FleQ from *Pseudomonas aeruginosa* as a c-diGMP-responsive transcription factor. *Mol Microbiol* **69**, 376–389 (2008).
125. Chu, E. K., Kilic, O., Cho, H., Groisman, A. & Levchenko, A. Self-induced mechanical stress can trigger biofilm formation in uropathogenic *Escherichia coli*. *Nature Communications* **9**, (2018).
126. Harshey, R. M. & Partridge, J. D. Shelter in a swarm. *J Mol Biol.* **427**, 3683–3694 (2016).
127. Kawagishi, I., Imagawa, M., Imae, Y., McCarter, L. & Homma, M. The sodium-driven polar flagellar motor of marine *Vibrio* as the mechanosensor that regulates lateral flagellar expression. *Molecular Microbiology* **20**, 693–699 (1996).
128. McCarter, L., Hilmen, M. & Silverman, M. Flagellar dynamometer controls swarmer cell differentiation of *V. parahaemolyticus*. *Cell* **54**, 345–351 (1988).
129. McCarter, L. L. Dual flagellar systems enable motility under different circumstances. *Journal of Molecular Microbiology and Biotechnology* **7**, 18–29 (2004).
130. Belas, R. & Suvanasuthi, R. The ability of *Proteus mirabilis* to sense surfaces and regulate virulence gene expression involves FliL, a flagellar basal body protein. **187**, 6789–6803 (2005).
131. Cusick, K., Lee, Y. Y., Youchak, B. & Belas, R. Perturbation of *fliL* interferes with *Proteus mirabilis* swarmer cell gene expression and differentiation. *Journal of Bacteriology* **194**, 437–447 (2012).

132. Patrick, J. E. & Kearns, D. B. Swarming motility and the control of master regulators of flagellar biosynthesis. *Mol Microbiol* **83**, 14–23 (2012).
133. Majdalani, N. & Gottesman, S. The *rcs* phosphorelay: A complex signal transduction system. *Annual Review of Microbiology* **59**, 379–405 (2005).
134. Moens, S. & Vanderleyden, J. Functions of bacterial flagella. *Critical Reviews in Microbiology* **22**, 67–100 (1996).
135. Stecher, B. *et al.* Motility allows *S. Typhimurium* to benefit from the mucosal defence. *Cellular Microbiology* **10**, 1166–1180 (2008).
136. Adler, J. A method for measuring chemotaxis and use of the method to determine optimum conditions for chemotaxis by *Escherichia coli*. *Journal of General Microbiology* **74**, 77–91 (1973).
137. Macnab, R. M. How bacteria assemble flagella. *Annual Review of Microbiology* **57**, 77–100 (2003).
138. Suzuki, K., Itabashi, T. & Ishiwata, S. Structural differences in the bacterial flagellar motor among bacterial species. *Biophysics and Physicobiology* **14**, 191–198 (2017).
139. Khan, S. & Scholey, J. M. Assembly, functions and evolution of archaella, flagella and cilia. *Current Biology* **28**, R278–R292 (2018).
140. Lim, S., Guo, X. & Boedicker, J. Q. Connecting single-cell properties to collective behaviour in multiple wild isolates of the *Enterobacter cloacae* complex. *PLoS ONE* **14**, (2019).
141. Ortega, Á., Zhulin, I. B. & Krell, T. Sensory repertoire of bacterial chemoreceptors. *Microbiol Mol Biol Rev* **81**, 1–28 (2017).
142. Yuan, W. *et al.* The importance of the interaction of CheD with CheC and the chemoreceptors compared to its enzymatic activity during chemotaxis in *Bacillus subtilis*. *PLoS ONE* **7**, 1–7 (2012).
143. Sonia L. Bardy, Ariane Briegel, Simon Rainville, T. K. Recent advances and future prospects and signal transduction. *J Bacteriol* **199**, 1–17 (2017).
144. Wuichet, K. & Zhulin, I. B. Origins and diversification of a complex signal transduction system in prokaryotes. *Sci signal* **3**, 1–13 (2012).
145. García-Fontana, C. *et al.* High specificity in CheR methyltransferase function: CheR2 of *Pseudomonas putida* is essential for chemotaxis, whereas CheR1 is involved in biofilm formation. *Journal of Biological Chemistry* **288**, 18987–18999 (2013).

146. Xu, H. *et al.* *Borrelia burgdorferi* CheY2 is dispensable for chemotaxis or motility but crucial for the infectious life cycle of the spirochete. *Infection and Immunity* **85**, 1–14 (2017).
147. Colin, R. & Sourjik, V. Emergent properties of bacterial chemotaxis pathway. *Current Opinion in Microbiology* **39**, 24–33 (2017).
148. Salah Ud-Din, A. I. M. & Roujeinikova, A. Methyl-accepting chemotaxis proteins: a core sensing element in Prokaryotes and Archaea. *Cellular and Molecular Life Sciences* **74**, 3293–3303 (2017).
149. Wilde, A. & Mullineaux, C. W. Light-controlled motility in prokaryotes and the problem of directional light perception. *FEMS Microbiology Reviews* **41**, 900–922 (2017).
150. Hou, S. *et al.* Globin-coupled sensors: A class of heme-containing sensors in Archaea and Bacteria. *Proc Natl Acad Sci U S A* **98**, 9353–9358 (2001).
151. Schlesner, M. *et al.* Identification of Archaea-specific chemotaxis proteins which interact with the flagellar apparatus. *BMC Microbiology* **9**, 1–15 (2009).
152. Berleman, J. E. & Bauer, C. E. Involvement of a Che-like signal transduction cascade in regulating cyst cell development in *Rhodospirillum centenum*. *Molecular Microbiology* **56**, 1457–1466 (2005).
153. Luu, R. A. *et al.* Integration of chemotaxis, transport and catabolism in *Pseudomonas putida* and identification of the aromatic acid chemoreceptor PcaY. *Molecular Microbiology* **96**, 134–147 (2015).
154. Black, W. P. & Yang, Z. *Myxococcus xanthus* chemotaxis homologs DifD and DifG negatively regulate fibril polysaccharide production. *Journal of Bacteriology* **186**, 1001–1008 (2004).
155. Harkey, C. W., Everiss, K. D. & Peterson, K. M. The *Vibrio cholerae* toxin-coregulated-pilus gene *tcpI* encodes a homolog of methyl-accepting chemotaxis proteins. *Infection and Immunity* **62**, 2669–2678 (1994).
156. Li, Z. *et al.* Methyl-accepting chemotaxis proteins 3 and 4 are responsible for *Campylobacter jejuni* chemotaxis and jejuna colonization in mice in response to sodium deoxycholate. *Journal of Medical Microbiology* **63**, 343–354 (2014).
157. Choi, Y. *et al.* Plasmid-encoded MCP is involved in virulence, motility, and biofilm formation of *Cronobacter sakazakii* ATCC 29544. *Infection and Immunity* **83**, 197–204 (2015).
158. Nishiyama, S. I. *et al.* Identification of a *Vibrio cholerae* chemoreceptor that senses taurine and amino acids as attractants. *Scientific Reports* **6**, 1–11 (2016).

159. Hazelbauer, G. L., Falke, J. J. & Parkinson, J. S. Bacterial chemoreceptors: high-performance signalling in networked arrays. *Trends in Biochemical Sciences* **33**, 9–19 (2008).
160. Lubkowski, J. *et al.* The structure of MCP-1 in two crystal forms provides a rare example of variable quaternary interactions. *Nature Structural Biology* **4**, 64–69 (1997).
161. Boldog, T., Grimme, S., Li, M., Sligar, S. G. & Hazelbauer, G. L. Nanodiscs separate chemoreceptor oligomeric states and reveal their signalling properties. *Proceedings of the National Academy of Sciences* **103**, 11509–11514 (2006).
162. Falke, J. J. & Hazelbauer, G. L. Transmembrane signalling in bacterial chemoreceptors. *Trends Biochem Sci.* **26**, 257–265 (2001).
163. Khursigara, C. M., Wu, X., Zhang, P., Lefman, J. & Subramaniam, S. Role of HAMP domains in chemotaxis signalling by bacterial chemoreceptors. *Proc Natl Acad Sci U S A* **105**, 16555–16560 (2008).
164. Bunney, P. E., Zink, A. N., Holm, A. A., Billington, C. J. & Kotz, C. M. Orexin activation counteracts decreases in non-exercise activity thermogenesis (NEAT) caused by high-fat diet. *Physiology & Behavior* **176**, 139–148 (2017).
165. Khalatbari, L., Kangavari, M. R., Hosseini, S., Yin, H. & Cheung, N. M. MCP: A multi-component learning machine to predict protein secondary structure. *Computers in Biology and Medicine* **110**, 144–155 (2019).
166. Greenswag, A. R. *et al.* Preformed soluble chemoreceptor trimers that mimic cellular assembly states and activate CheA autophosphorylation. *Biochemistry* **54**, 3454–3468 (2015).
167. Endres, R. G., Falke, J. J. & Wingreen, N. S. Chemotaxis receptor complexes: From signalling to assembly. *PLoS Computational Biology* **3**, 1385–1393 (2007).
168. Falke, J. J., Bass, R. B., Butler, S. L., Chervitz, S. A. & Danielson, M. A. The two-component signalling pathway of bacterial Chemotaxis: A molecular view of signal transduction by receptors, kinases, and adaptation enzymes. *Annual review of Cell and Developmental Biology* **13**, 1–55 (2010).
169. Huang, Z., Pan, X., Xu, N. & Guo, M. Bacterial chemotaxis coupling protein: Structure, function and diversity. *Microbiological Research* **219**, 40–48 (2019).
170. Griswold, I. J. & Dahlquist, F. W. The dynamic behavior of CheW from *Thermotoga maritima* in solution, as determined by nuclear magnetic resonance: Implications for potential protein-protein interaction sites. *Biophysical Chemistry* **101**, 359–373 (2002).



171. Piñas, G. E., Frank, V., Vaknin, A. & Parkinson, J. S. The source of high signal cooperativity in bacterial chemosensory arrays. *Proceedings of the National Academy of Sciences* **113**, 3335–3340 (2016).
172. Ortega, D. R. & Zhulin, I. B. Evolutionary genomics suggests that CheV is an additional adaptor for accommodating specific chemoreceptors within the chemotaxis signalling complex. *PLoS Computational Biology* **12**, 1–19 (2016).
173. Alexander, R. P., Lowenthal, A. C., Harshey, R. M. & Ottemann, K. M. CheV: CheW-like coupling proteins at the core of the chemotaxis signalling network. *Trends in Microbiology* **18**, 494–503 (2010).
174. Wuichet, K., Alexander, R. P. & Zhulin, I. B. Comparative genomic and protein sequence analyses of a complex system controlling bacterial chemotaxis. *Methods in Enzymology* **422**, 3 (2007).
175. Nakamura, S. & Minamino, T. Flagella-driven motility of bacteria. *Biomolecules* **9**, (2019).
176. Samatey, F. A. *et al.* Structure of the bacterial flagellar hook and implication for the molecular universal joint mechanism. *Nature* **431**, 1062–1068 (2004).
177. Altegoer, F., Schuhmacher, J., Pausch, P. & Bange, G. From molecular evolution to biobricks and synthetic modules: A lesson by the bacterial flagellum. *Biotechnology and Genetic Engineering Reviews* **30**, 49–64 (2014).
178. Huang, Z. *et al.* Cross talk between chemosensory pathways that modulate chemotaxis and biofilm formation. *mBio* **10**, 1–15 (2019).
179. Frankel, N. W. *et al.* Adaptability of non-genetic diversity in bacterial chemotaxis. *Elife* **3**, 1–30 (2014).
180. Kirsch, M. L. *et al.* Chemotactic methyltransferase promotes adaptation to repellents in *Bacillus subtilis*. *Journal of Biological Chemistry* **268**, 25350–25356 (1993).
181. Rao, C. v., Glekas, G. D. & Ordal, G. W. The three adaptation systems of *Bacillus subtilis* chemotaxis. *Trends in Microbiology* **16**, 480–487 (2008).
182. Szurmant, H., Muff, T. J. & Ordal, G. W. *Bacillus subtilis* CheC and FliY are members of a novel class of CheY-P-hydrolyzing proteins in the chemotactic signal transduction cascade. *Journal of Biological Chemistry* **279**, 21787–21792 (2004).
183. Muff, T. J., Foster, R. M., Liu, P. J. & Ordal, G. W. CheX in the three-phosphatase system of bacterial chemotaxis. *Journal of Bacteriology* **189**, 7007–7013 (2007).

184. Motaleb, M. A. *et al.* CheX is a phosphorylated CheY phosphatase essential for *Borrelia burgdorferi* chemotaxis. *Journal of Bacteriology* **187**, 7963–7969 (2005).
185. Rao, C. v. & Ordal, G. W. The molecular basis of excitation and adaptation during chemotactic sensory transduction in Bacteria. *Contributions to Microbiology* **16**, 33–64 (2009).
186. Briegel, A. *et al.* Bacterial chemoreceptor arrays are hexagonally packed trimers of receptor dimers networked by rings of kinase and coupling proteins. *Proceedings of the National Academy of Sciences* **109**, 3766–3771 (2012).
187. Lai, R. Z. *et al.* Cooperative signalling among bacterial chemoreceptors. *Biochemistry* **44**, 14298–14307 (2005).
188. Sourjik, V. & Berg, H. C. Functional interactions between receptors in bacterial chemotaxis. *Nature* **428**, 437–441 (2004).
189. Underbakke, E. S., Zhu, Y. & Kiessling, L. L. Protein foot-printing in a complex milieu: Identifying the interaction surfaces of the chemotaxis adaptor protein chew. *Journal of Molecular Biology* **409**, 483–495 (2011).
190. Yang, W. *et al.* *In situ* conformational changes of the *Escherichia coli* serine chemoreceptor in different signalling states. *mBio* **10**, 1–14 (2019).
191. Khursigara, C. M. *et al.* Lateral density of receptor arrays in the membrane plane influences sensitivity of the *E. coli* chemotaxis response. *EMBO Journal* **30**, 1719–1729 (2011).
192. Li, X. *et al.* The 3.2 Å resolution structure of a receptor: CheA:CheW signalling complex defines overlapping binding sites and key residue interactions within bacterial chemosensory arrays. *Biochemistry* **52**, 3852–3865 (2013).
193. Liu, J. *et al.* Molecular architecture of chemoreceptor arrays revealed by cryoelectron tomography of *Escherichia coli* minicells. *Proc Natl Acad Sci U S A* **109**, (2012).
194. Cassidy, C. K. *et al.* CryoEM and computer simulations reveal a novel kinase conformational switch in bacterial chemotaxis signalling. *Elife* **4**, 1–20 (2015).
195. Akkaladevi, N., Bunyak, F., Stalla, D., White, T. A. & Hazelbauer, G. L. Flexible hinges in bacterial chemoreceptors. *Journal of Bacteriology* **200**, 1–16 (2018).
196. Frank, V., Piñas, G. E., Cohen, H., Parkinson, J. S. & Vaknin, A. Networked chemoreceptors benefit bacterial chemotaxis performance. *mBio* **7**, 1–9 (2016).
197. Briegel, A. *et al.* Universal architecture of bacterial chemoreceptor arrays. *Proc Natl Acad Sci U S A* **106**, 17181–17186 (2009).

198. Pollard T., Earnshaw W., Lippincott-Schwartz J., Johnson G. *Cell Biology*. (2016).
199. Jones, C. W. & Armitage, J. P. Positioning of bacterial chemoreceptors. *Trends in Microbiology* **23**, 247–256 (2015).
200. Thiem, S., Kentner, D. & Sourjik, V. Positioning of chemosensory clusters in *E. coli* and its relation to cell division. *EMBO Journal* **26**, 1615–1623 (2007).
201. Koler, M., Peretz, E., Aditya, C., Shimizu, T. S. & Vaknin, A. Long-term positioning and polar preference of chemoreceptor clusters in *E. coli*. *Nature Communications* **9**, 1–10 (2018).
202. Shiomi, D., Yoshimoto, M., Homma, M. & Kawagishi, I. Helical distribution of the bacterial chemoreceptor via colocalization with the Sec protein translocation machinery. *Molecular Microbiology* **60**, 894–906 (2006).
203. Daniel, R. A. & Errington, J. Control of cell morphogenesis in bacteria: Two distinct ways to make a rod-shaped cell. *Cell* **113**, 767–776 (2003).
204. Porter, S. L., Wadhams, G. H. & Armitage, J. P. *Rhodobacter sphaeroides*: complexity in chemotactic signalling. *Trends in Microbiology* **16**, 251–260 (2008).
205. Briegel, A. *et al.* Structure of bacterial cytoplasmic chemoreceptor arrays and implications for chemotactic signalling. *Elife* **2014**, 1–16 (2014).
206. von Hoven, G. *et al.* Cytotoxin-and chemotaxis-genes cooperate to promote adhesion of photobacterium damsela. *Frontiers in Microbiology* **9**, 1–16 (2018).
207. Antunez-Lamas, M. *et al.* Bacterial chemoattraction towards jasmonate plays a role in the entry of *Dickeya dadantii* through wounded tissues. *Molecular Microbiology* **74**, 662–671 (2009).
208. Wu, H. *et al.* Identification and characterization of two chemotactic transducers for inorganic phosphate in *Pseudomonas aeruginosa*. *Journal of Bacteriology* **182**, 3400–3404 (2000).
209. Englert, D. L., Adase, C. A., Jayaraman, A. & Manson, M. D. Repellent taxis in response to nickel ion requires neither Ni<sup>2+</sup> transport nor the periplasmic NikA binding protein. *Journal of Bacteriology* **192**, 2633–2637 (2010).
210. Pasupuleti, S. *et al.* Chemotaxis of *Escherichia coli* to norepinephrine (NE) requires conversion of NE to 3,4-dihydroxymandelic acid. *Journal of Bacteriology* **196**, 3992–4000 (2014).
211. Hegde, M. *et al.* Chemotaxis to the quorum-sensing signal AI-2 requires the Tsr chemoreceptor and the periplasmic LsrB AI-2-binding protein. *Journal of Bacteriology* **193**, 768–773 (2011).

212. Cerda, O., Rivas, A. & Toledo, H. *Helicobacter pylori* strain ATCC700392 encodes a methyl-accepting chemotaxis receptor protein (MCP) for arginine and sodium bicarbonate. *FEMS Microbiology Letters* **224**, 175–181 (2003).
213. Huang, Y., Sweeney, E., Guillemin, K. & Amieva, M. Multiple acid sensors control *Helicobacter pylori* colonization of the stomach. *PLoS Pathogens* **13**, 1–28 (2017).
214. Yao, J. & Allen, C. The plant pathogen *Ralstonia solanacearum* needs aerotaxis for normal biofilm formation and interactions with its tomato host. *Journal of Bacteriology* **189**, 6415–6424 (2007).
215. Hickman, J. W., Tifrea, D. F. & Harwood, C. S. A chemosensory system that regulates biofilm formation through modulation of cyclic diguanylate levels. *Proceedings of the National Academy of Sciences* **102**, 14422–14427 (2005).
216. Flemming, H. C. Biofouling and me: My *Stockholm* syndrome with biofilms. *Water Research* **173**, 115576 (2020).
217. Ma, Y. F. *et al.* The complete genome of *Comamonas testosteroni* reveals its genetic adaptations to changing environments. *Applied and Environmental Microbiology* **75**, 6812–6819 (2009).
218. Huang, Z., *et al.* Cross talk between chemosensory pathways that modulate chemotaxis and biofilm formation. *mBio* **10**, 1–15 (2019).
219. Moreira, L. M. *et al.* Chemotactic signal transduction and phosphate metabolism as adaptive strategies during citrus canker induction by *Xanthomonas citri*. *Functional and Integrative Genomics* **15**, 197–210 (2015).
220. Fàbrega, A. & Vila, J. *Salmonella enterica* serovar Typhimurium skills to succeed in the host: Virulence and regulation. *Clinical Microbiology Reviews* **26**, 308–341 (2013).
221. Brands, D. *Salmonella. Deadly Diseases and Epidemics.* (2005).
222. Hoffmann, S. & Ahn, W. Economic cost of major foodborne illnesses increased \$2 billion from 2013 to 2018. *USDA Economic Research Service* <https://www.ers.usda.gov/amber-waves/2021/april/economic-cost-of-major-foodborne-illnesses-increased-2-billion-from-2013-to-2018/> (2021).
223. *Salmonella* subcommittee of the nomenclature committee of the international society for microbiology. The genus *Salmonella* Lignières, 1900. *J Hyg (Lond)* **34**, 333–50 (1934).
224. Centers for disease control and prevention. Incidence and trends of infection with pathogens transmitted commonly through food - foodborne diseases

- active surveillance network, 10 U.S. sites, 1996–2012. *Morbidity and Mortality Weekly Report* **62**, 283–287 (2013).
225. Gordon, M. A. *Salmonella* infections in immunocompromised adults. *Journal of Infection* **56**, 413–422 (2008).
226. Gal-Mor, O., Boyle, E. C. & Grassl, G. A. Same species, different diseases: How and why typhoidal and non-typhoidal *Salmonella enterica* serovars differ. *Frontiers in Microbiology* **5**, 1–10 (2014).
227. *Salmonella* (non-typhoidal). *World Health Organization* [https://www.who.int/news-room/fact-sheets/detail/salmonella-\(non-typhoidal\)](https://www.who.int/news-room/fact-sheets/detail/salmonella-(non-typhoidal)) (2018).
228. Ohl, M. E. & Miller, S. I. *Salmonella*: A model for bacterial pathogenesis. *Annual Review of Medicine* **52**, 259–274 (2001).
229. Majowicz, S. E. *et al.* The global burden of nontyphoidal *Salmonella* gastroenteritis. *Clinical Infectious Diseases* **50**, 882–889 (2010).
230. Blaser, M. & Newman, L. A review of human salmonellosis: I. Infective dose. *Rev Infect Dis* **4**, 1096–1106 (1982).
231. Ibarra, A. & Steele-Mortimer, O. *Salmonella* - the ultimate insider. *Salmonella* virulence factors that modulate intracellular survival. *Cellular Microbiology* **11**, 1579–1586 (2009).
232. Sano, G. I. *et al.* Flagella facilitate escape of *Salmonella* from oncotic macrophages. *Journal of Bacteriology* **189**, 8224–8232 (2007).
233. Gart, E. V. *et al.* *Salmonella* Typhimurium and multidirectional communication in the gut. *Frontiers in Microbiology* **7**, 1–18 (2016).
234. Francis, C. L., Ryan, T. A., Jones, B. D., Smith, S. J. & Falkow, S. Ruffles induced by *Salmonella* and other stimuli direct macropinocytosis of bacteria. *Nature* **364**, 639–642 (1993).
235. Coburn, B., Grassl, G. A. & Finlay, B. B. *Salmonella*, the host and disease: A brief review. *Immunology and Cell Biology* **85**, 112–118 (2007).
236. Madan, R., Krishnamurthy, G. & Mukhopadhyay, A. SopE-mediated recruitment of host Rab5 on phagosomes inhibits *Salmonella* transport to lysosomes. *Methods in Molecular Biology* **445**, 417–437 (2008).
237. Steinbach, E. C. & Scott E. Plevy, M. D. The role of macrophages and dendritic cells in the initiation of inflammation in IBD. *Bone* **20**, 166–175 (2014).

238. Micoli, F. *et al.* Comparative immunogenicity and efficacy of equivalent outer membrane vesicle and glycoconjugate vaccines against nontyphoidal *Salmonella*. *Proc Natl Acad Sci U S A* **115**, 10428–10433 (2018).
239. Worley, M. J., Nieman, G. S., Geddes, K. & Heffron, F. *Salmonella* Typhimurium disseminates within its host by manipulating the motility of infected cells. *Proc Natl Acad Sci U S A* **103**, 17915–17920 (2006).
240. Orenstein, S. R. Oral rehydration versus intravenous therapy for treating dehydration due to gastroenteritis in children. *Curr Gastroenterol Rep* **7**, 209–211 (2005).
241. Acheson, D., Hohmann, L. Nontyphoidal salmonellosis. *Clinical Infectious Diseases* **32**, 263–269 (2001).
242. Salmonella: For health professionals. Treatment & Outcomes. *Centers for Disease Control and Prevention* <https://www.cdc.gov/salmonella/general/technical.html>.
243. Burke, L. *et al.* Resistance to third-generation cephalosporins in human nontyphoidal *Salmonella enterica* isolates from England and Wales, 2010–12. *Journal of Antimicrobial Chemotherapy* **69**, 977–981 (2014).
244. Grayson, L., *et al.* Kucers' *The use of antibiotics* vol. 1 (2017).
245. CDC. National Antimicrobial Resistance Monitoring System (NARMS) Now: human data. *Department of Health and Human Services, CDC* <https://wwwn.cdc.gov/narmsnow/> (2018).
246. Irazoki, O., Mayola, A., Campoy, S. & Barbé, J. SOS system induction inhibits the assembly of chemoreceptor signalling clusters in *Salmonella enterica*. *PLoS ONE* **11**, 1–22 (2016).
247. Mayola, A. *et al.* RecA protein plays a role in the chemotactic response and chemoreceptor clustering of *Salmonella enterica*. *PLoS ONE* **9**, (2014).
248. Michel, B. After 30 years of study, the bacterial SOS response still surprises us. *PLoS Biology* **3**, 1174–1176 (2005).
249. Sassanfar, M. & Roberts, J. W. Nature of the SOS-inducing signal in *Escherichia coli*. *Journal of Molecular Biology* **212**, 79–96 (1990).
250. Chen, Z., Yang, H. & Pavletich, P. Mechanism of homologous recombination from the RecA-ssDNA/dsDNA structures. *Nature* **453**, 489–494 (2008).
251. Patel, M., Jiang, Q., Woodgate, R., Cox, M. & Goodman, F. A new model for SOS-induced mutagenesis: How RecA protein activates DNA polymerase V. *Critical Reviews in Biochemistry and Molecular Biology* **45**, 171–184 (2010).

252. Horii, T. *et al.* Regulation of SOS functions: Purification of *E. coli* LexA protein and determination of its specific site cleaved by the RecA protein. *Cell* **27**, 515–522 (1981).
253. Maslowska, K. H., Makiela-dzbenska, K. & Fijalkowska, I. J. The SOS system: A complex and tightly regulated response to DNA damage. *Environmental and Molecular Mutagenesis* **60**, 368–384 (2019).
254. Kreuzer, K. N. DNA damage responses in prokaryotes: regulating gene expression, modulating growth patterns, and manipulating replication forks. *Cold Spring Harbor Perspectives in Biology* 159–163 (2013) doi:10.1101/cshperspect.a012674.
255. Erental, A., Sharon, I. & Engelberg-Kulka, H. Two programmed cell death systems in escherichia coli: An apoptotic-like death is inhibited by the mazef-mediated death pathway. *PLoS Biology* **10**, (2012).
256. Jaszczur, M. *et al.* Mutations for worse or better: Low fidelity DNA synthesis by SOS DNA polymerase V is a tightly-regulated double-edged sword. *Biochemistry* **55**, 2309–2318 (2016).
257. Cirz, R. T. *et al.* Inhibition of mutation and combating the evolution of antibiotic resistance. *PLoS Biology* **3**, 1024–1033 (2005).
258. Kohanski, M., DePristo, M. & Collins, J. Sub-lethal antibiotic treatment leads to multidrug resistance via radical-induced mutagenesis. *Mol Cell* **37**, 311–320 (2010).
259. Song, L. Y. *et al.* Mutational consequences of ciprofloxacin in *Escherichia coli*. *Antimicrobial Agents and Chemotherapy* **60**, 6165–6172 (2016).
260. Barrett, T. C., Mok, W. W. K., Murawski, A. M. & Brynildsen, M. P. Enhanced antibiotic resistance development from fluoroquinolone persisters after a single exposure to antibiotic. *Nature Communications* **10**, 1–11 (2019).
261. Nautiyal, A., Patil, K. N. & Muniyappa, K. Suramin is a potent and selective inhibitor of *Mycobacterium tuberculosis* RecA protein and the SOS response: RecA as a potential target for antibacterial drug discovery. *Journal of Antimicrobial Chemotherapy* **69**, 1834–1843 (2014).
262. Crane, J. K., Cheema, M. B., Olyer, M. A. & Sutton, M. D. Zinc blockade of SOS Response inhibits horizontal transfer of antibiotic resistance genes in enteric Bacteria. *Front Cell Infect Microbiol* **8**, 410 (2018).
263. Rossi, F., Dellaglio, F. & Torriani, S. Evaluation of recA gene as a phylogenetic marker in the classification of dairy propionibacteria. *Systematic and Applied Microbiology* **29**, 463–469 (2006).

264. Eisen, J. A. The RecA protein as a model molecule for molecular systematic studies of Bacteria: comparison of trees of RecAs and 16S rRNAs from the same species. *J Mol Evol* **41**, 1105–1123 (1995).
265. Thompson, C. C. *et al.* Use of *recA* as an alternative phylogenetic marker in the family Vibrionaceae. *International Journal of Systematic and Evolutionary Microbiology* **54**, 919–924 (2004).
266. Vispé, S., Cazaux, C., Lesca, C. & Defais, M. Overexpression of Rad51 protein stimulates homologous recombination and increases resistance of mammalian cells to ionizing radiation. *Nucleic Acids Research* **26**, 2859–2864 (1998).
267. Yoshida, K. *et al.* The mouse RecA-like gene Dmc1 is required for homologous chromosome synapsis during meiosis. *Molecular Cell* **1**, 707–718 (1998).
268. Clark, A. J. & Margulies, A. D. Isolation and characterization of recombination-deficient mutants of *Escherichia coli* K12. *Proceedings of the National Academy of Sciences of the United States of* **53**, 451–459 (1965).
269. Yu, X. & Egelman, E. H. The RecA hexamer is a structural homologue of ring helicases. *Nature* **4**, 101–104 (1997).
270. Aihara, H. *et al.* An interaction between a specified surface of the C-terminal domain of RecA protein and double-stranded DNA for homologous pairing. *Journal of Molecular Biology* **274**, 213–221 (1997).
271. Vanloock, M. S. *et al.* ATP-mediated conformational changes in the RecA filament. *Nature* **11**, 187–196 (2003).
272. Prentiss, M., Prévost, C. & Danilowicz, C. Structure/function relationships in RecA protein-mediated homology recognition and strand exchange. *Critical Reviews in Biochemistry and Molecular Biology* **50**, 453–476 (2015).
273. Eldin, S., Forget, A. L., Lindenmuth, D. M., Logan, K. M. & Knight, K. L. Mutations in the N-terminal region of RecA that disrupt the stability of free protein oligomers but not RecA-DNA complexes. *Journal of Molecular Biology* **299**, 91–101 (2000).
274. Story, R. M. & Steitz, T. A. Structure of the *recA* protein-ADP complex. *Nature* **355**, 374–376 (1992).
275. Story M, R., Weber T., I. & Steitz A., T. The structure of the *E. coli recA* protein monomer and polymer. *Nature* **355**, 318–325 (1992).
276. Lusetti, S. L. *et al.* C-terminal deletions of the *Escherichia coli* RecA protein: Characterization of *in vivo* and *in vitro* effects. *Journal of Biological Chemistry* **278**, 16372–16380 (2003).



277. Haber, J. E. DNA Repair: The search for homology. *BioEssays* **40**, 1–24 (2018).
278. Rajendram, M. *et al.* Anionic phospholipids stabilize RecA filament bundles in *Escherichia coli*. *Mol Cell* **60**, 374–384 (2015).
279. Gómez-Gómez, J. M., Manfredi, C., Alonso, J. C. & Blázquez, J. A novel role for RecA under non-stress: Promotion of swarming motility in *Escherichia coli* K-12. *BMC Biology* **5**, 1–15 (2007).
280. Arifuzzaman, M. *et al.* Large-scale identification of protein–protein interaction of *Escherichia coli* K-12. *Genome Research* **16**, 686–691 (2006).
281. Corral, J., Pérez-Varela, M., Barbé, J. & Aranda, J. Direct interaction between RecA and a CheW-like protein is required for surface-associated motility, chemotaxis and the full virulence of *Acinetobacter baumannii* strain ATCC 17978. *Virulence* **11**, 315–326 (2020).
282. Medina-Ruiz, L. *et al.* Overexpression of the *recA* gene decreases oral but not intraperitoneal fitness of *Salmonella enterica*. *Infection and Immunity* **78**, 3217–3225 (2010).
283. Irazoki, O., Aranda, J., Zimmermann, T., Campoy, S. & Barbé, J. Molecular interaction and cellular location of RecA and CheW proteins in *Salmonella enterica* during SOS response and their implication in swarming. *Frontiers in Microbiology* **7**, 1–15 (2016).
284. Källberg, M. *et al.* Template-based protein structure modeling using the RaptorX web server. *Nature Protocols* **7**, 1511–1522 (2012).
285. Comeau, S. R., Gatchell, D. W., Vajda, S. & Camacho, C. J. ClusPro: A fully automated algorithm for protein–protein docking. *Nucleic Acids Research* **32**, (2004).
286. Cunningham, B. C. & Wells, J. A. *High-resolution epitope mapping of hGH-receptor interactions by alanine-scanning mutagenesis*. <https://www.science.org>.
287. Zaitsev E, Kowalczykowski S. Enhanced monomer–monomer interactions can suppress the recombination deficiency of the *recA142* allele. *Mol Microbiol* **34** 1–9 (1999).
288. Skiba, M. C., Logan, K. M. & Knight, K. L. Intersubunit proximity of residues in the RecA protein as shown by engineered disulfide cross-links. *Biochemistry* **38**, 11933–11941 (1999).
289. Schrödinger, L. The PyMOL Molecular Graphics System, Version 1.3r1. (2010).
290. Natale, A. M., Duplantis, J. L., Piasta, K. N. & Falke, J. J. Structure, function, and on-off switching of a core unit contact between CheA kinase and CheW

- adaptor protein in the bacterial chemosensory array: A disulfide mapping and mutagenesis study. *Biochemistry* **52**, 7753–7765 (2013).
291. Hell, S. W. & Wichmann, J. Breaking the diffraction resolution limit by stimulated emission: stimulated-emission-depletion fluorescence microscopy. *Optics Letters* **19**, 780 (1994).
  292. Keppler, A. *et al.* A general method for the covalent labelling of fusion proteins with small molecules in vivo. *Nature Biotechnology* **21**, 86–89 (2003).
  293. Gautier, A. *et al.* An engineered protein tag for multiprotein labelling in living cells. *Chemistry and Biology* **15**, 128–136 (2008).
  294. Partridge, J. D., Nhu, N. T. Q. Q., Dufour, Y. S. & Harshey, R. M. *Escherichia coli* remodels the chemotaxis pathway for swarming. *mBio* **10**, 1–16 (2019).
  295. Cardozo, M. J., Massazza, D. A., Parkinson, J. S. & Studdert, C. A. Disruption of chemoreceptor signalling arrays by high levels of CheW, the receptor-kinase coupling protein. *Molecular Microbiology* **75**, 1171–1181 (2010).
  296. Sourjik, V. & Berg, H. C. Localization of components of the chemotaxis machinery of *Escherichia coli* using fluorescent protein fusions. *Molecular Microbiology* vol. 37 (2000).
  297. Greenfield, D. *et al.* Self-organization of the *Escherichia coli* chemotaxis network imaged with super-resolution light microscopy. *PLoS Biology* **7**, (2009).
  298. Lesterlin, C., Ball, G., Schermelleh, L. & Sherratt, D. J. RecA bundles mediate homology pairing between distant sisters during DNA break repair. *Nature* **506**, 249–253 (2014).
  299. Lusetti, S. L. & Cox, M. M. The bacterial RecA protein and the recombinational DNA repair of stalled replication forks. *Annual Review of Biochemistry* vol. 71 71–100 (2002).
  300. Vu, A., Wang, X., Zhou, H. & Dahlquist, F. W. The receptor-CheW binding interface in bacterial chemotaxis. *Journal of Molecular Biology* **415**, 759–767 (2012).
  301. Maki, N., Gestwicki, J. E., Lake, E. M., Kiessling, L. L. & Adler, J. *Motility and Chemotaxis of Filamentous Cells of Escherichia coli*. *Journal of Bacteriology* vol. 182 (2000).
  302. Bano, S., Vankemmelbeke, M., Penfold, C. N. & James, R. Detection of induced synthesis of colicin E9 using ColE9p::gfpmut2 based reporter system. *World Journal of Microbiology and Biotechnology* **30**, 2091–2099 (2014).

303. Chaveroche, M. K., Ghigo, J. M. & Enfert, C. A rapid method for efficient gene replacement in the filamentous fungus *Aspergillus nidulans*. *Nucleic Acids Res* **28**, 97 (2000).
304. Datsenko, K. A. & Wanner, B. L. One-step inactivation of chromosomal genes in *Escherichia coli* K-12 using PCR products. *Proc Natl Acad Sci USA* **97**, 6640–5 (2000).
305. Irazoki, O. *et al.* Molecular interaction and cellular location of RecA and CheW proteins in *Salmonella enterica* during SOS response and their implication in swarming. *Front Microbiol* **7**, 1560 (2016).
306. Campoy, S. *et al.* Intracellular cyclic AMP concentration is decreased in *Salmonella Typhimurium* fur mutants. *Microbiology* vol. 148 (2002).
307. Davis, R., Botstein, D. & Roth, J. Advance Bacterial Genetics: Manual for Genetic Engineering. *Cold Spring Harbor, NY: Cold Spring Harbor Laboratory. Erhardt, M* (1980).
308. Lazova, M. D., Butler, M. T., Shimizu, T. S. & Harshey, R. M. *Salmonella* chemoreceptors McpB and McpC mediate a repellent response to L-cystine: A potential mechanism to avoid oxidative conditions. *Molecular Microbiology* **84**, 697–711 (2012).
309. Melton, T., Hartman, P. E., Stratis, J. P., Lee, T. L. & Davisstif, A. T. Chemotaxis of *Salmonella Typhimurium* to amino acids and some sugars. *Journal of Bacterology* (1978).
310. Dower, W. J., Miller, J. F. & Ragsdale', C. W. *High efficiency transformation of E.coli by high voltage electroporation. Nucleic Acids Research* vol. 16 (1988).
311. O'Callaghan, D. & Charbit, A. High efficiency transformation of *Salmonella Typhimurium* and *Salmonella typhi* by electroporation. **223**, 156–158 (1990).
312. McWilliam, H. *et al.* Analysis tool web services from the EMBL-EBI. *Nucleic Acids Research* **41**, (2013).
313. Raterman, E. L. & Welch, R. A. Chemoreceptors of *Escherichia coli* CFT073 play redundant roles in chemotaxis toward urine. *PLoS ONE* **8**, (2013).
314. Kroupitski, Y. *et al.* Internalization of *Salmonella enterica* in leaves is induced by light and involves chemotaxis and penetration through open stomata. *Applied and Environmental Microbiology* **75**, 6076–6086 (2009).

# 11 ACKNOWLEDGEMENTS



## 11. Acknowledgements

*Empecé esta aventura en el 2017 y aunque esta etapa acabe, para siempre me llevaré conmigo los buenos recuerdos y la sabiduría que he conseguido. Esto no hubiera sido posible sin la ayuda de todos los que me han apoyado, ayudado, animado y querido. Y por ello, quiero agradecerse:*

*A mis directores de tesis Jordi Barbé, Susana Campoy y María Marsal, por dedicarme parte de vuestro tiempo, depositar en mí la confianza, conocimientos y el apoyo tanto logístico como emocional que he necesitado. Destacar a Susana, por brindarme oportunidades y motivación desde el 2015; has sido un gran pilar todos estos años y quien más me ha ayudado en tener la ilusión por cerrar esta etapa y así abrir y continuar con más proyectos científicos.*

*A la Profesora Montserrat Llagostera y la Doctora Pilar Cortés, por los sabios consejos y el asesoramiento que he necesitado a lo largo de estos años.*

*A Jesús Aranda, Joan Ruiz y Susana Escribano. No sólo me habéis ayudado científicamente y dotado del material y los medios que he requerido, sino que me habéis transmitido que un grupo de trabajo puede ser tan cercano como una familia.*

*A mis compañeros de laboratorio, por hacerme reír y soñar, despertarme de esos frustrados días en los que nada sale, por ayudarme en cuanto he necesitado...*

*Miquel, Jordi y María, las risas tanto dentro como fuera del laboratorio y la estima que os tengo son incalculables. ¡Os debo muchas sesiones de psicología y logopedia! Ojalá volver a trabajar los cuatro juntos y cumplir nuestras metas. Junto a vosotros he madurado científica y personalmente.*

*A mi pequeño Marc. Me honra de orgullo y satisfacción haberte tenido de prácticas y finalmente de compañero. Has crecido mucho y me ha encantado verlo de cerca.*

*A Gabi. Por la alegría que desprendes. ¡Desde que te conozco, tengo muchísimas ganas de ver México! Juntas con Marc, para siempre el equipo ESKAPE.*

*A Jenni y Júlia. Gracias por los ratos en los que nos colamos entre nuestros despachos o en el césped para comer y ponernos al día.*

*A mis compañeros que llegaron y se fueron: Miquel Àngel, Pau, Dani, Andrea, Paula, Alba, Àngela y Oihane.*

*A mis compañeros de los laboratorios próximos: "Ambiental" y "Tercera planta".*

*A mis alumnos de prácticas, por mostrarme lo bonita y agradecida que es la enseñanza.*

*A mis amigos de Sant Boi, "los de toda la vida": Cris, David y Mario. No hace falta escribir una tesis para saber que siempre seguiremos juntos.*

*A mis amigos de Cerdanyola-Barcelona y Sant Vicenç, por integrarme y por todas esas experiencias inolvidables que he tenido con vosotros. Habéis formado parte de mi vida, para lo bueno y lo malo.*

*A Alex y su familia.*

*Gua guaa, guauguau gua guaa (Traducción: A Wendy, por enseñarme lo que es el amor incondicional).*

*A mi familia por el cariño y siempre mostrar interés cuando les explico qué hago en el laboratorio sin dormirse. En especial destacar a mi abuela, quien más me ha ayudado en todo el mundo, y más haría si pudiera. Gracias a mi madre por preguntarme siempre que qué he descubierto. También a Sergi y Rafa, aunque seáis pesados os elegiría infinidad de veces como hermanos.*

*A mis compañeros de kárate, que me han enseñado a liberar el estrés con tsukis y geris.*

*Ich danke A. Hensel dafür, dass er mich in seinem Labor empfangen und so gastfreundlich wie möglich aufgenommen hat. Dank Ihnen und dem gesamtem IPBP werde ich ein Stück Deutschland in meinem Herzen tragen.*

*A Salmonella y Enterobacter por ser mis modelos bacterianos sujeto de estudio estos años. Aunque a veces hayamos tenido nuestras riñas, habéis sido geniales y espero seguir trabajando con vosotros en mis futuras investigaciones.*

*Eternamente agradecida*





